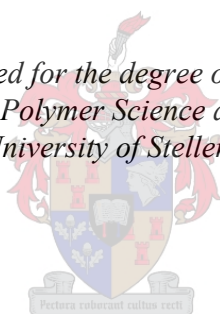


Synthesis of Permanent Non-Leaching Antimicrobial Polymer Nanofibers

by
Osama E. S. Bshena

*Dissertation presented for the degree of Doctor of Philosophy in
Polymer Science at the
University of Stellenbosch*



Promoter: Prof Bert Klumperman
Faculty of Science
Department of Chemistry and Polymer Science

March 2012

Declaration

I, the undersigned, hereby declare that the work contained in the thesis is my own original work and that I have not previously in its entirety or in part submitted it at any university for a degree

Osama Bshena

March 2012

Abstract

Antimicrobial fibers are very useful in various fields such as air and water purification, wound dressings and protective bandages, where sterile environments are essential. The non-woven nanofiber mats or membranes are able to filter out microorganisms and potentially kill several threatening pathogenic bacteria. In this thesis, a variety of styrene-maleimide copolymer derivatives were prepared based on the modification of poly(styrene-*co*-maleic anhydride with various primary amine compounds.

All prepared copolymer derivatives were electrospun to nanofiber mats using the needle electrospinning technique. For the characterization, differential scanning calorimetry (DSC) and thermogravimetric analysis (TGA) were used to study the thermal properties of the electrospun fiber mats. Scanning electron microscopy (SEM) was carried out to observe fiber dimensions and morphology.

The antibacterial activity of electrospun fiber mats was evaluated against different bacteria including *Staphylococcus aureus* (Gram-positive), *Escherichia coli* and *Pseudomonas aeruginosa* (Gram-negative). The evaluation study utilized different tools to test for antibacterial activity and mode of cell death, including bioluminescent imaging, fluorescence imaging and the viable cell counting method. Excellent antimicrobial activity was obtained against the different strains especially against *Staphylococcus aureus*. Fiber mats containing tertiary amino groups, phenol or quaternary ammonium groups had the strongest antimicrobial properties.

Opsomming

Antimikrobiese vesels is baie nuttig in verskeie toepassingsgebiede, soos lug- en watersuiwering, wondbedekkings en beskermende verbande, waar 'n steriele omgewing noodsaaklik is. Die ongeweeftde nanovesel matte of membrane is in staat om mikro-organismes te verwyder deur filtrasie, maar kan ook verskeie patogeeniese bakterieë doodmaak. In hierdie proefskrif is 'n verskeidenheid stireen-maleimied kopolimeer afgeleides gesintetiseer, gebaseer op die modifikasie van poli(stireen-ko-maleïne anhidried) met verskeie primêre amien verbindings.

Nanovesel matte van al die gesintetiseerde kopolimeer afgeleides is gemaak deur gebruik te maak van die naald-elektrospinn tegniek. Die termiese eienskappe van hierdie nanovesel matte is bestudeer deur gebruik te maak van differensiële skandeer kalorimetrie (DSK) en termogravitasie analiese (TGA) as karakteriseringsmetodes. Die vesel dimensies en morfologie is bestudeer deur skandeer elektronmikroskopie as karakteriseringsmetode te gebruik.

Die antibakteriële aktiwiteit van die gespinde vesel matte is geëvalueer teen verskillende bakterieë, naamlik *Staphylococcus aureus* (Gram-positief), *Escherichia coli* en *Pseudomonas aeruginosa* (Gram-negatief). Die evalueringstudie het verskillende instrumente gebruik om vir antibakteriële aktiwiteit en meganisme van seldood te toets, insluitend bioluminiseringsbeelding, fluoressensie beelding en die lewensvatbare sel tellingsmetode. Uitstekende antimikrobiese aktiwiteit is verkry teen die verskillende rasse, veral teen *Staphylococcus aureus*. Vesel matte met tersiêre aminogroepe, fenol of kwaternêre ammoniumgroepe het die sterkste antimikrobiese eienskappe gehad.

Acknowledgments

Firstly, I would like to thank God Almighty who is the creator of everything for blessing me with the gift of life during my study.

Secondly I would like to thank and acknowledge the institutions that have made this Study possible. The Libyan International Centre for Macromolecules Chemistry and Technology, the Libyan higher education department, the department of chemistry and polymer science and the department of microbiology at the University of Stellenbosch.

Without whose generous sponsorship this would not have been possible. I would also like to convey thanks to the Netherlands Organization for Applied Scientific Research (TNO) for their contribution in the antimicrobial assays.

I am heartily thankful to my supervisor, Prof Bert Klumperman, who was abundantly helpful and offered invaluable assistance, support and guidance. I would like to take this opportunity to thank Prof Ron Sanderson, for giving me the opportunity to study at this polymer science institution.

I owe a lot of gratitude to my friend Tiaan Hueins who helped me in conducting the antimicrobial assessments. Your help and kind efforts are highly appreciated. I also would like to thank all students and staff of Prof. Leon Dicks Lab, at the department of microbiology. I appreciate their warm and friendly hospitality. Special thanks go to Michele De Kwaadsteniet, her fruitful discussions and endless assistance are gratefully acknowledged and much appreciated.

I am thankful to Wolfgang Weber for his help in and guidance in the experimental work, also want thank Ben Loos for his assistance using the Fluorescence microscopy tool in my evaluation study

I thank all my friends and colleagues in the polymer science department for their support and encouragement. I offer my regards and blessings to all of those who supported me in any respect during the completion of the project

Finally, I would like to express love and gratitude to my beloved parents for their patience, understanding and support as well as their unequivocal belief in me. I cannot thank enough my wife Hana for her endless love, courage and support through the duration of my studies.

Contents

DECLARATION	I
ABSTRACT	II
OPSOMMING.....	III
ACKNOWLEDGMENTS	IV
LIST OF FIGURES	IX
LIST OF TABLES.....	XIII
LIST OF SCHEMES	XIII
LIST OF ACRONYMS.....	XIV
CHAPTER 1 INTRODUCTION AND AIMS.....	1
1.1 INTRODUCTION.....	1
1.2 OBJECTIVES.....	2
1.3 LAYOUT OF THE DISSERTATION.....	3
CHAPTER 2: LITERATURE REVIEW	5
2.1 ABSTRACT	5
2.1 INTRODUCTION.....	5
2.2 ANTIMICROBIAL AGENTS.....	7
2.2.1 <i>Low molecular weight inorganic and organic antimicrobial agents</i>	<i>7</i>
2.2.2. <i>High molecular weight antimicrobial agents</i>	<i>11</i>
2.2.3. <i>Natural and synthetic peptides.....</i>	<i>11</i>
2.2.4 <i>Chitosan and its derivatives.....</i>	<i>13</i>
2.3 SYNTHETIC ANTIMICROBIAL POLYMERIC MATERIALS	14
2.3.1. <i>Antimicrobial polymers.....</i>	<i>15</i>

2.3.2. Antimicrobial surface modification.....	16
2.3.2. Synthesis and activity of antimicrobial polymers.....	22
2.4. ANTIMICROBIAL POLYMER FIBERS.....	25
2.5. POTENTIAL CANDIDATES FOR NON-LEACHING ANTIMICROBIAL NANOFIBERS	32
2.6 CONCLUSIONS AND OUTLOOK	39
2.7 REFERENCES.....	40
CHAPTER 3: SYNTHESIS AND CHARACTERIZATION OF STYRENE-MALEIMIDE COPOLYMER DERIVATIVES.....	56
3.1 ABSTRACT	56
3.1 SYNTHESIS OF STYRENE-MALEIMIDE BASED COPOLYMERS.....	56
3.1.1 Materials.....	56
3.1.2 Synthesis of Styrene-maleic anhydride copolymer (SMA-P)	57
3.2 MODIFICATION OF SMA WITH VARIOUS AMINO-COMPOUNDS	60
3.2.1 Preparation of styrene-dimethylaminopropylmaleimide copolymer (SMI-P).....	61
3.2.2 Preparation of Styrene-n-butylmaleimide copolymer (SMI-NB)	65
3.2.3 Preparation of styrene-N-(2-hydroxyethyl)maleimide copolymer (SMI-AE).....	69
3.2.4 Preparation of styrene-N-(p-hydroxyphenyl)maleimide copolymer (SMI-AP)	72
3.2.4.1 Preparation of 4-hydroxyphenyl maleimide monomer (HPM)	72
3.2.4.2 Free radical copolymerization of HPM and styrene	75
3.3 QUATERNIZATION OF SMI COPOLYMER WITH ALKYL HALIDES.....	78
3.3.1 Methyl iodide quaternized styrene-N,N-dimethylaminopropyl maleimide) copolymer . 79	
3.3.1.1 Preparation of SMI-Pq1	79
3.3.1.2 Preparation of SMI-Cq1	79
3.3.2 Styrene-[(N-butyl)-N,N-dimethyl]-3-propyl maleimide] copolymer.....	81
3.3.2.1 Preparation of SMI-Pq4	81
3.3.2.2 Preparation of SMI-Cq4.....	82

3.3.3 Styrene-[(<i>N</i> -octyl- <i>N,N</i> -dimethyl)-3-propyl maleimide] copolymer.....	84
3.3.2.1 Preparation of SMI-Pq8.....	84
3.3.2.2 Preparation of SMI-Cq8.....	84
3.3.2.1 Preparation of SMI-Pq12.....	86
3.3.2.2 Preparation of SMI-Cq12.....	86
3.4 CONCLUSIONS:.....	90
3.5 REFERENCES:.....	90
CHAPTER 4: ELECTROSPINNING OF MALEIMIDE-STYRENE COPOLYMER DERIVATIVES.....	92
4.1 ABSTRACT.....	92
4.2. THE ELECTROSPINNING PROCESS.....	92
4.3 ELECTROSPINNING STYRENE-MALEIMIDE (SMI) COPOLYMER DERIVATIVES.....	94
4.4 RESULTS AND DISCUSSION.....	97
4.4.1 SEM analysis.....	97
4.4.2 Thermal analysis.....	99
4.5 SOLUBILITY PROPERTIES OF THE QUATERNIZED ELECTROSPUN FIBERS.....	102
4.5.1 Thermal curing of water-soluble fibers.....	103
4.6 CONCLUSIONS:.....	109
4.7 REFERENCES.....	109
CHAPTER 5: ANTIMICROBIAL EVALUATION.....	112
5.1 ABSTRACT.....	112
5.1 BIOLUMINESCENT IMAGING.....	113
5.1.1 Sample and culture preparation.....	114
5.2 ANTIMICROBIAL ASSAY OF FIBER MATS USING SHAKE FLASK METHOD (ASTM E2149).....	119
5.3 EXTERNAL ANTIMICROBIAL TESTS.....	129
5.4 EVALUATION USING FLUORESCENT MICROSCOPY.....	132

5.5 CYTOTOXICITY ASSAY	134
5.6. CONCLUSION:.....	139
5.7 REFERENCES:.....	139
CHAPTER 6: CONCLUSIONS AND RECOMMENDATIONS	143
6.1 CONCLUSIONS	143
<i>Modification of Poly(styrene-co-maleic anhydride) (SMA) copolymers</i>	<i>143</i>
<i>Electrospinning of styrene-maleimide copolymer derivatives</i>	<i>144</i>
<i>Antimicrobial evaluation</i>	<i>144</i>
6.2 RECOMMENDATIONS:	146

List of figures

Figure 2.1: Mode of action of various antimicrobial compounds. CRA's : chlorine-releasing agents, QA's: quaternary ammonium compounds.....	9
Figure 2.2: General structure of QACs.....	10
Figure 2.3: Examples of QACs.....	10
Figure 2.4: Chemical structure (a) of chitin poly(N-acetyl- β -d-glucosamine) and (b) of chitosan (poly(d-glucosamine) repeat units. (c) Structure of partially acetylated chitosan, a copolymer characterized by its average degree of acetylation (DA). 14	14
Figure 2.5: Immobilization of alkoxysilanes to reactive surface substrate.....	17
Figure 2.6: ATRP polymerization of DMEAMA from glass or paper surfaces.....	19
Figure 2.7: Modification of ATRP initiator followed by surface immobilization, polymerization, and quaternization of PDMEAMA on glass or paper with available hydroxyl groups.....	20
Figure 2.8: Modification of silicon-based surface.....	21
Figure 2.9: Poly (trialkyl-3-(and 4-)vinylbenzylammonium chlorides).....	22
Figure 2.10: Acrylic and methacrylic biguanide monomers.....	23
Figure 2.11: (Tributyl 4-vinylbenzyl)phosphonium salt monomer.	24
Figure 2.12: Copolymers of acrylamide and maleimide derivatives.....	25
Figure 2.13: Nano sized fiber diameters have higher surface areas compared with textile fibers. Reprinted from reference.....	26
Figure 2.14: Synthesis of VBDCC and subsequent copolymerization with PFAEA and MMA.....	27
Figure 2.15: Preparation of PVP sulfonated derivatives.....	28
Figure 2.16: Schematic shows preparation of P(DMAEMA-c-GMA)-b-PPCPA microfibers via ATRP and electrospinning.....	30
Figure 2.17: Preparation of P4VP-b-PPCPA via RAFT polymerization.....	31

Figure 2.18: Anchoring Acriflavine to PSMA and PMMA.....	34
Figure 2.19: PSMA modification with aromatic functionalized biocides.....	35
Figure 2.20: Attachment of antimicrobial agents to PSMA fiber mats.....	36
Figure 2.21: Polystyrene–Tertiary amine bonded fibers.....	38
Figure 2.22: Antimicrobial polystyrene derivatives (MIC = Minimum inhibitory concentration).....	39
Figure 3.1: ¹ H-NMR and ¹³ C-NMR spectra of SMA-P in acetone- <i>d</i> ₆	59
Figure 3.2: ATR-FTIR spectrum of SMA-P.....	60
Figure 3.3 ATR–FTIR spectra of SMI-P modification steps from SMA-P.....	63
Figure 3.4: ¹³ C-NMR spectra of SMI-P and SMA-P in DMSO- <i>d</i> ₆	64
Figure 3.5: ¹ H-NMR spectrum of SMI-P in DMSO- <i>d</i> ₆	65
Figure 3.6: ¹ H and C NMR spectra of SMI-NB in DMSO- <i>d</i> ₆	67
Figure 3.7: ATR-FTIR spectra of SMI-NB modified from SMA-P.....	68
Figure 3.8: ¹ H-NMR spectrum of SMI-AE in DMSO- <i>d</i> ₆	70
Figure 3.9: ¹³ C-NMR spectrum of SMI-AE in DMSO- <i>d</i> ₆	71
Figure 3.10: ATR-FTIR spectra of SMI-AE, illustrating the imidization reaction steps from SMA-P.....	72
Figure 3.11: ¹ H and ¹³ C-NMR spectra of HPM in DMSO- <i>d</i> ₆	74
Figure 3.12: ¹ H and ¹³ C-NMR spectra of SIM-AP in DMSO- <i>d</i> ₆	76
Figure 3.13: ATR-FTIR spectra of HPM and SMI-AP.....	77
Figure 3.14: Chemical structure of quaternized SMI derivatives. * The letter P here refers to modified copolymers from SMI-P. **The letter C refers to modified copolymers prepared from SMI-C.....	78
Figure 3.15: ¹ H-NMR spectra of SMI-Pq1 (top) and SMI-P in DMSO- <i>d</i> ₆	80
Figure 3.16: ¹³ C-NMR spectra of SMI-Pq1 and SMI-P in DMSO- <i>d</i> ₆	81

Figure 3.17: ¹ H and ¹³ C-NMR spectra of SMI-Pq4 and SMI-P in DMSO- <i>d</i> ₆	83
Figure 3.18: ¹ H and ¹³ C-NMR spectra of SMI-Pq8 in DMSO- <i>d</i> ₆	85
Figure 3.19: ¹ H and ¹³ C-NMR spectra of SMI-Pq12 in DMSO- <i>d</i> ₆	87
Figure 3.20: ATR-FTIR spectra of SMA-P and its modified derivatives.....	88
Figure 3.21: ATR-FTIR of N-quaternized SMI-C derivatives.....	89
Figure 4.1: representation of the electrospinning setup used in this work.....	93
Figure 4.2: Mean average diameter of the electrospun polymer derivatives.....	97
Figure 4.3: SEM images of some electrospun SMI copolymer derivatives.....	98
Figure 4.4: TGA thermograms of SMI copolymer derivatives.....	99
Figure 4.5: TGA thermograms of quaternized SMI-C (top) and SMI-P copolymer derivatives.....	100
Figure 4.6: SMI copolymer derivatives.....	104
Figure 4.7: ATR-FTIR spectra of soluble and insoluble SMI-P fiber mats.....	105
Figure 4. 8: SEM images of SMI-P fibers (A) untreated (B) treated at 80 °C, (C) treated at 130 °C.....	106
Figure 4.9: DSC curves of the treated and untreated SMI-P fibers.....	107
Figure 4.10: SEM image of the SMI-Pq4 fibers before and after crosslinking.....	108
Figure 5.1: the IVIS® imaging system that was used in this study.....	114
Figure 5.2: Photo Samples of electrospun SMI-P fibers, plate (1) (60 mg fiber mat), plate (2) (~20 mg fiber mat) taken inside the imaging chamber.....	115
Figure 5.3: Bioluminescence of (<i>S. aureus</i> Xen 36) imaged with an IVIS® camera (exposure time 20 sec). (1) SMI-P fiber and 10 mL concentration ~ 10 ⁶ cell.mL ⁻¹ culture after 2 minutes of contact. (2) A control plate containing (<i>S. aureus</i> Xen 36) culture at time 0. (3) Sample from image (1) after one hour of contact (4) Control after 4 hours incubation.....	115

Figure 5.4: Bioluminescence of (*S. aureus* Xen 36) imaged with an IVIS® camera (exposure time 20 sec). (1) SMI-P fiber sample mat, (2) sample and bacteria solution (20 mL ~ 10⁷ cell.mL⁻¹) time 0, (3) time 1 hour incubation, (4) 2 hours incubation, (5) 3:15 hours incubation, (6) 5:15 hours incubation 116

Figure 5.5: Bioluminescence of *E. coli* (Xen14) imaged with an IVIS camera (exposure time 20 sec). (1) SMI-P fibers and *E. Coli* after 10 minutes contact, (2) after 80 minutes..... 117

Figure 5.6: Tubes containing the fibers and bacterial culture used in the AM assay. 120

Figure 5.7: Phenol functionlized styrene maleic anhydride and maleimide derivatives. 122

Figure 5.8: Agar plate photos (*S. aureus*). Comparative view of the plated 10⁻³ diluted solutions between the control and the treated culture with SMI-AE fibers..... 124

Figure 5.9: Agar plate photos (*S. aureus*). Comparative view of the plated 10⁻¹ diluted solutions between the control and the treated culture with SMI-P fibers. 125

Figure 5.10: Agar plate images (*S. aureus*). Comparative view of the plated 10⁻¹ diluted solutions between the control and the treated culture with SMI-Cq1 fibers..... 126

Figure 5.11: Agar plate images (*S. aureus*). Comparative view of the plated 10⁻¹ diluted solutions between the control and the treated culture with SMI-Pq1 and SMI-Pq4 fibers. 127

Figure 5.12: Incubated plates of the triplicates treated with *B. Anthracis*, from time 2h-48 hr 131

Figure 5.13: Incubated plates of the triplicates treated with *Y. pestis* from time 2h-48 hr... 131

Figure5.14: Fluorescent microscope images of incubated fibers (SMI-Pq12) with *S. aureus* is saline solution 134

Figure 5.15: (PI) uptake of H9c-2 Cells treated with various antimicrobial fibers. The H9c-2 Cells were incubated with the fibers at room temperature for up to 4 hours. Assays were calculated from fluorescence results acquired after 1, 2 and 4 hours incubation..... 136

Figure 5.16: Fluorescence microscopy images of H9c-2 cells after incubation for 4 hours with various fibers as indicated in the figure..... 138

List of tables

Table 2.1: Classification of antimicrobial agents (adapted from reference 43).....	8
Table 2.2: Classes of bacteriocins and bacteriocin-like peptides and proteins from LAB (Rea <i>et al</i>).	12
Table 4.1: Dielectric constants of solvents copied from reference.....	95
Table 4.2: Experimental electrospinning conditions of the SMI copolymer derivatives	96
Table 4.3: Measured T_g s of the electrospun fibers.....	101
Table 4.4: The T_g of quaternized SMI-P copolymer derivatives.	107
Table 4.5: Average fiber diameters before and after crosslinking of quaternized SMI-P derivatives.....	108
Table 5.1: Chemical structure and Polymer codes prepared in this work	112
Table 5.2: Antibacterial assessment results using bioluminescence imaging by IVIS.....	118
Table 5.3: Antibacterial activity of the fibers against <i>S. Aureus</i>	121
Table 5.4: A summary of antimicrobial tests against <i>P. aeruginosa</i>	128
Table 5.5: A summary of antimicrobial assessment of SMI-P fibers against various bacteria	130

List of Schemes

Scheme 3.1: Free radical copolymerization of SMA.....	58
Scheme 3.3: Ring closure of reacted SMA with DAMPA (imidization step).....	62
Scheme 3.4: preparation of SMI-NB	66
Scheme 3.5: representation of SMI-AE preparation.....	69
Scheme 3.6: preparation of HPM.....	73
Scheme 3.7: free radical copolymerization of HPM and styrene.	75

List of Acronyms

ABA	4- aminobenzoic acid
ADMMAPS	styrene/acrylamide)- <i>N,N</i> -dimethylmaleimidopropyl ammoniopropane
AIBN	2,2'-azo bis(isobutyronitrile)
AP	4-aminophenol
ATP	adenosine triphosphate
ATR-FTIR	attenuated total reflection Fourier transform infrared
ATRP	atom transfer radical polymerization
BLI	Bioluminescence imaging
CFU	colony forming units
CHX	chlorhexidine
CNTs	carbon nanotubes
CRP	controlled radical polymerization
Đ	dispersity
DMAEMA	2-(<i>N,N</i> -dimethylamino)ethyl methacrylate
DMAPA	3-dimethylaminopropylamine
DMF	dimethylformamide
DSC	differential scanning calorimetry
HBA	4-hydroxybenzoic acid
HPM 4-	hydroxyphenyl maleimide
LiSPVP	lithium salt sulfonated poly(vinyl phenol)
MAnh	maleic anhydride
\bar{M}_w	weight average molecular weight
\bar{M}_n	number average molecular weight
MEK	methyl ethyl ketone
MIC	minimum inhibitory concentration

MMA	methyl methacrylate
MRSA	methicillin-resistant strains of <i>staphylococcus aureus</i>
NMR	nuclear magnetic resonance
OD	optical density
P(DMAEMA- <i>c</i> -GMA)	poly[[(2-dimethylamino)ethyl methacrylate)- <i>co</i> -(glycidyl methacrylate)]
PCPA	pentachlorophenyl acrylate
PI	propidium iodide
PMF	proton motive force
poly(MIQADMAMP)	poly(methyl iodide quaternized (acrylamide)- <i>N,N</i> -dimethylaminopropyl maleimide) copolymer
PPCPA	poly(pentachlorophenyl acrylate)
PSMA	Styrene-maleic anhydride copolymer
PTMSPMA	poly(3-(trimethoxysilyl)propyl methacrylate)
QACs	quaternary ammonium compounds
QAS	quaternary ammonium salt
RAFT	reversible addition fragmentation transfer
SEC	size exclusion chromatography
SEM	Scanning electron microscopy
SMA	poly(styrene- <i>co</i> -maleic anhydride)
SMI	poly(styrene- <i>co</i> -maleimide)
SMI-AE	styrene- <i>N</i> -(2-hydroxyethyl)maleimide copolymer
SMI-AP	<i>N</i> -(<i>p</i> -hydroxyphenyl)maleimide copolymer
SMI-NB	Styrene- <i>n</i> -butylmaleimide copolymer
SMI-C	styrene-dimethylaminopropylmaleimide copolymer, based on a commercial statistical poly(styrene- <i>co</i> -maleic anhydride) grade
SMI-P	styrene-dimethylaminopropylmaleimide copolymer based on an alternating poly(styrene- <i>co</i> -maleic anhydride) grade.

SMI-Pq1 & SMI-Cq1	Methyl iodide quaternized styrene- <i>N,N</i> -dimethylaminopropyl maleimide copolymer
SMI-Pq12, SMI-Cq12	Styrene-[(N-dodecyl)- <i>N,N</i> -dimethyl]-3-propyl maleimide] copolymer
SMI-Pq4, SMI-Cq4	Styrene-[(N-butyl- <i>N,N</i> -dimethyl)-3-propyl maleimide]) copolymer
SMI-Pq8, SMI-Cq8	Styrene-[(N-octyl- <i>N,N</i> -dimethyl)-3-propyl maleimide]) copolymer
SPVP)	Sulfonated poly(vinyl phenol
TGA	thermogravimetric analysis
THF	Tetrahydrofuran
TiO ₂	titanium dioxide
TNO	The Netherlands Organization for Applied Scientific Research
UV	ultraviolet
VBC	4-vinyl benzyl chloride
VBDCC	vinylbenzyl-dimethylcocoammonium chlorides
4VP	4-vinyl pyridine
VRE	vancomycin-resistant enterococci
zinc oxide	ZnO

Chapter 1 Introduction and Aims

1.1 Introduction

Nosocomial infections, microbial contamination and infection risks especially in medical related sectors have led to the growing demand to prevent such microbial infection in these areas. In the past decade, research efforts have notably increased to synthesize and design new effective antimicrobial polymeric materials. These materials can be divided in different categories such as the incorporation of effective biocides previously known to impart antimicrobial effects by default or rendered by an external stimulus such as light. Surface modification has been utilized to minimize or inhibit microbial growth. Another approach is the inclusion of naturally occurring antimicrobial substances in fibrous or other polymeric substrates. Many chemical agents including silver, hydrogen peroxide, iodine, and polypeptides have been incorporated into polymers to kill bacterial pathogens. However, some of these current approaches have certain disadvantages. For example, the continuous release of low molecular weight antibacterial agents from matrices can lead to diminishing effectiveness over time. Also, the cytotoxicity of some antibacterial agents, such as silver that binds to DNA and prevents replication, adversely impacts the promise of these low molecular weight antibacterial agents in treating infections.

There is considerable demand to synthesize new polymeric materials with inherent antimicrobial properties. To date there are limited studies reported on the synthesis of non-leaching antimicrobial fibers. It is of interest to design new materials with antimicrobial activities, *taking into consideration a suitable polymer system and its synthetic method*. Poly(styrene-co-maleic anhydride) (SMA) is a good example of a functionalized polymer system that is conveniently post-modified and/or processed.

Electrospinning is a simple, low-cost, and effective technology to produce polymer nanofibers, or polymer composite materials. Electrospun nanofibers have very large surface area to volume ratio, which enables such nanofibrous scaffolds to have many biomedical and industrial applications. Membranes or fiber mats made out of these nanofibers can be used in

a variety of applications like filtration, tissue engineering, drug delivery, etc. Therefore, nanofibers are considered an effective candidate to be utilized as antimicrobial materials.

1.2 Objectives

The basic motivation for this work is to investigate the antimicrobial activity of new polymer materials based on poly(styrene-*co*-maleimide) derivatives. The polymer precursor utilized is poly(styrene-*co*-maleic anhydride) (SMA). The advantage of this particular material is that it can be readily modified through its highly reactive anhydride groups. Furthermore, SMA is easily prepared via radical polymerization of styrene and maleic anhydride. It is also commercially available in different grades varying in molar mass and anhydride content. The goal of this work is to develop new permanent antimicrobial compounds in the form of insoluble non-woven fiber mats based on styrene-maleimide copolymer derivatives. The polymers prepared were inspired by introducing previously known biocidal groups and chemically attaching them onto the polymer chain. The objectives of the study can be summarized as follows:

1. To synthesize a high molar mass alternating styrene-maleic anhydride (SMA) copolymer that has approximately 50% maleic anhydride units.
2. To post-modify the alternating SMA copolymer with various primary amine compounds namely, 3-dimethylaminopropylamine (DMAPA), *n*-aminobutane and 2-aminoethanol to obtain fully imidized copolymer derivatives.
3. To prepare 4-hydroxyphenyl maleimide monomer and copolymerize it with styrene to synthesize poly(styrene-*co*-*N*-(*p*-hydroxyphenyl)maleimide).
4. To synthesize a series of quaternized derivatives based on the DMAPA imidized copolymers of both SMA grades (alternating and commercial). Four alkyl halide compounds including, methyl iodide, 1-bromobutane, 1-bromooctane, and 1-dodecylbromide are selected to quaternize the tertiary amino groups into quaternary ammonium moieties.
5. To synthesize non-woven nanofiber mats via electrospinning of all prepared copolymer derivatives and optimize the electrospinning conditions for each polymer system.

6. Evaluate the antimicrobial activity of the electrospun fiber mats against different Gram-positive and Gram-negative bacteria. Also, to investigate the mode of action of cell death via fluorescence microscopy.

1.3 Layout of the Dissertation

Chapter 1: A brief introduction to the scope of the study is described and the specific objectives are highlighted in this chapter.

Chapter 2: An overview of previous research studies and protocols related to this project are presented here. The survey provides an introduction into different classes of antimicrobial materials. The main focus is on strategies for the introduction of antimicrobial properties in polymer materials to date.

Chapter 3: This chapter describes the synthetic protocols and the characterization of alternating styrene-maleic anhydride copolymer, and styrene-maleimide copolymer derivatives.

Chapter 4: In this chapter the electrospinning conditions of the maleimide derivatives is presented. The thermal properties of the produced fiber mats were discussed as well as fiber morphology.

Chapter 5: This chapter presents an antimicrobial evaluation study of all synthesized electrospun polymer fiber mats. Various Gram-negative and Gram-positive bacteria were used for the study. An indication of cytotoxicity on mammalian cells was also addressed on potent fiber mats.

Chapter 6: Conclusions and recommendations for future research are highlighted in this chapter.

CHAPTER 2

CHAPTER 2: Literature Review

This chapter is a full review paper published in Future Medicinal Chemistry:

Bshena, O.; Heunis, T.D.J.; Dicks, L.M.T.; Klumperman, B. - Antimicrobial fibres: Therapeutic possibilities and recent advances – [Future Med. Chem. 2011, 3, 1821-1847](#)

2.1 Abstract

The emergence of multi-drug-resistant bacteria such as methicillin-resistant strains of *Staphylococcus aureus* (MRSA), vancomycin-resistant enterococci, *Pseudomonas aeruginosa*, *Acinetobacter baumannii* and extended-spectrum β -lactamase (carbapenemase)-producing Enterobacteriaceae is becoming a serious threat. New-generation antimicrobial agents need to be developed. This includes the design of novel antimicrobial compounds and drug-delivery systems. This review provides an introduction into different classes of antimicrobial materials. The main focus is on strategies for the introduction of antimicrobial properties in polymer materials. These can be roughly divided into surface modification, inclusion of antimicrobial compounds that can leach from the polymer, and the introduction of polymer-bound moieties that provide the polymer with antimicrobial properties. One of the main challenges in the development of antimicrobial polymers for the use in contact with human tissue is the concomitant demand of non-cytotoxicity. Current research is strongly focused on the latter aspect.

2.1 Introduction

Microbial contamination is of great concern, especially in hospitals^{1,2}, water purification systems, animal feed and food.³⁻⁵ Hospital-acquired infections are caused by several species, of which *Escherichia coli*, *Klebsiella pneumoniae*, *Serratia marcescens*, *Citrobacter freundii*, *Morganella morganii*, *Enterobacter* spp., *Proteus mirabilis*, *Burkholderia* spp., *Stenotrophomonas maltophilia*, *Pseudomonas aeruginosa* and *Acinetobacter baumannii* are the most common. The emergence of multi-drug resistant bacteria, such as methicillin-

resistant strains of *Staphylococcus aureus* (MRSA) and vancomycin-resistant enterococci (VRE), is increasing and the control of these bacteria is considered one of the biggest challenges the medical world is facing.⁶⁻⁸ A large number of *S. aureus* strains resistant to oxacillin, nafcillin, quinopristin-dalfopristin, rifampicin, ciprofloxacin, teichoplanin, cefazolin and cephalothin A have been reported.⁹ Multi-drug resistant strains of *Pseudomonas aeruginosa*, *Acinetobacter baumannii* and extended-spectrum β -lactamase (carbapenemase)-producing Enterobacteriaceae are also on the list of extreme pathogens.^{10,11} In the USA alone, approximately two million cases of bacterial infections are annually reported.¹² More than 90,000 patients die from, or have been associated with, bacterial infections.¹⁰

Pathogens sensitive to antibiotics may become resistant by acquiring genes from resistant microorganisms in the same niche, or they develop novel ways to prevent antibiotics from entering the cell. Resistance to β -lactam antibiotics is conferred by expression of the NDM-1 gene that encodes a broad-spectrum β -lactamase (carbapenemase).¹³ A recent study reported that the NDM-1 gene was mostly present in Gram-negative bacteria, including *Escherichia coli* and *K. pneumoniae*.¹⁴ Bacteria containing the NDM-1 gene usually exhibit resistance to a number of antibiotics.¹⁴

Some organisms are naturally more resistant to antimicrobials, a characteristic that seems to be strain-specific. In general, Gram-negative bacteria are more resistant to antibacterial agents compared to Gram-positive bacteria. This is mainly due to structural differences in their cell walls and the resistance is not specific towards a certain antimicrobial compound.^{15,16} Organisms may also become resistant to antimicrobial agents through production of enzymes that inactivate the antimicrobial agent, efflux pumps that remove an antimicrobial agent from the cell, down regulation (or alteration) of genes encoding an outer membrane protein channel, or through alteration of their cell walls.^{17,18} In a few rare cases, the antimicrobial agent serves as energy source and is degraded. A typical example is the metabolism of benzoate to succinic acid and acetyl coenzyme A by species of *Bacillus*, *Pseudomonas*, *Corynebacterium*, *Micrococcus* and *Aspergillus* through a β -ketoadipate pathway.¹⁹

Incentive strategies have been proposed to minimise and control the progression of multi-drug resistant bacteria.^{20,21} There is no question that the effective prevention and control of bacterial infections is an increasingly important part of any medical procedure. To prevent

bacterial contamination, responsible steps in the practice and application of antimicrobial agents need to be closely monitored.

In this survey, the following approach will be taken. The initial sections are focused on known antimicrobial agents, ranging from low molecular weight compounds, via polypeptides and (other) natural polymers to synthetic polymers with antimicrobial activity. These sections are used as an introduction into some concepts of antimicrobial activity. The subsequent sections focus on strategies to introduce antimicrobial activity in polymer materials. These include surface modifications, inclusion of compounds that leach from the polymer and introduction of polymer-bound (non-leaching) groups that invoke antimicrobial activity. In a variety of cases, the antimicrobial polymers are inspired by the approaches presented in the initial sections of the review.

2.2 Antimicrobial agents

Antimicrobial agents are classified according to their mode of action (Table 1). Most of these agents are used as bactericides or fungicides and are mostly aimed at the treatment of infections. The classification of antibiotics, antibacterial- and antifungal agents is discussed in the book authored by André Bryskier.²² Novel antimicrobial agents have been developed by combining low and high molar mass compounds and have been chemically modified to produce specific antimicrobial properties. The mode of action of various antimicrobial compounds on spores, bacteria, fungi and viruses is summarized in Figure 2.1.

2.2.1 Low molecular weight inorganic and organic antimicrobial agents

Metals are well known for their antimicrobial properties and are arranged in the following descending order, based on antifungal properties: Ag > Hg > Cu > Cd > Cr > Ni > Pb > Co > Zn > Fe > Ca.²³ Extensive studies have been devoted to the incorporation of silver compounds and silver ions into different polymers.²⁴⁻²⁶ The practical application of silver as antimicrobial agent has been tested in water and air filters,²⁷⁻³⁰ food packaging material,³¹ wound dressings^{32,33} and textiles.³⁴⁻³⁷ Health risks associated with excess silver are discussed in the review by Singh *et al.*³⁸ Silver-stabilized citrate and silver-stabilized poly(vinylpyrrolidone) nanoparticles slowly dissolve in water and release silver ions.³⁹

Chapter 2: Literature Review

These ions interact with DNA⁴⁰ by binding to the guanine N7 atom or between the A-T or G-C base pairs.⁴¹ Ultimately DNA replication is hampered.⁴²

Table 2.1: Classification of antimicrobial agents (adapted from reference 43)

Term	Concise definition
<i>Antibiotic</i>	A synthetic or natural organic chemical substance that, in diluted form, prevents microbial growth or causes the death of microorganisms.
<i>Bacteriostat</i>	Agent that prevents growth of bacteria, but not necessarily kills them or their spores.
<i>Sanitizer</i>	An agent that reduces the number of microorganisms to prescribed safe levels. Usually applied only to inanimate objects.
<i>Antiseptic</i>	A substance that prevents growth of microorganisms on living tissue by static or biocidal activity.
<i>Disinfectant</i>	An agent that frees from infection, usually chemical but could be physical like UV light. Pathogenic vegetative cells, but not necessarily spores, are killed. Usually used on inanimate objects.
<i>Sterilization</i>	Act or process that destroys all forms of life, especially microorganisms.

The photocatalytic properties of titanium dioxide (TiO₂) have received great attention in recent decades due to its photocatalytic disinfection performance.⁴⁴ TiO₂ metallic and non-metallic nano-composites, coatings, as well as polymer complexes have been investigated extensively for the killing or growth inhibition of bacteria under ultraviolet (UV) and visible light.⁴⁵⁻⁵⁰ Metallic oxides such as zinc oxide (ZnO) nano-particles,⁵¹ and calcium and magnesium oxides⁵² have received significant interest as possible antibacterial agents. Antibacterial agents based on CdTe quantum dots,^{53,54} carbon nanotubes (CNTs),⁵⁵⁻⁵⁷ gallium, fullerenes, nano clay and modified nano clay composites were also reported to have antimicrobial activity.^{37,57,58}

Chapter 2: Literature Review

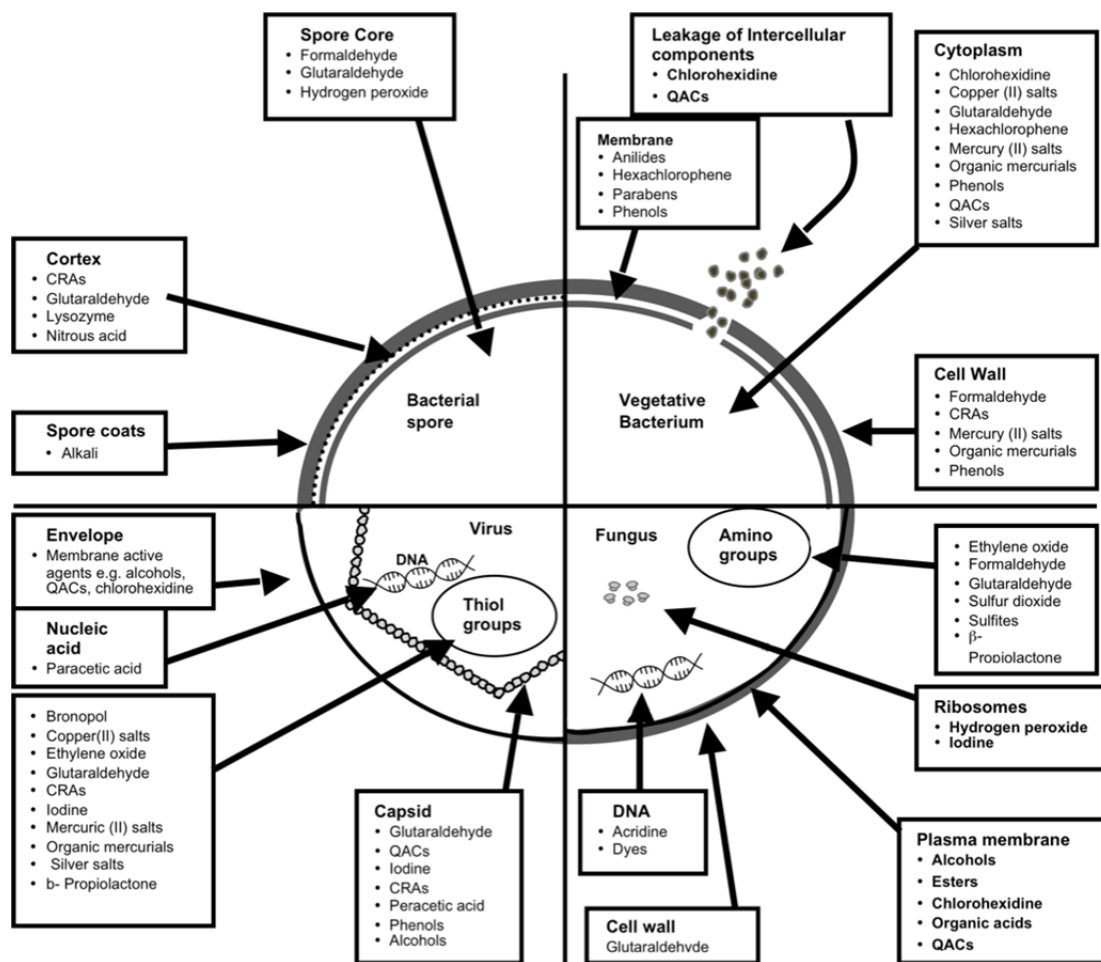


Figure 2.1: Mode of action of various antimicrobial compounds. CRA's : chlorine-releasing agents, QA's: quaternary ammonium compounds.⁵⁹

Organic-based antimicrobial materials of low molecular weight are mainly used as antimicrobial drugs, disinfectants and food preservatives. Formic, sorbic, acetic, citric, benzoic, lactic, tartaric, and propionic acids and their salts are used as food preservatives⁶⁰⁻⁶². Triclosan (5-chloro-2-(2,4-dichlorophenoxy)phenol) is used as a broad-spectrum antimicrobial agent in contemporary consumer and professional health-care products^{63,64}. However, some strains of *E. coli* and *Salmonella enterica* have developed resistance to triclosan.⁶⁵ Derivatives of quinolones and fluoroquinolones are also used as antimicrobial agents⁶⁶⁻⁶⁹. Aromatic alcohols such as phenol have bactericidal, fungicidal and virucidal properties^{70,71}. Phenolic derivatives such as ortho-phenylphenol and ortho-benzyl-para-chlorophenol are used as disinfectants in hospitals. The antimicrobial activity of these agents compare well to that of phenol. The antimicrobial properties of organic agents have been

Chapter 2: Literature Review

listed by Centers for Disease Control and Prevention⁷² and are reviewed by McDonnell *et al.*⁷³ and by Fraise *et al.*⁷⁴.

Quaternary ammonium compounds (QACs)⁷⁵⁻⁷⁷, also known as “quats”, have a broad spectrum of antimicrobial activity and are used as disinfectants in hospitals. Four of the substituents (R^1 – R^4) are alkyl or heterocyclic groups and the fifth (X^-) is either chloride, iodide or bromide (Figure 2.2).

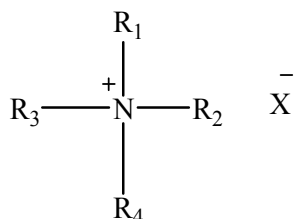


Figure 2.2: General structure of QACs.

Benzalkonium chloride and cetrimonium chloride (Figure 2.3) are common antimicrobial QACs.⁷⁸ More details on QACs compounds will be discussed in the section on antimicrobial polymeric materials.

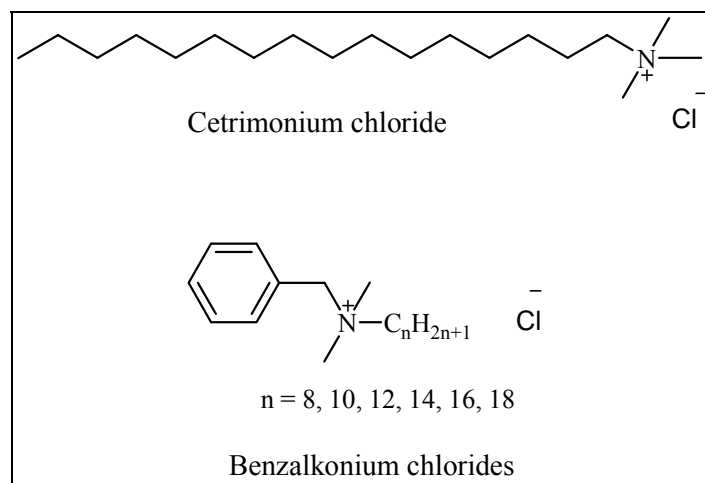


Figure 2.3: Examples of QACs.

Antimicrobial properties of maleimides are also well known.⁷⁹ Several studies have been conducted on the antimicrobial activity of maleimide derivatives such as N-alkylmaleimides,⁸⁰ 2-arylthio maleimides, N-substituted 3 and 4-nitrophthalimides,⁸¹ N-

substituted maleimides and succinimides,^{82,83} *N*-(fluorophenyl)maleimides,⁸⁴ and *N*-phenyl and *N*-phenylalkyl-maleimides.⁸⁵

Antimicrobial materials extracted from herbs and plants have also been extensively studied (reviewed by Martin *et al.*⁸⁶). Honey has also been investigated as an antimicrobial agent. The high viscosity, high osmolarity, low pH and nutrient content of the honey contribute to its antimicrobial activity (Subrahmanyam *et al.*⁸⁷; Jalali *et al.*⁸⁸).

2.2.2. High molecular weight antimicrobial agents

Materials of a high molecular weight are mainly natural and synthetic polymers. In this section, the focus will be on discussing different classes of antimicrobial polymeric materials. Selected examples of synthetic routes to produce antimicrobial polymeric materials will be discussed.

2.2.3. Natural and synthetic peptides

Antimicrobial peptides are part of the innate defense system of bacteria, insects, plants, animals and humans.⁸⁹ These peptides are grouped into different classes, i.e. α -helical peptides (e.g. cecropins), cysteine-rich peptides (e.g. α -defensin) and peptides with modified amino acids (e.g. nisin and colicin). Most antimicrobial peptides are cationic with an overall net positive charge and generally possess amphiphilic characteristics. Synthetic amphiphilic polymers with hydrophobic and hydrophilic side chains (protonated amines) have been designed based on these structures and are classified as synthetic mimics of antimicrobial peptides (SMAMPs).^{90,91} Examples are α - and β -amino acids, peptoids and aromatic oligomers.^{92,93} Although many antimicrobial peptides have been described, large scale production is expensive. Furthermore, the stability of these peptides *in vivo* has only been reported in a few studies. Nisin F retained antimicrobial activity *in vivo* for only 15 min after which the peptide was inactivated.⁹⁴ The authors attributed the inactivation to proteolytic degradation of the peptide.

Perron *et al.*⁹⁵ reported resistance against some of the cationic antimicrobial peptides. The use of antimicrobial peptides should thus be regulated to minimize the emergence of resistant microorganisms. Antimicrobial peptides produced by bacteria are known as bacteriocins and probably the best studied are the bacteriocins from lactic acid bacteria.

Chapter 2: Literature Review

These bacteriocins are ribosomally synthesized, generally cationic, have less than 100 amino acid residues^{96,97} and contain a substantial portion (30% or more) hydrophobic residues.⁹⁸ Mature peptides are produced after the cleavage of inactive pre-peptides.^{99,100} The positively charged section of the peptide interacts with the negatively charged bacterial outer membrane of the target cell. This is followed by the interaction between the hydrophobic region of the peptide and the cell membrane, entering of the double lipid structure and the formation of a permanent pore. Efflux of cell constituents through the channel causes an imbalance in the proton motive force (PMF), leading to cell death.¹⁰¹ Some bacteriocins prevent peptidoglycan synthesis¹⁰² or inhibit the germination of endospores.¹⁰³ Most bacteriocins have a narrow spectrum of antimicrobial activity, i.e. they are active against closely related species,^{104,105} and are grouped into two major classes (Table 2.2).

Table 2.2: Classes of bacteriocins and bacteriocin-like peptides and proteins from LAB (Rea *et al.* ¹⁰⁶)

<i>Subclass</i>	<i>Class I modified peptides</i>
IA	Lantibiotics and lantipeptides Subclasses I and II (modified by LanBC and LanM proteins) can also be further divided into 12 further subclasses based on amino acid sequences. Subclasses III and IV (modified by RamC-like and LanL proteins, respectively).
IB	Labyrinthopeptins
IC	Sactibiotics Two subclasses: single- and two-peptide bacteriocins
	<i>Class II Non-modified peptides</i>
IIA	Pediocin-like Four subclasses I–IV
IIB	Two-peptide bacteriocins Two subclasses (i.e., A and B)
IIC	Circular bacteriocins Two subclasses (i.e., 1 and 2)
IID	Linear non-pediocin-like one peptide bacteriocins
	<i>Bacteriolysins</i>
	Non-bacteriocin lytic proteins (formerly Class III bacteriocins)

Some bacteriocins exhibit a much broader spectrum of antimicrobial activity and may extend beyond the borders of bacteria to include protozoa, yeast, fungi and viruses.⁸⁹ A few bacteriocins are active against MRSA and VRE strains, and pathogens such as *P. aeruginosa* and *Streptococcus pneumoniae*.^{107,108} Although most of the research on bacteriocins focuses on food preservation, these peptides may also be used as an alternative to antibiotics.¹⁰⁹ The potential biomedical applications of bacteriocins from lactic acid bacteria have recently been reviewed.¹¹⁰ Bacteriocins may thus offer an alternative to control bacterial infections, administered alone or in combination with antibiotics.¹⁰¹

2.2.4 Chitosan and its derivatives

Chitosan is a linear polysaccharide composed of randomly distributed β -(1-4)-linked D-glucosamine (deacetylated unit) and N-acetyl-D-glucosamine (acetylated unit) (Figure 2.4). Chitosan is produced commercially by deacetylation of chitin, which is one of the most abundant natural polymers in the exoskeleton of crustaceans (crabs, shrimp, etc.) and in the cell walls of fungi and yeast.¹¹¹ The broad spectrum of antimicrobial activity of chitosan has been shown against a wide range of algae, bacteria, yeasts and fungi.¹¹² However, the activity of chitosan is limited to acidic conditions due to its poor solubility above pH 6.5.¹¹³ Furthermore, the antimicrobial properties of chitosan depend on average molecular weight¹¹⁴, degree of deacetylation and temperature.

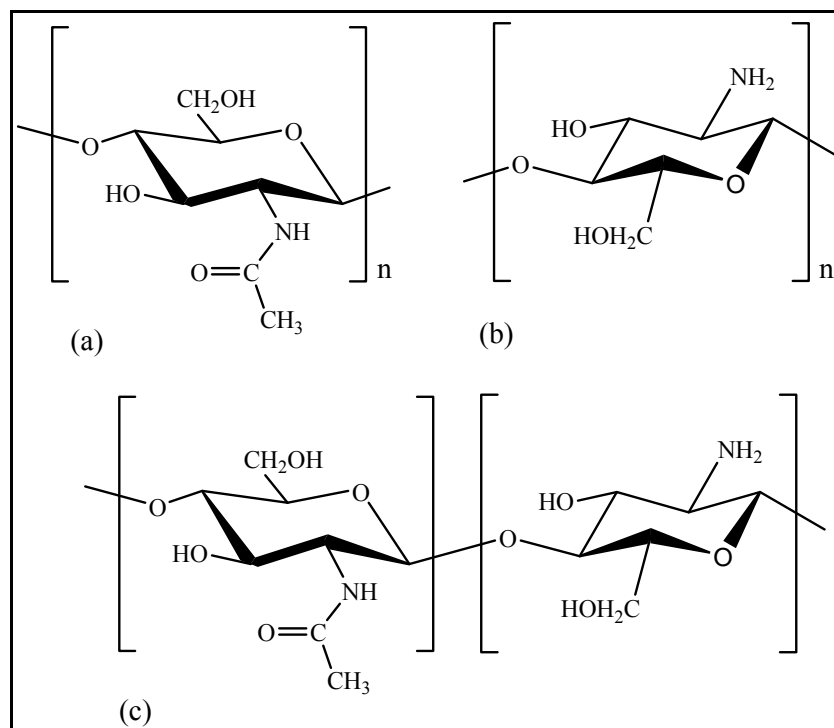


Figure 2.4: Chemical structure (a) of chitin poly(N-acetyl- β -D-glucosamine) and (b) of chitosan (poly(D-glucosamine) repeat units. (c) Structure of partially acetylated chitosan, a copolymer characterized by its average degree of acetylation (DA).

The polycationic nature of chitosan renders the molecule non-toxic, biocompatible, biodegradable and bioactive^{115,116}. Chitosan is used in food science, agriculture, medicine, pharmaceuticals, and textiles.^{111,117} Chitosan derivatives (e.g. chitosan acetate and quaternized chitosan derivatives) enhance antimicrobial activity and solubility at neutral pH values. The antimicrobial activity and biocompatibility of chitosan derivatives are discussed in several reviews.^{112,118-122}

2.3 Synthetic Antimicrobial polymeric materials

Polymer chemistry allows the design and synthesis of antimicrobial structures for specific applications, e.g. medical devices such as catheters, implants, bandages and filters. Incorporation of antimicrobial agents in plastics protects the polymer from degradation by microbes and provides a hygienic surface.¹²³⁻¹²⁵ Biocide additives are carefully selected based on their function and intended application. Several other factors also need to be taken

into account, e.g. thermal and light stability as well as toxicity of leachable components from the polymer.

Antimicrobial polymers are divided into two categories. The first category contains polymers impregnated with antimicrobial agents that are released over time (triclosan in the product Microban[®]) or polymers containing metal ions (such as Ag⁺), that slowly diffuses from the matrix¹²⁶. In all of these polymers, the slow release of the antimicrobial compound, and hence low concentrations, may lead to the development of resistance in microorganisms. With so many products on the market containing leachable antimicrobial agents and disproportionate use of antibiotics, the rate at which resistance develops is likely to increase. For instance, the excessive use of antibiotics in animal production has increased the risk of development of resistance in human and animal pathogens.¹²⁷ The second category of antimicrobial polymers is those with inherent antimicrobial or antiseptic properties. Such polymers can be applied or used in a variety of substrates, namely textiles, metal, cellulosic materials or plastics. These polymers are referred to as antimicrobial polymers and will be addressed as such throughout the text.

2.3.1. Antimicrobial polymers

Self-sterilizing antimicrobial polymers are environmentally friendly in that potentially toxic chemicals are not incorporated and hence cannot leach out.¹²⁸ Furthermore, they are easily incorporated into fibers, extruded to fibers or electrospun into nanofibers and prevent adhesion of microorganisms to their surface. Antimicrobial polymers are synthesized by covalent binding of biocidal functional groups in a post-polymerization modification, providing antimicrobial or antiseptic properties.¹² Modification is either to the bulk polymer or selectively to the surface via available reactive moieties.¹²⁸ Another form of synthesis is the chemical modification of a biocidal molecule into a polymerizable compound that can subsequently be polymerized or co-polymerized with another monomer.¹²⁹⁻¹³¹ Both these approaches have been valuable in establishing feasibility for the concept of non-leaching antimicrobial polymeric materials.

Researchers around the world have learnt to modify the already known low molecular weight antimicrobial agents, which are proven to have lethal actions against a broad spectrum of microorganisms.⁴³ This has probably helped to consider materials with bioactive functionalities as a start. Screening the organic biocides for example, one would find

numerous molecules that could be incorporated and modified to be immobilized to the bulk polymer or on the surface. A detailed discussion on the introduction of antimicrobial activity in polymers will follow in the next section.

Among the most potent antimicrobial materials that have been investigated in conjunction with polymers are the quaternary ammonium and phosphonium salts, and *N*-substituted halamines.¹³² The strategy of preparing antimicrobial polymers based on the quaternary salts is very attractive because it is fairly convenient to modify a polymer that contains reactive moieties such as tertiary or/and secondary amino groups on the polymer backbone. The biocidal activity of the cationic compounds is generally attributed to the positively charged nature of the (macro)-molecule. It is well known that the bacterial cell surface is usually negatively charged,¹³³ as evidenced by its susceptibility to electrophoresis. The bacterial cell membrane is negatively charged as a result of the negatively charged phosphate groups in the phospholipid heads of the bilayer. Thus, the polycations have a significant effect on the bacterial cell and in many cases have stronger biocidal effect compared to the same low molecular weight (MW) cation. This reasoning is based on the fact that the adsorption of the polycations onto the negatively charged bacterial surface is expected to take place to a greater extent than that of monomeric cations.

It is still challenging to some extent to synthesize biologically active polymers. Some of the challenges are the actual physical and mechanical properties that are required for the intended application. Although chemically some synthesized and modified polymer could be a successful bioactive material, their actual use in certain biomedical application is not possible. As example, the use of a water-soluble material as a coating or in a solid substrate will not be acceptable.

2.3.2. Antimicrobial surface modification.

The synthesis of an antimicrobial surface is one of the prime goals to combat microbial colonization and prevent cross contamination in medical sectors.^{1,134} Recently, considerable research interest has been dedicated to the development of non-leaching, permanent, sterile-surface materials especially for surface coatings. Details on the design, development, and chemistry of various antimicrobial coatings are extensively reviewed^{12,135-139} In many cases, the approach is that one end of a long-chained hydrophobic polycation containing antimicrobial polymer is attached covalently to the surface of a material such as, cotton, glass

or plastic. Antimicrobial surfaces are widely used to prevent microbial infection in a wide range of industrial and medical settings.

There are different techniques to develop antibacterial surfaces. A useful approach is to permanently attach the active antimicrobial agents to the surface through covalent interactions.¹²⁸ For example, quaternary ammonium compounds (QACs) are widely used as biocides,⁷³ and were successfully applied as antimicrobial coatings on various substrates.¹³⁴ Early work by Isquith *et al.*¹⁴⁰⁻¹⁴² have utilized well known coupling agents such as alkoxy silanes to various substrates. They have described the immobilization of (3-trimethoxysilyl)propyl dimethyloctadecyl ammonium chloride after hydrolysis in aqueous solution to surfaces of a variety of substrates (Figure 2.5). The antimicrobial assessment showed that the immobilized groups were active against a wide range of microorganisms.

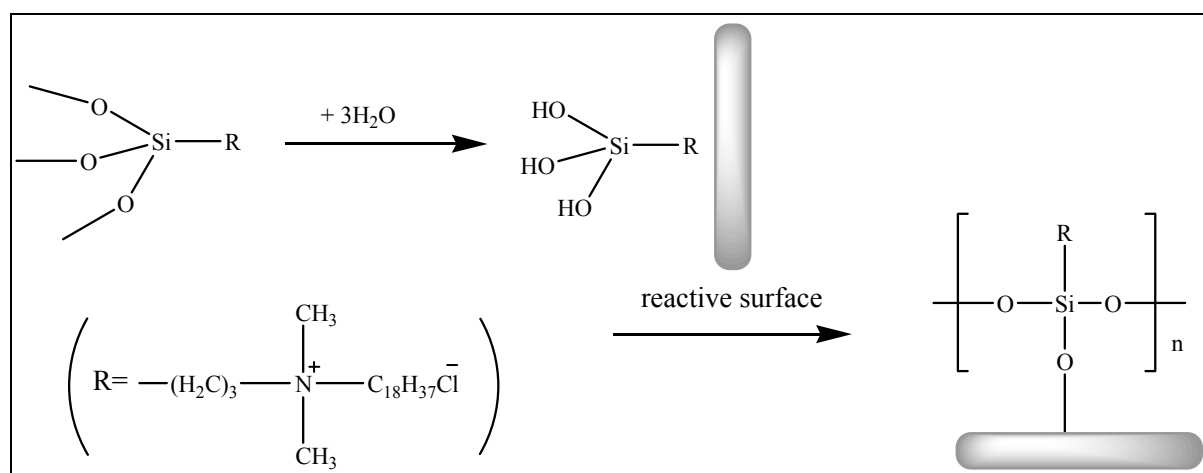


Figure 2.5: Immobilization of alkoxy silanes to reactive surface substrate.¹⁴⁰

Nakawaga *et al.*¹⁴³ have successfully attached QACs to porous glass beads by using 3-chloropropyltrimethoxysilane as a coupling agent. Porous glass beads were first covered with 3-chloropropyl-trimethoxysilane. Then, the immobilized chloropropyl moieties on the glass beads were quaternized with various N,N-dimethylalkylamines with alkyl groups $\text{C}_2\text{--C}_{18}$. Antibacterial activity of these surface treated glass beads were examined by passing bacterial cell suspensions through the column packed with the beads. Substrates that were not quaternized did not show much antibacterial activity. The results showed that the surface functionalized glass beads, with alkyl groups more than C_8 , exhibited high antibacterial activity compared to those of short alkyl group substituent.

Tiller *et al.* have described methods for successfully treating different material surfaces with partially quaternized poly(4-vinyl-pyridine). These materials included glass¹⁴⁴ and various polymer systems such as high-density polyethylene (HDPE), low-density polyethylene (LDPE), polypropylene (PP), nylon 6/6 and polyethylene terephthalate (PET).¹⁴⁵ The modified surfaces showed bactericidal activity against Gram-positive (*S. aureus* and *S. epidermidis*) and Gram-negative (*E. coli* and *P. aeruginosa*) species. Lin and co-workers¹⁴⁶ have developed a procedure for preparing a highly bactericidal and fungicidal polyolefin fabric/film, which involved a free-radical grafting of maleic anhydride on the surface followed by attachment of polyethylene amine and subsequent N-alkylation.

Another useful approach in developing antimicrobial surfaces is covalently attaching organic molecules capable of initiating polymerization from the surface of the material.^{147,148} Several researchers have investigated the utilization of controlled radical polymerization (CRP) techniques to confer biocidal action to various materials specifically by surface modification. For example, Lee *et al.*¹⁴⁹ have successfully prepared non-leaching antibacterial surfaces of glass and paper utilizing the CRP technique. The surface modification was applied via the polymerization of tertiary amine-containing monomer 2-(N,N-dimethylamino)ethyl methacrylate (DMAEMA) using the “grafting from” technique via atom transfer radical polymerization (ATRP). Subsequent quaternization of the amino groups of PDMAEMA brushes by an alkyl halide produces the biocidal functionality on the polymer-modified surfaces. In the study a Whatman #1 paper surface was modified by the immobilization of an ATRP initiator (2-bromoisobutyryl bromide) (Figure 2.6). The following step involved ATRP polymerization of DMAEMA, and finally quaternization of PDMAEMA brushes with different alkyl bromides.

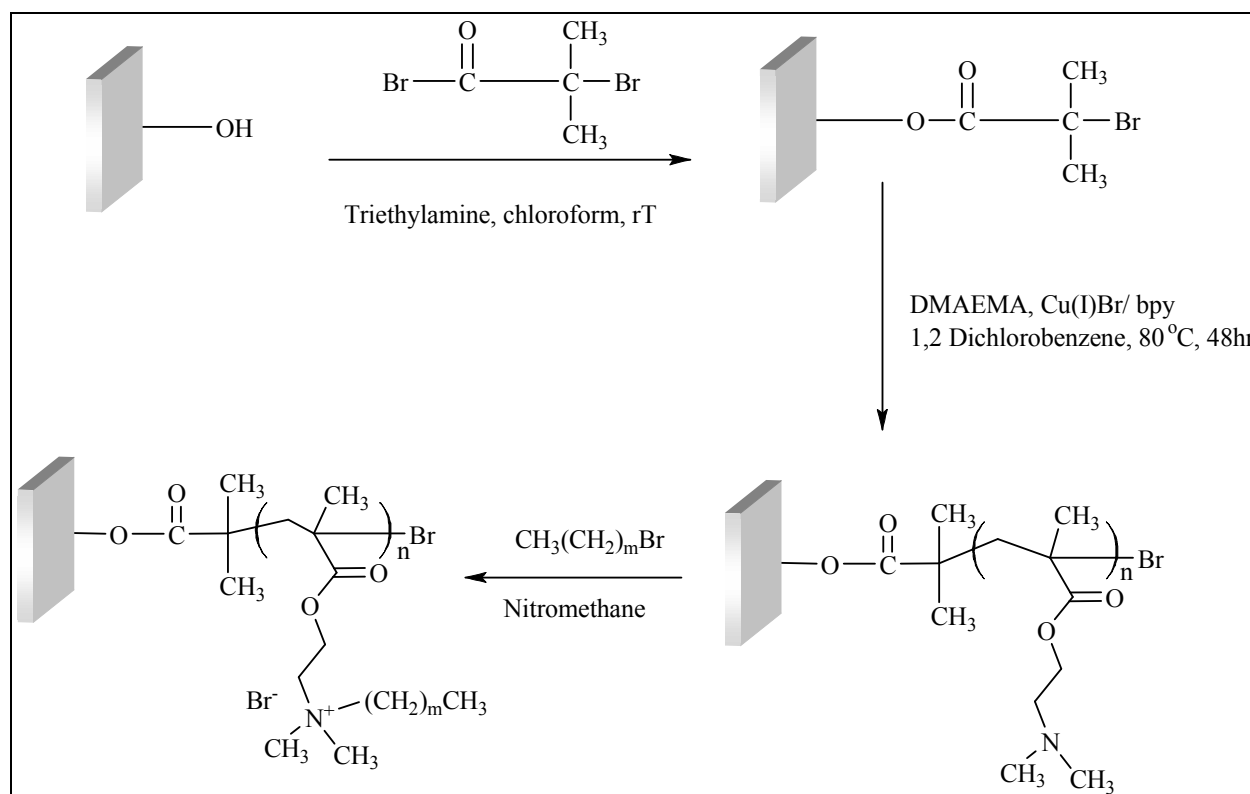


Figure 2.6: ATRP polymerization of DMEAMA from glass or paper surfaces.¹⁴⁹

The modified surfaces were active against *E. coli* and *Bacillus subtilis*. Murata *et al.*¹⁵⁰ have further investigated the effect of charge density on the biocidal efficiency using the same polymerization technique to synthesize antimicrobial paper and glass surfaces. A modified ATRP initiator 3-(2-bromoisobutyryl)-aminopropyltrimethoxysilane or 3-(2-bromoisobutyryl)-propyltrimethoxysilane was prepared and immobilized on glass slides and paper. This was followed by polymerization from the surface and subsequent quaternization. The modification and immobilization steps are shown in Figure 2.7. The modified surfaces exhibited substantial antimicrobial activity against *E. coli* and *B. subtilis*. Antibacterial activity was independent on polymer chain length. The important criterion for antibacterial activity appeared to be the available surface charge density of the quaternized PDMAEMA brushes.

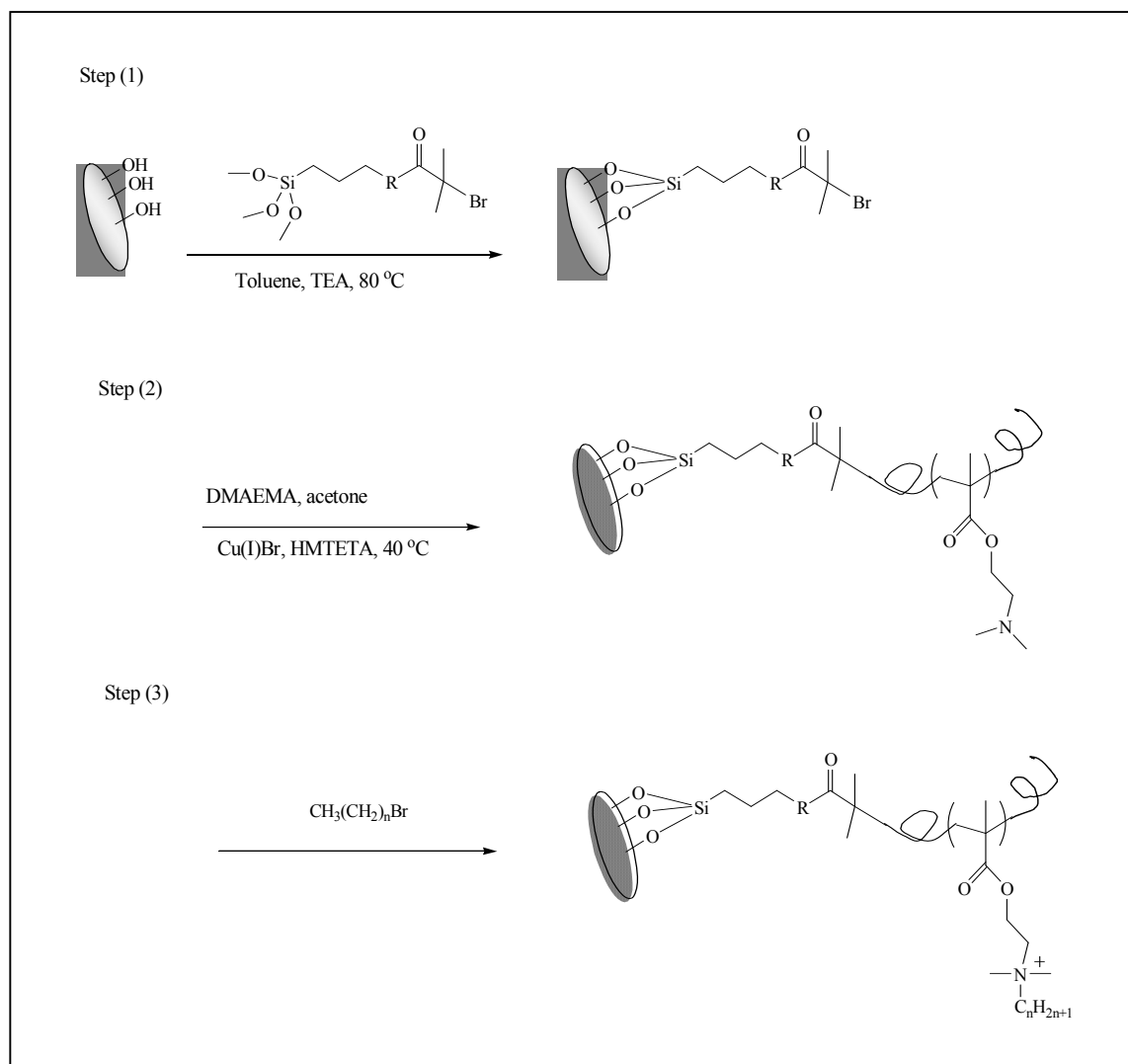


Figure 2.7: Modification of ATRP initiator followed by surface immobilization, polymerization, and quaternization of PDMEAMA on glass or paper with available hydroxyl groups.¹⁵⁰

Xu *et al.*¹⁵¹ have also utilized the “grafting from” method to modify a silicon-based surface via the ATRP technique. The silicon surfaces were modified by UV-induced reaction of 4-vinyl benzyl chloride (VBC) followed by grafting of PDMAEMA via ATRP and subsequently quaternization by an alkyl halide or viologen to induce the biocidal functionality (Figure 2.8). Viologen quaternized surfaces exhibited enhanced antibacterial properties over those of the alkyl halide quaternized PDMAEMA~Si surfaces, and effectively inhibited *Pseudomonas* growth and biofilm formation on these surfaces.

A more recent study by Huang *et al.*¹⁵² described the preparation of an antimicrobial glass surface by combining ATRP technique for the preparation of block copolymers consisting of

Chapter 2: Literature Review

a poly(DMAEMA) functional segment and a poly(3-(trimethoxysilyl)propyl methacrylate) (PTMSPMA) anchoring segment. The surface modification was performed using the “grafting onto” technique via the reaction between the anchoring trimethoxysilyl groups in the copolymers and silanol groups from the surface. Subsequent quaternization of the PDMAEMA segments in the copolymers was utilized to induce antimicrobial properties.

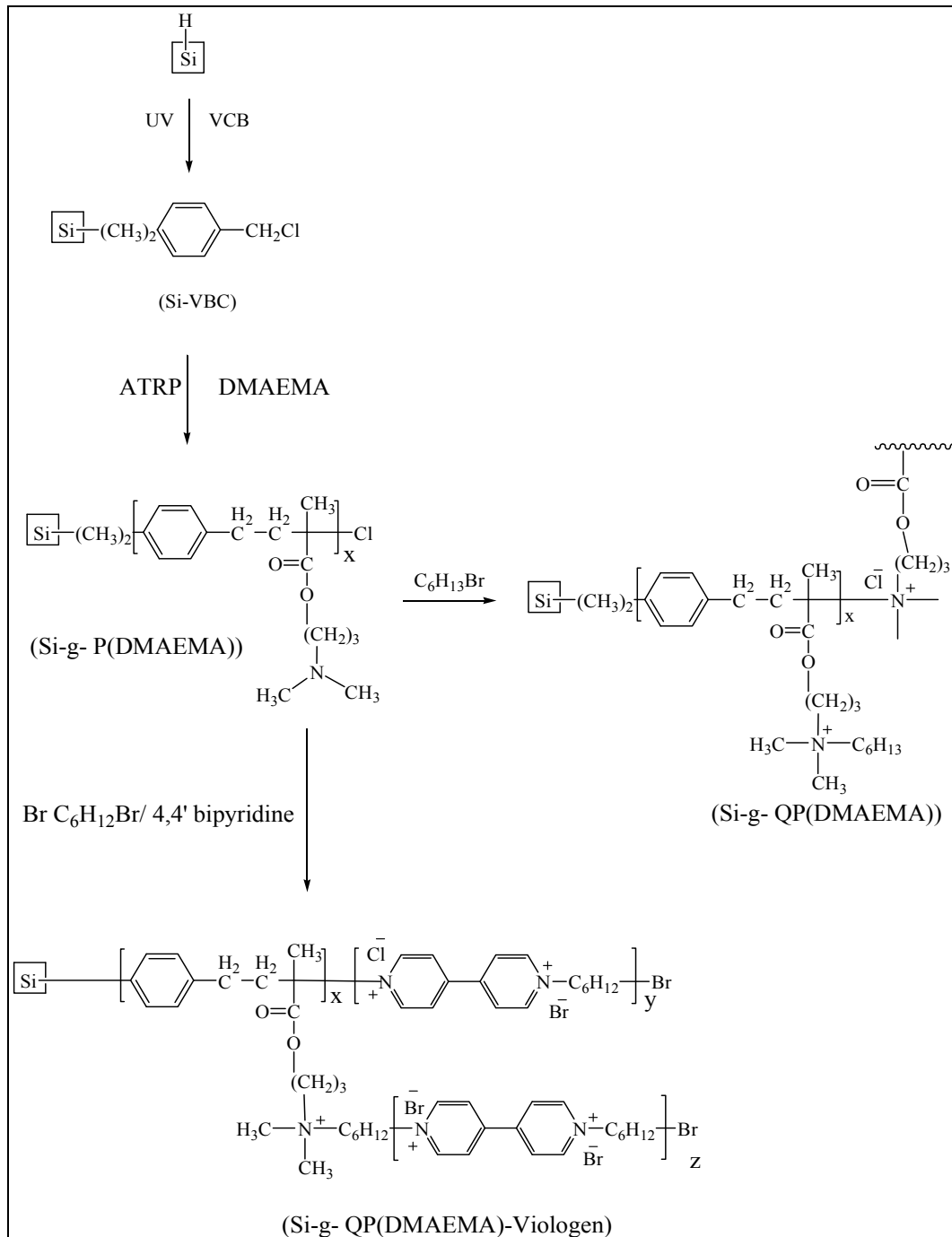


Figure 2. 8: Modification of silicon-based surface¹⁵²

2.3.2. Synthesis and activity of antimicrobial polymers.

It is rational to first consider an already known antimicrobial agent that can be chemically modified into a polymerizable derivative and still retains the bioactive functional groups after polymerization. Alternatively, the modification can be done on a preformed polymer bearing reactive moieties. In this way, the polymer backbone or its pendent groups are carrying functional moieties that can be chemically modified by linking a complementary reactive antimicrobial agent bearing e.g. hydroxyl, carboxyl, or amino groups.

Benzalkonium chloride derivatives, as mentioned earlier, possess a broad spectrum antimicrobial activity. Since the cationic character is mainly produced from the quaternized group, styrene derivatives are ideal to transform the small cation molecule into a polycation. In fact, (3- and 4-)chloromethylstyrene have been used for the synthesis of QAC by free radical polymerization of the monomer followed by a quaternization reaction with dialkyl amines. Ikeda *et al.*¹⁵³ have prepared various poly(trialkyl-3-vinylbenzylammonium chloride)s and poly(trialkyl-4-vinylbenzylammonium chloride)s (Figure 2.9). The antimicrobial activity of these water-soluble polymers was assessed against different Gram-negative and Gram-positive bacteria. The quaternized polymer with the longest alkyl halide C₁₆ (hexadecyl) was found to exhibit the highest activity in general, and being more active against Gram-positive bacteria, such as *B. subtilis* and *S. aureus*, than Gram-negative species (*E. coli*, *Aerobacter aerogenes* and *P. aeruginosa*).

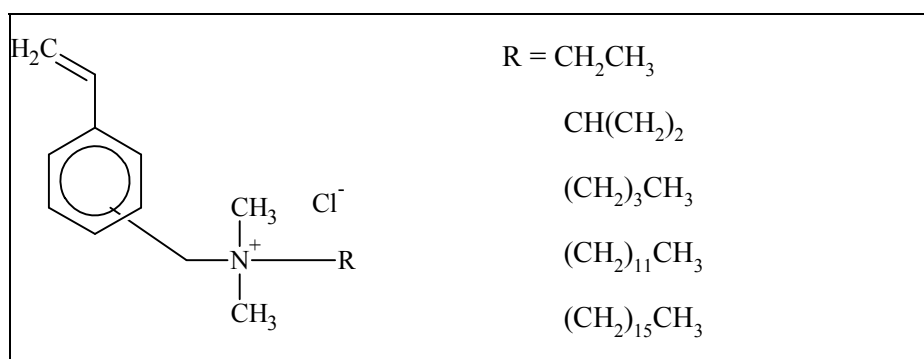


Figure 2.9: Poly (trialkyl-3-(and 4-)vinylbenzylammonium chlorides).

Polymers with biguanides are also interesting candidates. As example, polyhexamethylene biguanide was demonstrated to have antibacterial and antifungal properties and is used widely as contact lens disinfectant.^{154,155} The growth inhibition and bactericidal activity of

some polyhexamethylene biguanides are molecular weight dependent.¹⁵⁶ For example Broxton *et al.*¹⁵⁷ showed that the growth inhibition effect on *E. coli* in liquid culture increased with increasing chain length.

Acrylic and methacrylic monomers bearing biguanides have also been successfully prepared (Figure 2.10).^{156,158} The monomers with biguanides side groups were polymerized and copolymerized with other monomers such as acrylamide. The biguanide polymers showed very good antibacterial activity especially against Gram-positive bacteria, e.g. *S. aureus*. Antimicrobial studies have shown that the activity was dependent on the molecular weight, where the optimal activity was seen between 5×10^4 and 1.2×10^5 Da.

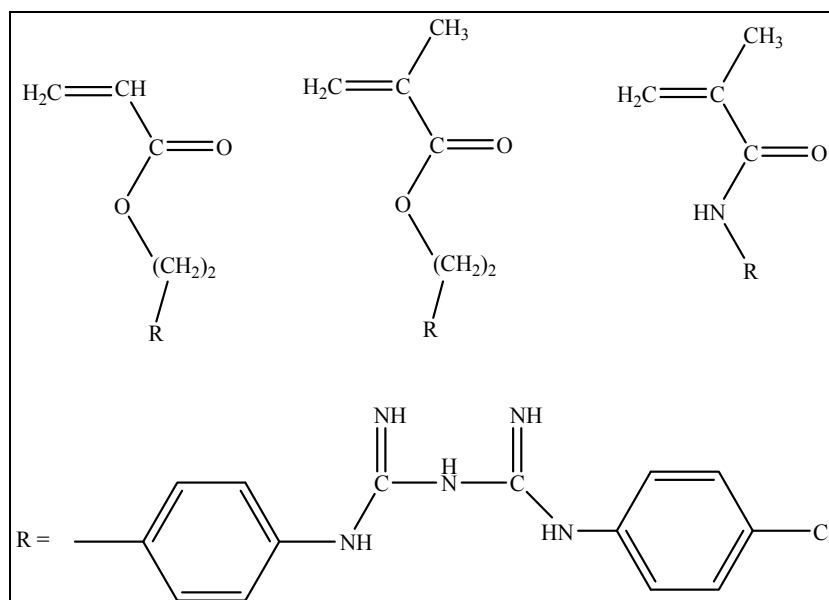


Figure 2.10: Acrylic and methacrylic biguanide monomers.

The role of polymer molecular weight on the antimicrobial activity was found to be critical in other polymer systems as well, such as that described by Kanazawa and co-workers.^{159,160} They investigated the molecular weight dependence of poly(tributyl 4-vinylbenzyl phosphonium chloride) (Figure 2.11) against *S. aureus* and revealed that the antibacterial properties increased with increase in molecular weight from 1.6×10^4 to 9.4×10^4 Da.

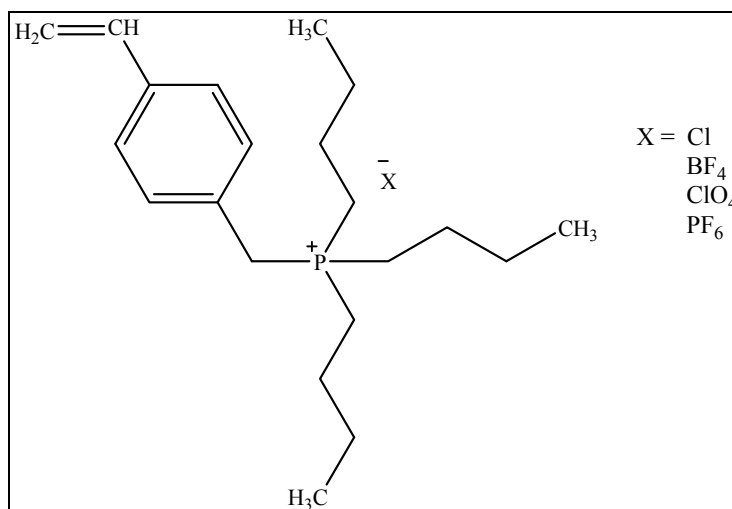


Figure 2.11: (Tributyl 4-vinylbenzyl)phosphonium salt monomer.

Many other antimicrobial polymers have been synthesized and their bioactivity investigated. A (2001) review on antibacterial macromolecules by Tashiro¹⁶¹ focused mainly on biocidal cationic polymers containing functional groups such as biguanide, quaternary ammonium salts, quaternary pyridinium salts, and phosphonium salts. A more recent review by Kenawy *et al.* (2007) discussed the chemistry and applications of a wide range of antimicrobial polymers.¹⁶² A 2010 review by Timofeeva and Kleshcheva¹³² have highlighted and summarized the results of various studies in the past decade that concern the mechanism of action of different antimicrobial polymers, and factors influencing their activity, and as well as major applications of antimicrobial polymers. Many of the demonstrated antimicrobial systems were based on macromolecules carrying a positive charge (e.g. quaternized phosphonium and ammonium compounds) and other systems that contained biocidal moieties as pendent groups. Some of the polymer systems will be addressed in the next section on antimicrobial polymer fibers.

A comprehensive 2010 review by Jaeger *et al.*¹⁶³ discussed the synthetic routes and chemistry of various charged polymer systems that are bearing quaternary ammonium moieties. Numerous examples have been addressed, some of which have been reported elsewhere as an active bactericide or fungicide.

Other quaternized polymer systems that have not yet been investigated for antimicrobial properties include (styrene/acrylamide)-*N,N*-dimethylmaleimidopropyl ammoniopropane sulfonate (ADMMAPS)^{164,165} copolymer and poly(methyl iodide quaternized (acrylamide)-*N,N*-dimethylaminopropyl maleimide) copolymer [poly(MIQADMAMP)]¹⁶⁶ (Figure 2.12).

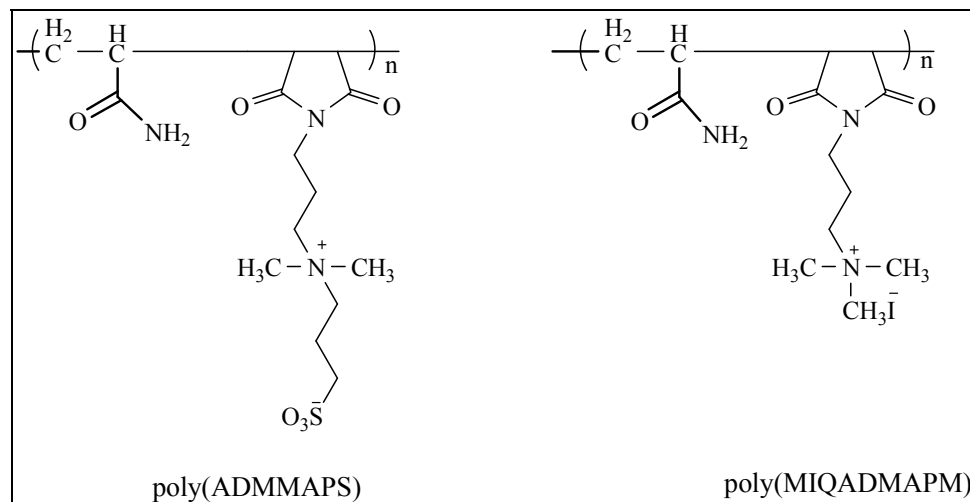


Figure 2.12: Copolymers of acrylamide and maleimide derivatives.^{165, 166}

2.4. Antimicrobial polymer fibers

Polymeric nanofibers can be produced by electrospinning. Electrospinning is a simple and cost effective process to prepare polymeric nanofibers.¹⁶⁷ It uses an electrical field to draw a polymer solution from the tip of a capillary to a collector, during which a high voltage is applied to the polymer solution.¹⁶⁸ This causes a polymer jet to be drawn towards a grounded collector. By choosing a suitable polymer and solvent system, nanofibers with diameters ranging from tens of nanometers to a few microns can be obtained.¹⁶⁹ One apparent advantage of nanofibers is the huge increase in the surface area to volume and mass ratio compared to larger fiber dimensions, (see Figure 2.13 for an example), which enables such nanofibrous scaffolds to have many biomedical and industrial applications.

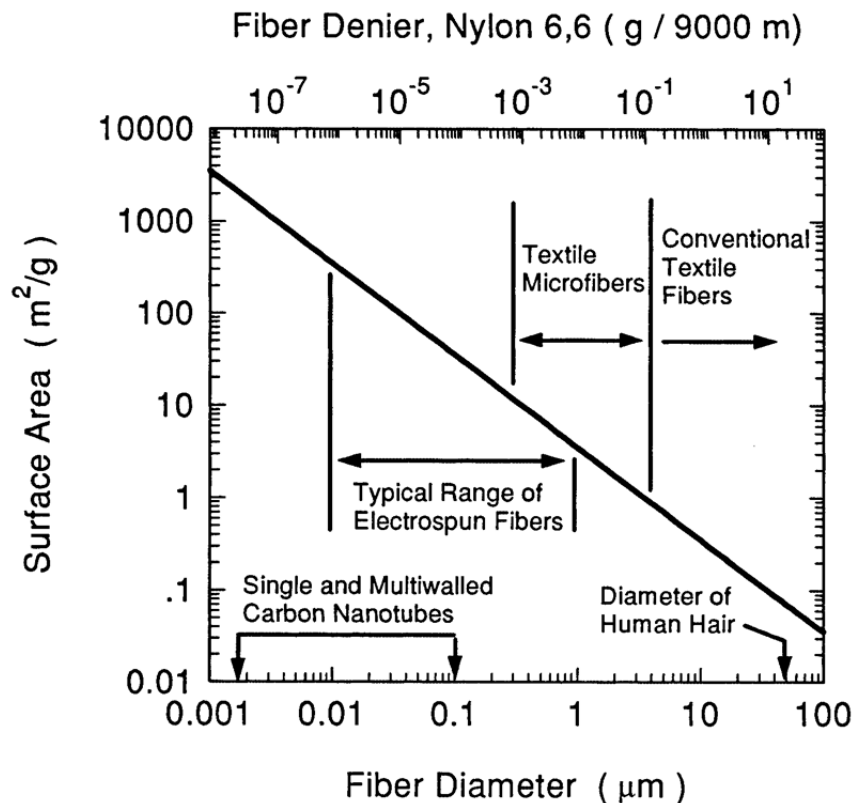


Figure 2.13: Nano sized fiber diameters have higher surface areas compared with textile fibers. Reprinted from reference.¹⁷⁰

However, there are many process parameters that influence the ability of a polymer to form fibers by electrospinning. Solution properties, process conditions (operational parameters) and ambient conditions are all variables that affects the electrospinning process and hence fiber morphology.¹⁷¹ For example suitable solution viscosity and high enough polymer molecular weight are among the critical solution properties for successful electrospinning to occur.^{172,173} Detailed description on the electrospinning technique and factors influencing the process is described in literature^{167,171,174}.

To date, a large number of polymers have been successfully electrospun, which found applications in industrial, consumer and defense filtrations for more than twenty years. Numerous of electrospun polymers and their electrospinning conditions, applications in various fields have been listed and discussed in comprehensive reviews by Huang *et al.*¹⁷⁵, Greiner *et al.*¹⁷⁶ and Agarwal *et al.*^{177,178}

With the increased academic research on the fabrication of various polymer systems into nanofibers, significant progress has been achieved in different fields such as protective textiles,^{170,179-181} advanced composites,¹⁸²⁻¹⁸⁶ high performance filters,^{187,188} sensors,¹⁸⁹⁻¹⁹¹

Chapter 2: Literature Review

photovoltaic cells,¹⁹² wound dressing¹⁹³⁻¹⁹⁷, drug delivery,^{198,199} and as scaffolds in tissue engineering.²⁰⁰⁻²⁰⁷ However, very limited studies have been published on fabrication of nanofibers having inherent or permanent antimicrobial properties, yet the research in this area is growing rapidly, where the development of new antimicrobial materials is of continuous interest.

For example, Acatay *et al.*²⁰⁸ have prepared a bioactive quaternary ammonium salt (QAS) containing monomer (vinylbenzyl-dimethylcocoammonium chlorides) (VBDCC). The quaternary monomer was then subsequently copolymerized in different molar ratios (0%, 1%, 5%, 10%, 25%) with MMA and perfluoro alkyl ethyl acrylate (PFAEA) via conventional free radical polymerization reaction (Figure 2.14). The copolymers were successfully electrospun to nanofibers and evaluated for antibacterial activity against *E. coli*.

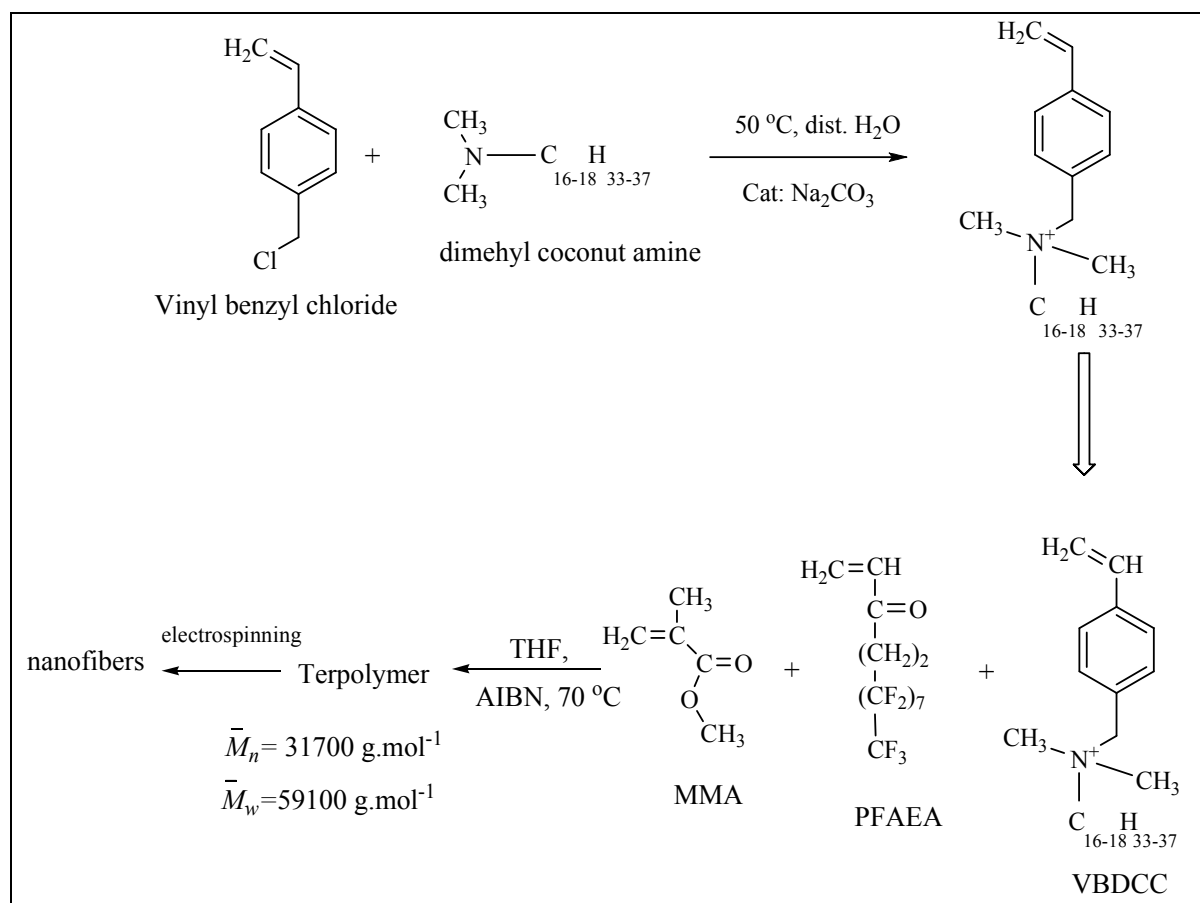


Figure 2.14.: Synthesis of VBDCC and subsequent copolymerization with PFAEA and MMA.²⁰⁸

Kenaway *et al.*²⁰⁹ prepared sulfonated derivatives of ($\bar{M}_w = 20k$ and $100k$) polyvinyl phenol (Figure 2.15), the polymeric materials were electrospun into microfiber mats. The prepared derivatives were evaluated for antimicrobial activity in both powder and fiber forms against a range of organisms including Gram-negative (*E. coli* and *Salmonella choleraesuis*), as well as Gram-positive (*B. subtilis* and *S. aureus*) species. It was also tested for fungicidal activity against *Aspergillus niger*, *T. rubrum* and *Candida albicans*.

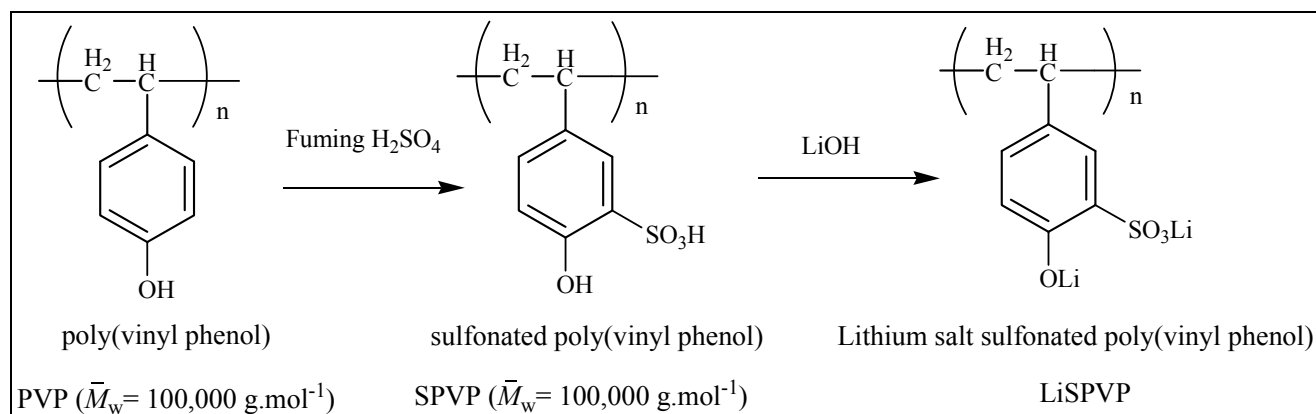


Figure 2.15: Preparation of PVP sulfonated derivatives.

All electrospun fibers showed good antimicrobial activity. Sulfonated poly(vinyl phenol) (SPVP) (100K) at a concentration of 2.5 mg/ml was able to kill *B. subtilis*, *S. choleraesuis*, *S. aureus* and *E. coli*. The lithium salt-based fibers (LiSPVP) killed 100% of *B. subtilis*, *S. choleraesuis* and *C. albicans* within 12 hours, whereas at the same concentration only killed 50% of *A.niger*. An increase in concentration, or incubation time, only slightly elevated the antimicrobial effect. Interaction of the sulfonated or lithium salt of the SPVP with the cell wall of organisms was suggested as a mode of action of these polymers, which will lead the disruption of the membrane and cell death. It was also shown that poly vinyl phenol (20k) fibers were active against *B. subtilis*, whereas no effect was observed for the same polymer in its powder form. They concluded that the small fiber diameter ($4.33 \mu\text{m}$) and an increased surface area will increase the contact between the polymer and organism.

Recent development in polymer synthesis techniques such as controlled radical polymerization (CRP) and Click Chemistry provides a feasible approach to prepare well-defined macromolecules with various functionalities.²¹⁰ This allowed for the design of various polymeric materials by synthesizing smart block and graft copolymers from two or

more different monomers. Many researchers have been utilizing CRP techniques to synthesize antimicrobial polymers and subsequent fabrication of nanofibers by electrospinning.

Guo-Dong *et al.*²¹¹ prepared solvent-resistant antibacterial microfibers of self-quaternized block copolymers via combined ATRP and electrospinning. Diblock copolymers with one block of poly[[(2-dimethylamino)ethyl methacrylate)-co-(glycidyl methacrylate)] P(DMAEMA-*c*-GMA) and another of poly(pentachlorophenyl acrylate) (PPCPA) (P(DMAEMA-*c*-GMA)-*b*-PPCPA) were successfully synthesized. (Figure 2.16). The antimicrobial properties of these electrospun cross-linked microfibers were investigated against bacterial cultures in a 200 ml flask (containing 10^5 cells mL^{-1}) *S. aureus* or *E. coli*. The antibacterial assay showed that 95% *E. coli* and 97% *S. aureus* were killed after being treated with about 50 mg P(DMAEMA-*c*-GMA)-*b*-PPCPA microfibers in 10 min.

Chapter 2: Literature Review

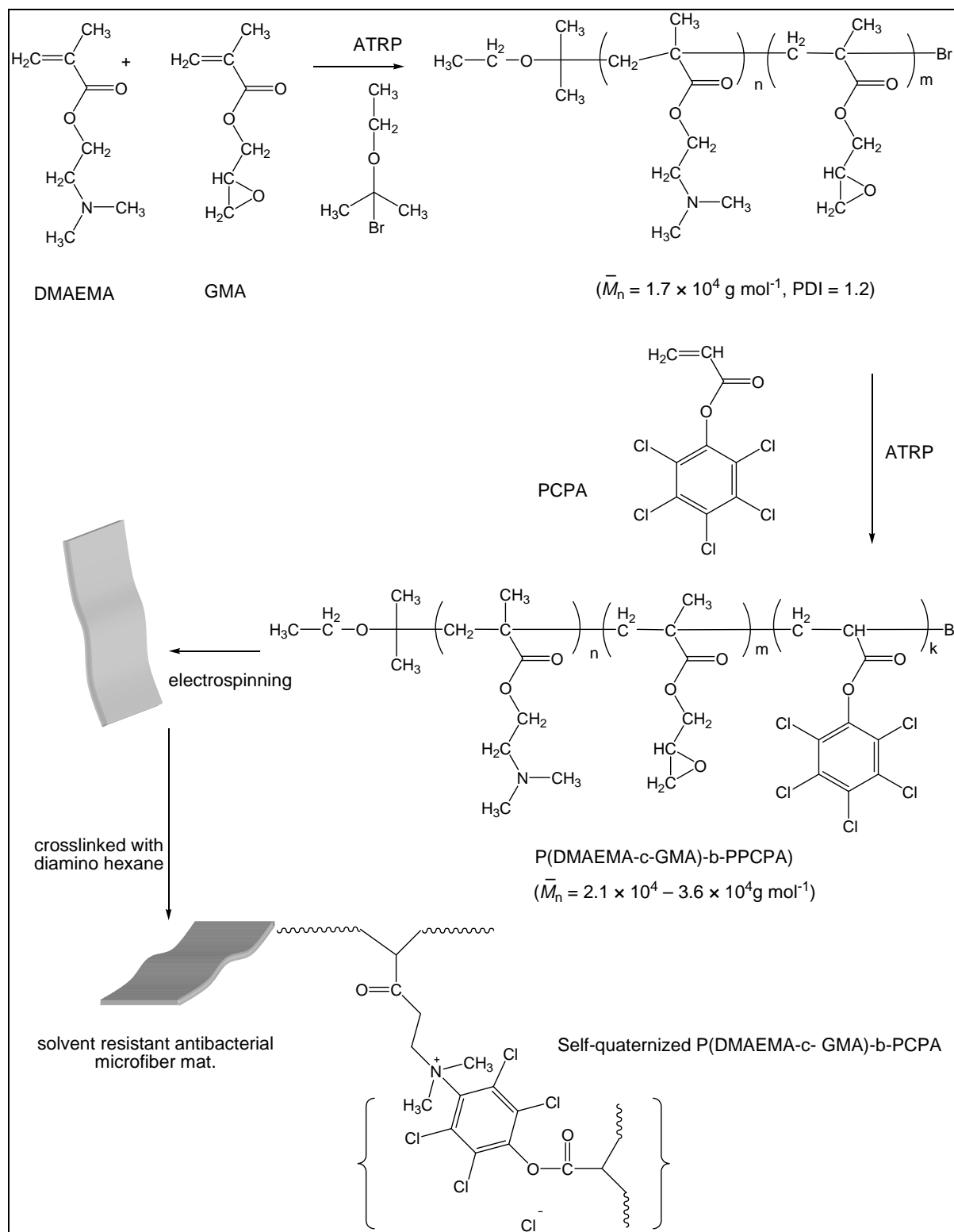


Figure 2.16: Schematic shows preparation of P(DMAEMA-c-GMA)-b-PPCPA microfibers via ATRP and electrospinning.²¹¹

In a similar study Qun *et al.*²¹² reported the synthesis of block copolymers of 4-vinyl pyridine (4VP) and pentachlorophenyl acrylate (PCPA) via reversible addition fragmentation transfer (RAFT) polymerization technique (Figure 2.17). The block copolymer was then electrospun into nanofibers. The QASs were generated by N-alkylation of the pyridine groups of P4VP block and chloro-aromatic compounds of PPCPA block, which the authors referred to as self-quaternization of P(4VP-b-PCPA). The nanofibers were subjected to antibacterial assays against *S. aureus* and *E. coli*. The results showed that the self-quaternized nanofibers exhibited high antibacterial efficiency, whereby 99.6% of *E. coli* and 99.1% *S. aureus* were killed after being in contact with 50 mg of nanofibers in a suspension of 10^5 cells mL⁻¹ for 10 min.

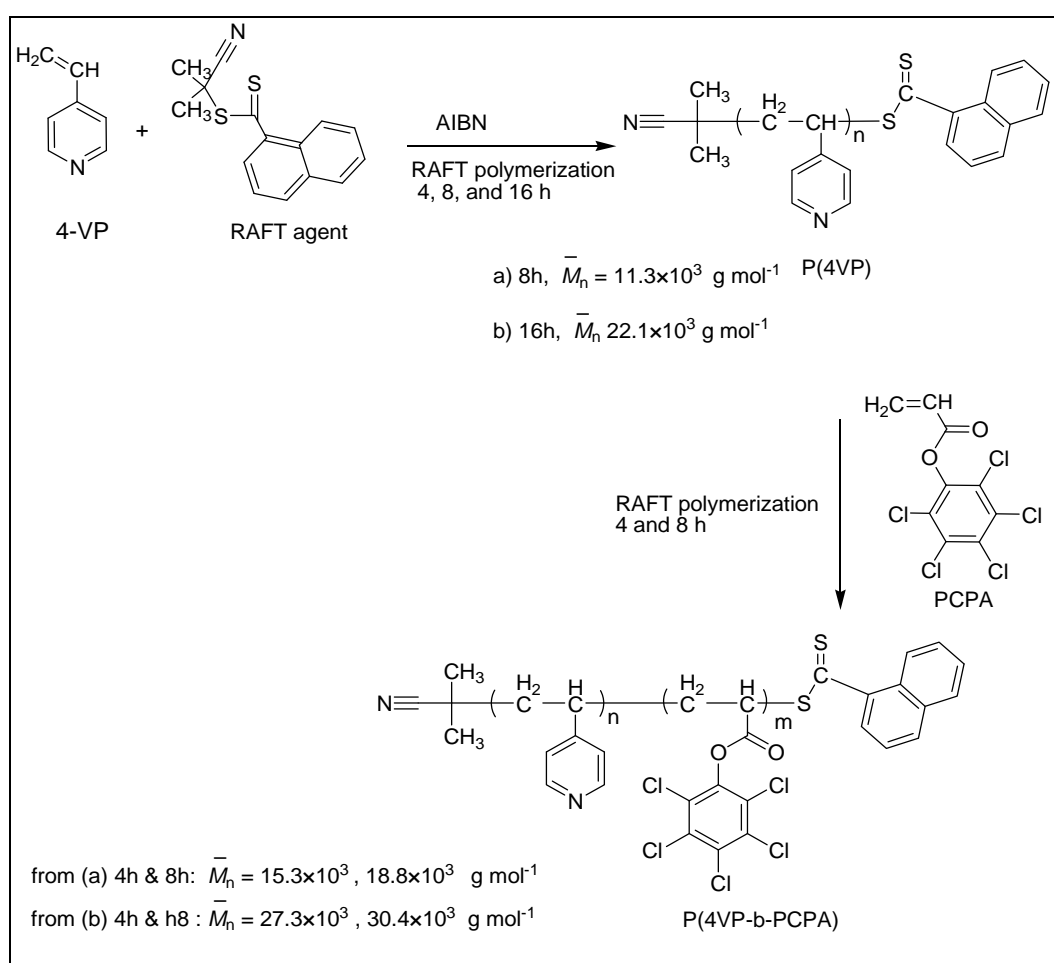


Figure 2.17: Preparation of P4VP-b-PPCPA via RAFT polymerization.²¹²

2.5. Potential candidates for non-leaching antimicrobial nanofibers

There are several antimicrobial systems that have been successfully prepared as mentioned in the previous sections. The challenge though, is to successfully produce nanofibers from these antimicrobial polymeric systems. Very few of the synthesized antimicrobial polymers have yet been explored for their ability to be electrospun. Some of the materials might not be suitable because of solubility and stability issues, because water-soluble fibers are not desirable and cannot be used in applications such as air and water filtration or water purification systems.

Many antimicrobial polymers bearing QASs are water soluble, for example. They show very good bactericidal and fungicidal activity, however these materials are not suitable as fibers and cannot be used in important applications such as air and water purification systems. Nevertheless, macromolecular design can be utilized to overcome this problem. For instance, the introduction of a hydrophobic monomer via copolymerization is one of the very useful methods for the modification of polymer properties.

Physical and chemical crosslinking is another very useful approach to transform a soluble fiber mat into a stable and insoluble one. Antimicrobial polymers with biocides and/or with iodine-polymer complexes have been used in conjunction with crosslinkable water soluble polymers.²¹³ For example, Ignatova et al.²¹⁴ determined that the minimum inhibitory concentration (MIC) of a quaternized chitosan derivative (QCh) was 169 µg/ml and 2.070 mg/ml against *S.aureus* and *E.coli*, respectively. Aqueous solutions of quaternized chitosan derivative and poly(vinyl pyrrolidone) (PVP) was electrospun into fibers and crosslinked via UV irradiation. Crosslinked QCh/PVP fibers, containing 3 mg/ml QCh, were exposed to either 10^5 cells mL⁻¹ *S. aureus* or *E. coli* cells. The fibers were able to kill the majority of *S. aureus* cells within 30 min and after 1 hour all cells were killed. These fibers showed less reduction of *E.coli* numbers within 30 min, however, most of the cells were killed within 120 min. In another study conducted by Ignatova et al.²¹⁵ it was shown that the MIC for a PVP-iodine complex was 380 µg/ml, 840 µg/ml and 424 µg/ml against *S. aureus*, *E. coli* and *C. albicans*, respectively. Electrospun mats, containing 840 µg/ml available iodine, killed *S.aureus* cells within 30 min after contact. The same fibers were also able to kill 99.8% of *E. coli* and 98% *C. albicans* cells in 90 min and 60 min, respectively.

There are some insoluble polymers that acquired good antimicrobial reputation such as poly[2-(tert-butylamino)ethyl methacrylate (PTBAEMA) which belongs to a class of water insoluble biocides,²¹⁶⁻²¹⁸ this polymer is a useful candidate and could be copolymerized with other monomers. However, to the best of our knowledge at the time of this survey, no attempts on electrospinning PTBAEA were reported.

One of the most interesting polymer systems that can easily be modified, consists of polymeric materials containing anhydride units in or attached to the backbone. Maleic anhydride is a very well known compound in this respect and extensively applied in various polymer systems as an efficient compatibilizer in polymer blends, and for surface functionalization of polyolefins. In addition, although maleic anhydride does not homopolymerize, it is readily copolymerized with various methacrylic and styrenic monomers to produce copolymers with interesting properties. Poly(styrene-*co*-maleic anhydride) (PSMA) for example can easily be prepared and has found significant interest in a variety of applications. PSMA can easily be chemically modified with hydroxyl and primary amine compounds. In fact, the reaction between the anhydride units and a primary amine is known to be very rapid and quite straight forward. The advantage of having these reactive moieties makes them attractive candidates for the design and synthesis of bioactive compounds.

Maleic anhydride copolymers proved to have good binding capability even to biological molecules such as nucleic acids and proteins.²¹⁹⁻²²¹

Petal and co-workers have prepared bioactive copolymers containing anhydride functionalities as drug carriers, whereby an antiseptic agent Acriflavine (3,6-diamino-10-methylacridinium) was covalently bound on the surface of poly[styrene (S)-*co*-(maleic anhydride) (MAnh)]²²² and poly (methyl methacrylate-*co*-MAnh)²²³(Figure 2.18). The controlled release of the Acriflavine in weak base was evaluated by antibacterial assessment of the released drug against *B. subtilis*. The same group has also described the synthesis of a macromolecular prodrug of Ampicillin bound to the anhydride groups of a matrix of PSMA via an amide bond.²²⁴ The release profiles of Ampicillin with different percentage of MAnh in the polymeric carrier were obtained using *E. coli*, *B. subtilis* and *S. aureus*, and found that the rate of drug release could be controlled by the fraction of incorporated anhydride moieties in the copolymer.

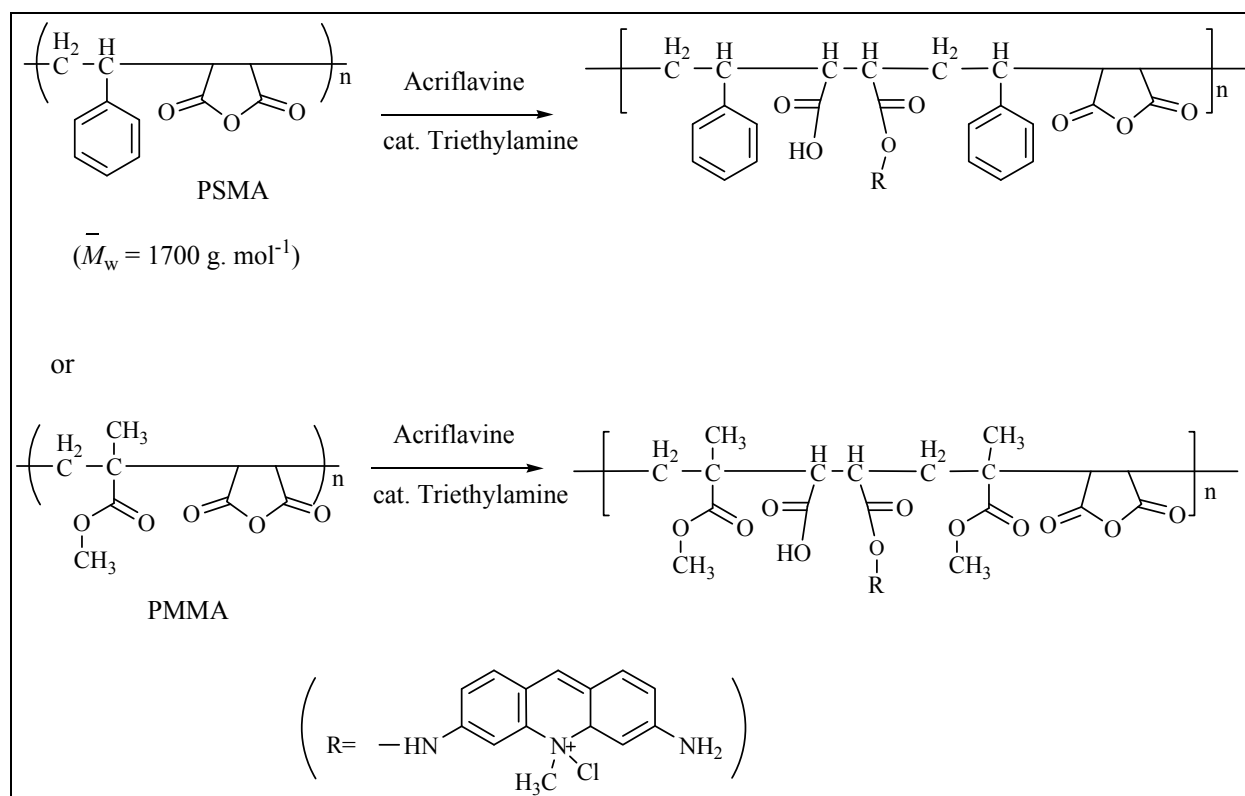


Figure 2. 18: Anchoring Acriflavine to PSMA and PMMA.

Obviously the goal in the previous example was not to prepare a non-leaching antibacterial polymer, but it illustrates the modification feasibility with these polymer systems in the drug delivery field.

Jeong *et al.* have described PSMA modifications with antimicrobial agents such as 4-aminobenzoic acid (ABA) 4-hydroxybenzoic acid (HBA) and 4-aminophenol^{225,226} (Figure 2.19). The coupling reactions were efficient for all modification reactions. The modified polymers were then examined against *E. coli* and *S. aureus*. (1.0 mL) of each of the modified polymers in DMF (10 wt%) was added to a culture suspension (5×10^{-3} cells mL⁻¹) in a phosphate buffered solution (PBS). the results showed that the HBA-modified derivative had excellent activity against *E. coli* with 100% reduction in 24 hours compared to a low 44.6% reduction for ABA-modified PSMA. The activity against *S. aureus* showed 99.99% reduction for ABA-modified PSMA and 95.16% reduction in the case of HBA-modified PSMA.

On the other hand, the aminophenol based conjugate showed strong antibacterial activity against both *E. coli* 99.5% reduction and 99.9% reduction with *S. aureus*. From these findings, it was shown that different antimicrobial agents can be readily anchored to the anhydride moieties in the form of amide and ester bonds. Although these modified antimicrobial polymers have good biocidal activity, they are not suitable as antimicrobial nanofibers because of water solubility. Furthermore, potential leaching of the active groups cannot be avoided in basic media.

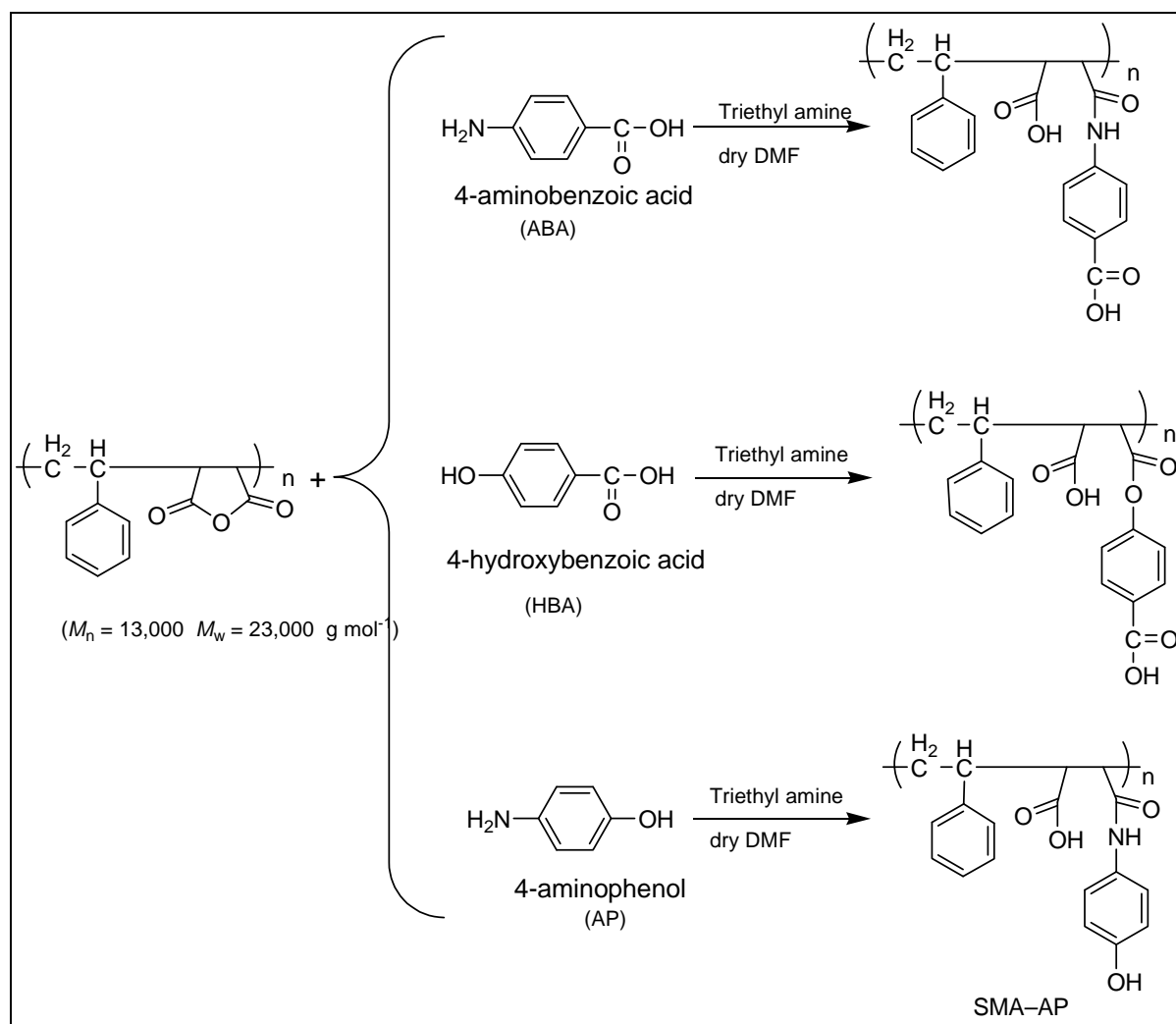


Figure 2. 19: PSMA modification with aromatic functionalized biocides.

Recently, Ignatova *et al.*²²⁷ were the first to attach known antimicrobial agents onto electrospun PSMA (7 wt% MAnh) microfiber mats. Three different types of AM agents were used in the study, i.e 5-amino-8-hydroxyquinoline, chlorhexidine (CHX) and poly(propylene glycol) monoamine (Jeffamine M-600). Each of those compounds was covalently attached

Chapter 2: Literature Review

via the anhydride groups present on the surface of PSMA fibers (Figure 2.20). The M-600 grafted mat was further treated to form a iodine-complex-containing mat. All modified and unmodified fiber mats were assessed for antibacterial activity against the bacteria (*S. aureus* or *E. coli*) or fungi (*C. albicans*) cell suspension (5 mL containing about 10^5 cells mL⁻¹).

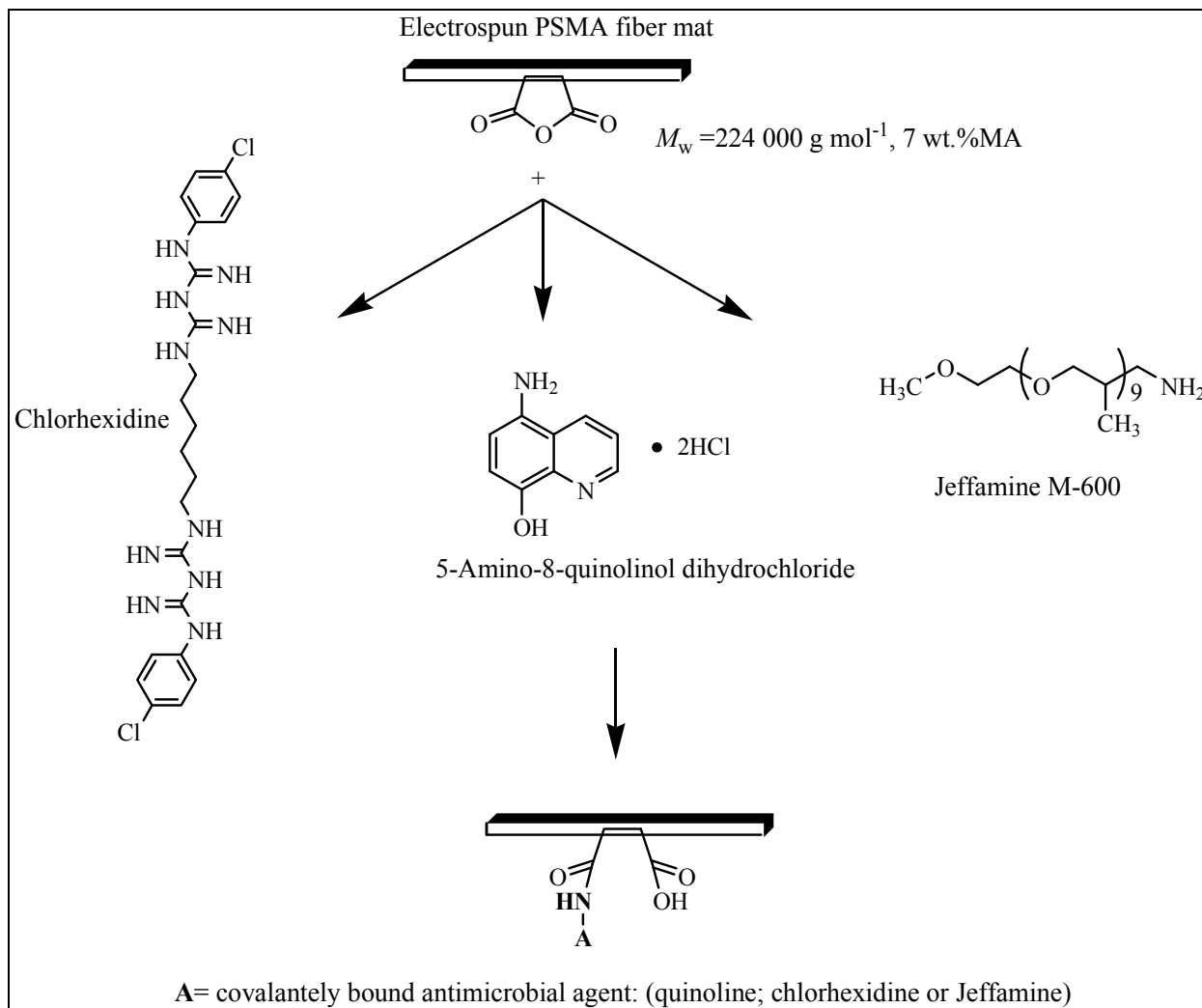


Figure 2.20: Attachment of antimicrobial agents to PSMA fiber mats.

All modified mats were active against the tested microorganisms. In general the complex bound iodine (treated with iodine solution) grafted Jeffamine mats and (CHX)-modified mats showed the strongest biocidal and fungicidal activity. For example, the CHX-modified mats had the fastest killing rate, as it killed all *S. aureus* cells in 30 min, and *E. coli* in 120 min. In addition the fibers killed all *C. albicans* cells after 30 minutes contact.

However, no stability assessments on the modified mats were reported, which would have added important information on the durability and the end use application of these modified mats.

There are many factors that need to be considered when designing a new antimicrobial polymer, some of which have been mentioned earlier. It is illustrated in the previous sections that many antimicrobial polymers have been successfully prepared. In the vast majority of these materials, the bioactive compound can be attached or immobilized by different methods to the polymer backbone. Thus, in principle, potential adjustments and modifications of polymeric materials are possible. Current macromolecular design of novel antimicrobial polymers can be inspired by a combination of factors. These include reported antimicrobial polymers that have been successfully prepared, such as polymers containing quaternized and unquaternized amino compounds. Furthermore, practicality and the simplicity of both chemical and physical adjustments are amongst important factors to prepare inexpensive biocidal and applicable antimicrobial polymers.

Polymers that contain secondary or tertiary amine moieties have been reported to have good antibacterial properties. According to our present understanding, there is very limited information on antimicrobial polymers bearing tertiary amine moieties. In 1987, Endo *et al.*²²⁸ were the first to investigate antimicrobial activity of an insoluble tertiary amino polymer compound. The study was carried out on polystyrene–tertiary amine bonded fibers (Figure 2.21) and evaluated against Gram-positive (*S. aureus* and *Streptococcus faecalis*) and Gram-negative (*E. coli*; *P. aeruginosa*; *Klebsiella pneumonia*; *S. typhimurium* and *Serratia marcescens*). The fibers were also examined for antifungal activity against *Candida albicans*.

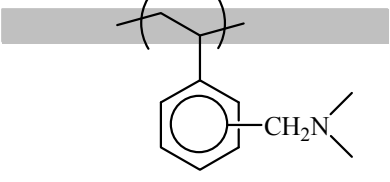
	Microorganism(s)	Viability (%) after 1 h contact
0.25g dry fiber samples used for the assay bacterial suspensions were used at 10^6 CFU/mL	Gram-negative bacteria	
	<i>E. coli</i>	0.007
	<i>P. aeruginosa</i>	0.0017
	<i>K. pneumoniae</i>	0.42
	<i>Salmonella typhimurium</i>	1.2
	<i>Serratia marcescens</i>	0.018
	Gram-positive bacteria	
	<i>Staphylococcus aureus</i>	20
	<i>Streptococcus faecalis</i>	6.3
	<i>C. albicans</i>	48

Figure 2.21: Polystyrene–Tertiary amine bonded fibers.

Fiber samples (0.25g dry) were treated with bacterial suspensions containing 10^6 CFU/mL. The antimicrobial evaluation revealed that the fibers exhibited stronger bactericidal activity against Gram-negative bacteria than Gram-positive bacteria see (Fig. 21).

A similar study by Gelman *et al.*²²⁹ was focused on the biocidal activity of poly((4-dimethylaminoethyl)-styrene) and its quaternized derivative (Figure 2.22). The tertiary amine-functional styrene derivative was copolymerized with 4-octylstyrene in different molar ratios. In part, the investigation was carried out to compare between the biocidal activity of poly((4-dimethylaminoethyl)-styrene) and a host-defense alpha-peptide (magainin-2 amide) which is known to display potent activity. In addition, 4-octylstyrene was introduced as a hydrophobic material and copolymerized with 4-(dimethylaminoethyl)-styrene in different molar ratios. The biocidal activity was examined against *E. coli*, *B. subtilis*, MRSA and vancomycin-resistant *E. faecium* (VRE). Interestingly, the tertiary amine-derivative of polystyrene exhibited bactericidal activity against all four strains, in contrast to the monomer itself, which was completely inactive. Copolymers containing up to mol 20% of octylstyrene units showed similar or slightly improved activity to tertiary amine polymer derivative. However, the activity of the copolymer drops with increasing the octylstyrene content.

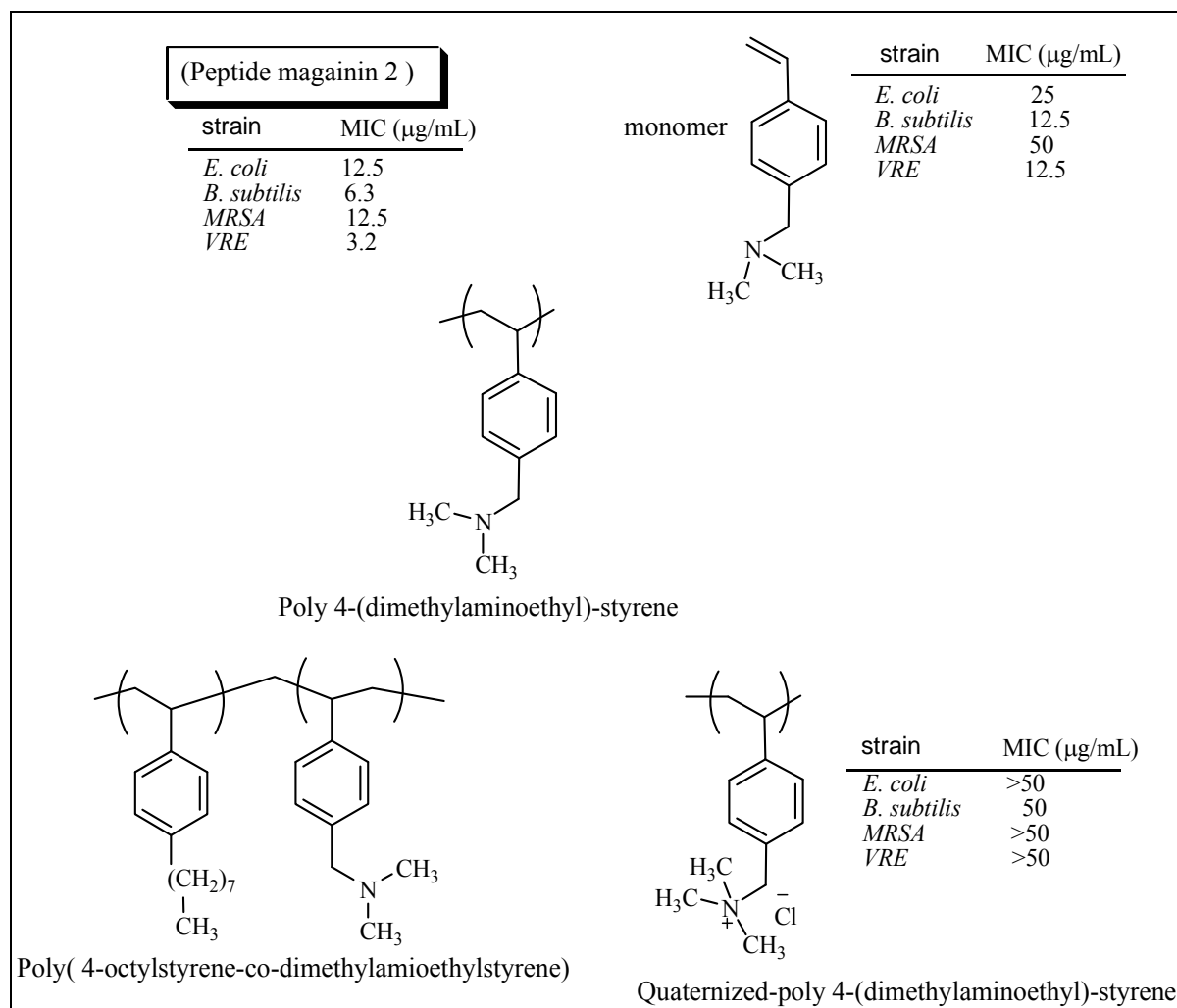


Figure 2.22: Antimicrobial polystyrene derivatives (MIC = Minimum inhibitory concentration)

2.6 Conclusions and Outlook

With the increasing development of resistance against classical antibiotics, there is a growing demand for alternatives to sterilize medical equipment and devices, and treat patients systemically or topically. New antimicrobial materials are being developed that meet requirements of specific applications. Antimicrobial polymers proved to be successful in the growth control of a wide range of microorganisms. The advantage of producing antimicrobial polymers arises from the possibility of incorporating these materials and applying them in different physical forms, e.g. coatings, films, emulsions and fibers. Antimicrobial fibers produced via electrospinning are probably the most efficient and cost effective. This is because of the huge surface area to volume ratio of the fibers. Many antimicrobial polymers are modified before or after electrospinning. This provides the

opportunity to design and modify functional polymers in an intelligent way to specifically target different types of microorganisms. An example that has shown great activity against a wide spectrum of microorganisms consists of quaternary ammonium, phosphonium, and pyridinium compounds. There are other challenges when it comes to the final application of these materials, especially when applied in human therapy practices as wound dressings, protective bandages, etc. Cytotoxicity evaluations need to be performed to assess whether such antimicrobial materials are non-toxic and safe. It is expected that natural and synthetic polymers and polypeptides will play an increasing role in the fight against bacteria that have developed resistance against antibiotics.

2.7 References

1. Page, K.; Wilson, M.; Parkin, I. P. *Journal of Materials Chemistry* 2009, 19, (23), 3819-3831.
2. Gottenbosa, B.; Grijpmab, D. W.; van der Meia, H. C.; Feijenb, J.; Busscher, H. J. *Journal of Antimicrobial Chemotherapy* 2001, 48, 7-13.
3. Mitesh, B. P.; Samir, A. P.; Arabinda, R.; Rajni, M. P. *Journal of Applied Polymer Science* 2003, 89, (4), 895-900.
4. Eun-Soo, P.; Hyoung-Joo, L.; Hye Young, P.; Mal-Nam, K.; Kyoo-Hyun, C.; Jin-San, Y. *Journal of Applied Polymer Science* 2001, 80, (5), 728-736.
5. Montegut, D.; Indictor, N.; Koestler, R. J. *International Biodeterioration* 1991, 28, (1-4), 209-226.
6. Guggenheim, M.; Zbinden, R.; Handschin, A. E.; Gohritz, A.; Altintas, M. A.; Giovanoli, P. *Burns* 2009, 35, (4), 553-560.
7. Lesseva, M. I.; Hadjiiski, O. G. *Burns* 1996, 22, (4), 279-282.
8. Taylor, G. D.; Kibsey, P.; Kirkland, T.; Burroughs, E.; Tredget, E. *Burns* 1992, 18, (4), 332-335.
9. Gould, D.; Chamberlaine, A. *Journal of Clinical Nursing* 1995, 4, (1), 5-12.
10. Peleg, A. Y.; Hooper, D. C. *New England Journal of Medicine* 2010, 362, (19), 1804-1813.
11. Frieden, T., Congressional Testimony: Antibiotic Resistance and the Threat to Public Health In Services, U.S. Department of Health and Human, Ed. Centers for Disease Control and Prevention: Washington, April 28, 2010.

Chapter 2: Literature Review

12. Madkour, A. E.; Tew, G. N. *Polymer International* 2008, 57, (1), 6-10.
13. Walsh, T. R.; Toleman, M. A.; Poirel, L.; Nordmann, P. *Clinical Microbiology Reviews* 2005, 18, (2), 306–325.
14. Kumarasamy, K. K.; Toleman, M. A.; Walsh, T. R.; Bagaria, J.; Butt, F.; Balakrishnan, R.; Chaudhary, U.; Doumith, M.; Giske, C. G.; Irfan, S.; Krishnan, P.; Kumar, A. V.; Maharjan, S.; Mushtaq, S.; Noorie, T.; Paterson, D. L.; Pearson, A.; Perry, C.; Pike, R.; Rao, B.; Ray, U.; Sarma, J. B.; Sharma, M.; Sheridan, E.; Thirunarayan, M. A.; Turton, J.; Upadhyay, S.; Warner, M.; Welfare, W.; Livermore, D. M.; Woodford, N. *The Lancet Infectious Diseases* 2010, 10, (9), 597-602.
15. Wright, G. D. *Advanced Drug Delivery Reviews* 2005, 57, (10), 1451-1470.
16. Russell, A.; Chopra, I., In *Understanding antibacterial action and resistance*, 2nd ed.; Ellis Horwood: London, 1996.
17. McManus, M. C. *American Journal of Health-System Pharmacy* 1997, 54, (12), 1420-1433.
18. Zapun, A.; Contreras-Martel, C.; Vernet, T. *FEMS Microbiology Reviews* 2008, 32, (2), 361-385.
19. Chipley, J. R., Sodium benzoate and benzoic acid. In *Antimicrobials in foods*, 2nd ed.; P. Michael Davidson; Branen, A. L., Ed. M. Dekker New York, 1993; pp 11–48.
20. DiazGranados, C. A.; Cardo, D. M.; McGowan Jr, J. E. *International Journal of Antimicrobial Agents* 2008, 32, (1), 1-9.
21. Bush-Knapp, M. E.; Brinsley-Rainisch, K. J.; Lawton-Ciccarone, R. M.; Sinkowitz-Cochran, R. L.; Dressler, D. D.; Budnitz, T.; Williams, M. V. *American Journal of Infection Control* 2007, 35, (10), 656-661.
22. Bryskier., A., *Antimicrobial Agents: Antibacterials and Antifungals* ASM Press Washington, D.C 2005.
23. Berger, T. J.; Spadaro, J. A.; Bierman, R.; Chapin, S. E.; Becker, R. O. *Antimicrobial Agents and Chemotherapy* 1976, 10, (5), 856–860.
24. Percival, S. L.; Bowler, P. G.; Russell, D. *Journal of Hospital Infection* 2005, 60, (1), 1-7.
25. Silver, S. *FEMS Microbiology Reviews* 2003, 27, (2-3), 341-353.

Chapter 2: Literature Review

26. Trevors, J. T. *Enzyme and Microbial Technology* 1987, 9, (6), 331-333.
27. Lee, B.; Yun, S.; Ji, J.; Bae, G. *Journal of Microbiology and Biotechnology* 2008, 18, (1), 176-182.
28. Miaśkiewicz-Peska, E.; Lebkowska, M. *Fibres & Textiles in Eastern Europe* 2011, 11, (1), 73-77.
29. Phuong Phong, N. T.; Thanh, N. V. K.; Phuong, P. H. *Journal of Physics: Conference Series* 2009, 187, (1).
30. Sheikh, F. A.; Barakat, N. A. M.; Kanjwal, M. A.; Chaudhari, A. A.; Jung, I.-H.; Lee, J. H.; Kim, H. Y. *Macromolecular Research* 2009, 17, (9), 688-696.
31. Appendini, P.; Hotchkiss, J. H. *Innovative Food Science & Emerging Technologies* 2002, 3, (2), 113-126.
32. Kang, M.; Jung, R.; Kim, H.-S.; Youk, J. H.; Jin, H.-J. *Journal of Nanoscience and Nanotechnology* 2007, 7, 3888-3891.
33. Rujitanaroj, P.-o.; Pimpha, N.; Supaphol, P. *Polymer* 2008, 49, (21), 4723-4732.
34. Chadeau, E.; Oulahal, N.; Dubost, L.; Favergeon, F.; Degraeve, P. *Food Control* 2010, 21, (4), 505-512.
35. Dubas, S. T.; Kumlangdudsana, P.; Potiyaraj, P. *Colloids and Surfaces A: Physicochemical and Engineering Aspects* 2006, 289, (1-3), 105-109.
36. Yuranova, T.; Rincon, A. G.; Pulgarin, C.; Laub, D.; Xantopoulos, N.; Mathieu, H. J.; Kiwi, J. *Journal of Photochemistry and Photobiology A: Chemistry* 2006, 181, (2-3), 363-369.
37. Dastjerdi, R.; Montazer, M. *Colloids and Surfaces B: Biointerfaces* 2010, 79, (1), 5-18.
38. Singh, N.; Manshian, B.; Jenkins, G. J. S.; Griffiths, S. M.; Williams, P. M.; Maffeis, T. G. G.; Wright, C. J.; Doak, S. H. *Biomaterials* 2009, 30, (23-24), 3891-3914.
39. Kittler, S.; Greulich, C.; Diendorf, J.; Köllner, M.; Epple, M. *Chemistry of Materials* 2010, 22, (16), 4548-4554.
40. Ahamed, M.; Karns, M.; Goodson, M.; Rowe, J.; Hussain, S. M.; Schlager, J. J.; Hong, Y. *Toxicology and Applied Pharmacology* 2008, 233, (3), 404-410.

Chapter 2: Literature Review

41. Arakawa, H.; Neault, J. F.; Tajmir-Riahi, H. A. *Biophysical Journal* 2001, 81, (3), 1580-1587.
42. Feng, Q. L.; Wu, J.; Chen, G. Q.; Cui, F. Z.; Kim, T. N.; Kim, J. O. *Journal of Biomedical Materials Research* 2000, 52, (4), 662-668.
43. Vigo Tyrone, L., Antimicrobial Polymers and Fibers: Retrospective and Prospective. In *Bioactive Fibers and Polymers*, American Chemical Society: 2001; Vol. 792, pp 175-200.
44. Kong, H.; Song, J.; Jang, J. *Environmental Science & Technology* 2010, 44, (14), 5672-5676.
45. Wei, C.; Lin, W. Y.; Zainal, Z.; Williams, N. E.; Zhu, K.; Kruzic, A. P.; Smith, R. L.; Rajeshwar, K. *Environmental Science & Technology* 1994, 28, (5), 934-938.
46. Kwak, S.-Y.; Kim, S. H.; Kim, S. S. *Environmental Science & Technology* 2001, 35, (11), 2388-2394.
47. Fu, G.; Vary, P. S.; Lin, C.-T. *The Journal of Physical Chemistry B* 2005, 109, (18), 8889-8898.
48. Zhang, X.; Su, H.; Zhao, Y.; Tan, T. *Journal of Photochemistry and Photobiology A: Chemistry* 2008, 199, (2-3), 123-129.
49. Vilas Desai, S.; Meenal, K. *Research Journal of Microbiology* 2009, 4, (3), 97-103.
50. Erdural, B. K.; Yurum, A.; Bakir, U.; Karakas, G. *Journal of Nanoscience and Nanotechnology* 2008, 8, (2), 878-886.
51. Jones, N.; Ray, B.; Ranjit, K. T.; Manna, A. C. *FEMS Microbiology Letters* 2008, 279, (1), 71-76.
52. Sawai, J. *Journal of Microbiological Methods* 2003, 54, (2), 177-182.
53. Dumas, E.; Gao, C.; Suffern, D.; Bradforth, S. E.; Dimitrijevic, N. M.; Nadeau, J. L. *Environmental Science & Technology* 2010, 44, (4), 1464-1470.
54. Lu, Z.; Li, C. M.; Bao, H.; Qiao, Y.; Toh, Y.; Yang, X. *Langmuir* 2008, 24, (10), 5445-5452.
55. Kang, S.; Pinault, M.; Pfefferle, L. D.; Elimelech, M. *Langmuir* 2007, 23, (17), 8670-8673.
56. Yang, C.; Mamouni, J.; Tang, Y.; Yang, L. *Langmuir* 2010, 26, (20), 16013-16019.
57. Narayan, R. J.; Berry, C. J.; Brigmon, R. L. *Materials Science and Engineering: B* 2005, 123, (2), 123-129.

Chapter 2: Literature Review

58. Li, Q.; Mahendra, S.; Lyon, D. Y.; Brunet, L.; Liga, M. V.; Li, D.; Alvarez, P. J. J. *Water Research* 2008, 42, (18), 4591-4602.
59. Russell, A.; Furr, R.; Maillard, J. *American Society for Microbiology News* 1997, 63, (9), 481–487
60. Borick, P. M.; Bratt, M. *Applied Microbiology* 1961, 9, (6), 475–477.
61. Ricke, S. C. *Poultry Science* 2003, 82, (4), 632-639.
62. Jamilah, M. B.; Abbas, K. A.; Rahman, R. A. *American Journal of Agricultural and Biological Sciences* 2008, 3, (3), 566-574.
63. Davies, R. H.; Wray, C. *Poultry Science* 1995, 74, (4), 638-647.
64. Zafar, A. B.; Butler, R. C.; Reese, D. J.; Gaydos, L. A.; Mennonna, P. A. *American Journal of Infection Control* 1995, 23, (3), 200-208.
65. Birosova, L.; Mikulasova, M. *Journal of Medical Microbiology* 2009, 58, (4), 436-441.
66. Christian, J. S. *Primary Care Update for OB/GYNS* 3, (3), 87-92.
67. Tomioka, H. *Journal of Infection and Chemotherapy* 2000, 6, (1), 8-20.
68. Oliphant, C. M.; Green, G. M. *American Family Physician* 2002, 65, (3), 455-464.
69. Appelbaum, P. C.; Hunter, P. A. *International Journal of Antimicrobial Agents* 2000, 16, (1), 5-15.
70. Lucchini, J. J.; Corre, J.; Cremieux, A. *Research in Microbiology* 1990, 141, (4), 499-510.
71. Corre, J.; Lucchini, J. J.; Mercier, G. M.; Cremieux, A. *Research in Microbiology* 1990, 141, (4), 483-497.
72. Rutala, W. A.; Weber, D. J.; HICPAC, Guideline for Disinfection and Sterilization in Healthcare Facilities, 2008. In *Healthcare Infection Control Practices Advisory Committee Centers for Disease Control and Prevention*: 2008.
73. McDonnell, G.; Russell, A. D. *Clinical Microbiology Reviews* 1999, 12, (1), 147-179.

Chapter 2: Literature Review

74. Fraise, A. P.; Lambert, P. A.; Maillard, J.-Y., *Russell, Hugo & Ayliffe's principles and practice of disinfection, preservation & sterilization* 4th ed.; Blackwell Pub: Malden, Mass 2004.
75. Rahn, O.; Van Eseltine, W. P. *Annual Review of Microbiology* 1947, 1, (1), 173-192.
76. Grönholm, L.; Wirtanen, G.; Ahlgren, K.; Nordström, K.; Sjöberg, A. M. *Zeitschrift für Lebensmitteluntersuchung und -Forschung A* 1999, 208, (4), 289-298.
77. Isquith, A. J.; Abbott, E. A.; Walters, P. A. *Applied Microbiology* 1972, 24, (6), 859-863.
78. Shimizu, M.; Okuzumi, K.; Yoneyama, A.; Kunisada, T.; Araake, M.; Ogawa, H.; Kimura, S. *Dermatology* 2002, 204, (Suppl. 1), 21-27.
79. Hargreaves, M. K.; Pritchard, J. G.; Dave, H. R. *Chemical Reviews* 1970, 70, (4), 439-469.
80. Igarashi, Y.; Yagami, K.; Imai, R.; Watanabe, S. *Journal of Industrial Microbiology & Biotechnology* 1990, 6, (3), 223-225.
81. Rosario, D. C.; Joe, D. S. *Proceedings: Plant Sciences* 1974, 80, (2), 68-75.
82. Zentz, F.; Hellio, C.; Valla, A.; De La Broise, D.; Bremer, G.; Labia, R. *Marine Biotechnology* 2002, 4, (4), 431-440.
83. Shetgiri, N. P.; Nayak, B. K. *Indian Journal of Chemistry* 2005, 44B, 1933-1936.
84. Watanabe, S.; Igarashi, Y.; Yagami, K.; Imai, R. *Pesticide Science* 1991, 31, 45-51.
85. Sortino, M.; Cechinel Filho, V.; Corrêa, R.; Zacchino, S. *Bioorganic & Medicinal Chemistry* 2008, 16, (1), 560-568.
86. Martin, K. W.; Ernst, E. *J. Antimicrob. Chemother.* 2003, 51, (2), 241-246.
87. Subrahmanyam, M.; Sahapure, A. G.; Nagane, N. S.; Bhagwat, V. R.; Ganu, J. V. *Annals of Burns and Fire Disasters* 2003, 16, (3).
88. Jalali, F. S. S.; Tajik, H.; Saifzadeh, S.; Farshid, A. A. *Journal of Animal and Veterinary Advances* 2007, 6, (2), 179-184.
89. Reddy, K. V. R.; Yedery, R. D.; Aranha, C. *International Journal of Antimicrobial Agents* 2004, 24, (6), 536-547.

Chapter 2: Literature Review

90. Al-Badri, Z. M.; Som, A.; Lyon, S.; Nelson, C. F.; Nußslein, K.; Tew, G. N. *Biomacromolecules* 2008, 9, (10), 2805-2810.
91. Song, A.; Walker, S. G.; Parker, K. A.; Sampson, N. S. *ACS Chemical Biology* 2011, 6, (6), 590-599.
92. Tang, H.; Doerksen, R. J.; Tew, G. N. *Chemical Communications* 2005, (12), 1537-1539.
93. Gabriel, G. J.; Som, A.; Madkour, A. E.; Eren, T.; Tew, G. N. *Materials Science and Engineering: R: Reports* 2007, 57, (1-6), 28-64.
94. Brand, A. M.; De Kwaadsteniet, M.; Dicks, L. M. T. *Letters in Applied Microbiology* 2010, 51, (6), 645-649.
95. Perron, G. G.; Zasloff, M.; Bell, G. *Proceedings of the Royal Society B: Biological Sciences* 2006, 273, (1583), 251-256.
96. Marcus, J. P.; Green, J. L.; Goulter, K. C.; Manners, J. M. *The Plant Journal* 1999, 19, (6), 699-710.
97. Jenssen, H.; Hamill, P.; Hancock, R. E. W. *Clinical Microbiology Reviews* 2006, 19, (3), 491-511.
98. Dijkshoorn, L.; Brouwer, C. P. J. M.; Bogaards, S. J. P.; Nemeč, A.; van den Broek, P. J.; Nibbering, P. H. *Antimicrobial Agents and Chemotherapy* 2004, 48, (12), 4919-4921.
99. Nes, I. F.; Holo, H. *Peptide Science* 2000, 55, (1), 50-61.
100. Sahl, H.-G.; Bierbaum, G. *Annual Review of Microbiology* 1998, 52, (1), 41-79.
101. Knoetze, H.; Todorov, S. D.; Dicks, L. M. T. *International Journal of Antimicrobial Agents* 2008, 31, (3), 228-234.
102. Bauer, R.; Dicks, L. M. T. *International Journal of Food Microbiology* 2005, 101, (2), 201-216.
103. McAuliffe, O.; Ross, R. P.; Hill, C. *FEMS Microbiology Reviews* 2001, 25, (3), 285-308.
104. Jack, R. W.; Tagg, J. R.; Ray, B. *Microbiol. Rev.* 1995, 59, (2), 171-200.
105. Klaenhammer, T. R. *FEMS Microbiology Reviews* 1993, 12, (1-3), 39-85.

Chapter 2: Literature Review

106. Rea, M. C.; Ross, R. P.; Cotter, P. D.; Hill, C., Classification of bacteriocins from gram-negative bacteria. In *Prokaryotic Antimicrobial Peptides*, Drider, Djamel; Rebuffat, Sylvie, Eds. Springer: New York, 2011; pp 29-53.
107. Chatterjee, S.; Chatterjee, D. K.; Jani, R. H.; Blumbach, J.; Ganguli, B. N.; Klesel, N.; Limbert, M.; Seibert, G. *The Journal of antibiotics* 1992, 45, (6), 839-45.
108. Galvin, M.; Hill, C.; Ross, R. P. *Letters in Applied Microbiology* 1999, 28, (5), 355-358.
109. Piper, C.; Hill, C.; Cotter, P. D.; Ross, R. P. *Microbial Biotechnology* 2010, doi:10.1111/j.1751-7915.2010.00207.x.
110. Dicks, L. M. T.; Heunis, T. D. J.; Van Staden, A. D.; Brand, A.; Sutyak Noll, K.; Chikindas, M. L., Medical and Personal Care Applications of Bacteriocins Produced by Lactic Acid Bacteria. In *Prokaryotic Antimicrobial Peptides: From Genes to Applications*, Drider, Djamel; Rebuffat, Sylvie, Eds. Springer: New York, 2011; pp 391-421.
111. Rinaudo, M. *Progress in Polymer Science* 2006, 31, (7), 603-632.
112. Lim, S.-H.; Hudson, S. M. *Journal of Macromolecular Science, Part C: Polymer Reviews* 2003, 43, (2), 223 - 269.
113. Pillai, C. K. S.; Paul, W.; Sharma, C. P. *Progress in Polymer Science* 2009, 34, (7), 641-678.
114. Shin, Y.; Yoo, D. I.; Jang, J. *Journal of Applied Polymer Science* 2001, 80, (13), 2495-2501.
115. Kean, T.; Thanou, M. *Advanced Drug Delivery Reviews* 2010, 62, (1), 3-11.
116. Chandy, T.; Sharma, C. P. *Artificial Cells, Blood Substitutes and Biotechnology* 1990, 18, (1), 1-24.
117. Ravi Kumar, M. N. V. *Reactive and Functional Polymers* 2000, 46, (1), 1-27.
118. Rúnarsson, Ö. V.; Holappa, J.; Malainer, C.; Steinsson, H.; Hjálmsdóttir, M.; Nevalainen, T.; Másson, M. *European Polymer Journal* 2010, 46, (6), 1251-1267.
119. Sajomsang, W. *Carbohydrate Polymers* 2010, 80, (3), 631-647.
120. Devlieghere, F.; Vermeulen, A.; Debevere, J. *Food Microbiology* 2004, 21, (6), 703-714.
121. Goy, R. C.; Britto, D. d.; Assis, O. B. G. *Polímeros* 2009, 19, 241-247.

Chapter 2: Literature Review

122. Rabea, E. I.; Badawy, M. E. T.; Stevens, C. V.; Smagghe, G.; Steurbaut, W. *Biomacromolecules* 2003, 4, (6), 1457-1465.
123. D'Arcy, N. *Plastics, Additives and Compounding* 2001, 3, (12), 12-15.
124. Pritchard, G., In *Rapra Market Report: Plastic Additives*, Rapra Technology Limited: Shropshire, 2005.
125. Nichols, D., Biocides in Plastics, *Rapra Review Reports*, 2004, 15, Report 12
126. Junhui, J.; Wei, Z. *Journal of Biomedical Materials Research Part A* 2009, 88A, (2), 448-453.
127. Witte, W. *Science* 1998, 279, (5353), 996-997.
128. Klibanov, A. M. *Journal of Materials Chemistry* 2007, 17, (24), 2479-2482.
129. Thamizharasi, S.; Vasantha, J.; Reddy, B. S. R. *European Polymer Journal* 2002, 38, (3), 551-559.
130. Moon, W.-S.; Chul Kim, J.; Chung, K.-H.; Park, E.-S.; Kim, M.-N.; Yoon, J.-S. *Journal of Applied Polymer Science* 2003, 90, (7), 1797-1801.
131. Dizman, B.; Elasri, M. O.; Mathias, L. J. *Journal of Applied Polymer Science* 2004, 94, (2), 635-642.
132. Timofeeva, L.; Kleshcheva, N. *Applied Microbiology and Biotechnology* 2010, 89, 1-18.
133. Dickson, J. S.; Koohmaraie, M. *Applied and Environmental Microbiology* 1989, 55, (4), 832-836.
134. Banerjee, I.; Pangule, R. C.; Kane, R. S. *Advanced Materials* 2011, 23, (6), 690-718.
135. Ferreira, L.; Zumbuehl, A. *Journal of Materials Chemistry* 2009, 19, (42), 7796-7806.
136. Larson, A. M.; Hsu, B. B.; Rautaray, D.; Haldar, J.; Chen, J.; Klibanov, A. M. *Biotechnology and Bioengineering* 2011, 108, (3), 720-723.
137. Chen, Y.; Han, Q. *Applied Surface Science* 2011, 257, (14), 6034-6039.
138. Karlsson, A. J.; Flessner, R. M.; Gellman, S. H.; Lynn, D. M.; Palecek, S. P. *Biomacromolecules* 2011, 11, (9), 2321-2328.

Chapter 2: Literature Review

139. Lichter, J. A.; Van Vliet, K. J.; Rubner, M. F. *Macromolecules* 2009, 42, (22), 8573-8586.
140. Isquith, A. J.; Abbott, E. A.; Walters, P. A. *Applied and Environmental Microbiology* 1972, 24, (6), 859-863.
141. Walters, P. A.; Abbott, E. A.; Isquith, A. J. *Appl. Environ. Microbiol.* 1973, 25, (2), 253-256.
142. Isquith, A. J.; McCollum, C. J. *Appl. Environ. Microbiol.* 1978, 36, (5), 700-704.
143. Nakagawa, Y.; Hayashi, H.; Tawaratani, T.; Kourai, H.; Horie, T.; Shibasaki, I. *Appl. Environ. Microbiol.* 1984, 47, (3), 513-518.
144. Tiller, J. C.; Liao, C.-J.; Lewis, K.; Klivanov, A. M. *Proceedings of the National Academy of Sciences of the United States of America* 2001, 98, (11), 5981-5985.
145. Tiller, J. C.; Lee, S. B.; Lewis, K.; Klivanov, A. M. *Biotechnology and Bioengineering* 2002, 79, (4), 465-471.
146. Lin, J.; Murthy, S. K.; Olsen, B. D.; Gleason, K. K.; Klivanov, A. M. *Biotechnology Letters* 2003, 25, (19), 1661-1665.
147. Roy, D.; Knapp, J. S.; Guthrie, J. T.; Perrier, S. b. *Biomacromolecules* 2007, 9, (1), 91-99.
148. Madkour, A. E.; Dabkowski, J. M.; Nul'sslein, K.; Tew, G. N. *Langmuir* 2008, 25, (2), 1060-1067.
149. Lee, S. B.; Koepsel, R. R.; Morley, S. W.; Matyjaszewski, K.; Sun, Y.; Russell, A. J. *Biomacromolecules* 2004, 5, (3), 877-882.
150. Murata, H.; Koepsel, R. R.; Matyjaszewski, K.; Russell, A. J. *Biomaterials* 2007, 28, (32), 4870-4879.
151. Xu, F.; Yuan, S.; Pehkonen, S.; Kang, E.; Neoh, K. *NanoBioTechnology* 2006, 2, (3), 123-134.
152. Huang, J.; Koepsel, R. R.; Murata, H.; Wu, W.; Lee, S. B.; Kowalewski, T.; Russell, A. J.; Matyjaszewski, K. *Langmuir* 2008, 24, (13), 6785-6795.
153. Ikeda, T.; Tazuke, S.; Suzuki, Y. *Die Makromolekulare Chemie* 1984, 185, (5), 869-876.
154. Messick, C. R.; Pendland, S. L.; Moshirfar, M.; Fiscella, R. G.; Losnedahl, K. J.; Schriever, C. A.; Schreckenberger, P. C. *Journal of Antimicrobial Chemotherapy* 1999, 44, (2), 297-298.

Chapter 2: Literature Review

155. Zhang, Y.; Jiang, J.; Chen, Y. *Polymer* 1999, 40, (22), 6189-6198.
156. Ikeda, T.; Hirayama, H.; Yamaguchi, H. *Antimicrobial Agents and Chemotherapy* 1986, 30, (1), 132-136.
157. Broxton, P.; Woodcock, P. M.; Gilbert, P. *Journal of Applied Microbiology* 1983, 54, (3), 345-353.
158. Ikeda, T.; Yamaguchi, H.; Tazuke, S. *Antimicrob. Agents Chemother.* 1984, 26, (2), 139-144.
159. Kanazawa, A.; Ikeda, T.; Endo, T. *Journal of Polymer Science Part A: Polymer Chemistry* 1993, 31, (2), 335-343.
160. Kanazawa, A.; Ikeda, T.; Endo, T. *Journal of Polymer Science Part A: Polymer Chemistry* 1993, 31, (6), 1441-1447.
161. Tashiro, T. *Macromolecular Materials and Engineering* 2001, 286, (2), 63-87.
162. Kenawy, E.-R.; Worley, S. D.; Broughton, R. *Biomacromolecules* 2007, 8, (5), 1359-1384.
163. Jaeger, W.; Bohrisch, J.; Laschewsky, A. *Progress in Polymer Science* 2010, 35, (5), 511-577.
164. Lee, W. F.; Chen, C. F. *Journal of Applied Polymer Science* 1997, 66, (1), 95-103.
165. Lee, W. F.; Chen, Y. M. *Journal of Applied Polymer Science* 2001, 80, (10), 1619-1626.
166. Lee, W. F.; Huang, G. Y. *Journal of Applied Polymer Science* 1996, 60, (2), 187-199.
167. Reneker, D. H.; Yarin, A. L.; Zussman, E.; Xu, H.; Hassan, A.; Erik van der, G., Electrospinning of Nanofibers from Polymer Solutions and Melts. In *Advances in Applied Mechanics*, Elsevier: 2007; Vol. Volume 41, pp 43-195, 345-346.
168. Doshi, J.; Reneker, D. H. *Journal of Electrostatics* 1995, 35, (2-3), 151-160.
169. Frenot, A.; Chronakis, I. S. *Current Opinion in Colloid & Interface Science* 2003, 8, (1), 64-75.
170. Gibson, P.; Schreuder-Gibson, H.; Rivin, D. *Colloids and Surfaces A: Physicochemical and Engineering Aspects* 2001, 187-188, 469-481.

Chapter 2: Literature Review

171. Chronakis, I. S., Micro-/Nano-Fibers by Electrospinning Technology: Processing, Properties and Applications. In *Micromanufacturing Engineering and Technology*, William Andrew Publishing: Boston, 2010; pp 264-286.
172. Deitzel, J. M.; Kleinmeyer, J.; Harris, D.; Beck Tan, N. C. *Polymer* 2001, 42, (1), 261-272.
173. Bhardwaj, N.; Kundu, S. C. *Biotechnology Advances* 2010, 28, (3), 325-347.
174. Arinstein, A.; Zussman, E. *Journal of Polymer Science Part B: Polymer Physics* 2011, 49, (10), 691-707.
175. Huang, Z.-M.; Zhang, Y. Z.; Kotaki, M.; Ramakrishna, S. *Composites Science and Technology* 2003, 63, (15), 2223-2253.
176. Greiner, A.; Wendorff, J. H. *Angewandte Chemie International Edition* 2007, 46, (30), 5633-5633.
177. Agarwal, S.; Greiner, A.; Wendorff, J. H. *Advanced Functional Materials* 2009, NA.
178. Agarwal, S.; Wendorff, J. H.; Greiner, A. *Polymer* 2008, 49, (26), 5603-5621.
179. Schreuder-Gibson, H.; Gibson, P.; Senecal, K.; Sennett, M.; Walker, J.; Yeomans, W.; Ziegler, D.; Tsai, P. P. *Journal of Advanced Materials* 2002, 34, (3), 44-55.
180. Gibson, P. W.; Schreuder-Gibson, H. L.; Rivin, D. *AIChE Journal* 1999, 45, (1), 190-195.
181. Bender, W.; Stutte, P., Antimicrobials for Synthetic Fibers. In *Bioactive Fibers and Polymers*, American Chemical Society: 2001; Vol. 792, pp 218-242.
182. Kim, J. s.; Reneker, D. H. *Polymer Composites* 1999, 20, (1), 124-131.
183. Bergshoef, M. M.; Vancso, G. J. *Advanced Materials* 1999, 11, (16), 1362-1365.
184. Sun, W.; Cai, Q.; Li, P.; Deng, X.; Wei, Y.; Xu, M.; Yang, X. *Dental Materials* 2010, 26, (9), 873-880.
185. Lin, S.; Cai, Q.; Ji, J.; Sui, G.; Yu, Y.; Yang, X.; Ma, Q.; Wei, Y.; Deng, X. *Composites Science and Technology* 2008, 68, (15-16), 3322-3329.
186. Baji, A.; Mai, Y.-W.; Wong, S.-C.; Abtahi, M.; Chen, P. *Composites Science and Technology* 2010, 70, (5), 703-718.

Chapter 2: Literature Review

187. Gopal, R.; Kaur, S.; Ma, Z.; Chan, C.; Ramakrishna, S.; Matsuura, T. *Journal of Membrane Science* 2006, 281, (1-2), 581-586.
188. Han, W.; Gaofeng, Z.; DaoHeng, S. In *Electrospun nanofibrous membrane for air filtration*, Nanotechnology, 2007. IEEE-NANO 2007. 7th IEEE Conference on, 2-5 Aug. 2007, 2007; 2007; pp 1244-1247.
189. Wang, X.; Drew, C.; Lee, S.-H.; Senecal, K. J.; Kumar, J.; Samuelson, L. A. *Nano Letters* 2002, 2, (11), 1273-1275.
190. Wang, X.; Kim, Y.-G.; Drew, C.; Ku, B.-C.; Kumar, J.; Samuelson, L. A. *Nano Letters* 2004, 4, (2), 331-334.
191. Davis, B. W.; Niamnont, N.; Hare, C. D.; Sukwattanasinitt, M.; Cheng, Q. *ACS Applied Materials & Interfaces* 2010, 2, (7), 1798-1803.
192. Drew, C.; Wang, X.; Senecal, K.; Schreuder-Gibson, H.; He, J.; Kumar, J.; Samuelson, L. A. *Journal of Macromolecular Science, Part A: Pure and Applied Chemistry* 2002, 39, (10), 1085 - 1094.
193. Verreck, G.; Chun, I.; Rosenblatt, J.; Peeters, J.; Dijck, A. V.; Mensch, J.; Noppe, M.; Brewster, M. E. *Journal of Controlled Release* 2003, 92, (3), 349-360.
194. Khil, M. S.; Cha, D. I.; Kim, H. Y.; Kim, I. S.; Bhattarai, N. *Journal of Biomedical Materials Research Part B: Applied Biomaterials* 2003, 67B, (2), 675-679.
195. Zhong, W.; Xing, M. M. Q.; Maibach, H. I. *Cutaneous and Ocular Toxicology* 2010, 29, (3), 143-152.
196. Heunis, T. D.; Dicks, L. M. *Journal of biomedicine & biotechnology* 2010, 2010.
197. Liu, X.; Lin, T.; Fang, J.; Yao, G.; Zhao, H.; Dodson, M.; Wang, X. *Journal of Biomedical Materials Research Part A* 2010, 94A, (2), 499-508.
198. Kenawy, E.-R.; Abdel-Hay, F. I.; El-Newehy, M. H.; Wnek, G. E. *Materials Chemistry and Physics* 2009, 113, (1), 296-302.
199. Heunis, T.; Bshena, O.; Klumperman, B.; Dicks, L. *International Journal of Molecular Sciences* 2011, 12, (4), 2158-2173.

Chapter 2: Literature Review

200. Saw, S. H.; Wang, K.; Yong, T.; Ramakrishna, S., *Polymeric Nanofibers in Tissue Engineering*. Wiley-VCH Verlag GmbH & Co. KGaA: 2007.
201. Matthews, J. A.; Wnek, G. E.; Simpson, D. G.; Bowlin, G. L. *Biomacromolecules* 2002, 3, (2), 232-238.
202. Yoshimoto, H.; Shin, Y. M.; Terai, H.; Vacanti, J. P. *Biomaterials* 2003, 24, (12), 2077-2082.
203. Min, B.-M.; Lee, G.; Kim, S. H.; Nam, Y. S.; Lee, T. S.; Park, W. H. *Biomaterials* 2004, 25, (7-8), 1289-1297.
204. Shin, M.; Ishii, O.; Sueda, T.; Vacanti, J. P. *Biomaterials* 2004, 25, (17), 3717-3723.
205. Sill, T. J.; von Recum, H. A. *Biomaterials* 2008, 29, (13), 1989-2006.
206. Barnes, C. P.; Sell, S. A.; Boland, E. D.; Simpson, D. G.; Bowlin, G. L. *Advanced Drug Delivery Reviews* 2007, 59, (14), 1413-1433.
207. Beachley, V.; Wen, X. *Progress in Polymer Science* 2010, 35, (7), 868-892.
208. Acatay, K.; Şimşek, E.; Akel, M.; Menceloğlu, Y. Z., Electrospinning of low surface energy quaternary ammonium salt containing polymers and their antibacterial activity. In *Nanoengineered Nanofibrous Materials*, Guceri, Selcuk; Gogotsi, Yury G.; Kuznetsov, Vladimir, Eds. Kluwer Academic Publishing Co: USA, 2004; pp 97-106.
209. Kenawy, E.-R.; Abdel-Fattah, Y. R. *Macromolecular Bioscience* 2002, 2, (6), 261-266.
210. Yao, F.; Xu, L.; Lin, B.; Fu, G.-D. *Nanoscale* 2010, 2, (8), 1348-1357.
211. Guo-Dong, F.; Fang, Y.; Zhigang, L.; Xinsong, L. *Journal of Materials Chemistry* 2008, 18, (8), 859-867.
212. Qun, X. L.; Fang, Y.; Shan, Y.; Fu, G. D.; Liang, S.; Shengzhe, N.; Meifang, Z. *High Performance Polymers* 2010, 22, 359-376
213. Ignatova, M.; Manolova, N.; Rashkov, I. *European Polymer Journal* 2007, 43, (5), 1609-1623.
214. Ignatova, M.; Manolova, N.; Rashkov, I. *European Polymer Journal* 2007, 43, (4), 1112-1122.
215. IGNATOVA, M.; MARKOVA, N.; MANOLOVA, N.; RASHKOV, I. *Journal of Biomaterials Science, Polymer Edition* 2008, 19, 373-386.

Chapter 2: Literature Review

216. Lenoir, S.; Pagnouille, C.; Galleni, M.; Compère, P.; Jérôme, R.; Detrembleur, C. *Biomacromolecules* 2006, 7, (8), 2291-2296.
217. Lenoir, S.; Pagnouille, C.; Detrembleur, C.; Galleni, M.; Jérôme, R. *Journal of Polymer Science Part A: Polymer Chemistry* 2006, 44, (3), 1214-1224.
218. Thomassin, J.-M.; Lenoir, S.; Riga, J.; Jérôme, R.; Detrembleur, C. *Biomacromolecules* 2007, 8, (4), 1171-1177.
219. Ladaviere, C.; Delair, T.; Domard, A.; Pichot, C.; Mandrand, B. *Journal of Applied Polymer Science* 1999, 71, (6), 927-936.
220. Ladavière, C.; Delair, T.; Domard, A.; Pichot, C.; Mandrand, B. *Journal of Applied Polymer Science* 1999, 72, (12), 1565-1572.
221. Türk, M.; Rzayev, Z. M. O.; Khalilova, S. A. *Bioorganic & Medicinal Chemistry* 2010, In Press, Corrected Proof.
222. Patel, H.; Raval, D. A.; Madamwar, D.; Patel, S. R. *Die Angewandte Makromolekulare Chemie* 1998, 263, (1), 25-30.
223. Patel, H.; Raval, D. A.; Madamwar, D.; Sinha, T. J. M. *Die Angewandte Makromolekulare Chemie* 1997, 245, (1), 1-8.
224. Patel, J. S.; Patel, S. V.; Talpada, N. P.; Patel, H. A. *Die Angewandte Makromolekulare Chemie* 1999, 271, (1), 24-27.
225. Jeong, J. H.; Byoun, Y. S.; Ko, S. B.; Lee, Y. S. *Journal of Industrial and Engineering Chemistry* 2001, 7, (5), 310-315.
226. Jeong, J.-H.; Byoun, Y.-S.; Lee, Y.-S. *Reactive and Functional Polymers* 2002, 50, (3), 257-263.
227. Ignatova, M.; Stoilova, O.; Manolova, N.; Markova, N.; Rashkov, I. *Macromolecular Bioscience* 2010, 10, (8), 944-954.
228. Endo, Y.; Tani, T.; Kodama, M. *Applied and Environmental Microbiology* 1987, 53, (9), 2050-2055.
229. Gelman, M. A.; Weisblum, B.; Lynn, D. M.; Gellman, S. H. *Organic Letters* 2004, 6, (4), 557-560.

CHAPTER 3

CHAPTER 3: Synthesis and Characterization of Styrene-Maleimide Copolymer Derivatives

3.1 Abstract

This chapter describes the experimental procedures and protocols used for the preparation and characterization of styrene-maleimide copolymer derivatives. Different primary amine compounds were used for the modification of two different styrene-maleic anhydride copolymer grades. The grades used are a random copolymer obtained commercially, and the second is an alternating copolymer prepared in this work. All synthesized and modified copolymers were utilized in the electrospinning process for producing nanofibers.

3.1 Synthesis of styrene-maleimide based copolymers

The polymers synthesized in this work were derivatives of styrene-maleic anhydride copolymers (SMA) reacted with primary amines. Two types of SMA copolymers were used as precursors. The grades differ in the anhydride content and thus molecular sequence and these are:

1. SMA-C: a commercial grade, $\bar{M}_w = 110\ 000$ containing about 28% maleic anhydride (MA) moieties as a statistical copolymer obtained from Polyscope, grade (SZ 28 110).
2. SMA-P: An alternating SMA copolymer prepared in this study as described in section 3.1.2.

3.1.1 Materials

Maleic anhydride (MAh) 99% (Merck), 3-dimethylaminopropylamine (DAMPA) 99% (Aldrich), Styrene (St) was washed with KOH solution for inhibitor removal and distilled before use, Tetrahydrofuran (THF) 99% (Aldrich); dimethylformamide (DMF), AIBN

(ACROS) recrystallized from methanol and dried before use, diethyl ether 99.5% , methyl ethyl ketone (MEK) 99%, methanol 99% and ethanol 99% were obtained from (Merck), 1-bromooctane 99% , 1-bromobutane 99%, 1-dodecylbromide 99% and methyl iodide 99% were purchased from (Sigma Aldrich).

Characterization:

- The $^1\text{H-NMR}$ and $^{13}\text{C-NMR}$ measurements were performed at 50 °C on a Varian Mercury 400 or Varian Gemini 300 spectrometer in either *deuterated dimethyl sulfoxide* (DMSO- d_6) or *deuterated acetone* (Acetone- d_6)
- Attenuated Total Reflection Fourier Transform Infrared (ATR-FTIR) spectroscopy was performed on a Nexus infrared spectrometer equipped with a Smart Golden Gate attenuated total reflectance diamond from Thermo Nicolet with ZnSe lenses. Each spectrum was scanned 32 times with 4.0 cm^{-1} resolution. The data analysis was performed with Omnic Software version 7.2.
- Molar mass and dispersity (\bar{M}_w), were obtained using size exclusion chromatography SEC. The SEC comprised of Waters Alliance apparatus fitted with a 5 mm mixed-D PLgel column from Polymer Laboratories, a Shimadzu LC-10AT isocratic pump, a Waters 171+ auto sampler, a refractive index detector and a Waters 2487 dual wavelength UV detector. The flow rate was set at 1 mL/min, and the injection volume was 100 μL . Dimethylacetamide HPLC grade was used for the solvent, with 0.05% (w/v) 2,6-di-*tert*-butyl-4-methylphenol and 0.3% (w/v) lithium chloride. The calculated molar masses were relative to a calibration curve for poly(methyl methacrylate) standards (molar mass range of 8.50×10^2 to $3.5 \times 10^5 \text{ g. mol}^{-1}$) of low dispersity from Polymer Laboratories. Data acquisition and processing were performed using Millennium software.

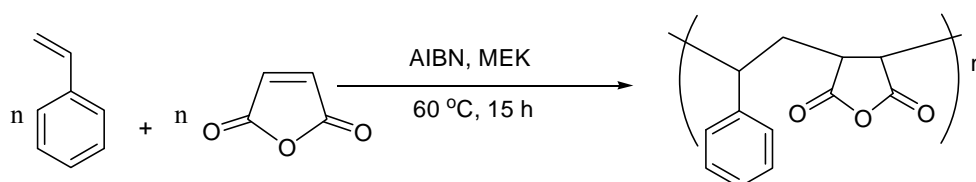
3.1.2 Synthesis of Styrene-maleic anhydride copolymer (SMA-P)

20 g (192 mmol) of styrene and 18.8 g (192 mmole) of MAnh were placed in a 500 mL three neck flask containing 250 mL MEK.¹ 0.65 g AIBN (1 mole-% based on monomer feed) was added to the flask under N_2 . After 15 min of purging, the flask was immersed in a preheated oil bath set with a temperature controller at 60 °C. Scheme 3.1 illustrates the chemical

reaction of the polymerization. The reaction was stopped after 15 h. The polymer was precipitated in 2-propanol to give SMA-P.

Yield: 39g of white solid.

The molecular weight and \bar{D} from SEC: $\bar{M}_n = 128\ 000$ g/mol, $\bar{D} = 2.7$.



Scheme 3.1: Radical alternating copolymerization of styrene and maleic anhydride

Characterization results:

NMR spectroscopy:

$^1\text{H-NMR}$ spectrum of SMA-P is shown in Figure 3.1 (A). Phenyl protons appear between $\delta = 6.0\text{--}7.6$ ppm, and the methine (c) protons appear between 2.94 and 3.65 ppm. The broad peak between 1.6–2.8 ppm corresponds to the chemical shift of ($-\text{CH}_2-$ and $-\text{CH}-$) protons of the copolymer backbone. The styrene/maleic anhydride ratio was calculated from the integration ratio of the (5H) aromatic protons of styrene and the (2H) methine protons of maleic anhydride. The ratio obtained is approximately 1:1 of styrene to anhydride units.

From the $^{13}\text{C-NMR}$ spectrum (Figure 3.1 (B)) the triad sequence of styrene and maleic anhydride was determined to have an alternating microstructure. As reported by Ha *et al*² and Leassard *et al*,³ the quaternary aromatic carbon (C7) and the methylene ($-\text{CH}_2-$) polymer chain carbon (C1), are the predominant markers to be sensitive to the centered triad sequence distribution observed by the $^{13}\text{C-NMR}$ spectra.

A perfectly alternating sequence has a C7 resonance in the range $\delta = 137\text{--}140$ ppm, and a C1 resonance around 33–37 ppm.³ From Figure 3.1 (B) it is clear that the quaternary carbon C7 appears in the same ppm range at $\delta = 136\text{--}141$ ppm. Furthermore the C1 has a resonance $\delta = 31.50\text{--}36.66$ ppm. The prepared SMA copolymer therefore has a highly alternating sequence of styrene and maleic anhydride units along the polymer backbone.

Chapter 3: Synthesis and characterization of styrene-maleimide copolymer derivatives

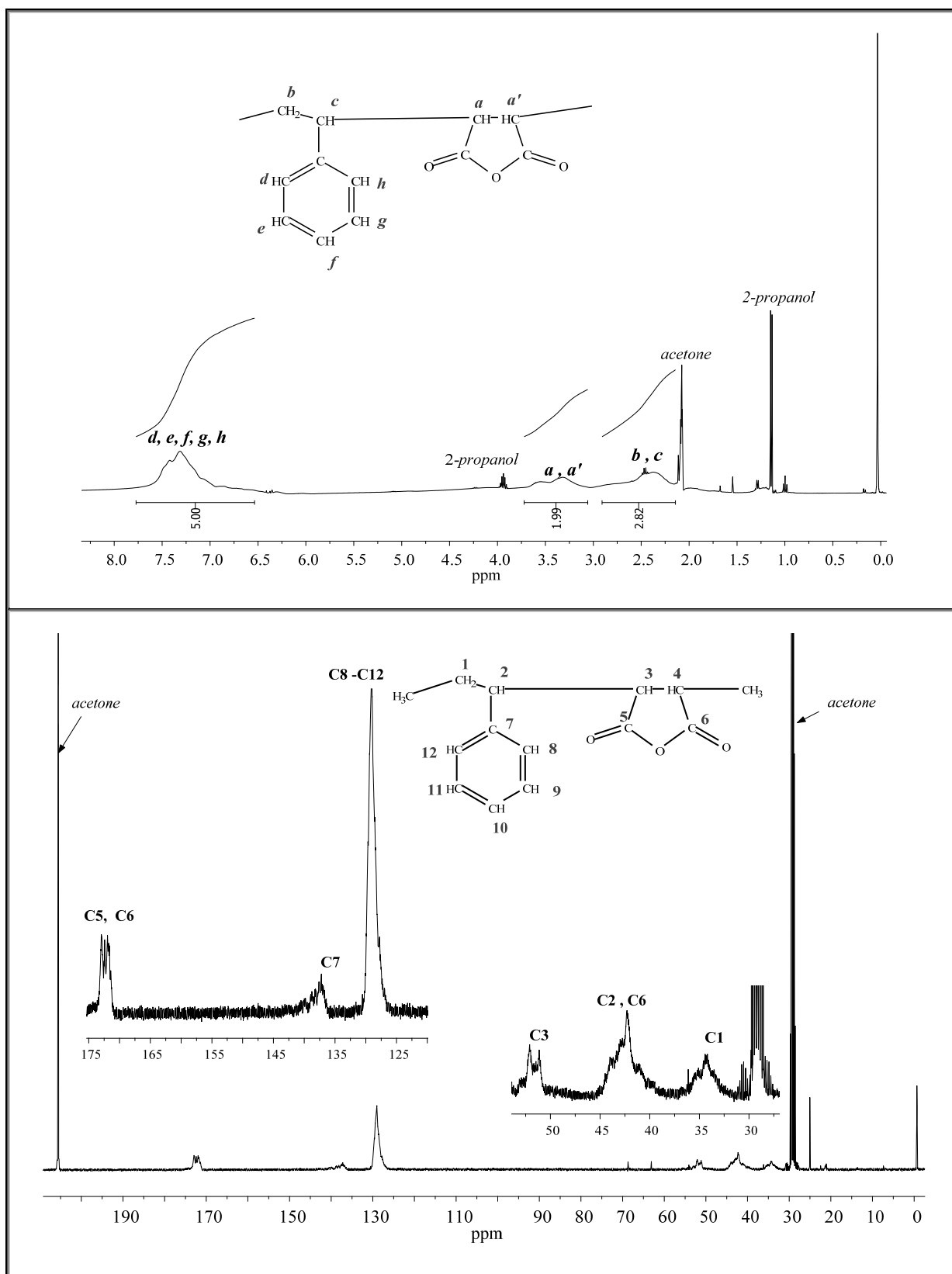


Figure 3.1: $^1\text{H-NMR}$ and $^{13}\text{C-NMR}$ spectra of SMA-P in acetone- d_6 .

ATR-FTIR spectroscopy

Figure 3.2 shows the ATR-FTIR spectrum of SMI-P. The absorption bands at 1855 and 1770 cm^{-1} are characteristic for asymmetric and symmetric C=O stretching vibrations from the anhydride groups, while the signals at 1605 cm^{-1} and 1500 cm^{-1} are caused by (C=C) stretching of the aromatic ring and (C-H) bending vibration of the aromatic ring respectively. Bands at 916, 1078 and 1220 cm^{-1} are due to cyclic anhydride groups.⁴

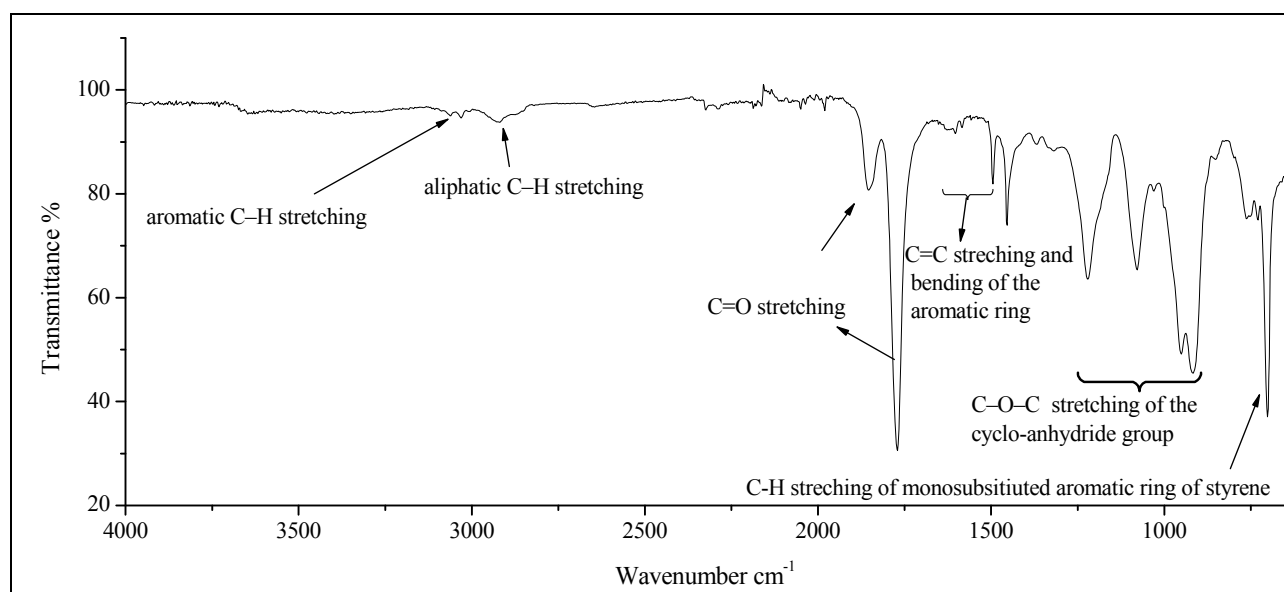


Figure 3.2: ATR-FTIR spectrum of SMA-P.

3.2 Modification of SMA with various amino-compounds

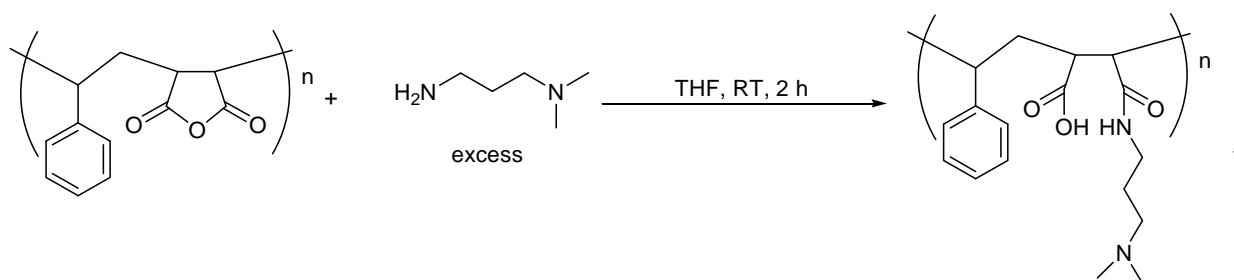
Three amino compounds, namely 3-dimethylaminopropylamine (DMAPA), *n*-aminobutane and 2-aminoethanol were used to modify the SMA copolymers. The fourth amino compound was used to synthesize a maleimide derivative from 4-aminophenol and MANh, then copolymerized with St.

3.2.1 Preparation of styrene-dimethylaminopropylmaleimide copolymer (SMI-P)

SMI-P and SMI-C were prepared by treating SMA with 3-dimethylaminopropylamine (DMAPA) as follows:

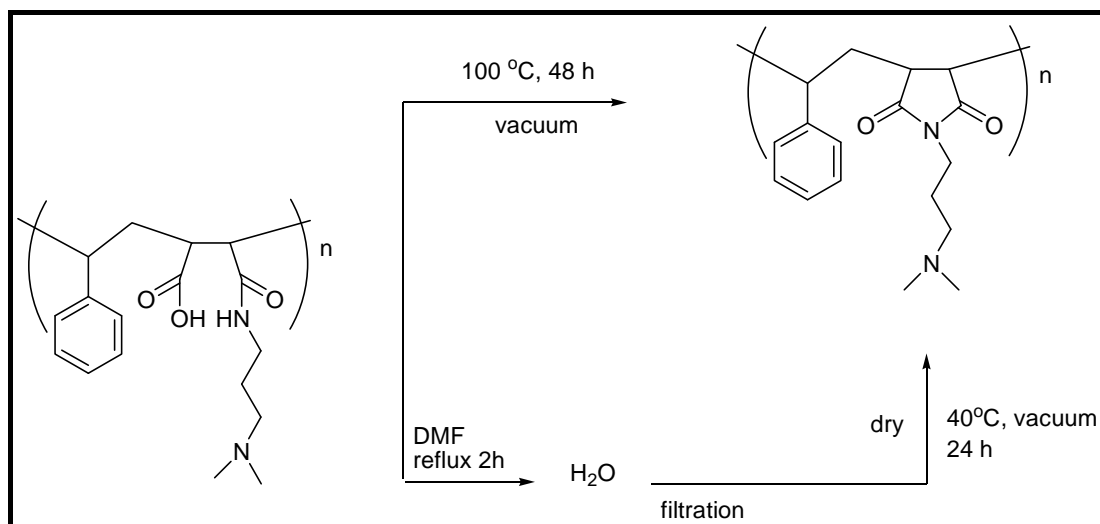
15 g of SMA-P was placed in a 1 L Erlenmeyer flask and 400 mL THF was added to dissolve the polymer. 30 mL (0.238 mol) (15 mL in the case when added to SMA-C) of DMAPA was placed in a dropping funnel with 100 mL THF. The DMAPA solution was added dropwise at room temperature over a period of 30 min and the mixture stirred for another 2 hours. The anhydride groups react rapidly with the primary amine of DMAPA, causing ring opening and formation of the amide linkages. (Scheme 3.2) The white precipitate was filtered off, washed with pentane and dried under vacuum at 100 °C for 24 h to obtain SMI-P.

Yield 19.0 g, of light yellow solid.



Scheme 3.2: Preparation of styrene-dimethylaminopropylmaleimide copolymer

Alternatively the SMI was also prepared by treating SMA with DMAPA in DMF.⁵ In a similar procedure to that previously described when using THF as a solvent, DMAPA was added to the polymer solution in DMF and precipitation of the polymer out of solution was also observed. The polymer suspension was heated gradually bringing it to reflux. The suspension gradually cleared up with increasing temperature and was refluxed for another 2 h. From literature, a reaction time of 4 to 8 hr at temperatures of 140 to 180 °C should be sufficient for complete imidization of Manh in organic solvents.⁶ The solution was cooled and precipitated in water and re-dissolved in methanol and precipitated in diethyl ether. The obtained polymer was dried in vacuum at 40 °C for 24 h.



Scheme 3.3: Ring closure of reacted SMA with DAMPA (imidization step).

Characterization results:

ATR-FTIR spectroscopy

Figure 3.3 shows the ATR-FTIR spectra of the SMA-P and its maleimide derivative and the intermediate ring opened derivative before the imidization step. The first step is the anhydride ring opening reaction that is demonstrated by the complete disappearance of the carbonyl anhydride peaks at 1855 and 1770 cm^{-1} , and the C-O-C stretching bands of the cyclic anhydride between 916 and 1220 cm^{-1} . The evidence of the imidization step was confirmed by observing the shift of C=O carbonyl anhydride peak to 1770 and 1689 cm^{-1} , which are characteristic to the asymmetric and symmetric C=O stretching vibrations of the formed imide groups.⁴ In this imidization step, the conversion of the anhydride into imide was complete, since no more anhydride or amic acid signals were observed.

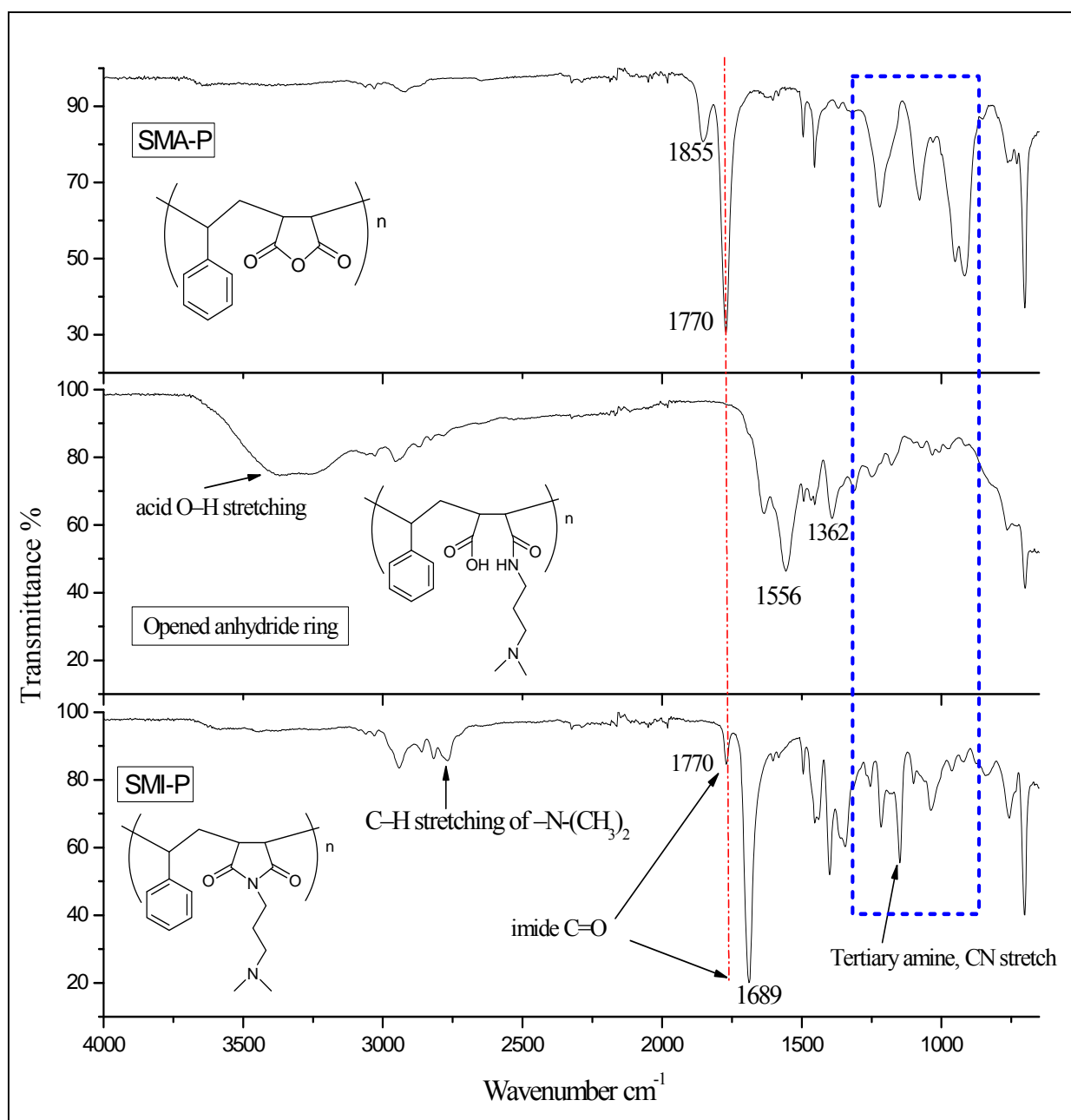


Figure 3. 3 ATR-FTIR spectra of SMI-P modification steps from SMA-P

NMR spectroscopy

Figure 3.4 shows stacked ^{13}C -NMR spectra of SMA-P and SMI-P. The peaks at 172.5 and 173.7 ppm in the upper spectra in the figure are characteristic to the carbonyl anhydride chemical shifts. The conversion of the anhydride to an imide can be seen in the lower spectrum as the peak shifts of (C_e , C_e') carbons are shifted downfield to 176.9 and 177.8 ppm. The complete absence of any resonance at the previous chemical shift values of the anhydride, suggests that all anhydride groups have been successfully opened and reacted

with DMAPA which supports the ATR- FTIR analysis results. Other new peaks appeared in the spectrum are the aliphatic signals of the methyl (C_a , C_a' Figure 3.4) at 45.23 ppm; and the methylene groups (C_b , C_c and C_d) at 56.14, 24.61 and 36.02 ppm respectively. The ^1H -NMR spectrum of SMI-P is shown in (Figure 3.5) with chemical shifts assigned to the individual protons of the polymer structure.

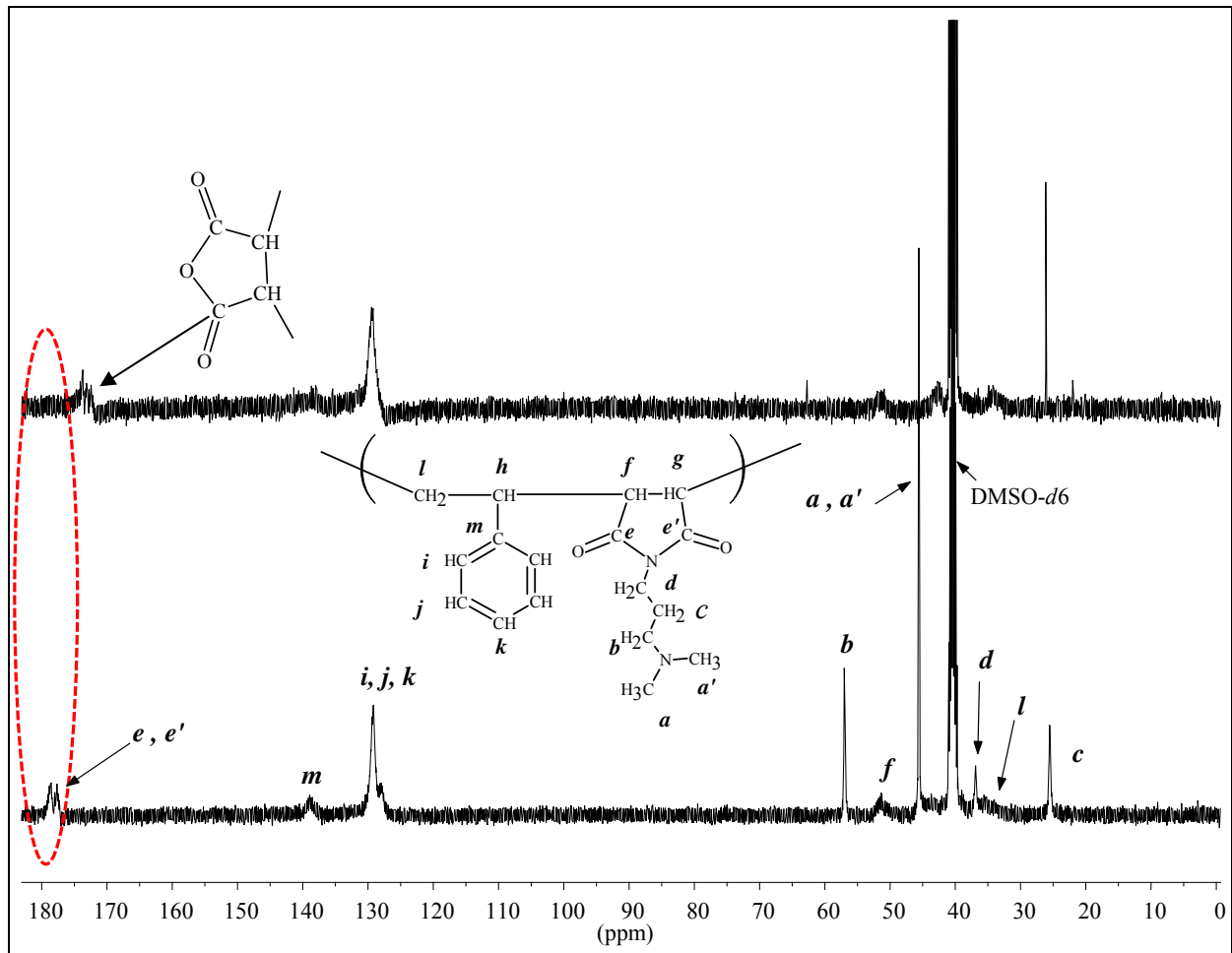


Figure 3.4: ^{13}C -NMR spectra of SMI-P and SMA-P in $\text{DMSO-}d_6$

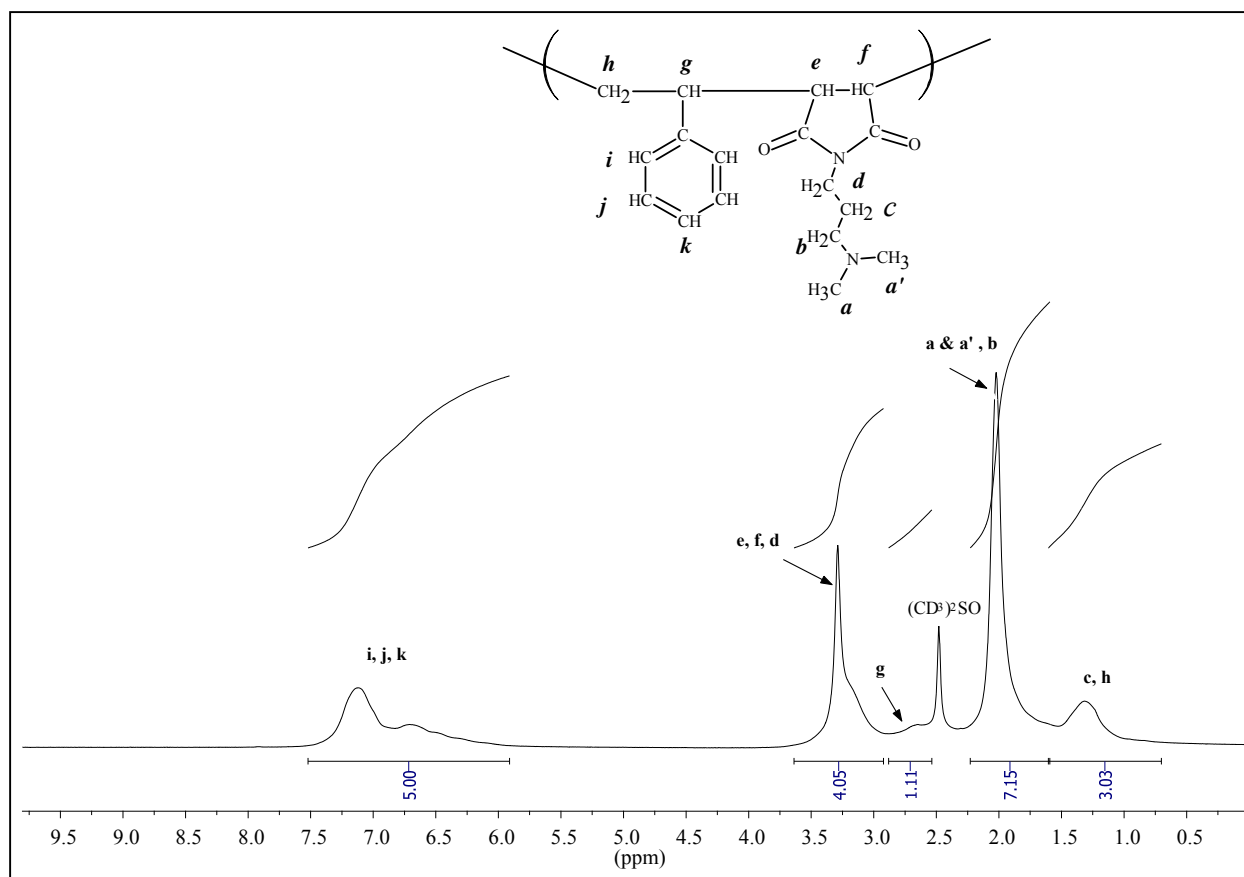
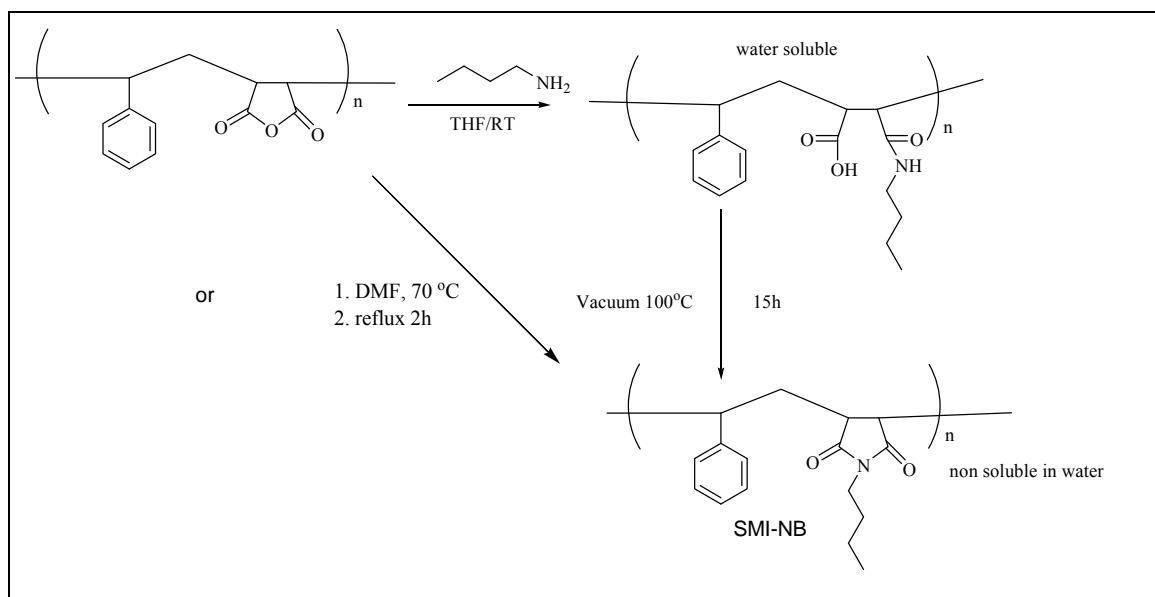


Figure 3. 5: ¹H-NMR spectrum of SMI-P in DMSO-*d*₆.

3.2.2 Preparation of Styrene-*n*-butylmaleimide copolymer (SMI-NB)

SMI-NB was prepared by treating SMA-P with *n*-butylamine. Typically, 5 g of SMA-P was dissolved in 70 mL of DMF. 7.5 mL (76 mmol) *n*-butylamine was then added drop wise at 70 °C. Immediate precipitation was observed during the addition of the butyl amine indicating the reaction of the anhydride groups with the primary amino groups forming amide linkages. The suspension was stirred and gradually heated to reflux. As the temperature increased, the suspension started to become clearer, most likely indicating ring closure and formation of the imide groups. The solution was refluxed for 2 hours, then cooled to room temperature and the product precipitated in diethylether. The solid polymer was dried under vacuum at 60 °C for 24 h. This polymer was also prepared in a two step reaction, using THF as a solvent. (See Scheme 3.4)

Yield 5.8g off-white solid.



Scheme 3.4: preparation of SMI-NB

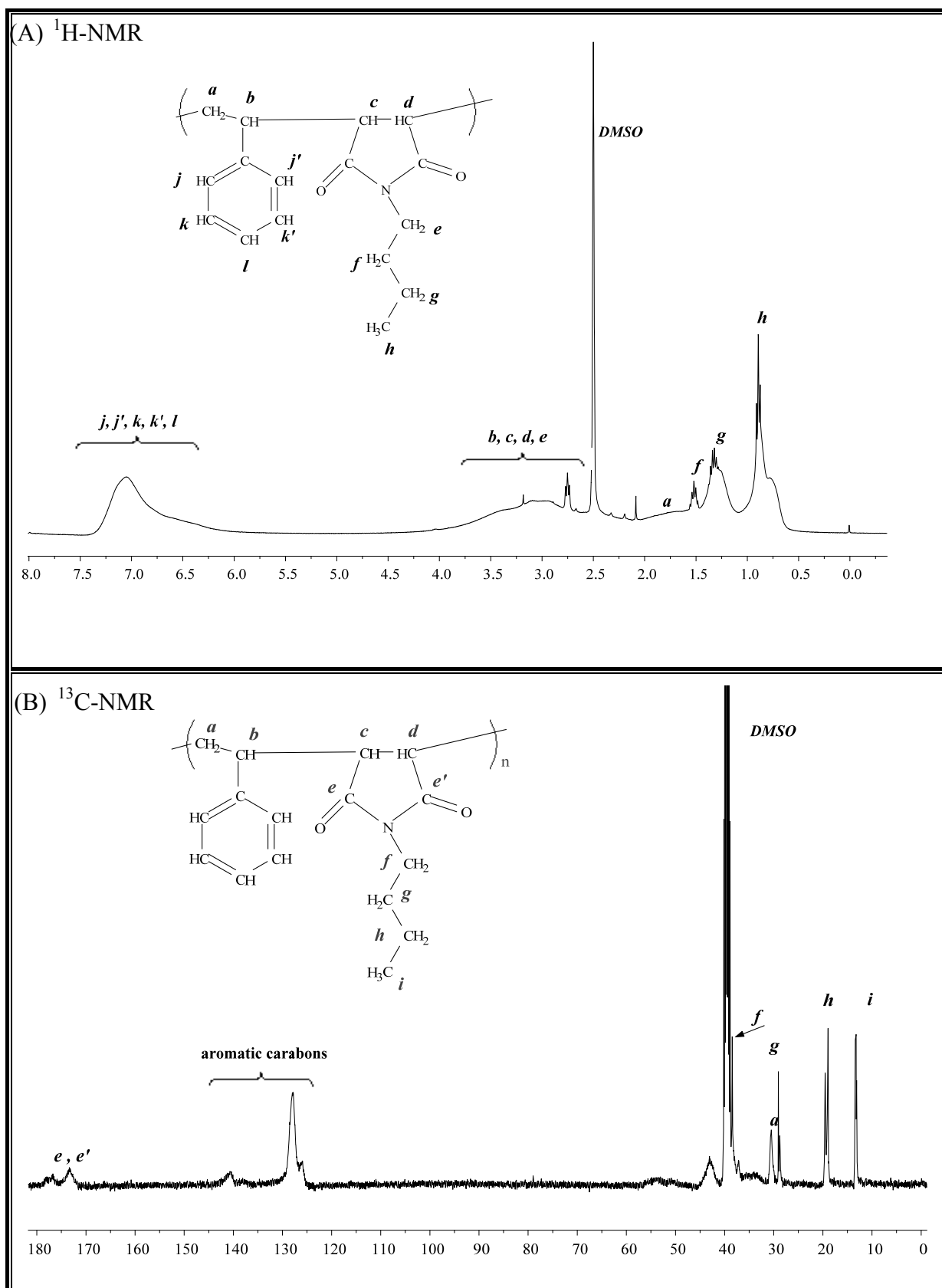
NMR spectroscopy

The ¹H-NMR spectrum of SMI-NB is shown in Figure 3.6. The signals between 0.6–1.6 are assigned to the (–CH₃ and –CH₂–) aliphatic hydrogen linked to the n-butyl chain.

The aromatic hydrogen in the phenyl ring are indicated by a broad peak between 6.2 and 7.5 ppm.

The ¹³C-NMR spectrum is shown in Figure 3.7. Chemical shift assignments of the aliphatic carbons of the butyl chain are assigned at 13.4 ppm (–CH₃); 19.2, 29 (–CH₂–); 38.5 ppm signal corresponds to (N–CH₂–) carbon. The (–CH₂–) of the backbone is assigned at 30.5 ppm. Resonance signals at 173 and 177 ppm are assigned to the carbonyl carbon of the imide group.

Chapter 3: Synthesis and characterization of styrene-maleimide copolymer derivatives



ATR-FTIR spectroscopy

Besides NMR spectroscopy, the imidization of the anhydride groups was further verified with ATR-FTIR. Figure 3.7 demonstrates the FTIR spectra of SMI-NB and the precursor SMA-P. It can be seen, that the peaks corresponding to asym./sym. (C=O stretching) have shifted from 1855 & 1770 cm^{-1} in the anhydride to 1690 cm^{-1} due to (C=O stretching) indicating the imidization step is complete. The C–H stretching vibration of the (–CH–) backbone is at 2871 cm^{-1} . Bands at 2930–2958 cm^{-1} are due to (C–H stretching of methyl and –CH₂– groups). Weak bands at 3028–3066 are assigned to the aromatic C–H stretching vibrations.

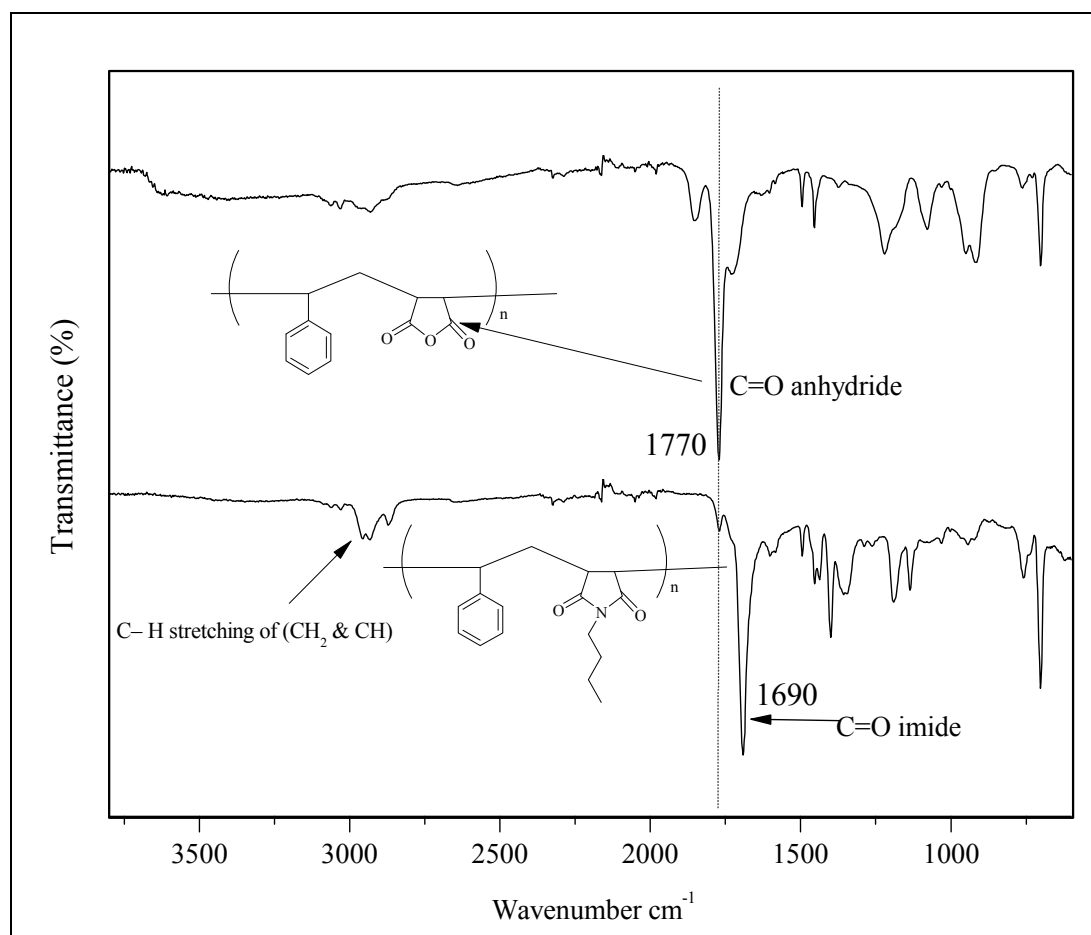
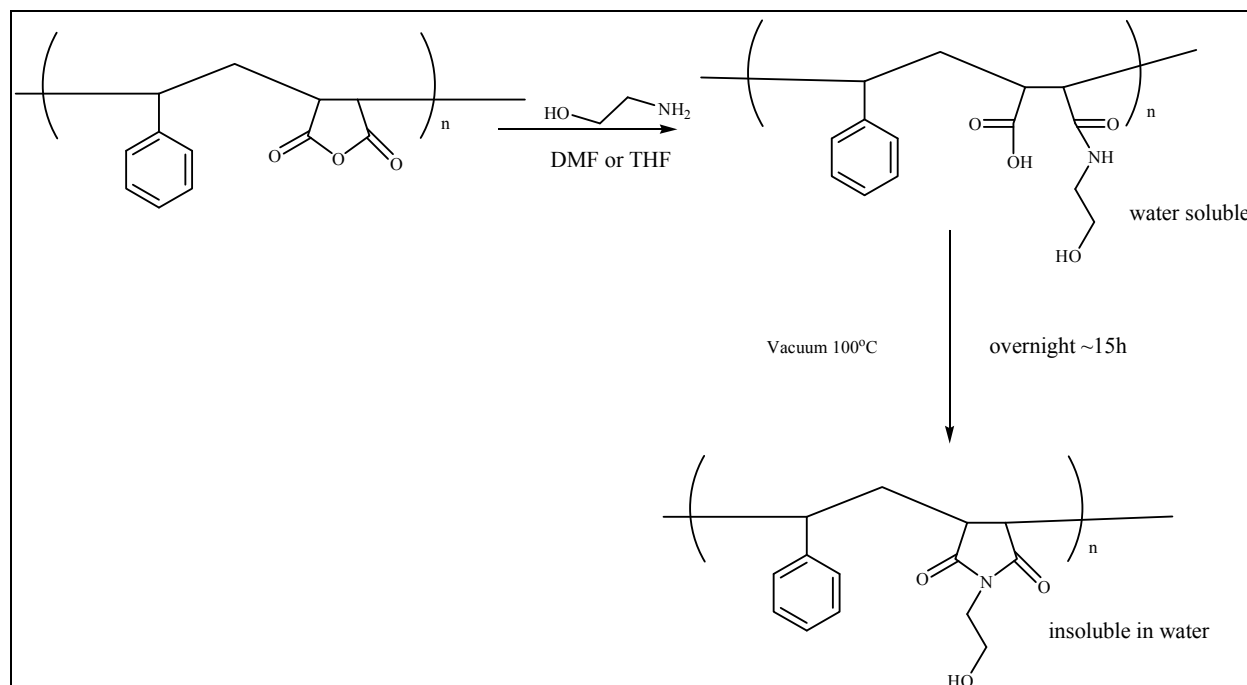


Figure 3.7: ATR-FTIR spectra of SMI-NB modified from SMA-P.

3.2.3 Preparation of styrene-N-(2-hydroxyethyl)maleimide copolymer (SMI-AE)

In a 250 mL round bottom flask, 5 g of SMA-P was dissolved in 70 mL DMF. 5 mL (83 mmol) of 2-aminoethanol was added dropwise at 70 °C. Immediate precipitation was noticed upon the addition. This indicated opening of the anhydride moieties when reacted with the primary amine. After complete addition, the suspension was heated to reflux. The solution gradually started to clear after reaching 120 °C and the clear solution was further refluxed for 2 hours for complete ring closure. In case of the reaction run in THF the precipitate was filtered off and resuspended in DMF and refluxed for the ring closing step. (Scheme 3.5)

The polymer solution was first poured into 200 mL diethylether. The sticky polymer precipitate was redissolved in THF and again precipitated in pentane. An alternative way to isolate the product is by centrifuge. Here the polymer solution was precipitated in water. The formed suspension was difficult to filter off as it sticks to the surface of the filter and was clogging the pores. After centrifuging the suspension, the solid polymer was removed and added to a beaker containing 150 mL distilled water. The suspension was stirred vigorously for 2 hours at room temperature. The polymer was then filtered and dried at 60 °C in a vacuum oven to yield 4.6 g of a white-cream solid.



Scheme 3.5: representation of SMI-AE preparation.

NMR spectroscopy

The ^1H -NMR spectrum of SMI-AE is shown in Figure 3.8. The broad singlet peak at approximately 4.6 ppm is assigned to the hydrogen in the hydroxyl ($-\text{OH}$) groups. The integral ratio of phenyl (5H) (6.2–7.5 ppm) to the hydroxyl protons was about (5:1) as shown in the figure. This result supports the fact that the SMA-P precursor was indeed an alternating copolymer and the imidization reaction went to completion.

The ^{13}C -NMR spectrum of SMI-AE is demonstrated in Figure 3.9. The peak at 57.1 ppm is attributed to the carbon adjacent to the hydroxyl groups. The imidization reaction was confirmed by the evident shift of the carbon signals from (172.3 and 171.5 ppm Figure 3.4) in the anhydride groups to 178.1 and 177.1 ppm of the imide carbonyl groups.

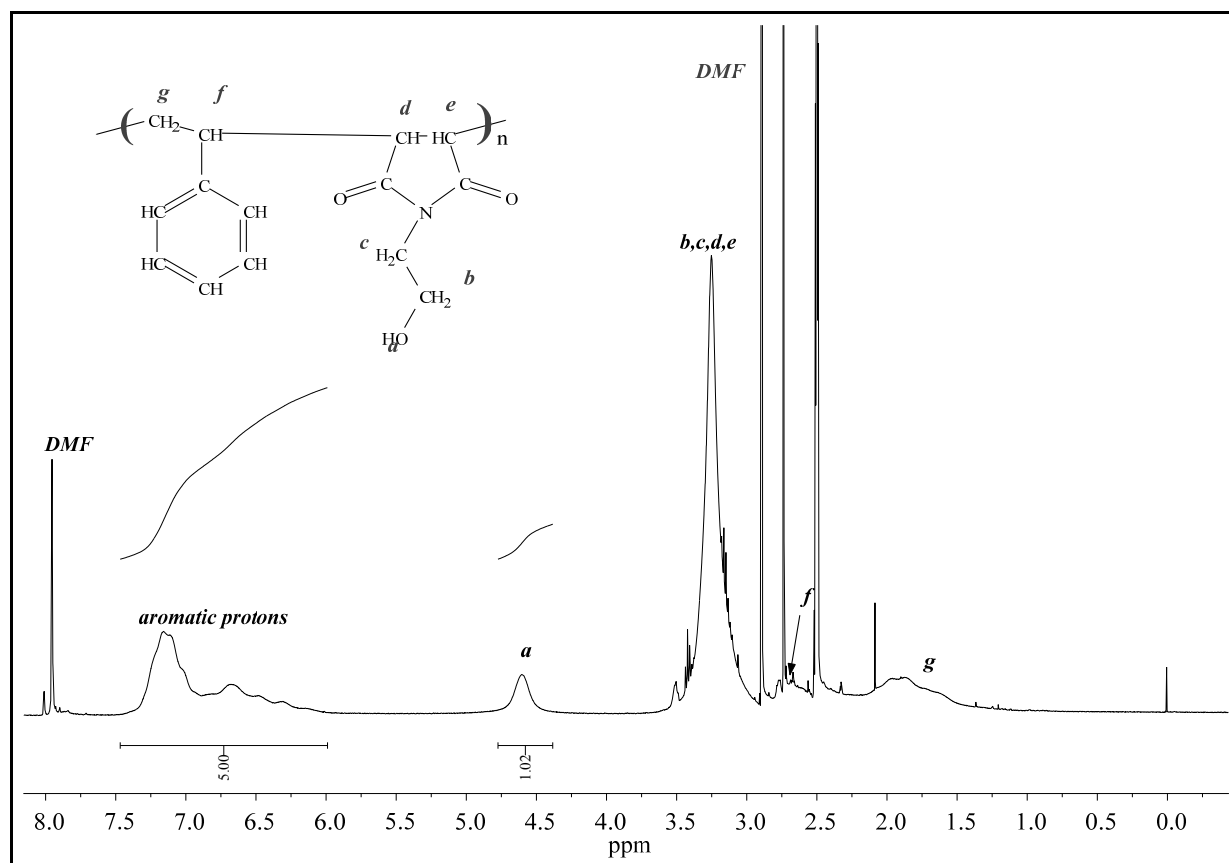


Figure 3.8: ^1H -NMR spectrum of SMI-AE in DMSO-d_6 .

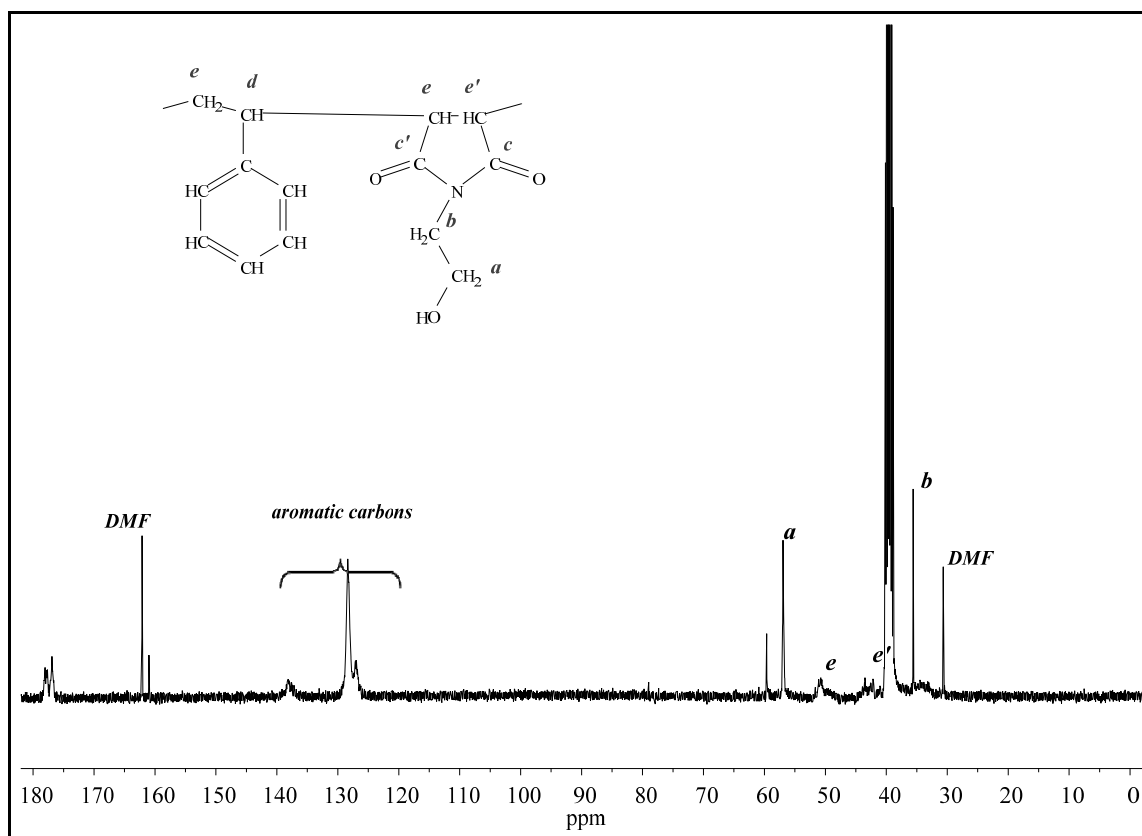


Figure 3.9: ^{13}C -NMR spectrum of SMI-AE in $\text{DMSO-}d_6$.

ATR-FTIR spectroscopy

ATR-FTIR spectroscopy was also used to follow the imidization reaction of SMA-P with 2-aminoethanol. Figure 3.10 demonstrates the ATR-FTIR spectra of imidization steps. It can be seen that the ring-opening reaction resulted in the formation of carboxylic and amide groups as the (C=O stretching) of the anhydride groups at 1853 and 1774 cm^{-1} completely disappeared. However, the formation of the imide groups of SMI-AE was evident by a clear shift of the (C=O stretching) to 1687 and 1768 cm^{-1} . The broad band centered at 3400 cm^{-1} is assigned to the stretching of hydroxyl O–H groups.

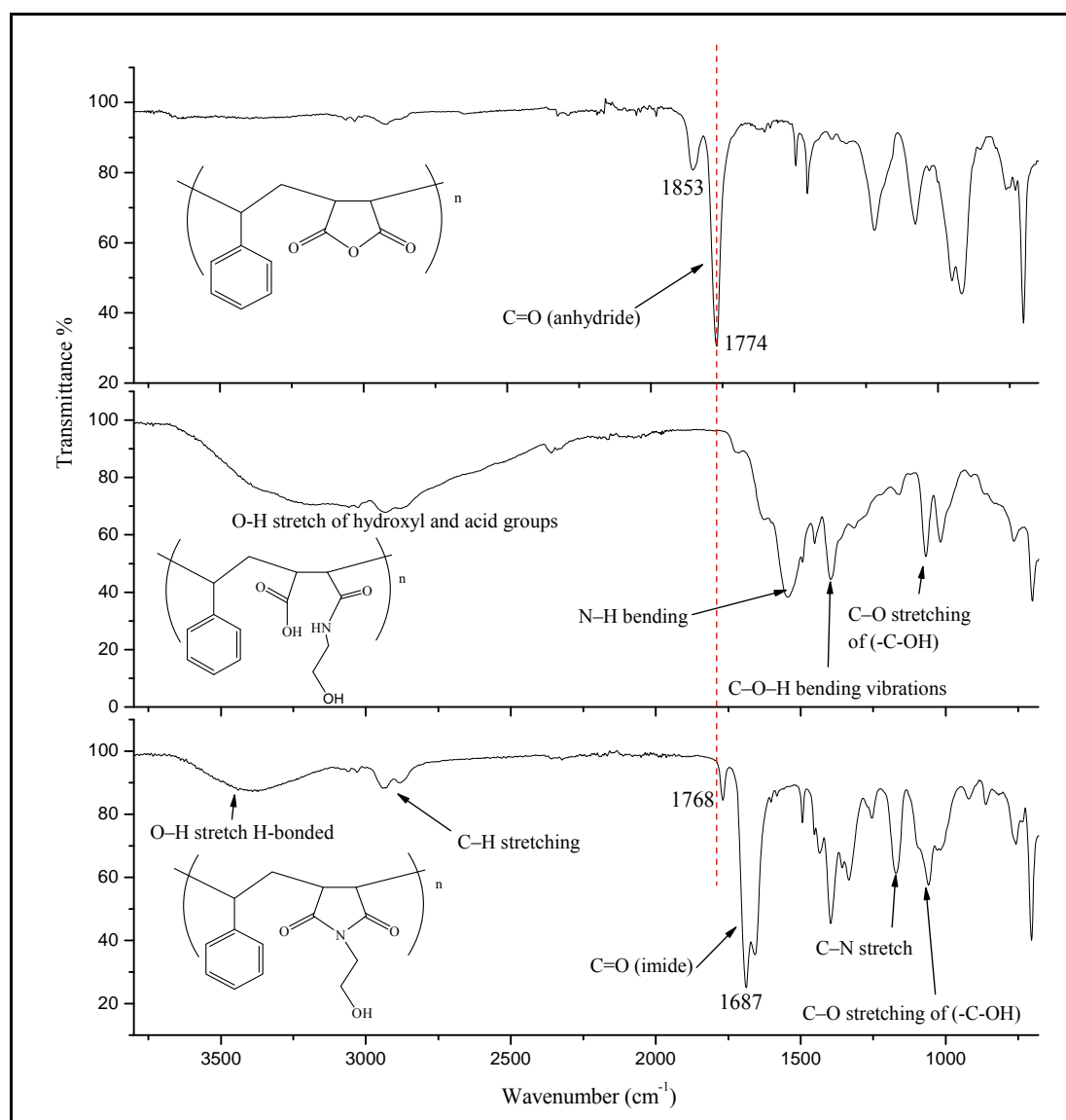


Figure 3.10: ATR-FTIR spectra of SMI-AE, illustrating the imidization reaction steps from SMA-P.

3.2.4 Preparation of styrene-N-(p-hydroxyphenyl)maleimide copolymer (SMI-AP)

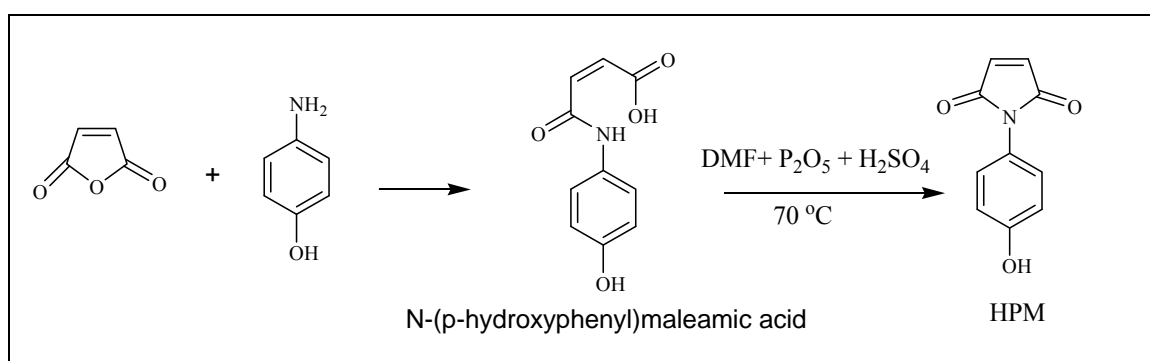
3.2.4.1 Preparation of 4-hydroxyphenyl maleimide monomer (HPM)

The preparation of HPM was carried out according to the procedure of Oba *et al.*⁷, whereby 21.6 g (220 mmol) of maleic anhydride were placed in a 250 mL round bottom flask containing 50 mL of DMF. 21.8 g (200 mmol) of p-aminophenol were gradually added at room temperature with thorough stirring. After completion of the addition, the reaction was allowed to proceed at room temperature for 2 hours to yield N-(p-hydroxyphenyl)maleamic

acid. To the reaction mixture, a previously formed solution containing 70 mL of DMF, 11.4 g (80.3 mmol) of phosphorus pentoxide and 5 g (49 mmol) of sulfuric acid was added dropwise using a dropping funnel. Thereafter, the reaction was continued at 70°C for 2 hours. After cooling to room temperature, the resulting reaction mixture was poured into 400 mL of ice water to precipitate HPM in the form of a yellow solid. The solid was separated by filtration, washed with water and then dried at 60 °C in vacuum overnight to obtain N-(p-hydroxyphenyl)maleimide.

Yield: m= 26.5g (70%) bright yellow crystals.

Melting point (mp): 184 °C. mp (literature ⁸)189 °C



Scheme 3.6: preparation of HPM

NMR spectroscopy

¹H-NMR (300 MHz, DMSO-*d*₆) δ 9.71 ppm (s, 1H, OH), 7.11 (s, 1H, *a*, *a'*), 7.11–7.05 (m, 2H, *b*, *b'*), 6.87–6.80 (m, 2H, *c*, *c'*). Figure 3.11 (A)

¹³C-NMR (75 MHz, DMSO-*d*₆) δ 170.26 ppm (*b*, *b'*), 157.05 (*f*), 134.53 (*a*, *a'*), 128.44(*d*, *d'*), 122.54 (*c*), 115.45 (*e*, *e'*). Figure 3.11 (B)

Chapter 3: Synthesis and characterization of styrene-maleimide copolymer derivatives

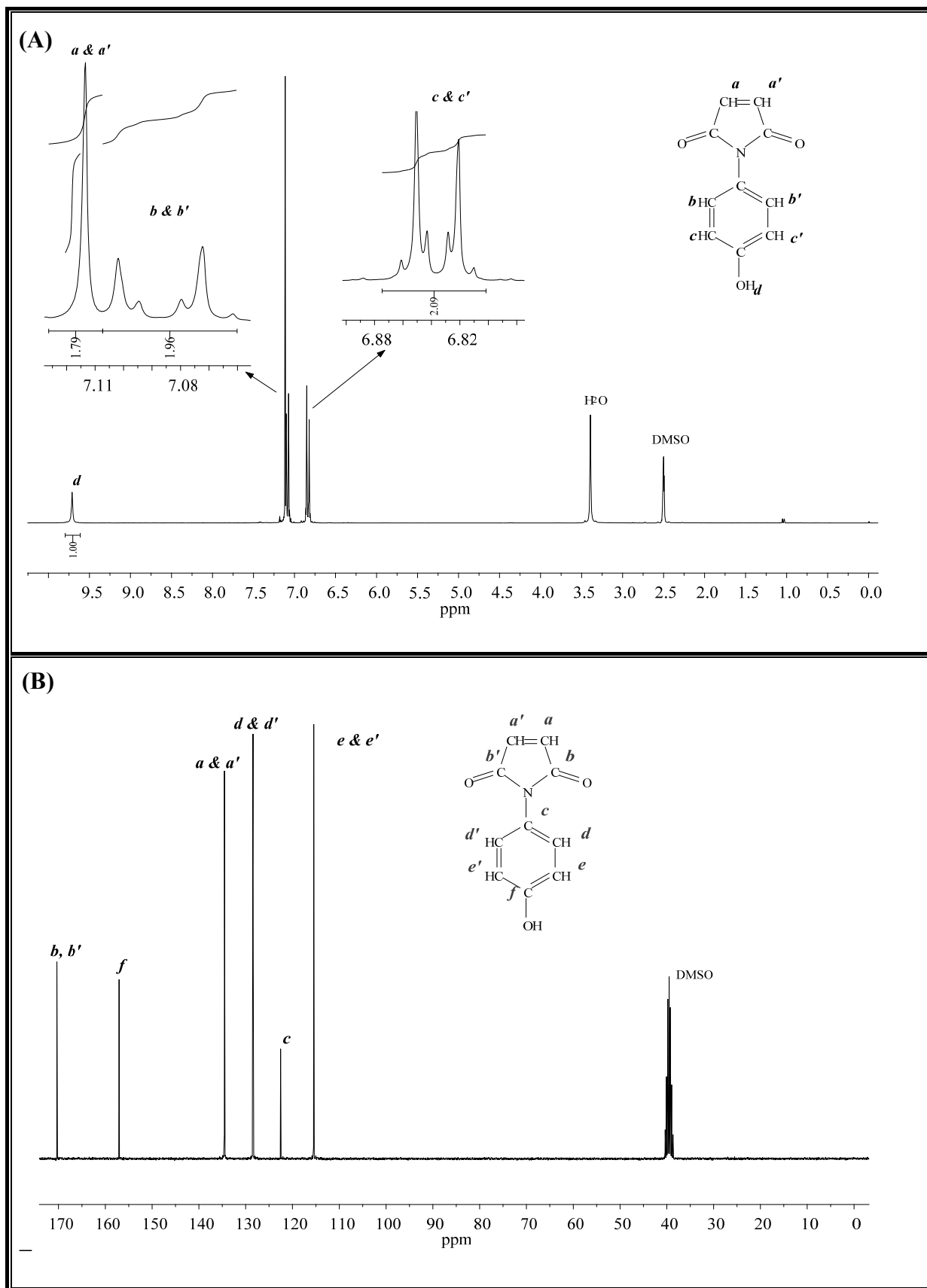


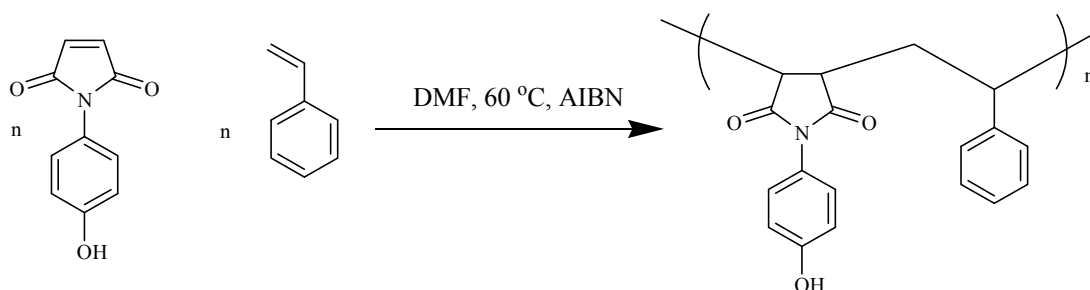
Figure 3.11: ^1H and ^{13}C -NMR spectra of HPM in $\text{DMSO-}d_6$.

3.2.4.2 Free radical copolymerization of HPM and styrene⁹

In a 250 mL round bottom flask, 100 mL of DMF was added followed by 10 g (52.8 mmol) of HPM and 5.15 g (25.8 mol) styrene. 0.15 g of AIBN initiator (1 % , based in total moles of both monomers) was then added to the reaction mixture. The flask was purged with N₂ gas for 10 minutes before it was immersed in a preheated oil bath at 60 °C. Scheme 3.8 shows the chemical reaction of the polymerization. After 16 hours, the reaction was cooled at room temperature and the product precipitated in methanol and dried in vacuum oven at 80 °C.

Yield 11.7 g of SMI-AP as white-pale solid.

The molecular weight and Đ were obtained using SEC $M_n = \sim 16\,000$ g/mol, Đ = 2.0;



Scheme 3.7: Radical copolymerization of HPM and styrene.

NMR spectroscopy

The ¹H-NMR spectrum of SMI-AP is presented in Figure 3.12 (A). The resonance signal at 9.6 ppm corresponds to the hydrogen of the phenolic OH. The aromatic hydrogen of the phenyl rings appear as two medium broad peaks centered at 7.1 and 6.7 ppm respectively. The sharp peak signal at 3.2 ppm is attributed to the aliphatic (–CH–) backbone protons. A weak broad peak centered around 2 ppm corresponds to the styrene (–CH₂–) protons. The integration ratio for OH and phenyl protons is about 1:9 which is consistent with the alternating polymer structure.

The ¹³C-NMR spectrum is demonstrated in Figure 3.12(B). The signal at 157.7 ppm is assigned to the phenolic carbon (–C–OH). Carbon signals corresponding to the phenyl rings appear typically between 115.8–138.3 ppm. The signals at 51.7 and 43.3 ppm are attributed to the backbone (–CH–) carbons, in addition the signal at 34.8 ppm is assigned to the (–CH₂–) carbon.

Chapter 3: Synthesis and characterization of styrene-maleimide copolymer derivatives

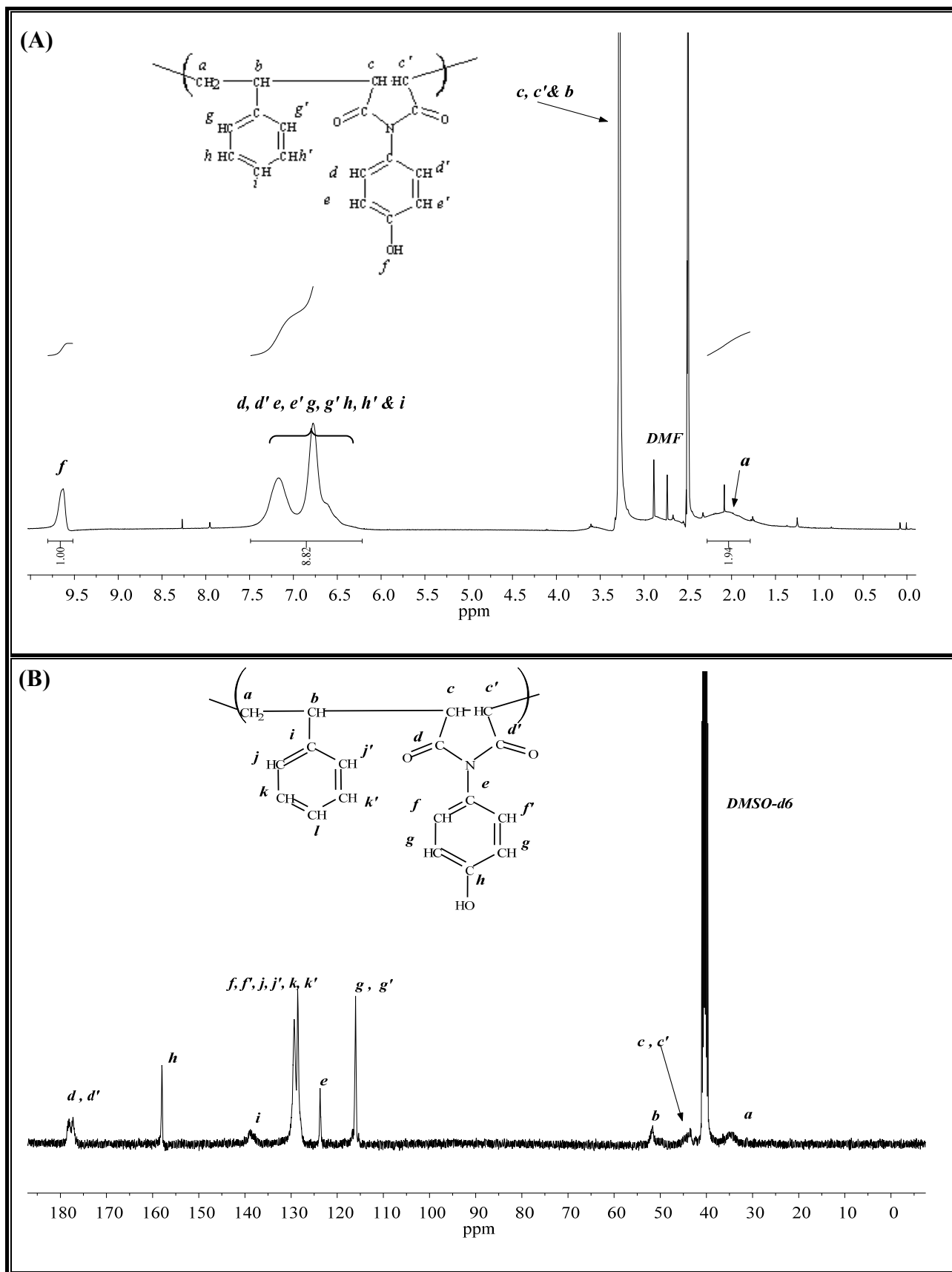


Figure 3.12: ^1H and ^{13}C -NMR spectra of SIM-AP in $\text{DMSO-}d_6$.

ATR-FTIR spectroscopy

ATR-FTIR spectra of HPM and SMI-AP are shown in Figure 3.13. In the HPM spectrum, it is observed that the (C=O) stretch of the imide groups appear at 1679 cm^{-1} and a band at 3110 cm^{-1} which is characteristic for the alkene C–H stretching of maleimide. The sharp peak at 820 cm^{-1} is attributed to the aromatic (C–H) 1,4-disubstitution (para) out-of-plane bend. The O–H stretch of the phenol is observed at 3477 cm^{-1} . The spectrum of SMI-AP clearly shows the disappearance of the alkene C–H stretching after copolymerization, and a new band at appears at 754 cm^{-1} attributed to the mono-substituted aromatic C–H bending. The C–H stretch of the aliphatic groups of the polymer backbone is observed as a weak band at 2925 cm^{-1} .

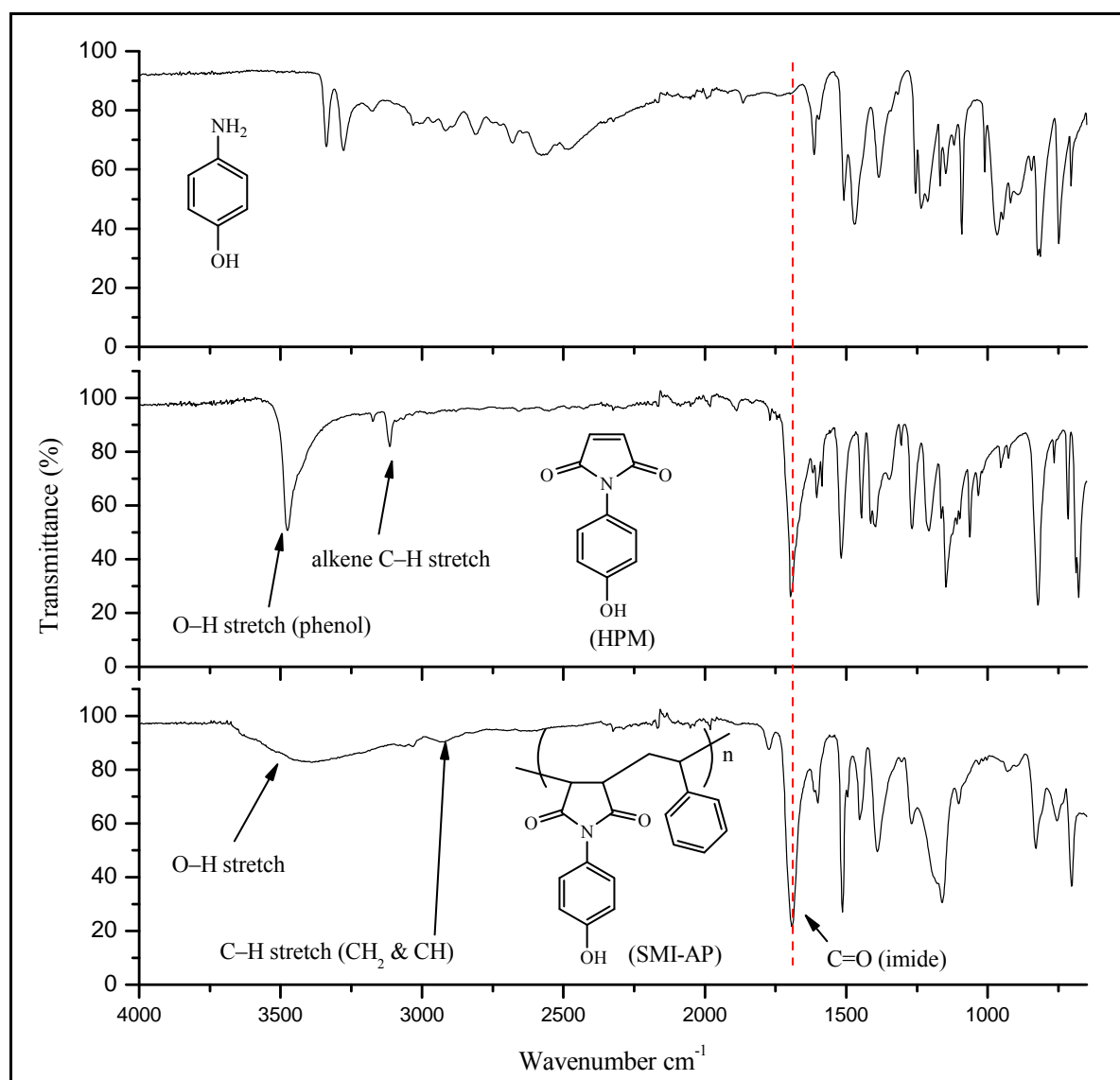


Figure 3.13: ATR-FTIR spectra of HPM and SMI-AP.

3.3 Quaternization of SMI copolymer with alkyl halides

A series of quaternized SMI copolymers was prepared by treating SMI-P and SMI-C with various alkyl halides. Figure 3.14 shows the chemical structures of the quaternized polymeric materials prepared in this study.

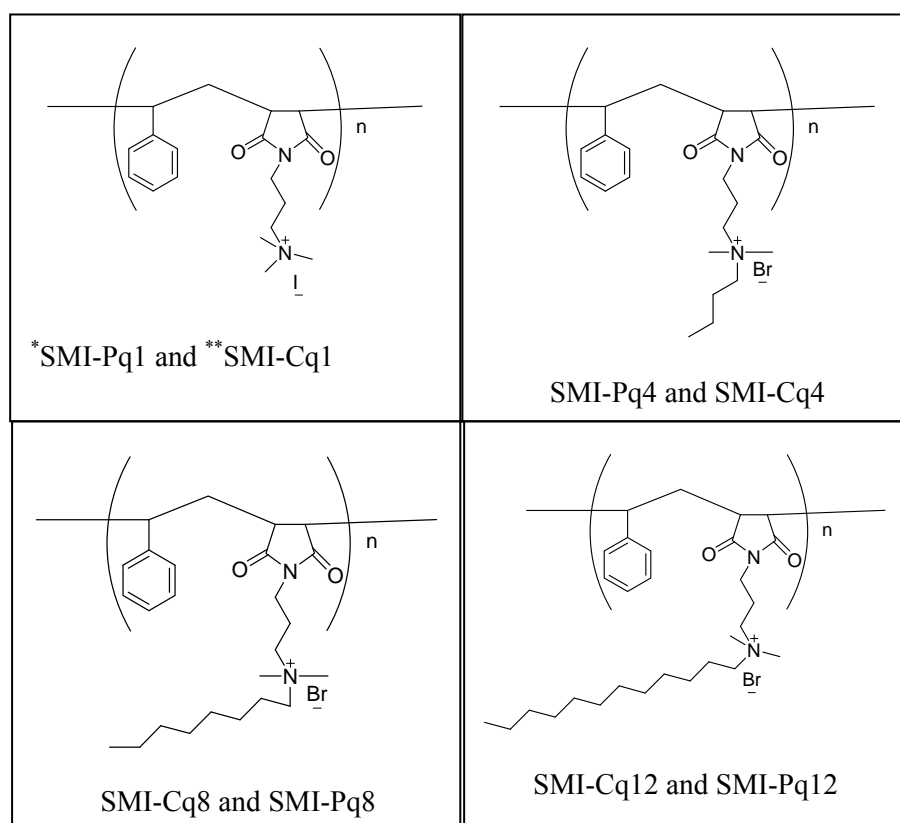


Figure 3.14: Chemical structure of quaternized SMI derivatives. * The letter P here refers to modified copolymers from the prepared alternating copolymer precursor SMI-P. **The letter C refers to modified copolymers prepared from the commercial precursor of SMI-C.

Methyl iodide was used for the preparation of methyl iodide quaternized styrene-dimethylaminopropylmaleimide (SMI-Pq1). Alkyl bromides containing 4, 8, and 12 carbon atoms were also used for the quaternization of SMI copolymers. The quaternized polymers will be described in abbreviation letters according to each class, for instance SMI-Cq_n represents the commercial based SMA derivatives and SMI-Pq_n for the prepared ones. The variable *n* refers to the number of carbons present in the alkyl halide quaternized polymer. For example SMI-Cq1 is a quaternized SMI-C polymer with methyl iodide which has only one carbon atom. Figure 3.14 illustrates the type of quaternized polymers that have been

prepared and their abbreviation codes. The polymers were characterized by $^1\text{H-NMR}$ and $^{13}\text{C-NMR}$ spectroscopy and ATR-FTIR. The assigned NMR spectra shown here are for the quaternized polymers based on alternating SMA-P copolymers, the same results were obtained for the commercial SMA-C based polymers.

3.3.1 Methyl iodide quaternized styrene-*N,N*-dimethylaminopropyl maleimide) copolymer

3.3.1.1 Preparation of SMI-Pq1

3 g of SMI-P was placed in a 100 mL round bottom flask containing 50 mL of DMF. After dissolving the polymer, the flask was allowed to cool in an ice bath to 10 °C, then 2 mL (16.4 mmol, excess) was added at once and stirred while cooled for 4 hours, followed by room temperature stirring for 20 hours. The quaternized polymer was precipitated in diethyl ether and dried in a vacuum oven at 50 °C for 25 h.

Yield 4.52 g of light-yellow flaky solid.

3.3.1.2 Preparation of SMI-Cq1

10 g of SMI-C was dissolved in 75 mL THF at room temperature and allowed to cool to 10 °C using an ice-bath. 5 mL (80 mmol, excess) of methyl iodide was then added and the mixture stirred. A change to light yellow color was observed after a few minutes of reaction. A yellow solid started to precipitate out of solution during the reaction time, which indicated that the quaternized polymer was forming. The reaction was allowed to stir overnight at room temperature. The resulting dark yellow slurry was filtered and the filtrate was washed several times with dry acetone and dried in vacuum oven at 50 °C.

Yield: 9.53g pale-yellow solid.

NMR spectroscopy

$^1\text{H-NMR}$ spectra of SMI-P and its derivative of SMI-Pq1 are shown in Figure 3.15. The quaternization of pendent amino groups of SMI-P with methyl iodide was successful. It can be seen that the signal peak corresponding to $-\text{N}-(\text{CH}_3)_2$ at 2.0 ppm has disappeared. A new signal is observed at 3.24 ppm corresponding to the methyl groups $[-\text{N}^+(\text{CH}_3)_3]$.

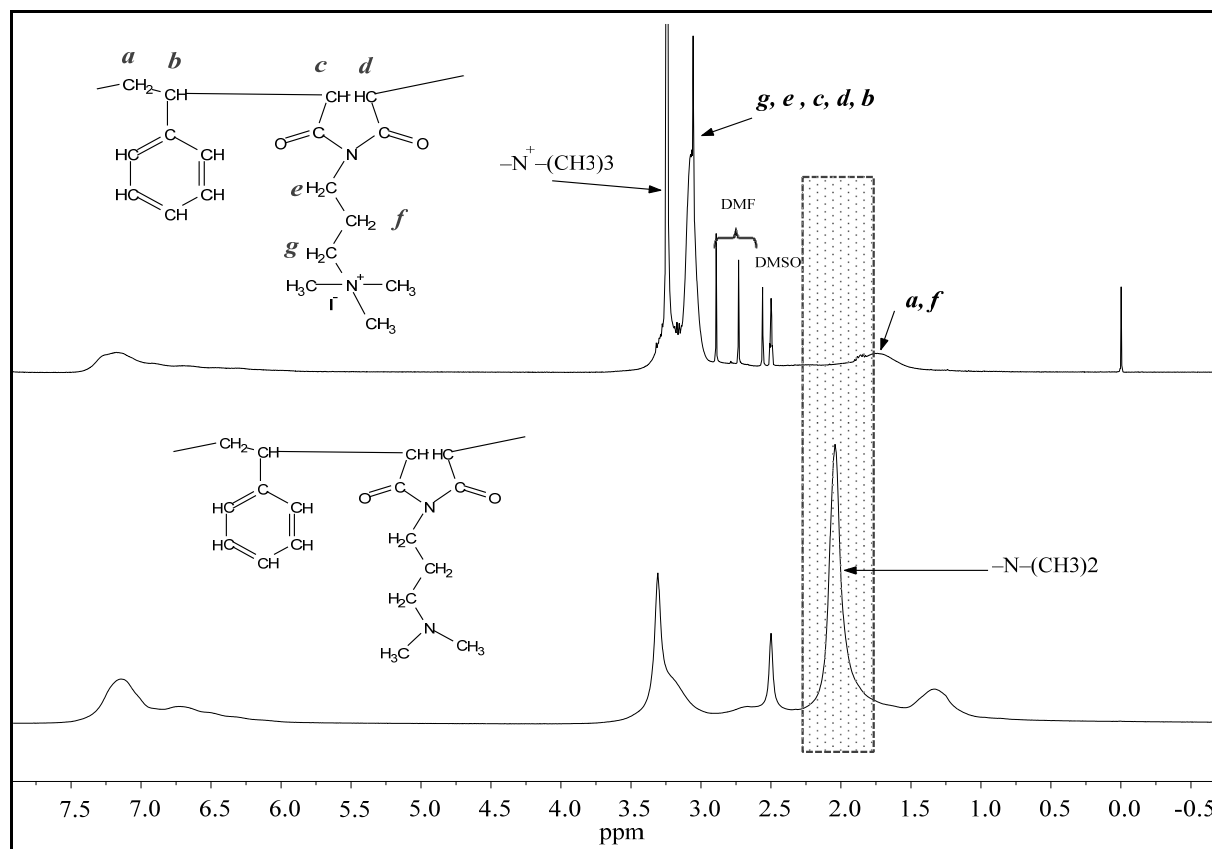


Figure 3.15: $^1\text{H-NMR}$ spectra of SMI-Pq1 (top) and SMI-P in $\text{DMSO-}d_6$

Figure 3.16 shows the $^{13}\text{C-NMR}$ spectra of SMI-Pq1 and the SMI-P. The highlighted area shows a clear downfield shift of the methyl carbon groups signal from 45.5 ppm of the

$[-\text{N}-(\text{CH}_3)_2]$ to 53.1 ppm of $[-\text{N}^+(\text{CH}_3)_2]$ carbon atoms. A downfield shift of the $[\text{N}-\text{CH}_2-]$ signal from 57.0 to 63.6 ppm for $[-\text{N}^+(\text{CH}_3)-\text{CH}_2-]$ was also observed.

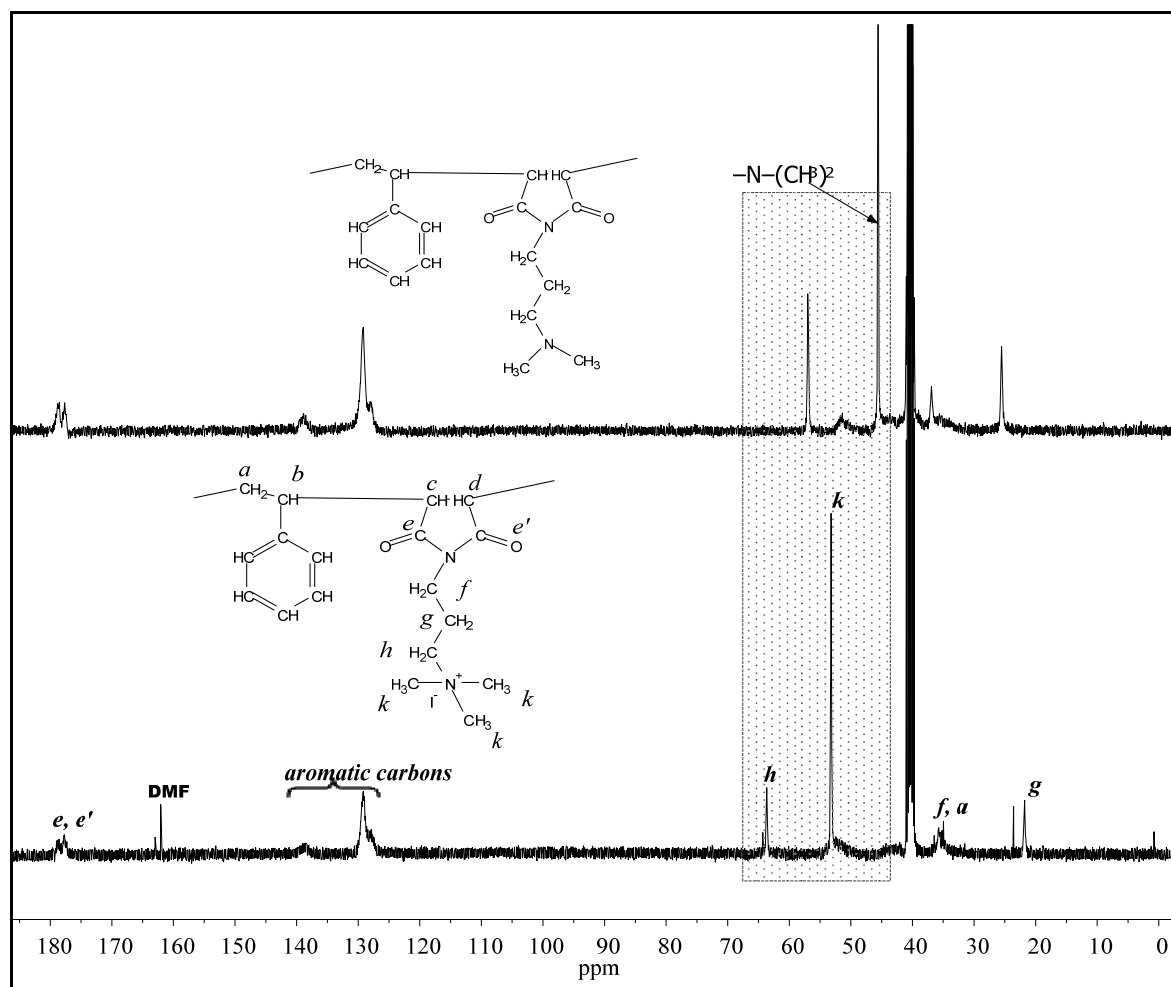


Figure 3.16: ^{13}C -NMR spectra of SMI-Pq1 and SMI-P in $\text{DMSO-}d_6$

3.3.2 Styrene-[(N-butyl)-N,N-dimethyl]-3-propyl maleimide] copolymer

3.3.2.1 Preparation of SMI-Pq4

In a round bottom flask equipped with a condenser and magnetic stirrer bar, 3 g of SMI-P was dissolved in 50 mL DMF. 1.8 mL (16 mmole) of 1-bromo butane was added to the polymer solution and the mixture stirred at 80 °C. The reaction was stopped after about 24 hours. The light brown solution was allowed to cool to room temperature. The quaternized product was precipitated in diethyl ether and dried in vacuum at 50 °C for 24 h.

Yield 4.3 g of pale-clay solid.

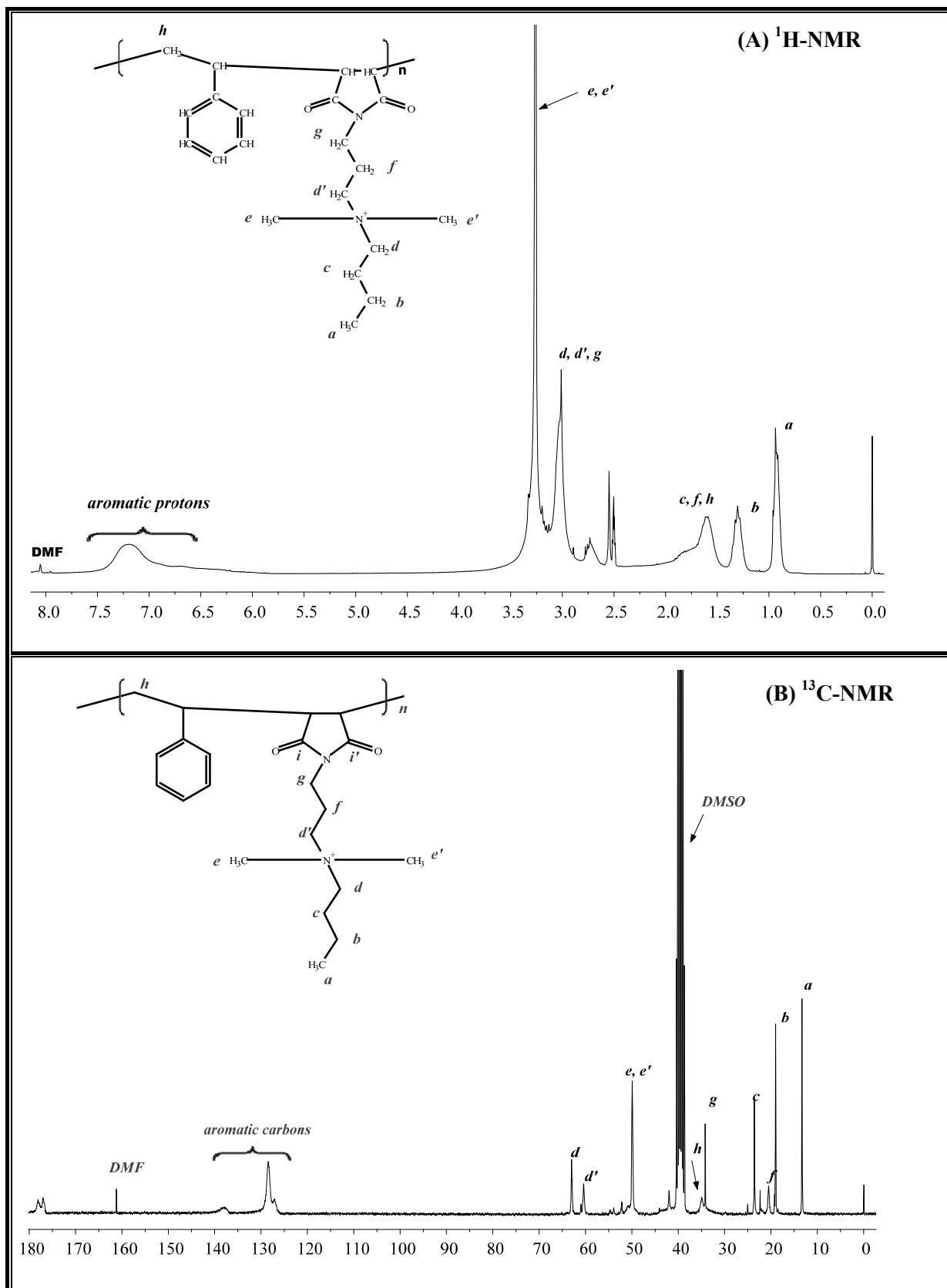
3.3.2.2 Preparation of SMI-Cq4

9.8 g of SMI-C was placed in a round bottom flask equipped with a condenser and a magnetic stirrer bar, 75 mL THF was added to the flask and stirred at room temperature. After the polymer had dissolved, 8 mL (74 mmol) of 1-bromo butane was added and the mixture was heated to 70 °C and stirred overnight. A yellow polymer lump had separated from the reaction which indicated the quaternization reaction had taken place. The solution surrounding the polymer lump was checked after 19 h by a precipitation test in diethyl ether and no indication of any polymer was observed as the solution remained clear in diethyl ether. The quaternized product was re-dissolved in methanol and precipitated in diethyl ether. The precipitate was dried under vacuum at 50 °C for 24h.

Yield 5.8 g light yellow solid.

NMR spectroscopy

¹H-NMR spectrum of SMI-Pq4 is shown in Figure 3.17 (A). Successful quaternization of SMI-P with C4 bromide was evident by observing the methyl group protons signals. A clear downfield shift at 3.25 ppm was assigned to the methyl [$-\overset{|}{\text{N}}^+\text{CH}_3)_2$] protons. The signal at 0.94 ppm corresponds to methyl protons of the C4 chain, and at 1.25 ppm, corresponding to the methylene protons ($-\text{CH}_2-\text{CH}_3$). Figure 3.17 (B) presents the ¹³C-NMR spectrum of SMI-Pq4. The characteristic signals of the C4 appeared at 13.3, 19.1 and 23.6 ppm (methyl and methylene respectively). The [$-\text{CH}_2-\overset{|}{\text{N}}^+-\underset{|}{\text{CH}_2}-$] signals are observed at 60.6 and 63.1 ppm. The signal at 50.0 ppm corresponds to the methyl [$-\overset{|}{\text{N}}^+-\text{(CH}_3)_2$] groups.



3.3.3 Styrene-[(N-octyl-N,N-dimethyl)-3-propyl maleimide] copolymer

3.3.2.1 Preparation of SMI-Pq8

In a round bottom flask equipped with a condenser and magnetic stirrer bar, 6 g of SMI-P was dissolved in 50 mL DMF, and then 7.3 mL (40 mmol) of 1-bromooctane was added to the polymer solution and stirred at 80 °C. The reaction was stopped after about 30 hours; the brown solution was allowed to cool at room temperature. The quaternized product was precipitated in diethyl ether and dried in vacuum at 50 °C for 24 h.

Yield: 8.7 g of pale solid.

3.3.2.2 Preparation of SMI-Cq8

10 g of SMI-C was placed in a round bottom flask and 75 mL THF was added. After dissolving the polymer, 10 mL (58 mmol) of 1-bromooctane was added to the polymer solution and then heated to 80 °C and stirred for 40 h. The sticky polymer lump was then redissolved in methanol, precipitated in diethylether and dried in vacuum at 50 °C for 24h.

Yield: 7.29 g light yellow solid.

NMR spectroscopy

The ¹H-NMR spectrum of SMI-Pq8 is shown in Figure 3.18 (A). The signal at 0.85 ppm corresponds to the terminal methyl groups of the C₈ chain. A sharp signal at 1.26 ppm was attributed to the methylene groups as indicated in the figure. The aliphatic protons of the CH₂ backbone and the methylene [-CH₂-CH₃] appear overlapped at 1.56 ppm. Protons adjacent to the quaternized N, and the imide groups are overlapped and appear between 2.7 and 3.5 ppm.

The ¹³C-NMR spectrum is shown in Figure 3.18 (B). The signal at 13.7 ppm is characteristic for the terminal methyl groups of the C₈ chain. The signals between 20 – 35 ppm correspond to the methylene groups of the polymer as indicated in the figure, except for the [-CH₂-N⁺(CH₃)₂-CH₂-] signals, that appears at 60.3 and 63.3 ppm. The signal at 49.7 ppm is attributed to the methyl [-N⁺(CH₃)₂] groups.

Chapter 3: Synthesis and characterization of styrene-maleimide copolymer derivatives

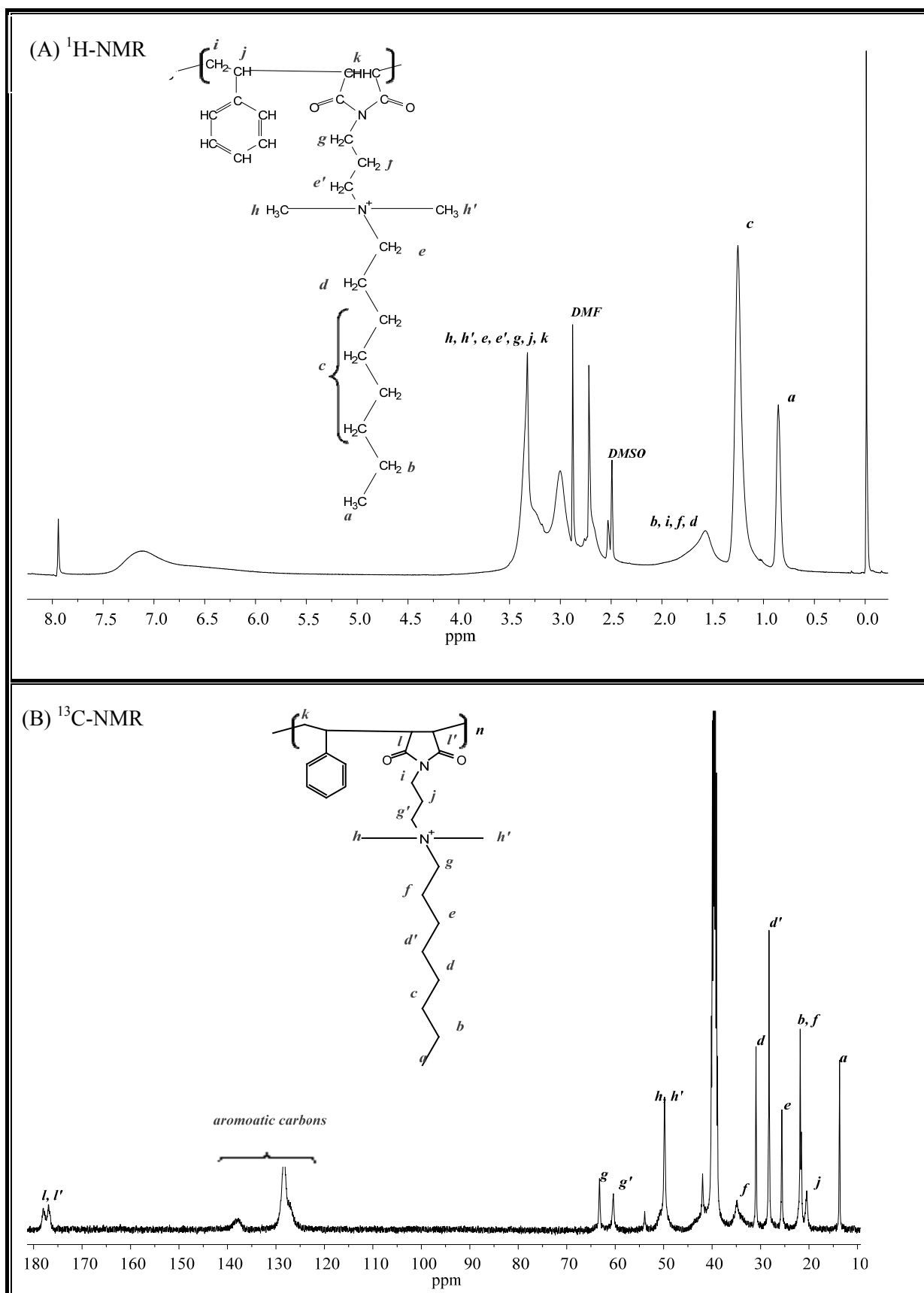


Figure 3.18: ^1H and ^{13}C -NMR spectra of SMI-Pq8 in $\text{DMSO-}d_6$

3.3.4 Styrene-[(N-dodecyl)-N,N-dimethyl-3-propyl maleimide] copolymer

3.3.2.1 Preparation of SMI-Pq12

In a round bottom flask equipped with a condenser and magnetic stirrer bar, 3.84 g of SMI-P was dissolved in 50 mL DMF, then 3.8 mL (16 mmol) of 1-bromododecane was added to the polymer solution and stirred heated to 100 °C with stirring for 24 hours. The resulting light brown solution was allowed to cool at room temperature and then the quaternized polymer was precipitated in diethyl ether and dried in vacuum at 50 °C for 24 h.

Yield: 6.63 g of clay-like solid.

3.3.2.2 Preparation of SMI-Cq12

10 g of SMI-C was placed in a round bottom flask followed by 75 mL DMF. After dissolving the polymer, 15 mL (55 mmol) of 1-bromododecane was added to the solution and the flask then heated to 100° C and stirred for 40 h. The resulting light yellow polymer solution was cooled to room temperature and the polymer precipitated in diethylether. After filtration the quaternized product was dried in vacuum at 50 °C for 24 h.

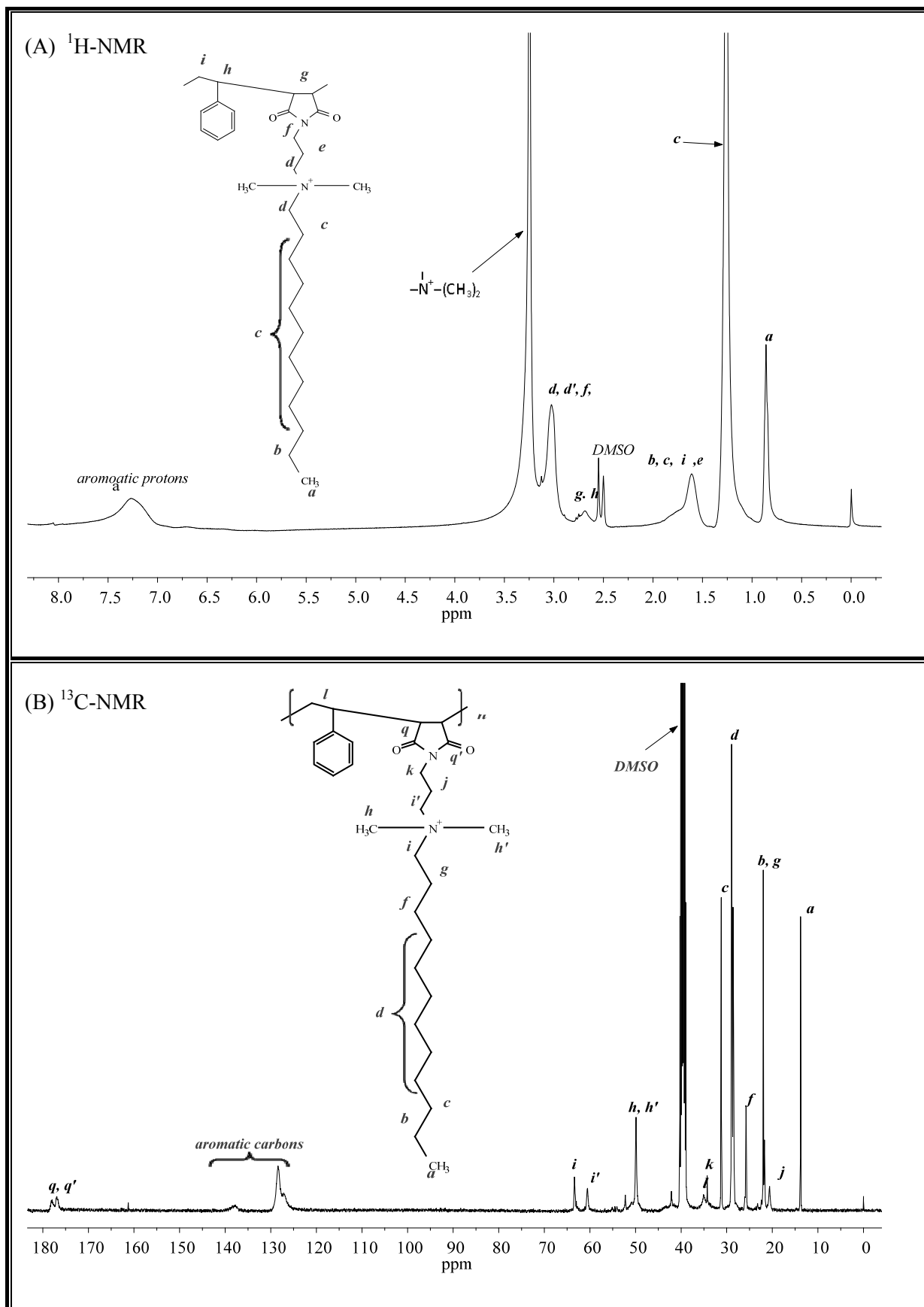
Yield: 15.4 g of pale white solid.

NMR spectroscopy

The ¹H-NMR spectrum of SMI-Pq12 is similar to SMI-Pq8, the assigned chemical shifts are shown in Figure 3.19 (A).

The ¹³C-NMR spectrum is shown in Figure 3.19 (B). The typical aliphatic signals appeared in the range between 13-35 ppm as indicated in the figure. The characteristic signals for the carbons adjacent to the quaternary N appear at 49.8 ppm for methyl [$-\overset{|}{\text{N}}^+(\text{CH}_3)_2$] groups, and 60.6–63.3 ppm for the [$-\overset{|}{\text{CH}_2}-\overset{|}{\text{N}}^+\text{CH}_2-$] methylene groups.

Chapter 3: Synthesis and characterization of styrene-maleimide copolymer derivatives



ATR-FTIR spectroscopy

Figure 3.20 illustrates the stacked ATR-FTIR spectra of all quaternized polymer derivatives prepared in this study. The Figure presents the results of modification steps starting from SMA-P at the bottom of the spectra. Above that are the imidized derivative SMI-P and the subsequent quaternized derivatives with C1, C4, C8 and C12 alkyl groups.

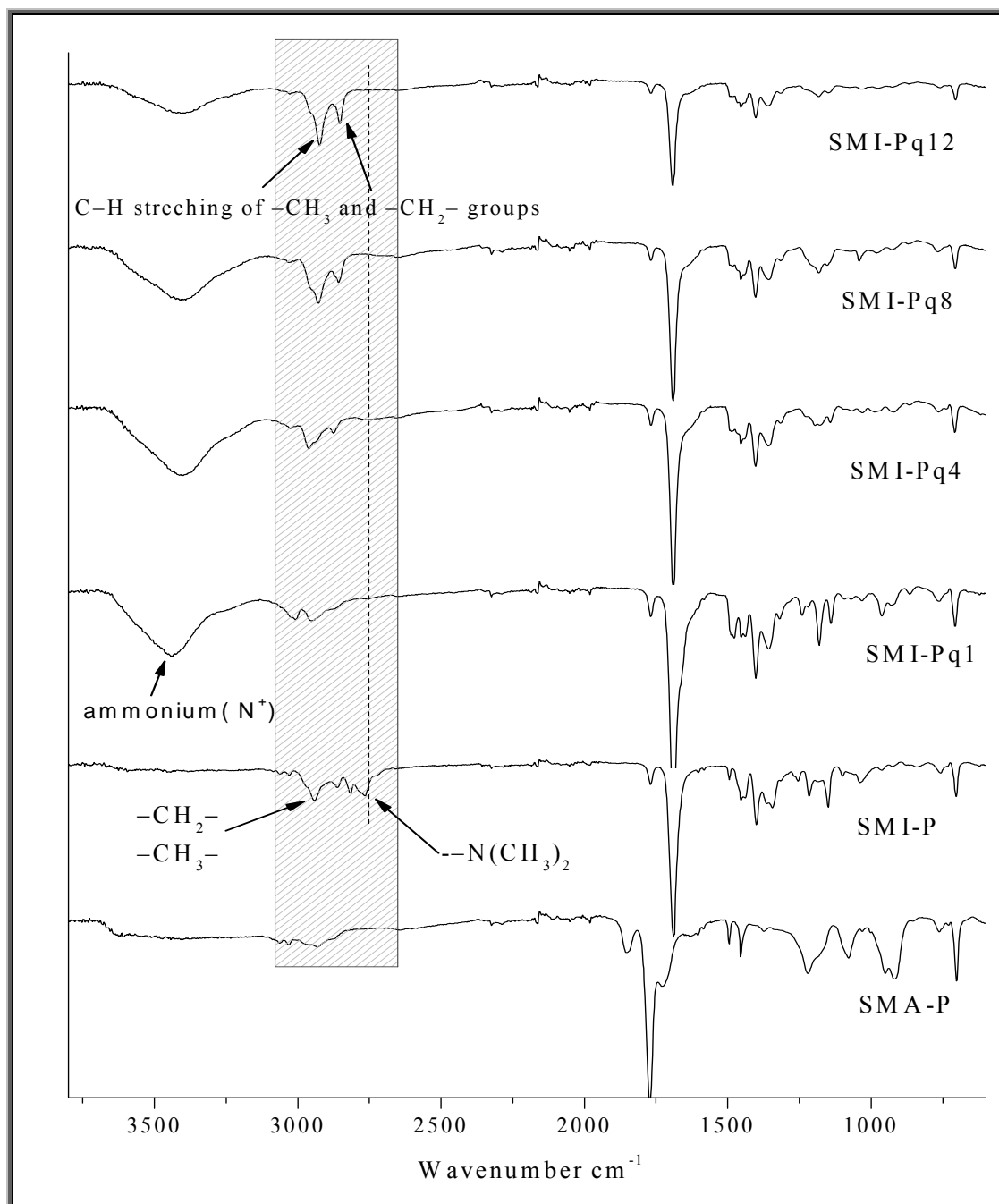


Figure 3.20: ATR-FTIR spectra of SMA-P and its modified derivatives.

It can be seen in Figure 3.20 that the absorption band (doublet) that corresponds to the C–H stretching of $[-N-(CH_3)_2]$ disappears in all of the quaternized polymers. Since alkyl halides were used in the quaternization, peaks in the range $2945\text{--}2851\text{ cm}^{-1}$ (C–H antisymmetric and symmetric stretching of $-CH_3$ and $-CH_2$ group) suggested the successful addition of alkyl chains to the polymer. The appearance of a new broad band centered at around 3400 cm^{-1} is attributed to the ammonium cation, thus confirms successful quaternization of the tertiary amino groups of SMI-P.

Similar results were obtained for the quaternized maleimide derivatives of the commercially modified SMI-C copolymer. Figure 3.21 demonstrates the ATR-FTIR spectra of the quaternized-SMI-C derivatives with C1, C4, C8 and C12 alkyl groups. The characteristic ammonium ion bands at around 3400 cm^{-1} and the C–H stretching of the aliphatic (methylene and methyl) groups are evidently a clear indication for the obtained quaternized derivatives.

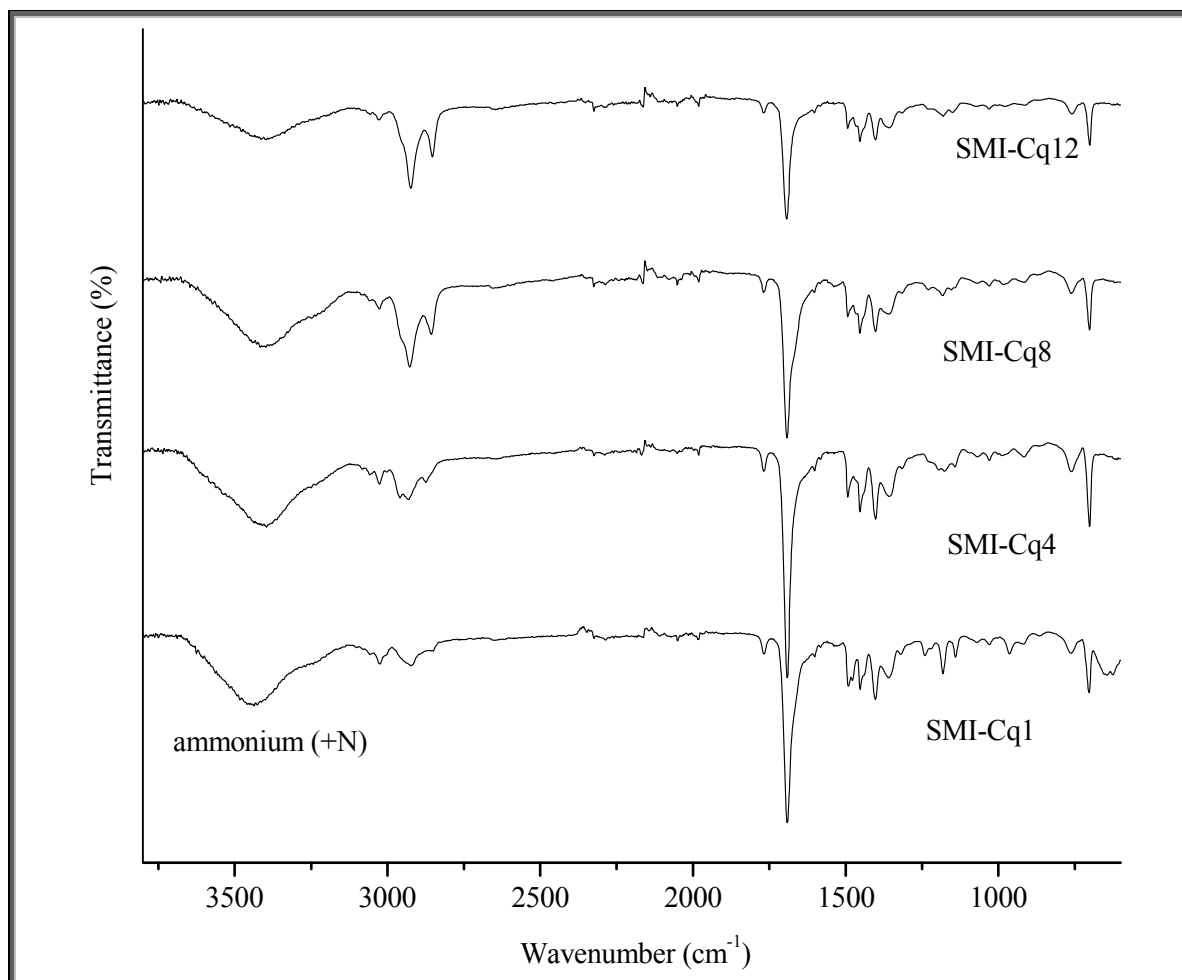


Figure 3.21: ATR-FTIR of N-quaternized SMI-C derivatives.

3.4 Conclusions:

In this chapter, the synthesis and characterization of various styrene-maleimide copolymer derivatives was presented.

The imidization of styrene-maleic anhydride copolymers (prepared and commercial grade) was successfully accomplished using various aliphatic amino compounds (2-amino ethanol, n-butyl amine, 3-dimethylaminopropylamine) to form the styrene-maleimide copolymer derivatives.

The imidized polymers (styrene-*N,N*-dimethylaminopropyl maleimide) copolymer) SMI-P and SMI-C were used as a precursor for the preparation of quaternized copolymer derivatives. The quaternization reactions were successfully accomplished using various alkyl halides, namely methyl iodide, 1-bromobutane, 1-bromooctane, and 1-dodecylbromide, as shown by the characterization results of each compound.

3.5 References:

1. Soer, W. J.; Ming, W.; Klumperman, B.; Koning, C.; van Benthem, R. *Polymer* 2006, 47, (22), 7621-7627.
2. Ha, N. T. H. *Polymer* 1999, 40, (4), 1081-1086.
3. Lessard, B. t.; Maricì , M. *Macromolecules* 2009, 43, (2), 879-885.
4. Samyn, P.; Deconinck, M.; Schoukens, G.; Stanssens, D.; Vonck, L.; Van den Abbeele, H. *Polymers for Advanced Technologies* 2010, n/a.
5. Lee, W.-F.; Hwong, G.-Y. *Journal of Applied Polymer Science* 1996, 59, (4), 599-608.
6. Gietzelt, T. *Journal of Materials Science* 2001, 36, (8), 2073-2079.
7. Oba, M.; Kawamata, M.; Tsuboi, H.; Koga, N.; States, U. Process for the production of N-(hydroxyphenyl) maleimides. US4289699, 1981.
8. Park, J. O.; Jang, S. H. *Journal of Polymer Science Part A: Polymer Chemistry* 1992, 30, (5), 723-729.
9. Nair, C. P. R.; Mathew, D.; Ninan, K. N. *European Polymer Journal* 1999, 35, (10), 1829-1840.

CHAPTER 4

CHAPTER 4: Electrospinning of Maleimide-Styrene Copolymer Derivatives

4.1 Abstract

In this chapter the utilization of the electrospinning process is described. All the prepared and modified copolymers in this study were electrospun into non-woven nanofibrous mats. The electrospun fibers were characterized by different analytical tools such Scanning Electron Microscopy (SEM) for morphological and size assessment, Differential Scanning Calorimetry (DSC) and Thermogravimetric analysis (TGA) analysis were conducted to investigate the thermal properties of the fibers.

4.2. The electrospinning process

Electrospinning is considered the most convenient and cheapest method to fabricate polymeric and inorganic nanofibers for filtration, textile and biomedical applications.^{1,2} Fibers with diameters in the range of tens to hundreds of nanometers can be readily electrospun into mats. In simple words, the electrospinning process is a process that creates nanofibers through an electrically charged jet of a polymer solution or polymer melt.³

In its simplest form, electrospinning uses an electric field to draw a polymer solution from the tip of a capillary to a collector. A positive voltage is applied to the polymer solution, which causes a jet of the solution to be drawn toward a grounded or negatively charged collector. The fine jets dry to form polymeric fibers.

A typical electrospinning setup in the laboratory consists of:

- A viscous polymer solution
- An electrode (hollow tubular or solid) that is maintained in contact with the polymer solution
- A high-voltage DC generator connected to the electrode

- A grounded or negatively charged surface to collect the fibers.

Figure 4.1 shows a diagram of the electrospinning setup employed in this work. A detailed explanation of the electrospinning process is presented in a valuable book by Andradý.⁴ The description of the process can be summarized in the following key stages:

- 1) Droplet generation
- 2) Taylor cone formation
- 3) Launching of the jet
- 4) Elongation of straight segment
- 5) Whipping instability region
- 6) Solidification into nanofiber

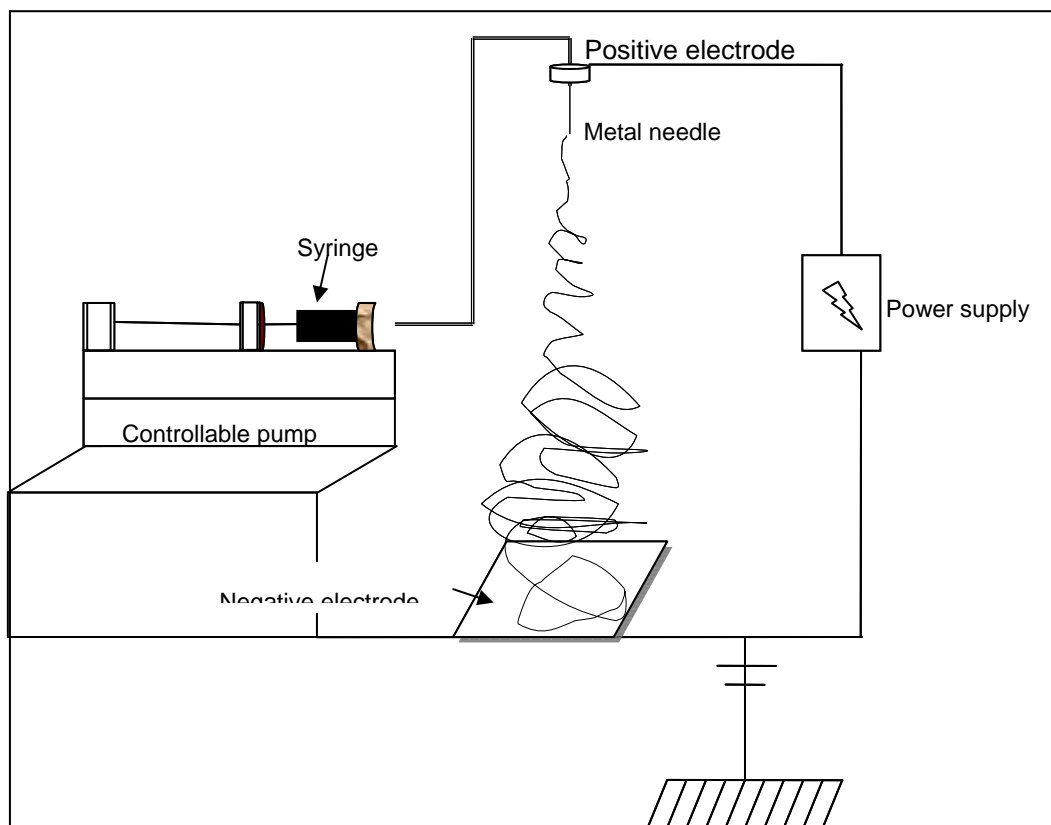


Figure 4.1: representation of the electrospinning setup used in this work

Chapter 4: Electrospinning of SMI copolymer derivatives

Briefly, in the electrospinning process, the polymer solution is pushed through the tip (most often metallic) of a needle by a control pump. The electrical field draws the solution droplet at the tip into a structure called Taylor cone (caused by equilibrium between the electrical force of the charged surface and the surface tension). If the viscosity and the surface tension of the solution are appropriately tuned, a stable jet is formed and travels across the gap from the highly charged tip to the ground collector surface. On the way to the collector, the solvent evaporates (or melt solidifies) and solid fibers are precipitated, typically forming a non-woven nanofibrous mat.

In general, the important features of electrospinning are³:

1. A suitable solvent to completely dissolve the polymer.
2. Vapor pressure of the solvent should be suitable to quickly evaporate and maintain fiber integrity, but also not too quickly, which would cause solidification before proper stretching of the polymer fibers.
3. Suitable viscosity and surface tension of the polymer solution.
4. A power supply that provides enough potential to overcome the viscosity and surface tension of the polymer solution to form a stable jet.

4.3 Electrospinning styrene-maleimide (SMI) copolymer derivatives

The prepared copolymer derivatives as described in Chapter 3 were electrospun after a series of optimization trials to set the electrospinning conditions for each polymer system. These conditions include polymer solution concentrations, feed rates, applied voltage, electrospinning distance, and the solvent system used. The solvent system was chosen according first to the ability to dissolve the polymer. Also, it was considered to minimize the use of very toxic solvents for each polymer system, taking into account the solvent properties such as dielectric constant, which has a significant influence on electrospinning. Generally, a solution with a greater dielectric property reduces the formation of beads and the diameter of the resulting electrospun fiber. Also, it has an effect on the morphology of the fibers. Table (4.1) shows the dielectric constants of some common solvents used for electrospinning, it was also used as a guide for solvent selection. It is beyond the scope of this study to thoroughly

focus on the actual surface morphology and the effect of different solvents on the electrospun fibers. Table 4.1 shows the dielectric constant of some common solvents used in literature for electrospinning and reported in a book by Ramakrishna *et al.*⁵

Table 4.1: Dielectric constants of solvents copied from reference (5).

Solvent	Dielectric constant
2-Propanol	18.3
Acetic acid	6.15
Acetone	20.7
Acetonitrile	35.92-37.06
Chloroform	4.8
Dichloromethane	8.93
Dimethylformamide	36.71
Ethyl acetate	6.0
Ethanol	24.55
m-Cersol	11.8
Methanol	32.6
Pyrrolidine	12.3
Tetrahydrofuran	7.47
Toluene	2.438
Trifluoroethanol	27.0
Water	80.2

After numerous optimization attempts of the electrospinning conditions of the copolymer derivatives, the final conditions that were set for each polymer system are tabulated in Table 4.2.

The fibers produced via these optimized conditions were observed in the scanning electron microscope (SEM) to determine the diameter sizes. The seemingly random selection of spinning conditions were optimized values that led to fiber diameters in the range of 400-800 nm. The fibers were then analyzed for thermal properties and subsequently used for antimicrobial evaluation discussed in Chapter 5.

Chapter 4: Electrospinning of SMI copolymer derivatives

Table 4.2: Experimental electrospinning conditions of the SMI copolymer derivatives

Polymer type	Solvent	Conc. (Wt. %)	Volts (KV)	Feed rate (mL/min)	Distance (cm)	Relative *Humidity & Temp.
SMI-P	EtOH	8	10	0.013	15	37% , 25 °C
SMI-NB	EtOH:MeOH 1:1	10	10	0.008	17	53% , 19 °C
SMI-AE	DMF:EtOH 1:3	10	11.25	0.022	17	64% , 20.5 °C
SMI-AP	DMF:EtOH 1:1	14	10	0.012	16	62 % , 21.5 °C
SMI-Cq1	DMF:Acetone 1:1	33	12.5	0.007	17	65 % , 21 °C
SMI-Cq4	EtOH	24	15	0.007	10	63.5% , 23 °C
SMI-Cq8	MeOH	28	12	0.008	15	50% , 22.5 °C
SMI-Cq12	EtOH:MeOH 1:1	28	11.25	0.01	15	63% , 24 °C
SMI-Pq1	DMF	35	12.5	0.01	15	66% , 22.5 °C
SMI-Pq4	MeOH	20	12.5	0.014	16	63% , 21.5 °C
SMI-Pq8	EtOH:MeOH 1:1	18	17.5	0.008	17	63% , 23.5 °C
SMI-Pq12	EtOH:MeOH 1:1	18	10	0.01	15	53% , 22 °C

* recorded by a temperature/humidity data logger OPT506H series (Optirion)

4.4 Results and Discussion

4.4.1 SEM analysis

SEM was performed on all electrospun fiber mats. Imaging of the samples was accomplished using a Leo® 1430VP Scanning Electron Microscope at Stellenbosch University. Prior to imaging, the samples were mounted on a stub with double-sided carbon tape. The sample was then coated with a thin layer of gold in order to make the sample surface electrically conducting. The scanning electron (SE) images show the surface structure of the material. Beam conditions during surface analysis were 7 kV and approximately 1.5 nA, with a working distance of 13 mm and a spot size of 150. Fiber diameters were estimated using digital image processing software AxioVision (V 4.4.0.0).⁶ The average fiber diameter was evaluated by randomly selecting up to 30-50 measurements of different portions of the fibrous mat and averaging the diameter over the number of single fiber measurements. The data collected is shown in Figure 4.2. The average diameter of the electrospun fiber mats is in general in the nanometer range if 400-800 nm. Figure 4.3 shows examples of SEM images of selected electrospun fibers.

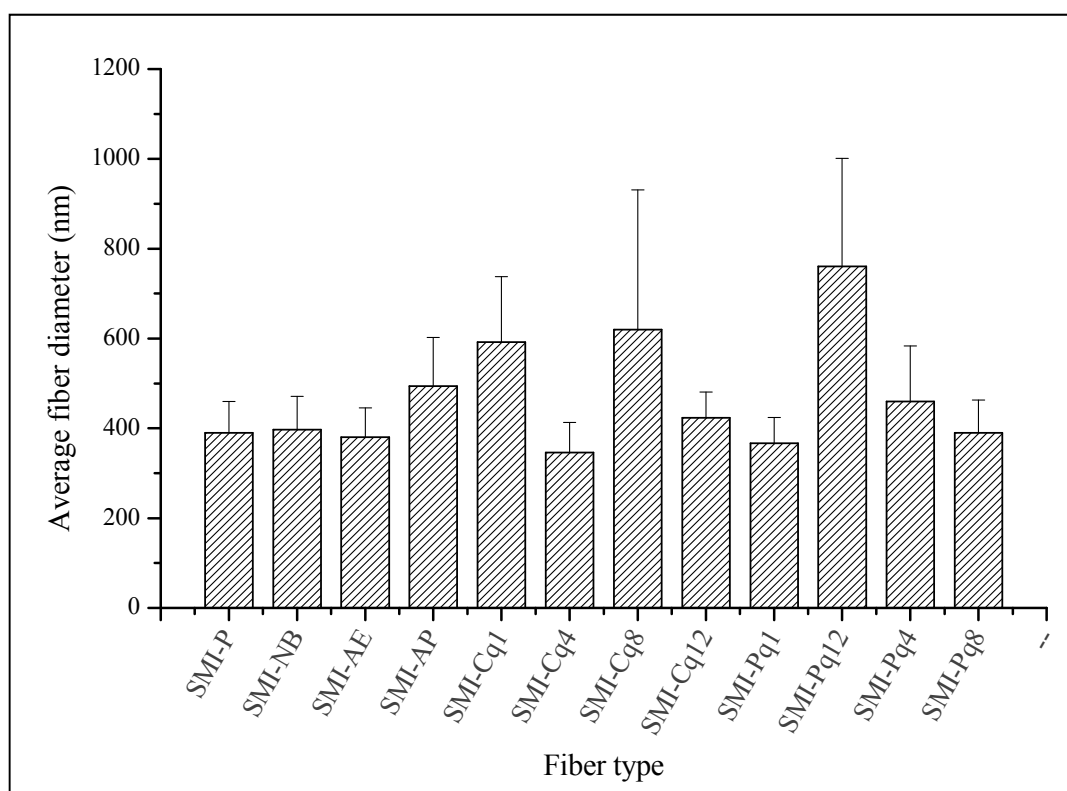


Figure 4.2: Mean average diameter of the electrospun polymer derivatives.

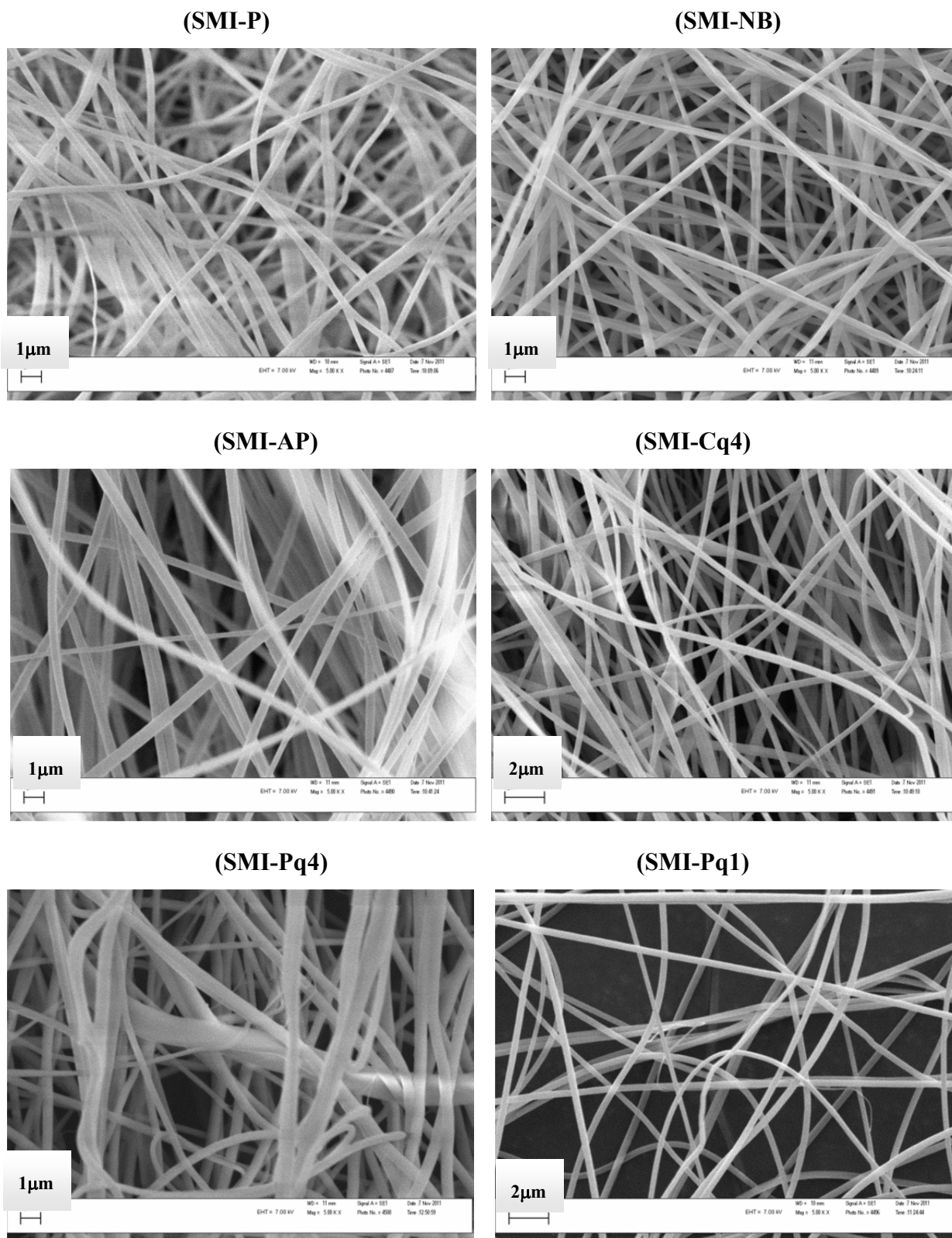


Figure 4.3: SEM images of some electrospun SMI copolymer derivatives.

4.4.2 Thermal analysis

The thermal properties of the fibers were investigated by TGA and DSC analysis.

DSC was carried out on a TA Instruments Advanced Q1000 calorimeter. Samples were heated from 50 to 200 °C at a rate of 10 °C/min followed by an isothermal step for 1 min. A cooling cycle to 50 °C with 10 °C/min was performed prior to a second heating run to 200 °C at 10 °C/min. The glass transition temperature (T_g) was determined from the second heating run.

The TGA instrument is a Perkin Elmer TGA 7, samples were heated from 20 °C to 920 °C at 20 °C/min under nitrogen atmosphere.

TGA thermograms of styrene-maleimide copolymer derivatives prepared from SMA-P precursor are shown in Figure 4.4. From the figure, the TGA curve of maleic anhydride SMA-P copolymer, undergoes a two-stage weight loss in the temperature 200-350 °C, where the major portion decomposes in the second stage at about 350 °C. The first-stage weight loss was approximately 10% started around 200 °C, These results are in good agreement with those corresponding to the thermogravimetric behavior of PSMA.⁷⁻⁹ The styrene-maleimide copolymer derivatives decomposed in a single step around 400 °C. However, the thermogram curve for SMA-NB showed two degradation steps, *i.e.* the first 20 % wt loss around 160 °C and the second was around 400 °C.

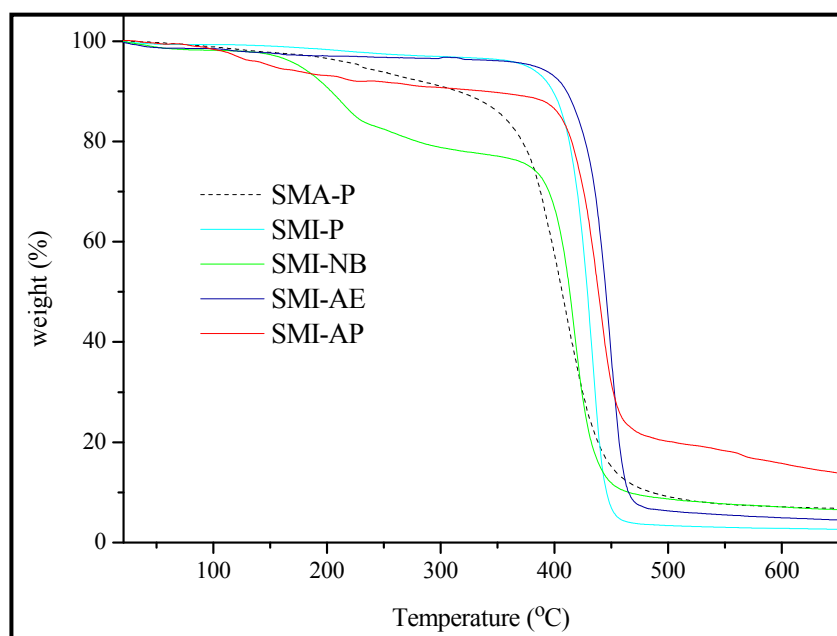


Figure 4.4: TGA thermograms of SMI copolymer derivatives.

Chapter 4: Electrospinning of SMI copolymer derivatives

TGA thermograms of the quaternized SMI-P and SMI-C with C₁, C₄, C₈ and C₁₂ substituents are presented in Figure 4.5. It was observed that the quaternized polymer fibers decomposed at lower temperatures than the non-quaternized precursors. It can be seen that the decomposition temperature of the quaternized SMI-C copolymer derivatives are around 235 °C, while the unquaternized precursor SMI-C decomposed at approximately 400 °C. In a similar trend the decomposition temperatures of the quaternized SMI-P copolymer derivatives were lower than the unquaternized SMI-P precursor due to the quaternary ammonium groups.

Slightly lower decomposition temperatures were observed for the SMI-P copolymer derivatives compared to the SMI-C derivatives due to the increase in the bromine or iodine content in the polymer.^{10,11}

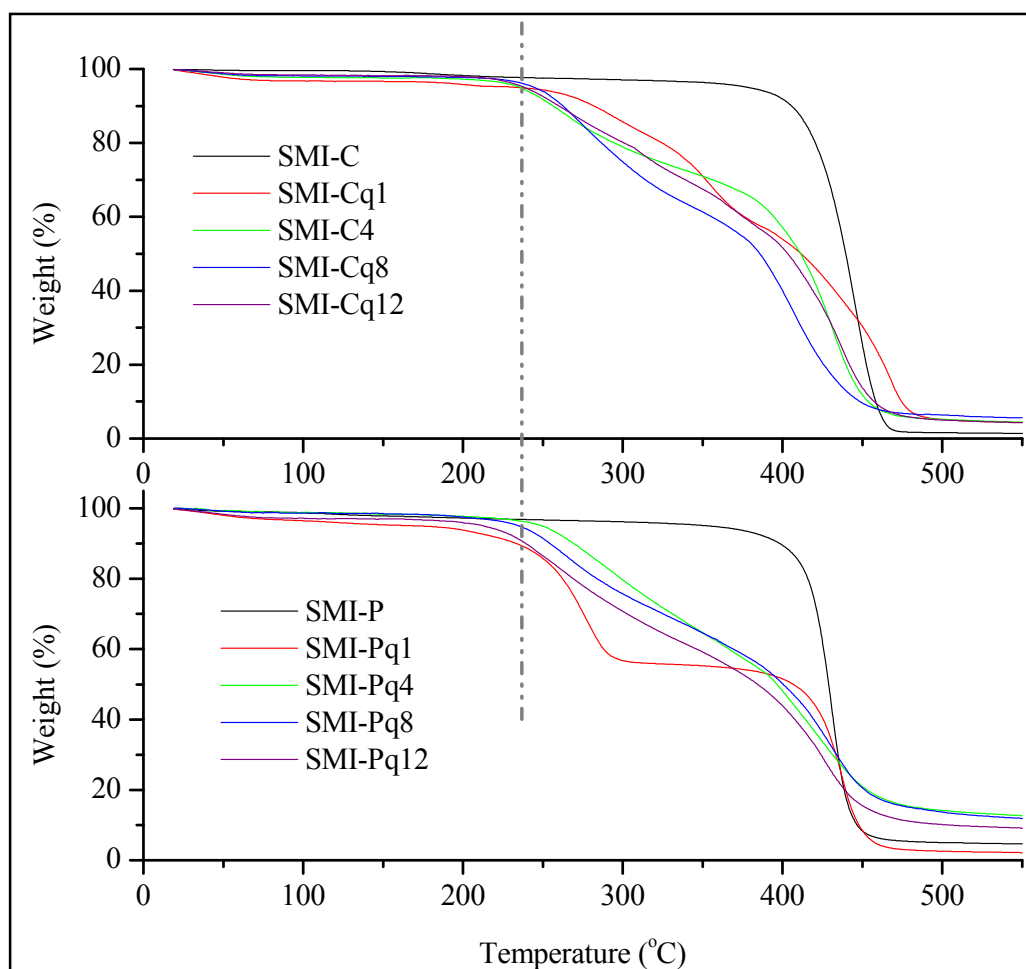


Figure 4.5: TGA thermograms of quaternized SMI-C (top) and SMI-P copolymer derivatives.

Chapter 4: Electrospinning of SMI copolymer derivatives

The glass transition temperatures T_g of the modified copolymers are summarized in Table 4.3. It can be seen from the Table that the T_g s of both styrene-maleic anhydride copolymer precursors SMA-P (206 °C) and SMA-C (160 °C) are strongly influenced by the anhydride content. It was shown that the T_g increases linearly with MANh at 2.67 °F per added MANh %.¹² The incorporation of MANh leads to an increased stiffness of the chain and thus to a higher T_g .

Furthermore, the SMA-P structure with approximately 50% anhydride units corresponds to a completely alternating copolymer, which is probably able to pack in a more efficient way than the more random (statistical) copolymer SMI-C with approximately 28% anhydride units.¹³

Table 4.3: Measured T_g s of the electrospun fibers

SMI fiber derivatives	T_g (°C)	Quaternized fiber derivatives	T_g (°C)
SMA-P	206	SMI-Cq1	173
SMA-C	160	SMI-Cq4	152
SMI-P	123	SMI-Cq8	149
SMI-NB	147	SMI-Cq12	130
SMI-AE	187	SMI-Pq1	140
SMI-AP	150	SMI-Pq4	153
		SMI-Pq8	154
		SMI-Pq12	146

N-substituted maleimides show a balance between increased stiffness (ring structures) and reduced chain packing (alkyl substituents). A significant decrease in the T_g of all imidized products compared to that of the SMA-P precursor have been recorded. For example the T_g of the imidized SMI-P derivative decreased significantly to 123 °C. Introduction of the aliphatic chain with a tertiary amino group acting as short chain branches would significantly affect the macromolecular behavior. The decrease in the T_g can be attributed to the restriction of the

polymer chains to pack, the short branched groups could provide more free chain mobility and that leads to having a lower T_g value. Vermeesch and Groeninckx¹⁴ have showed that an increasing chain length of grafted amine onto the PSMA backbone depressed the glass transition temperature of poly(styrene-*co*-*N*-alkylmaleimides) remarkably.

Similar thermal behavior was observed with other imidized products such SMI-NB, and SMI-AE where the T_g also decreased compared to that of SMA-P. These observations are in agreement with the thermal properties of similar imidized copolymers reported in literature.^{15,16} However every functional group has a different effect on the final T_g of the copolymer.

The quaternization of SMI-P and SMI-C also influenced the thermal properties. The introduction of an alkyl group to the tertiary amino moieties has resulted in an increase in the T_g of the copolymer derivatives. From Table 4.3, it can be seen in the case of the quaternized SMI-C derivatives, the T_g decreases with an increase of the *N*-alkyl chain attached to the quaternary ammonium group. However, this decreasing trend was not observed in the quaternized SMI-P derivatives. The quaternized SMI-P derivatives showed quite the opposite trend to that of the SMI-C quaternized derivatives in the following order SMI-Pq1 < SMI-Pq4 < SMI-Pq8, as the T_g showed an increasing trend up to the quaternized polymer with a C8 alkyl chain then a slight drop in the T_g was observed from a 154 °C in the case of SMI-Pq8 to 146 °C of SMI-Pq12.

It was not possible to compare the thermal property findings in this study with other results in the literature because of the lack of information on thermal studies with similar copolymer derivatives. Lee *et al.*^{17,18} have reported the synthesis of poly(methyl iodide quaternized styrene-*N*-(3-(*N*',*N*'-dimethylamino)propyl)maleimide) which is the same as SMI-Pq1. However, in their study they only focused on investigating the aqueous solution properties of the cationic copolymer derivatives without touching on the thermal properties of the polymers. Therefore the thermal properties of the quaternized derivatives are considered to be reported for the first time in this study.

4.5 Solubility properties of the quaternized electrospun fibers

The presence of an ionic group such as the quaternary ammonium group in the polymer can significantly affect its solubility and make the dissolution of the polymer in water possible. A solubility test on the quaternized fibers was performed. This was done by taking a small piece of

the fiber mat and placing it in a sample vial containing about 10 mL water. Because of the huge surface area of the fibers it was very easy to observe its solubility, as it is expected if the polymer is soluble, the mat will disappear immediately or at least in a few minutes. The experimental observations revealed that the quaternized SMI-C derivatives were insoluble in water. This is expected to be due to the hydrophobic character of the dominating styrene rings, as the sample fiber mats were clearly visible, suspended in the water. On the other hand the quaternized (alternating) SMI-P samples including SMI-Pq1, SMI-Pq4 and SMI-Pq8 dissolved immediately. This was attributed to the fact that the quaternized SMI-P derivatives have substantially larger amounts of cationic groups present in the polymer chain, which helps the molecule to dissolve in water. However, the quaternized polymer with C12 carbon was insoluble, which is most likely due to the long aliphatic tail that increased the hydrophobicity of the amphiphilic copolymer.

The water-solubility of the quaternized fibers after electrospinning limits their use for many applications, especially if intended for filtration purposes.¹⁹ One of the aims in this study was to investigate the copolymer derivatives in the form of electrospun fiber mats for filtration applications. Therefore, it was important to make the fibers water-insoluble after electrospinning. Furthermore, the effect of the availability of cationic groups on the antimicrobial properties is to be compared between the SMI-C and SMI-P quaternized derivatives. The crosslinking of the fibers was achieved by thermal treatment, which was advantageous because no external chemical crosslinking agents were required as will be explained in the following section.

4.5.1 Thermal curing of water-soluble fibers.

The water-soluble fibers SMI-Pq1, SMI-Pq4 and SMI-Pq8 were thermally cured in a vacuum oven at 130 °C for 24 hours. The solubility of the fibers was investigated after curing in the same way as explained earlier. After the thermal treatment, none of the fibers were soluble in water or solvents such as THF or DMF, which was a clear indication for success of the crosslinking process. The cured fibers were analyzed by DSC and SEM.

The actual crosslinking via heat treatment was inspired by the results found when treating the parent precursor (alternating) SMI-P copolymer. The thermal treatment of the SMI-P fibers

Chapter 4: Electrospinning of SMI copolymer derivatives

resulted in a crosslinked fiber mat that was insoluble in THF, DMF and DMSO, as evident by the stability of the fiber mat in the solvent for weeks. An attempt to understand the nature of the crosslinking process was carried out. All prepared imidized derivatives (Figure 4.6) were thermally treated to investigate the effect of the different N-substituted groups on the curability of the fibers

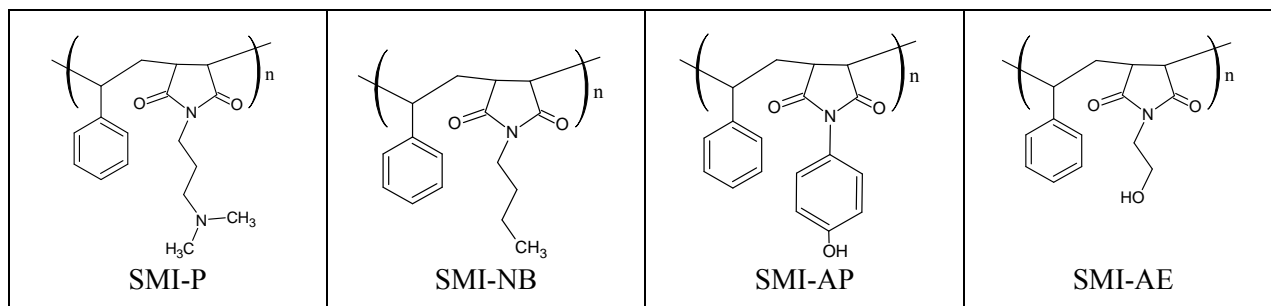


Figure 4.6: SMI copolymer derivatives.

It was found that no effect was noticed on the SMI derivatives (except for SMI-P), as they were still soluble in DMF after heat treatment. This led to conclude that the tertiary amine functionality was the key in promoting the crosslinking process to occur. The nature of the actual chemical or physical crosslinking process however, is not understood yet. From the ATR-FTIR spectra in of SMI-P (Figure 4.7) before and after curing, it was difficult to notice any differences or to extract useful information as both spectra are almost identical.

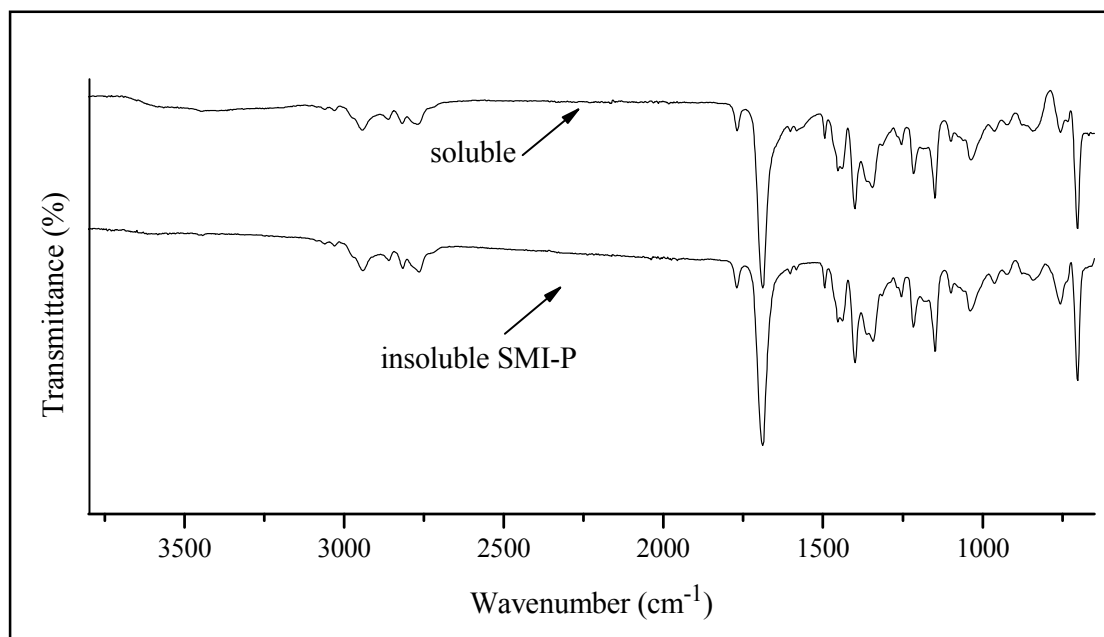


Figure 4.7: ATR-FTIR spectra of soluble and insoluble SMI-P fiber mats.

However, it was noticed that high temperature is not necessarily required for the crosslinking process to actually occur. The SMI-P fibers were crosslinked even at 80 °C under normal atmospheric pressure in less than 24 hours. Therefore, the temperature can promote the crosslinking to happen, but also influence the physical nature of the fiber mat. In the course of the investigation, SEM images were taken (Figure 4.8) of electrospun SMI-P fibers before and after treatment at 80 and 130 °C, and very interesting results were obtained. The fibers were visually examined and it can be seen that the high temperature treatment at 130 °C had a significant effect. This was noticed from the slight shrinkage of the mat on the aluminium foil compared to its original state. Also, when removed it can be easily seen that the fiber mat became noticeably brittle.

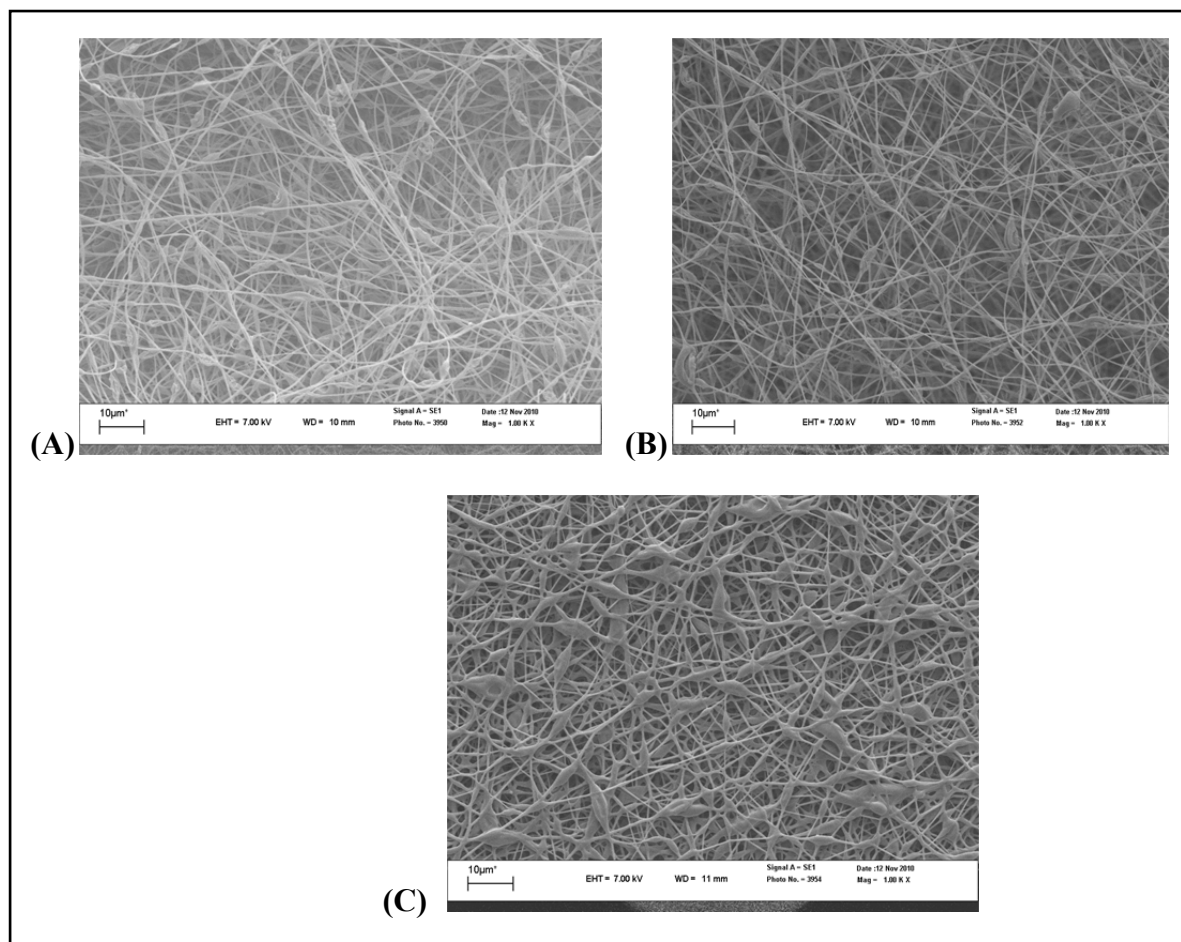


Figure 4. 8: SEM images of SMI-P fibers (A) untreated (B) treated at 80 °C, (C) treated at 130 °C.

From Figure 4.8 (C), on a macroscopic level, it can be seen that the fiber integrity has been lost compared to its original form. This could be due to heating the fibers above its T_g where the polymer chains are known to be mobile and hence the fibrous structure could be altered. However, the mat treated at 80 °C did not have any noticeable visual changes. According to the SEM images, it was difficult to see any differences between the untreated and treated fiber mat. It appeared flexible unlike the high temperature-treated mat. The interesting point is that both treated fibers were crosslinked, which was confirmed by the insolubility in various solvents such as DMF. The 80 °C treated mat and the untreated fibers were investigated further for thermal properties. Figure 4.9 shows the DSC thermograms of the untreated and the (crosslinked) 80 °C fibers. From the DSC analysis the T_g s of both fiber mats were almost identical at around 124 °C.

Chapter 4: Electrospinning of SMI copolymer derivatives

The actual nature and mechanism of crosslinking is still under investigation and conclusions cannot be drawn yet. However, the thermal treatment of SMI-P copolymer provided a starting point to treat the quaternized derivatives in the same manner.

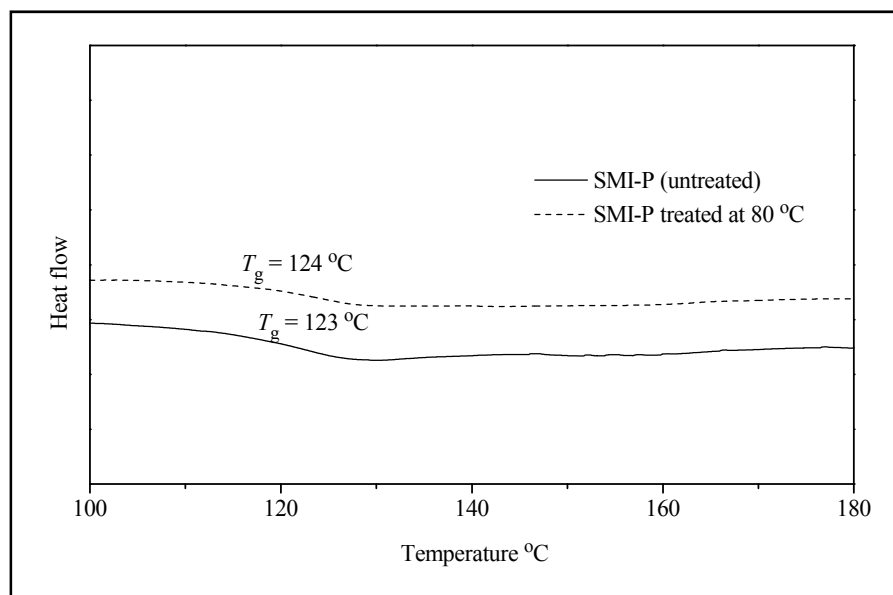


Figure 4.9: DSC curves of the treated and untreated SMI-P fibers

Thermal crosslinking of the quaternized fiber mats was only achievable at higher temperatures, unlike the parent macromolecule SMI-P. Therefore all the fibers were treated at 130 °C in a vacuum oven. Table 4.4 shows the T_g of the quaternized fibers obtained from the DSC. From the Table it can be seen that the T_g of all cured polymer fibers increased, which was expected. The increase in the T_g of the crosslinked fibers is attributed to the restriction of chain mobility and most likely leads to higher T_g compared to that of un-crosslinked fibers.

Table 4.4: The T_g of quaternized SMI-P copolymer derivatives.

Polymer	T_g °C	T_g (crosslinked) °C
SMI-Pq1	140	Difficult to detect
SMI-Pq4	153	165
SMI-Pq8	154	164
SMI-Pq12	146	154

Chapter 4: Electrospinning of SMI copolymer derivatives

The fiber diameters were analyzed by SEM after crosslinking, the results showed a slight decrease in fiber diameter compared to the un-crosslinked fibers. For example the SMI-Pq4 fibers (Figure 4.6) showed a slight decrease in the average fiber diameter from 460 ± 123 nm to 440 ± 95 nm, however, this decrease can be considered negligible if one takes the standard deviations of the averaged diameter values into account. A more significant decrease was observed with the SMI-Pq12 fibers as shown in Table 4.5. It is postulated that the fibers could have slightly shrunk because of polymer chains entropy changes during thermal treatment at 130 °C. Understanding the nature of the crosslinking process should provide useful information and thus thermal properties and fiber morphology can be correlated.

Table 4.5: Average fiber diameters before and after crosslinking of quaternized SMI-P derivatives.

Fiber	SMI-Pq1	SMI-Pq4	SMI-Pq8	SMI-Pq12
Average Diameter (nm) (not crosslinked)	420 ± 60	460 ± 123	430 ± 55	761 ± 220
Average Diameter (nm) crosslinked	360 ± 55	440 ± 95	390 ± 70	365 ± 55

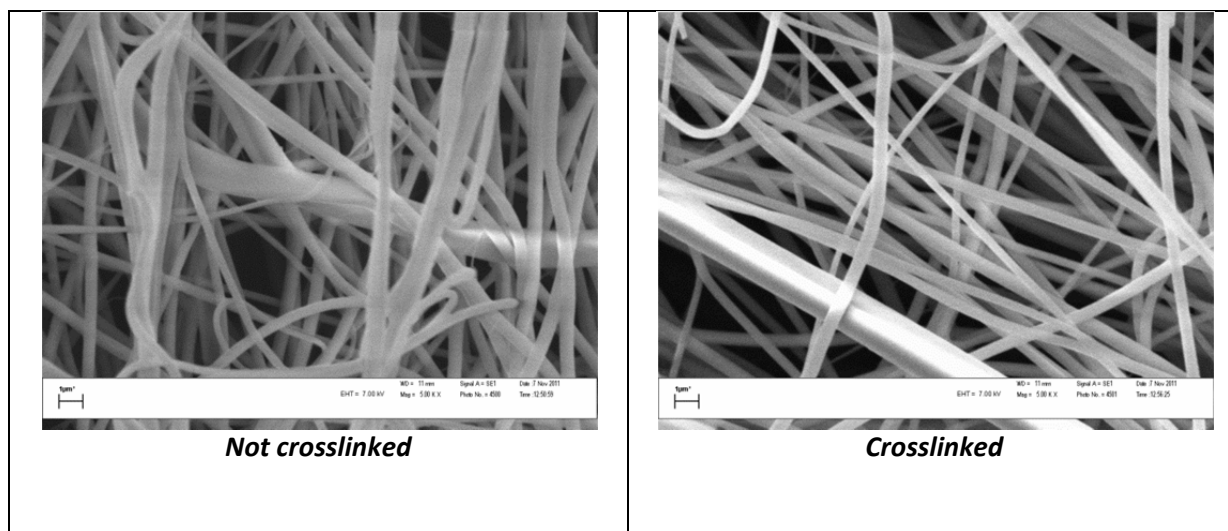


Figure 4.10: SEM image of the SMI-Pq4 fibers before and after crosslinking.

4.6 Conclusions:

The electrospinning of all synthesized styrene-maleimide copolymer derivatives was carried out. A successful set of conditions was found for each polymer system to produce non-woven fiber mats. The electrospun fibers were easily collected and analyzed by different analytical tools. According to the SEM imaging results, the average diameters were all in the nanometer range.

The TGA curves of the copolymer derivatives show an increase in thermal stability after imidization. The thermal stability of the quaternized precursors SMI-C and SMI-P have decreased substantially compared to the unquaternized polymers because of the presence of the bromide and iodide counter ions in the polymer.

Heat treatment of the soluble fiber was a successful method to transform the fibers into crosslinked insoluble mats. This adds an important and valuable property that may allow usage of the highly functionalized quaternary ammonium fiber mats in different conditions. Furthermore, it can motivate the investigation of various other alkyl halide derivatives that can be used in the quaternization and selectively tune the functional groups to meet specific requirements such as potency towards specific microorganisms.

4.7 References

1. Greiner, A.; Wendorff, J. H. *Angewandte Chemie International Edition* 2007, 46, (30), 5633-5633.
2. Agarwal, S.; Wendorff, J. H.; Greiner, A. *Polymer* 2008, 49, (26), 5603-5621.
3. Ramakrishna, S.; Fujihara, K.; Teo, W.-E.; Lim, T.-C.; Ma, Z., In *An introduction to electrospinning and nanofibers*, World Scientific Singapore 2005; pp 15-18.
4. Andrady, A. L., In *Science and technology of polymer nanofibers* Wiley Hoboken, N.J 2008; pp 7-110.
5. Ramakrishna, S.; Fujihara, K.; Teo, W.-E.; Lim, T.-C.; Ma, Z., In *An introduction to electrospinning and nanofibers*, World Scientific Singapore 2005; p 102.
6. Carl Zeiss Microscopy. <http://www.zeiss.de/C12567BE0045ACF1/Inhalt-Frame/668C9FDCBB18C6E2412568C10045A72E>

Chapter 4: Electrospinning of SMI copolymer derivatives

7. Billiani, G. H.; Vijayakumar, C. T.; Fink, J. K.; Lederer, K. *Journal of Analytical and Applied Pyrolysis* 1989, 16, (3), 221-227.
8. Maria Świtała-Żeliazkow. *Polymer Degradation and Stability* 2001, 74, (3), 579-584.
9. Baruah, S. D.; Laskar, N. C. *Journal of Applied Polymer Science* 1996, 60, (5), 649-656.
10. Roy, D.; Knapp, J. S.; Guthrie, J. T.; Perrier, S. b. *Biomacromolecules* 2007, 9, (1), 91-99.
11. Punyani, S.; Singh, H. *Journal of Applied Polymer Science* 2006, 102, (2), 1038-1044.
12. Moore, E. R. *Industrial & Engineering Chemistry Product Research and Development* 1986, 25, (2), 315-321.
13. Wästlund, C.; Maurer, F. H. J. *Polymer* 1998, 39, (13), 2897-2902.
14. Vermeesch, I.; Groeninckx, G. *Journal of Applied Polymer Science* 1994, 53, (10), 1365-1373.
15. Soer, W. J.; Ming, W.; Klumperman, B.; Koning, C.; van Benthem, R. *Polymer* 2006, 47, (22), 7621-7627.
16. Becker, H. G.; Schmidt-Naake, G. *Chemical Engineering & Technology* 2002, 25, (1), 37-41.
17. Lee, W.-F.; Hwong, G.-Y. *Journal of Applied Polymer Science* 1996, 59, (4), 599-608.
18. Lee, W. F.; Huang, G. Y. *Journal of Applied Polymer Science* 1996, 60, (2), 187-199.
19. Bhardwaj, N.; Kundu, S. C. *Biotechnology Advances* 2010, 28, (3), 325-347.

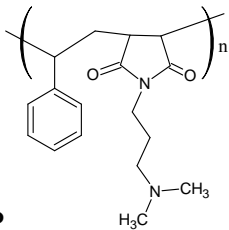
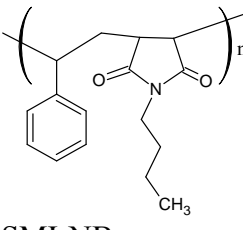
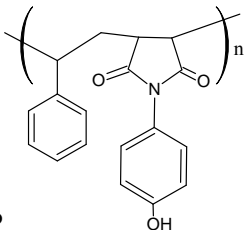
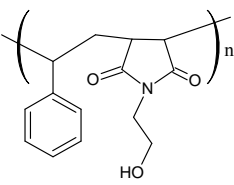
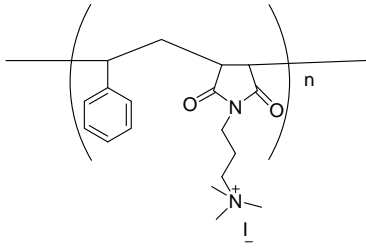
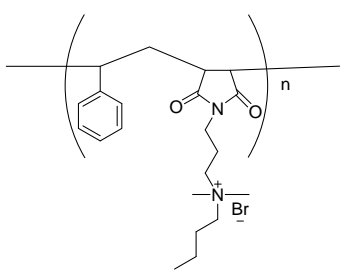
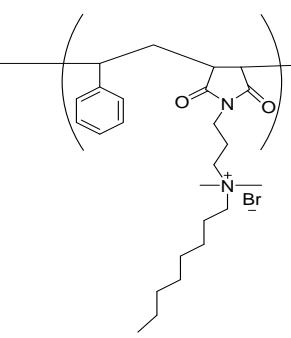
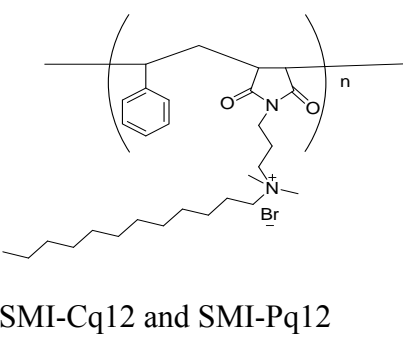
Chapter 5

Chapter 5: Antimicrobial Evaluation

5.1 Abstract

This chapter presents an antimicrobial evaluation study of all synthesized and modified electrospun polymer fibers. See Table 5.1 for chemical structures of the polymer fibers being assessed. The bactericidal activity of the fibers was examined against different bacteria including *Staphylococcus aureus* (Gram-positive), *Escherichia coli* and *Pseudomonas aeruginosa* (Gram-negative). The evaluation study utilized different tools to test for antibacterial activity and mode of cell death including bioluminescent imaging, fluorescence imaging and the viable cell counting method.

Table 5.1: Chemical structure and Polymer codes prepared in this work

 <p>SMI-P</p>	 <p>SMI-NB</p>	 <p>SMI-AP</p>
 <p>SMI-AE</p>	 <p>*SMI-Pq1 and **SMI-Cq1</p>	
 <p>SMI-Pq4 & SMI-Cq4</p>	 <p>SMI-Cq8 & SMI-Pq8</p>	 <p>SMI-Cq12 and SMI-Pq12</p>

*The letter P here refers to the copolymers modified copolymers from a prepared alternating SMA (~50% maleic anhydride) copolymer. **The letter C refers to modified copolymers prepared from a commercial SMA grade containing 28% maleic anhydride units

5.1 Bioluminescent imaging

Bioluminescence imaging (BLI) is a technique that has been developed over the past two decades for biomolecular imaging. It has been successfully used as a molecular imaging tool to obtain qualitative and semi-quantitative information of various biological processes *in vivo*.¹⁻³

Live animal imaging is one of the major techniques that rely on BLI, as it is non-invasive and allows real time monitoring of infectious disease, tumor cell growth, mammalian tissues, etc.⁴

BLI is based on the detection of visible light produced by enzyme (Luciferase)-mediated oxidation of a molecular substrate. The luciferase enzyme catalyzes a chemical reaction in the presence of oxygen and adenosine triphosphate (ATP) and emits light as one of the reaction products.⁵ The detectable photons can be captured by a charge coupled device (CCD) in a BLI system.⁶

In this work, a Xenogen IVIS[®] 200 Optical Imaging system (Figure 5.1) was used to detect the bioluminescence photons and convert them into an image of electrical charge patterns.

Monitoring the intensities generated in the processed image provides information on the biological processes of the organism.

In order to apply the BLI system in the antimicrobial evaluation, engineered bacterial strains obtained from (Caliper life sciences, Hopkinton MA, USA) were used for the assessment in this study. The bacterial strains have a *Photobacterium luminescens luxABCDE* operon (*lux* gene) to provide bioluminescence.

Metabolically active cells can be detected by monitoring the produced light detected by BLI such as the IVIS[®] imaging system.⁷ The light will evidently indicate that ATP is providing the energy required for cellular functions and it is metabolically active.¹ On the other hand, if the intensity of the photons decreases, it indicates a decrease in the concentration of ATP, and hence the cell becomes dormant or metabolically inactive and eventually dies. Thus bioluminescence is an indicator of the metabolic state of the cell.

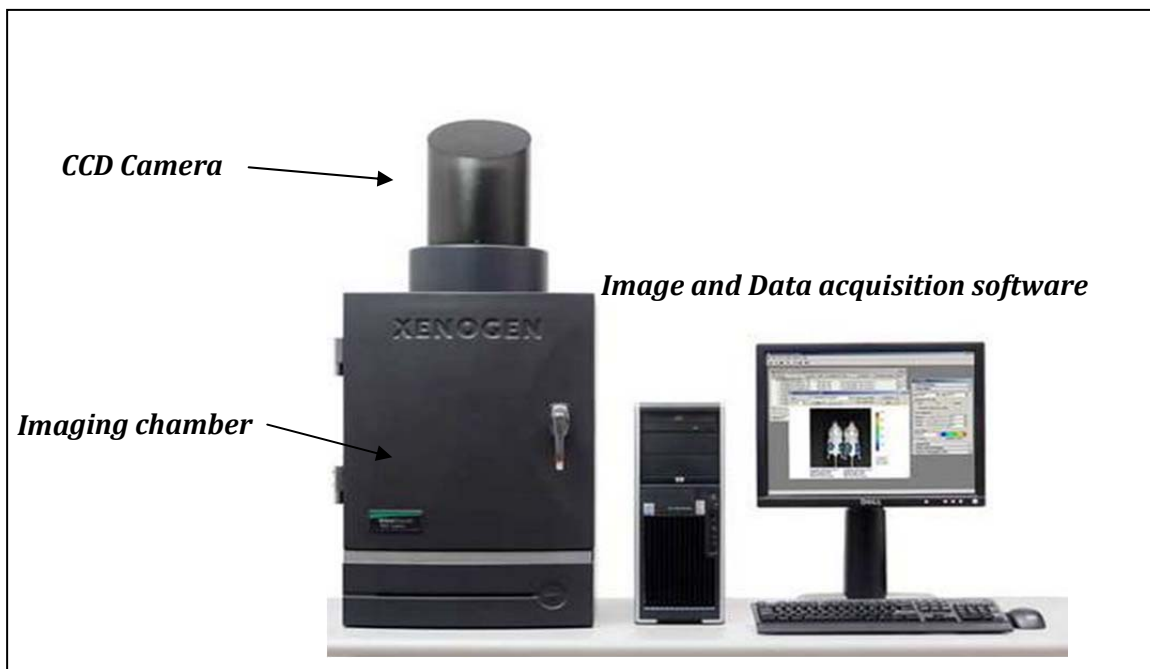


Figure 5.1: the IVIS® imaging system that was used in this study

5.1.1 Sample and culture preparation

In the antimicrobial efficacy tests, the bacterial cultures were grown in nutrient solutions (broth). Brain heart infusion (BHI, Biolab Diagnostic, Midrand, South Africa) for *S. aureus* and Luria Bertani broth (LB, Biolab Diagnostic, Midrand, South Africa) for *P. aeruginosa* or *E. coli*. Cultures were grown overnight at 37 °C. The cells were harvested in a centrifuge (8 000xg, 5 min), and resuspended in a sterile saline solution (prepared by dissolving 8.5 g of sodium chloride in 1 L of distilled deionized water in a “Schott” bottle followed by sterilization at 121 °C for 20 min).

The bacterial solution was further diluted in stock bottles to approximately $10^6 \sim 10^7$ cells.mL⁻¹ estimated by optical density (OD) measurement at 600 nm against a blank saline solution. Later will be presented as OD_{600 nm}.

In this section, only the bioluminescence imaging results of SMI-P fibers with *S. aureus* and *E. coli* cultures will be shown by this method. The other polymer fibers were also tested and their results will be illustrated.

A sample of a fiber mat was cut into pieces of different dimensions. A suitable fiber sample was then weighed and placed in a Petri dish (Figure 5.2).

Chapter 5: Antimicrobial evaluation

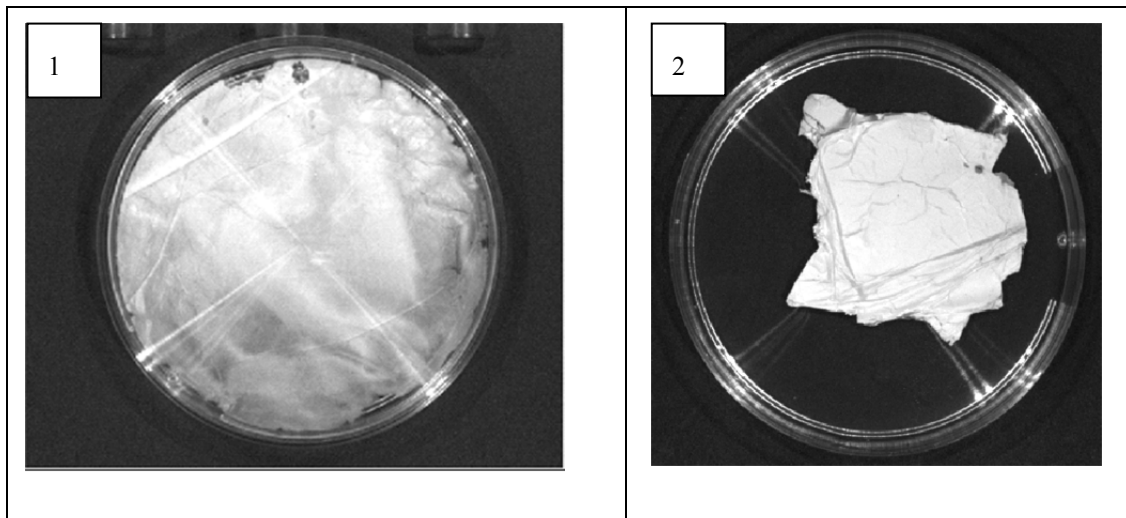


Figure 5.2: Photo Samples of electrospun SMI-P fibers, plate (1) (60 mg fiber mat), plate (2) (~20 mg fiber mat) taken inside the imaging chamber.

A specific bacterial culture (10 mL) for example of *S. aureus* Xen 36 (10^6 cfu/mL) was added to the plate containing the fiber. After gently swirling the solution for wetting the fiber mat, bioluminescent imaging was acquired at different time intervals using the IVIS[®] system. A culture plate (no fibers) was used as a control to compare the results.

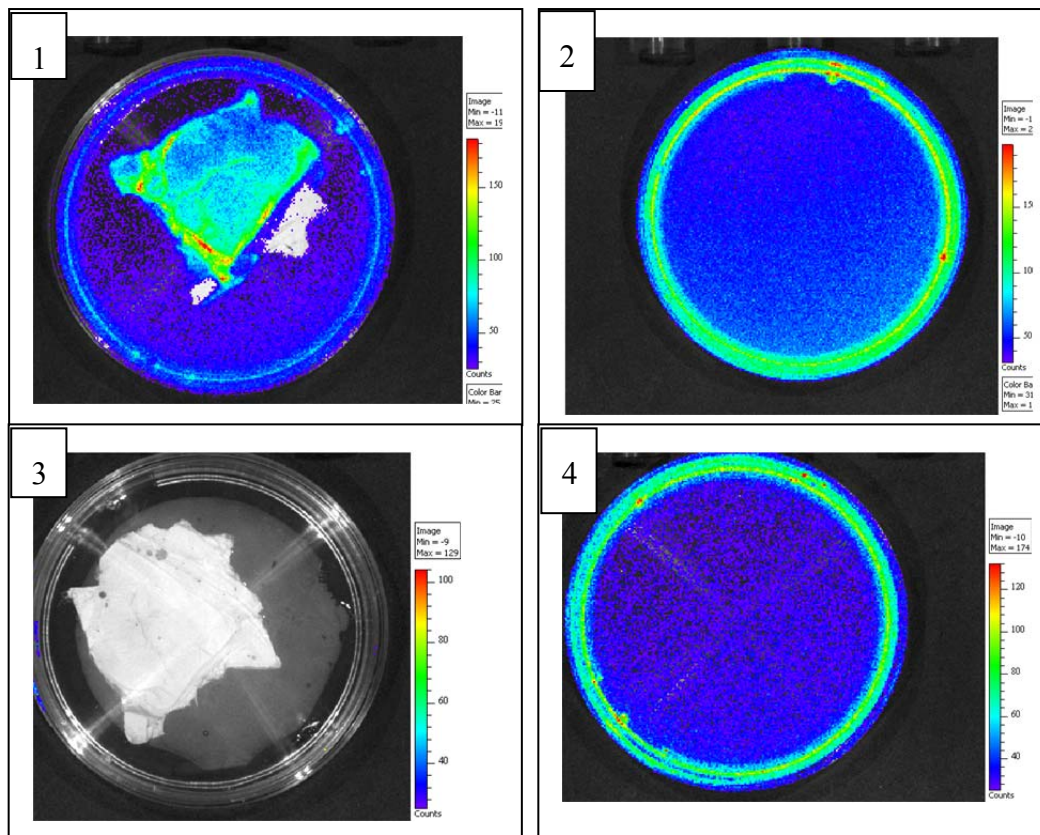


Figure 5.3: Bioluminescence of (*S. aureus* Xen 36) imaged with an IVIS[®] camera (exposure time 20 sec). (1) SMI-P fiber and 10 mL concentration $\sim 10^6$ cell.mL⁻¹ culture after 2 minutes of contact. (2) A control plate containing (*S. aureus* Xen 36) culture at time 0. (3) Sample from image (1) after one hour of contact (4) Control after 4 hours incubation.

Chapter 5: Antimicrobial evaluation

Figure 5.3 displays the bioluminescent imaging results of *S. aureus* (Xen 36) culture with and without SMI-P fibers contact. It is clearly shown that after around 1 hour of contact no bioluminescence of the culture was detected. However, the culture in the control plate was still able to show bioluminescence even after 4 hours.

The experiments were carried out at least three times and the same results were observed. Figure 5.4 shows the results of bioluminescence imaging of the same polymer but with a larger sample and a 20 mL culture. Observing the intensity of the bioluminescent bacteria culture over time gives an indication of the viability of the bacteria cells, where high intensity will be due to a large number of metabolically active cells present.

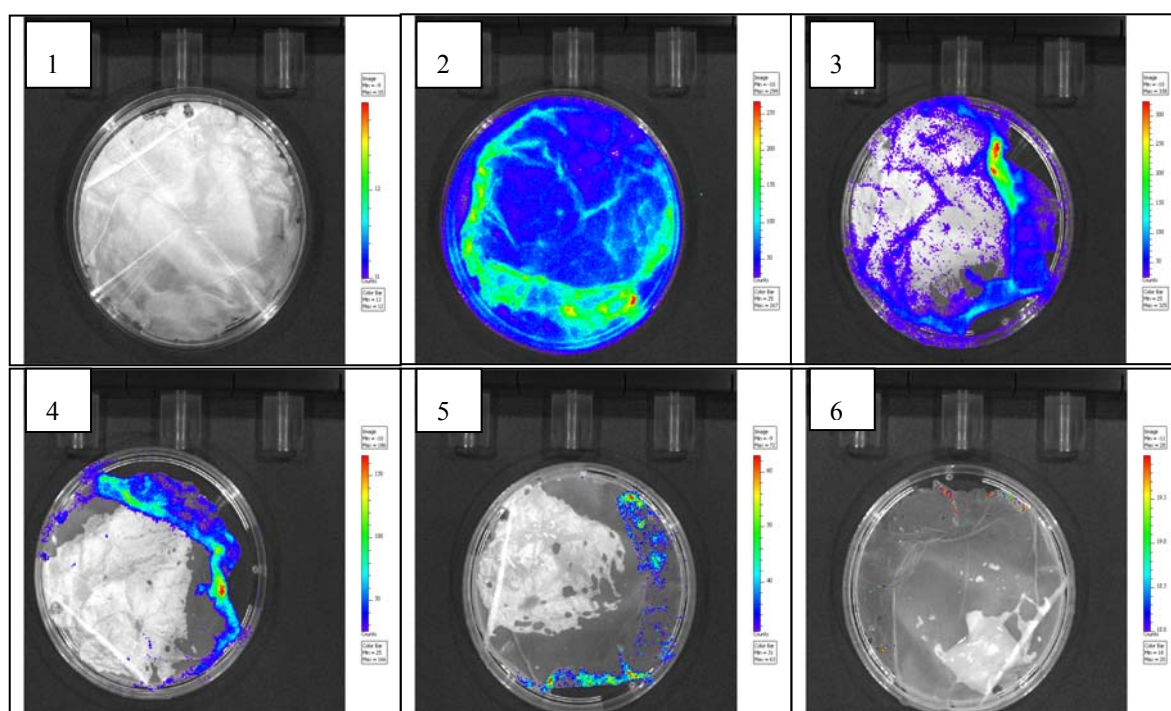


Figure 5.4: Bioluminescence of (*S. aureus* Xen 36) imaged with an IVIS[®] camera (exposure time 20 sec). (1) SMI-P fiber sample mat, (2) sample and bacteria solution (20 mL $\sim 10^7$ cell.mL⁻¹) time 0, (3) time 1 hour incubation, (4) 2 hours incubation, (5) 3:15 hours incubation, (6) 5:15 hours incubation

From both Figures (5.3 and 5.4), it can be seen that the presence of the fibers was responsible for causing the reduction and disappearance of detectable luminescence of the culture. This would imply that the fibers are active against the bacterial cells and probably affecting the ability of the bacteria to produce ATP as a result. Although all the other components for bioluminescence are present including luciferin (substrate), luciferase (enzyme) and oxygen,

Chapter 5: Antimicrobial evaluation

ATP remains the important element to produce light in this case. The reduction of luminescent intensity would most likely indicate that the cell becomes dormant and metabolically inactive or it is dead. In order to investigate whether the cells are still alive or not, 100 μ L was withdrawn from the culture that did not show any luminescence and inoculated in a liquid culture of BHI and incubated overnight at 37 °C. The incubated tubes have been monitored at least in the first 5 hours. Evidence of cell growth was noticed from the change of the clear BHI solution from being clear to opaque with time. This simply means that the culture sample taken from the Petri plates still contains living cells. The absence of detectable luminescence does not necessarily imply that all cells are actually dead. It is speculated that the surviving cells must be in a dormant state and metabolically inactive, yet if the right conditions and nutrition are found they may grow again.

The fibers were also tested against a culture of *E. coli* Xen 14 (10^6 cfu/ml) in the same way. Figure 5.5 shows the imaging results of a fiber mat in contact with an *E. coli* (Xen 14).

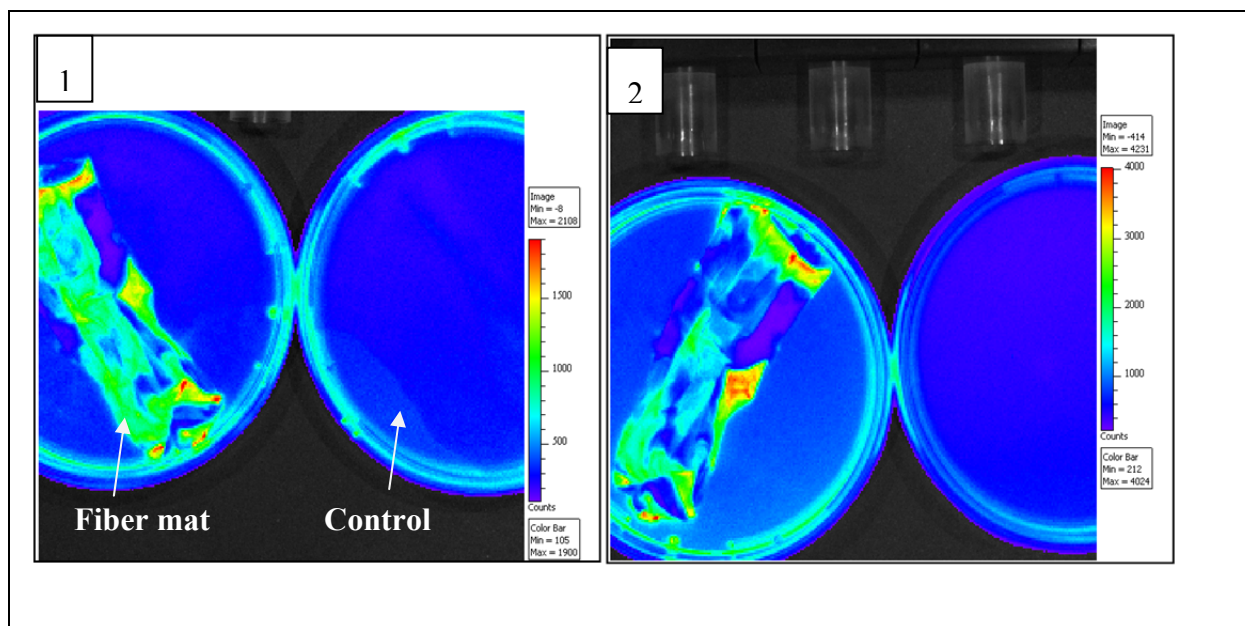


Figure 5. 5: Bioluminescence of *E. coli* (Xen14) imaged with an IVIS camera (exposure time 20 sec). (1) SMI-P fibers and *E. Coli* after 10 minutes contact, (2) after 80 minutes.

It is quite clear that the SMI-P fibers are less potent towards *E. coli* compared to its activity against *S. aureus*. As evident from the luminescence image of the bacterial culture, there was no significant change in the luminescent intensity after an hour of contact in contrast to the results observed when the same fibers were in contact with *S. aureus* culture.

Chapter 5: Antimicrobial evaluation

The bioluminescence imaging was carried out for all the fibers in the same way. Table 5.2 summarizes the bioactivity results of different polymer fibers using IVIS in conjunction with different strains.

Table 5. 2: Antibacterial assessment results using bioluminescence imaging by IVIS.

Strain	* Active fibers observed according to IVIS imaging system.		
	Incubation time -----> activity decreases		
	1 hour	2-5 hours	>5 hours
<i>E.coli</i> (Xen14)	SMI-Pq1, SMI-Pq 4, SMI-Pq 8, SMI-Pq 12 SMI-Cq1, SMI-Cq4, SMI-Cq8,	SMI-AP	SMI-P
<i>S. aureus</i> (Xen 36)	SMI-Pq1, SMI-Pq4, SMI-Pq8, SMI-Pq12 SMI-Cq1 SMI-Cq4, SMI-Cq8, SMI-Cq12		
<i>P. aeruginosa</i> (Xen5)	SMI-Pq1, SMI-Pq4 , SMI-Pq8, SMI-Pq12	SMI-AP	

* *The activity was based on significant reduction of bioluminescence as a function of incubation (example image 3 in Figure 5.5) time compared to the luminescence intensity of the control culture.*

The assessment was based on the observation of changes in luminescent intensity of the bacterial cultures when treated with the fibers compared to a control. The observation from this assessment indicated that all quaternized polymer fibers show significant activity against the bacterial cultures. It was considered that the fibers are active if appreciable bioluminescent reduction was observed within the first incubation hour. Non-quaternized maleimide-styrene copolymer fibers such as SMI-P and SMI-AP showed very good activity against *S aureus*. However, when *E. coli* was treated, the decrease in the luminescence was not as rapid as in the case of *S. aureus*. No significant activity was observed for any of the unquaternized type copolymer fibers when in contact with *P. aeruginosa* (Xen 5) except for SMI-AP that showed activity as indicated by comparing the IVIS images with time.

The IVIS imaging system is a powerful tool to qualitatively assess antimicrobial fiber mats. This is a qualitative evaluation and it cannot be considered as a quantitative indication of the antibacterial activity. In order to determine the antimicrobial activity in a quantitative way, other methods must be applied. Thus, in this study the shake flask (viable cell count) method was used for quantitative antimicrobial assessments.

5.2 Antimicrobial assay of fiber mats using shake flask method (ASTM E2149)

The ability of the modified electrospun fibers to kill bacteria was tested using the shake flask (viable cell count) method. This test ensures good contact between bacteria, and the polymer fibers by constant agitation of the test specimen in a bacterial suspension during the test period.

All modified electrospun fibers were tested against *S. aureus* and *E. coli*, however, only the potent fibers from the results against these strains were examined against *P. aeruginosa*.

The electrospun fiber mats of each polymer were tested in triplicate. Pieces of the fiber mats 25-26 mg were placed in a sterile centrifuge tube.(Figure 5.6). Aliquots of 5 mL from the stock culture solution (prepared as in the previous section) were added to each tube. Control experiments were run in which no fibers were present in the bacteria culture and treated in a similar way. After an incubation period of 24 hours at 37 °C, 1 mL of the solution was taken from each tube then added to 9 mL of sterile saline, and diluted (decimal serial dilutions until 10⁶) by mixing 1 mL with 9 mL of sterile saline solution.

Samples (100 μ L) of the decimal dilutions were spread on agar plates containing 2% agar for solid media. (BHI for *S.aureus* Xen 36 and LB for *E. coli* Xen 14 or *P. aeruginosa* Xen 5 as previously mentioned). Cells were incubated overnight at 37 °C. After incubation, the plates were examined and the number of colony forming units (CFU) was counted manually. The results, after multiplication by the dilution factor, were expressed as mean colony forming units per milliliter (CFU/mL).

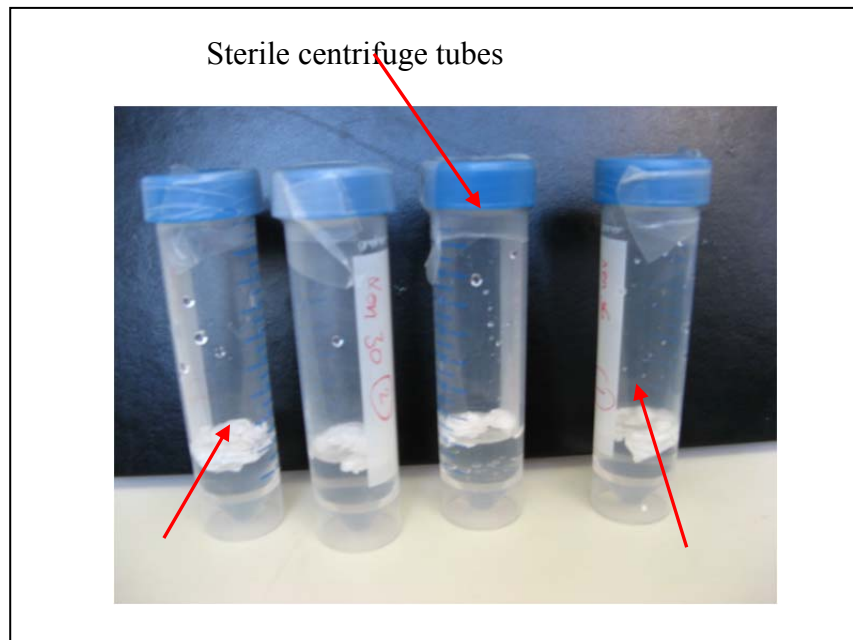


Figure 5.6: Tubes containing the fibers and bacterial culture used in the AM assay.

Table 5.3 shows the results of the antibacterial assessment against *S. aureus* and *E. coli* using the shake flask method. The viable cell count results correlates well with previous observations using the BLI system, although in this case quantitative measurements are achieved.

Chapter 5: Antimicrobial evaluation

Table 5. 3: Antibacterial activity of the fibers against *S. Aureus*

Initial cell concentration of <i>S. aureus</i> (OD _{600nm} , 0.019) $\sim 9.0 \times 10^6$ cell.mL ⁻¹		
Initial cell concentration of <i>E. Coli</i> (OD _{600nm} , 0.014) $\sim 7.0 \times 10^6$ cell.mL ⁻¹		
<u>Average Log reduction of CFU</u>		
<u>Fiber type</u>	<u><i>S. aureus</i></u>	<u><i>E. coli</i></u>
SMI-AE	no significant activity	no significant activity
SMI-NH	no significant activity	no significant activity
SMI-NB	no significant activity	2 Log
SMI-AP	6 Log (100% kill)	5 Log
SMI-P	5 Log	3 Log
SMI-Pq1	6 Log (100% kill)	5 Log
SMI-Pq4	6 Log (100% kill)	6 Log (100% kill)
SMI-Pq8	6 Log (100% kill)	4Log
SMI-Pq12	6 Log (100% kill)	6 Log (100% kill)
SMI-Cq1	3 Log	3 Log
SMI-Cq4	3 Log	2 Log
SMI-Cq8	3 Log	1 Log
SMI-Cq12	3 Log	1 Log
Control plates	1.5×10^6 CFU. mL ⁻¹	1.3×10^6 CFU. mL ⁻¹

Starting from the unquaternized maleimide-based copolymers, only fibers with tertiary amine or phenol functionalities (SMI-AP, SMI-P) showed significant antibacterial activity. This was not unexpected, as it was shown in previous studies that these groups have potential antibacterial properties. For instance Jeong *et al.*⁸ have modified electrospun SMA fibers to obtain SMA-AP conjugate (figure 5.7) The fibers in a 1 mL (10 wt%) sample exhibited bactericidal activity against *E. coli* and *S. aureus*.

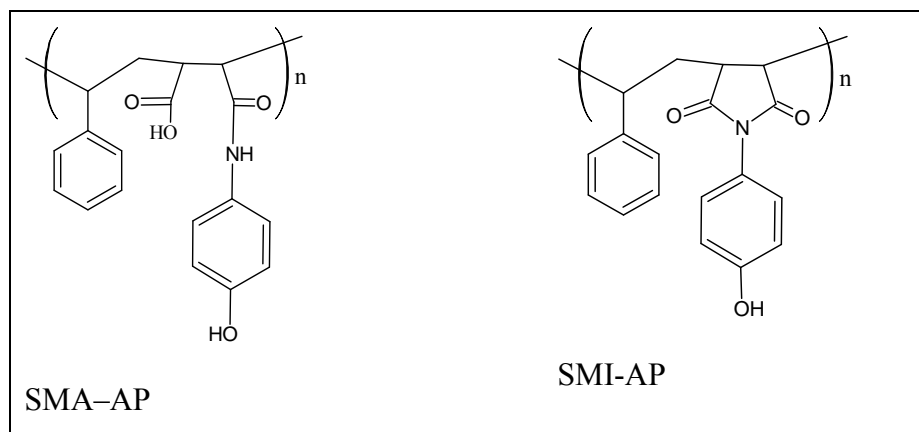


Figure 5.7: Phenol functionalized styrene maleic anhydride and maleimide derivatives.

In this study, the phenol functionality was also considered as an active agent to be introduced in the polymer. However, unlike the case of Jeong's work, the copolymer SMI-AP was prepared by the copolymerization of styrene and 4-hydroxyphenyl maleimide. The polymer in the imide form is more stable, compared to the SMA-AP conjugates prepared by Jeong's, where the opened ring structure is susceptible to hydrolysis through the amide bond. However, under the same antimicrobial test conditions, no hydrolysis of SMA-AP was detected.

Nonaka *et al.*⁹ reported that resins containing phenol derivatives with one, two, or three hydroxyl groups exhibited antibacterial properties. In their study the resins containing phenolic derivatives exhibited higher antibacterial activity against *E. coli* than against *S. aureus*. They also attributed the activity to the presence of phenolic hydroxyl groups in the resin, as the activity increased with increasing the phenolic hydroxyl groups in the resins.

Kenaway *et al.*¹⁰ prepared sulfonated derivatives of polyvinyl phenol ($\bar{M}_w = 20k$ and $100k$). They reported that electrospun polyvinyl phenol (20k) showed antimicrobial activity against *B. subtilis* while the higher molecular weight fibers do not show antimicrobial activity. However, the fibers were examined on a medium as a sole source of carbon with different strains including *bacilli*, *thermophilic bacilli*, *Pseudomonads*. It was found that no growth was obtained even for the high molecular weight polymer, indicating that neither polymer can be degraded by the testing strains. In this study, SMI-AP fibers were very active against *S. aureus* as it killed 100% cells in the 24 hours incubation. Very good activity against *E. coli* was also observed but not to the extent that all cells were killed.

Chapter 5: Antimicrobial evaluation

The activity of SMI-AP is attributed to the presence of phenol moieties. Phenol is known to induce progressive leakage of intracellular constituents,¹¹ including the release of K^+ , the first indicator of membrane damage.¹²

The viable-cell count was also reduced by the tertiary amine fiber derivative (SMI-P) showing good antibacterial properties. SMI-P fibers showed stronger activity against Gram-positive bacteria *S. aureus* as viable cell counts showed a log 5 reduction compared to a log 3 cell reduction of Gram-negative *E. coli*. The activity of a tertiary amine functionality covalently bonded to a polystyrene fiber was first tested by Endo *et al*¹³. The antimicrobial assessment of the functionalized fibers revealed that the fibers were more active against Gram-negative bacteria such as *E. coli*, *P. aeruginosa*, *K. pneumoniae*, *Salmonella typhimurium* and *Serratia marcescens* than against Gram-positive *S. aureus*. They have attributed the antimicrobial property of the modified fibers to the presence of the tertiary amine groups, in which electrostatic interaction between the tertiary amine moieties and the divalent cations such as Mg^{2+} , Ca^{2+} and Fe^{2+} . Because divalent cations normally function as cation bridges between adjacent phosphates of membrane lipids in Gram-negative bacteria, it was suggested that the cationic tertiary amine groups are competing with other cationic active sites in the outer membrane. This eventually damages the function of the outer membrane and causes cell death.

A more recent study by Gelman *et al*.¹⁴ also investigated the antibacterial activity of poly(2-(N,N-dimethylamino)ethyl)styrene), and its quaternized derivative against various bacteria such as *E. coli*, *B. subtilis*, VRE (vancomycin-resistant enterococci) and MRSA (methicillin-resistant *S. aureus*). They have shown that a dimethylamino functionalized styrene has greater antimicrobial activity than its analogous N-quaternized derivative suggesting reversible protonation has some impact on the biocidal activity.

In both of the mentioned studies it seems that the styrenic based tertiary amine polymers are more potent against Gram-negative bacteria than Gram-positive in general. However, unlike previous studies the tertiary amino containing fibers SMI-P in this study showed stronger potency to Gram-positive bacteria than Gram-negative bacteria. This can be attributed to the fact that, the modified polymers examined in this study all contained maleimide functionality, and had significant affect on the bioactivity of the macromolecule as a whole, compared to

Chapter 5: Antimicrobial evaluation

other macromolecules having the same bioactive moieties such as those prepared by Endo *et al.*¹³

The other styrene-maleimide derivatives including SMI-NB and SMI-AE did not show significant activity except for SMI-NB where a log 2 reduction was observed against *E. coli*.

The incubated plates for SMI-AE (Figure 5.8) and SMI-P (Figure 5.9) antimicrobial assessment against *S aureus* are shown as an example. It can be seen that the samples from SMI-AE assessment at 10^{-3} dilutions on agar plates are comparable to the control plates at the same dilution 10^{-3} which is an indication for inactivity of the fibers. On the other hand, in Figure 5.9 the difference is very clear, the control plates display complete coverage of the plates by cell growth. The fiber-treated plates only show a few colonies, indicative of the antimicrobial activity of the SMI-P fibers.

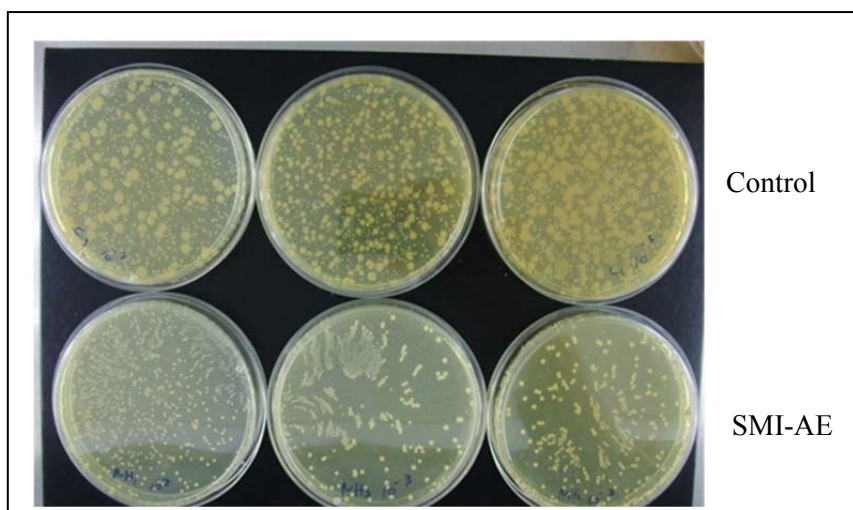


Figure 5.8: Agar plate photos (*S. aureus*). Comparative view of the plated 10^{-3} diluted solutions between the control and the treated culture with SMI-AE fibers (triplicate samples).

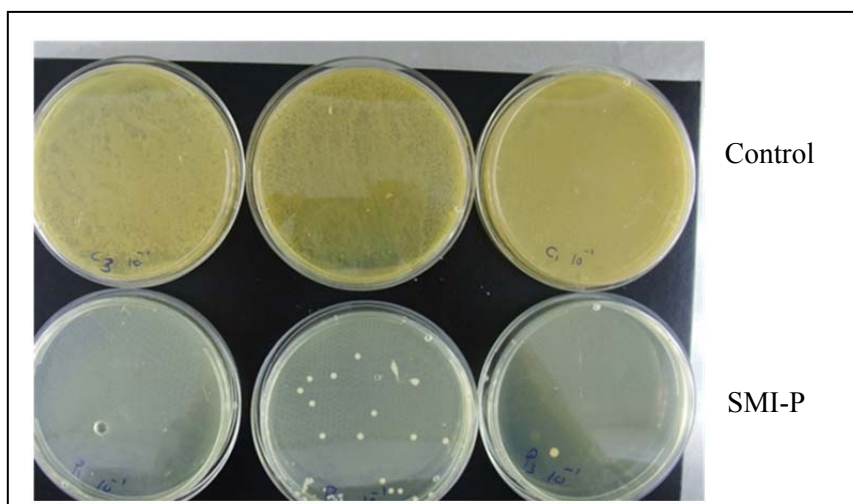


Figure 5.9: Agar plate photos (*S. aureus*). Comparative view of the plated 10^{-1} diluted solutions between the control and the treated culture with SMI-P fibers. S.

However, two different grades of polymer precursors were used. The first SMA precursor was a commercial grade containing about 28% wt maleic anhydride units, the modified polymers based on this precursor are assigned as SMI-C, the letter C is for the commercial grade. The second SMA grade was an alternating copolymer prepared in this study, having approximately 50% of maleic anhydride units, modified via imidization to obtain SMI-P precursor.

Both SMI-C and SMI-P are essentially the same type of copolymers, however, the number of functional tertiary amine groups in SMI-P is roughly twice that in SMI-C. The quaternized derivatives are indicated with the letter (q) and a number describing the number of carbon atoms of the alkyl halide that was used in the quaternization. In this study, a C_1 iodide and C_4 , C_8 , C_{12} bromides were used to investigate their effect on the antimicrobial properties.

From Table 5.3 the antimicrobial activity of all quaternized SMI-P derivatives was the strongest. The fibers of SMI-Cq1,4,8,12 are less active than the SMI-P quaternized derivatives by about 50% (logarithmic scale) when tested against *S. aureus* and *E. coli*. For example, the activity of SMI-Cq1 fibers against *S. aureus* showed a 3 log reduction (Figure 5.10) compared to a 6 log reduction (100% reduction) when treated with SMI-Pq1 as indicated by the incubated agar plate with not a single colony present. (Figure 5.11)

Murata *et al.*¹⁵ investigated the effect of charge density and chain length of polymeric quaternized brushes polyDMAEMA functionalized on an inorganic surface. They have found

Chapter 5: Antimicrobial evaluation

that surface charge density is a critical element in designing a surface for maximum kill efficiency.

The lower activity of the SMI-C quaternized derivatives compared to the SMI-P derivatives can be directly related to the number of tertiary amino groups present in each polymer. Since the SMI-P derivatives have more quaternized groups than the SMI-C derivatives, they are expected to have a larger number of charges, which provided stronger bactericidal activity.



Figure 5.10: Agar plate images (*S. aureus*). Comparative view of the plated 10^{-1} diluted solutions between the control and the treated culture with SMI-Cq1 fibers.

Regardless of the length of the alkyl chain used in the quaternized polymers, the activity against *S. aureus* was very strong for all SMI-P quaternized fibers as indicated by the complete killing of all the cells.

Figure 5.11 displays photo examples of the incubated agar plates resulting during the antimicrobial assay of SMI-Pq1 and SMI-Pq4 against *S. aureus*.

In order to verify that all cells were dead and not adhered to the fiber mat, the fibers were removed from the tube after counting the CFUs on the agar plates, and inoculated in a tube of BHI medium at 37 °C overnight. There was no sign of any growth in the tubes after 24h incubation. This implies that indeed the quaternized SMI-P fibers were very potent and have extremely good antibacterial activity against *S. aureus*.

Chapter 5: Antimicrobial evaluation

However, only SMI-Pq4 and SMI-Pq12 were able to 100% kill *E. coli* cells. It was expected that the variation in the alkyl chain length of the quaternary ammonium groups would have an influence on antibacterial activity of the fibers.

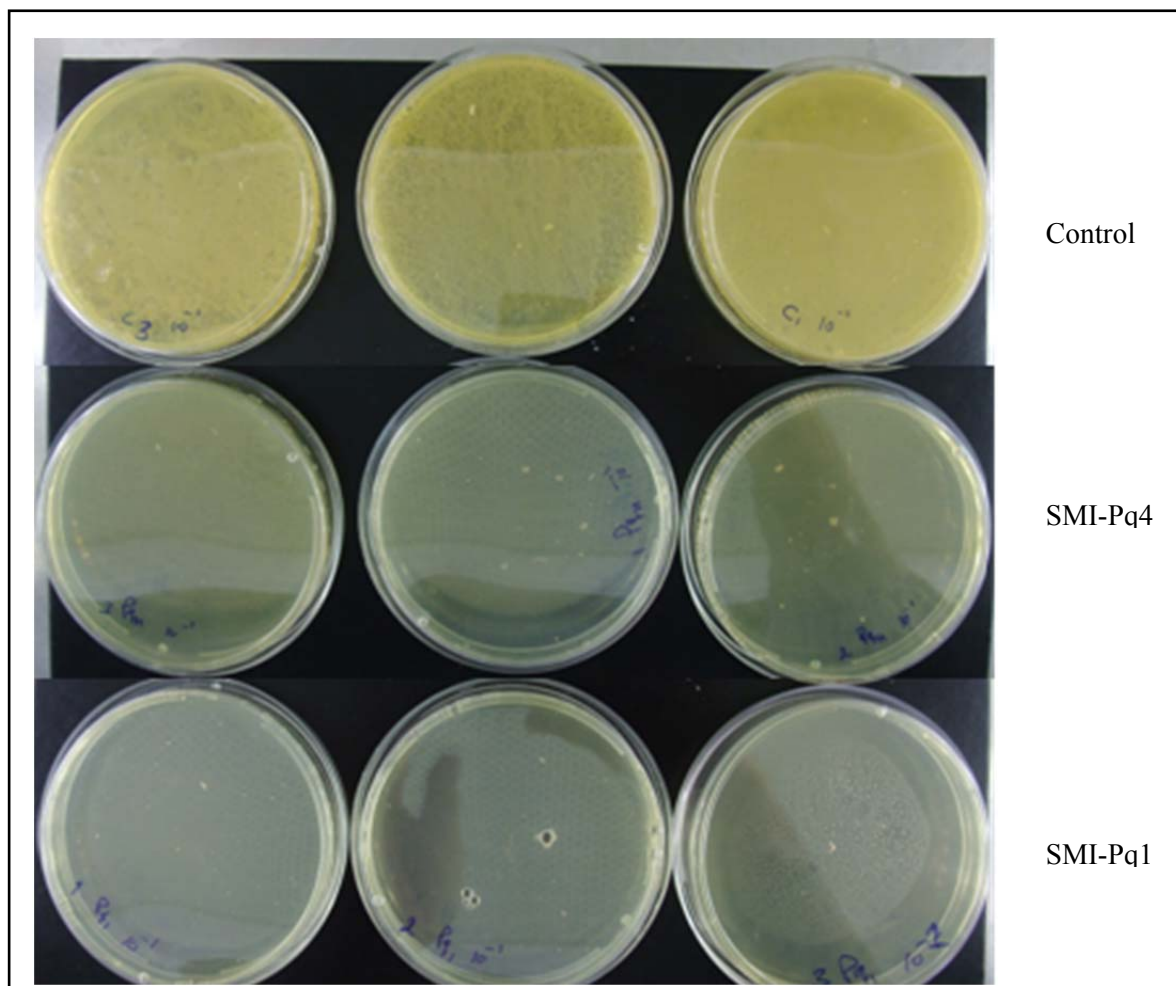


Figure 5.11: Agar plate images (*S. aureus*). Comparative view of the plated 10^{-1} diluted solutions between the control and the treated culture with SMI-Pq1 and SMI-Pq4 fibers.

The polymer fibers that exhibited good antimicrobial properties were tested against another pathogenic bacteria Gram-negative *P. aeruginosa*. The polymer fibers considered for activity evaluation included SMI-P, SMI-NB, SMI-AP and the quaternized derivatives of SMI-P.

The antimicrobial assessment results are summarized in Table 5.4.

Table 5.4: A summary of antimicrobial tests against *P. aeruginosa*

<i>Initial concentration ~ 10⁵ Cell.mL⁻¹ (600 nm)</i>	
Fiber type	Average Log reduction of CFU
SMI-P	no significant activity
SMI-NB	no activity
SMI-AP	3Log
SMI-Pq1	3Log
SMI-Pq4	2Log
SMI-Pq8	5 Log (100% kill)
SMI-Pq12	3Log
Control plates counted after 24 hr = 3.5 × 10 ⁵ CFU	

Many antimicrobial studies of polymers have shown that alkylation can influence antimicrobial efficacy in a different manner, depending on the alkyl chain length and the actual polymer system. For example, Ikeda *et al.*¹⁶ investigated the antimicrobial activity of quaternized poly(trialkylvinylbenzylammonium chloride)s, it was found that the quaternized C₁₂ derivative significantly enhanced its antimicrobial activity.

However, others have observed a decrease in antimicrobial activity with an increase in alkyl chain length. For instance, Roy *et al.*¹⁷ studied the antimicrobial activity of quaternized (C₈₋₁₆) poly-DMAEMA grafted on cellulose fibers against *E. coli*. The antimicrobial activity was found to depend on the alkyl chain length and on the degree of quaternization, whereby the C₈ quaternized copolymer derivative showed a greater activity than the longer alkyl chain derivatives. The authors discussed that the C₁₂ and C₁₆ have increased the hydrophobic character of the polymer. The increase in the hydrophobicity may therefore limit the interaction between the polymer and the bacteria cell membrane, as they are not as easily wetted by the aqueous medium. However, C₈ quaternized derivative is easily wetted and resulted in better antimicrobial properties.

Chapter 5: Antimicrobial evaluation

The results obtained in this study however do not follow the trend, as it can be clearly seen that the SMI-Pq8 was not very potent against *E. coli* as it was against *S. aureus*. However, the same fibers were able to kill 100% all *P. aeruginosa* cells.

On the other hand SMI-Pq4 and SMI-Pq12 fibers were consistently active against *S. aureus* and *E. coli* with 100% kill. However, the same fibers were not very active against *P. aeruginosa* as observed by a 3 log cell reduction for Pq12 and only 2 log cell count reduction in the case of Pq4 fibers.

The phenol containing derivative was also active and only resulted in a 3 log cell reduction, the tertiary amine SMI-P derivative as well as the alkyl maleimide derivative SMI-NB did not show any significant activity.

It is rational to consider that every polymer system with a different backbone behaves differently, even if the same antimicrobial agent is immobilized. The properties of the whole macromolecule can significantly change and react differently in various media. Polycationic antimicrobial agents are known to have a diffusion and binding tendency to the cytoplasmic membrane of the bacteria. This binding is in the form of both electrostatic and hydrophobic interactions in relation to the molecular weight /length of the alkyl chain of the cationic polymer.^{18,19} Thus it is believed that an optimal range of alkyl chain length and molecular weights exist for antimicrobial activity of polymers.²⁰

5.3 External antimicrobial tests

Since one of the advantages of electrospun fibers is their application as membrane filters, it was in part intended to provide protection against biological warfare agents that may be used in biodefense, or counterterrorism. Among different possible biological agents are considered viruses, bacteria, and their toxins. E.g. bacterial threats/diseases such as the following: bacillus anthracis/anthrax, yersinia pestis/plague, *V. cholerae*/plague, etc.

Fiber samples of SMI-P showed significant antimicrobial activity, the preparation of the polymer itself was easily managed and also was very easy to be electrospun with low toxicity solvents such as ethanol. It was therefore considered one of the interesting polymer materials to focus on and investigate its activity with other different Gram-negative and Gram-positive bacteria.

Chapter 5: Antimicrobial evaluation

The SMI-P fibers were tested against *Bacillus anthracis*, methicillin resistant *S. aureus* (MRSA), *Yersinia pestis* and *Vibrio cholerae* at the Netherlands Organization for Applied Scientific Research (TNO).

The tests were carried out by (TNO) personnel in a similar manner as previously described in this study. The fibers were treated with diluted overnight culture in a tube. The experiments were carried out in triplicates for each strain. At time intervals 2, 4, 6, 24 and 48 hours 0.1 mL was withdrawn and plated on agar plates for colony counts. All plates were incubated at 35 °C except for *Y. pestis* at 26 °C.

The results indicated that the fibers were able to inhibit the growth of all the strains except the spores as described in Table 5.6. As an example, Figures 5.12 and 5.13 show photos of agar plates during the antimicrobial evaluation of the fibers against *B. anthracis* and *Y. pestis*

Table 5.5: a summary of antimicrobial assessment of SMI-P fibers against various bacteria

Bacteria strain	Amount CFU	Antibacterial assessment
MRSA	4.6×10^6	3 log reduction was observed after 24 h, still inhibited but not killed even after 78 h.
<i>V. cholerae</i>	6×10^6	3 log reduction after 24 h
<i>Y. pestis</i>	3.2×10^6	6 log reduction and complete kill after 6 hours.
<i>B. anthracis</i>	8×10^4	5 log reduction, bacteria is inhibited but not killed even after 76 h.
<i>B. anthracis</i> spores	1.6×10^6	No activity

Chapter 5: Antimicrobial evaluation

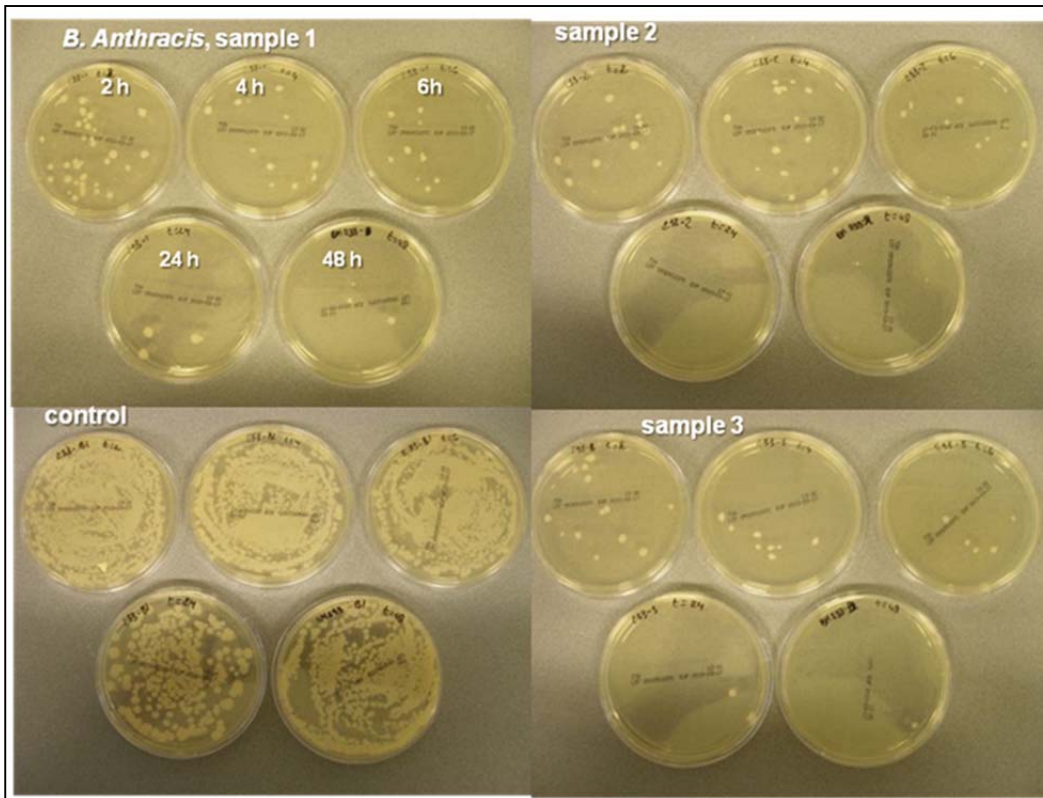


Figure 5.12: Incubated plates of the triplicates treated with *B. Anthracis*, from time 2h-48 hr

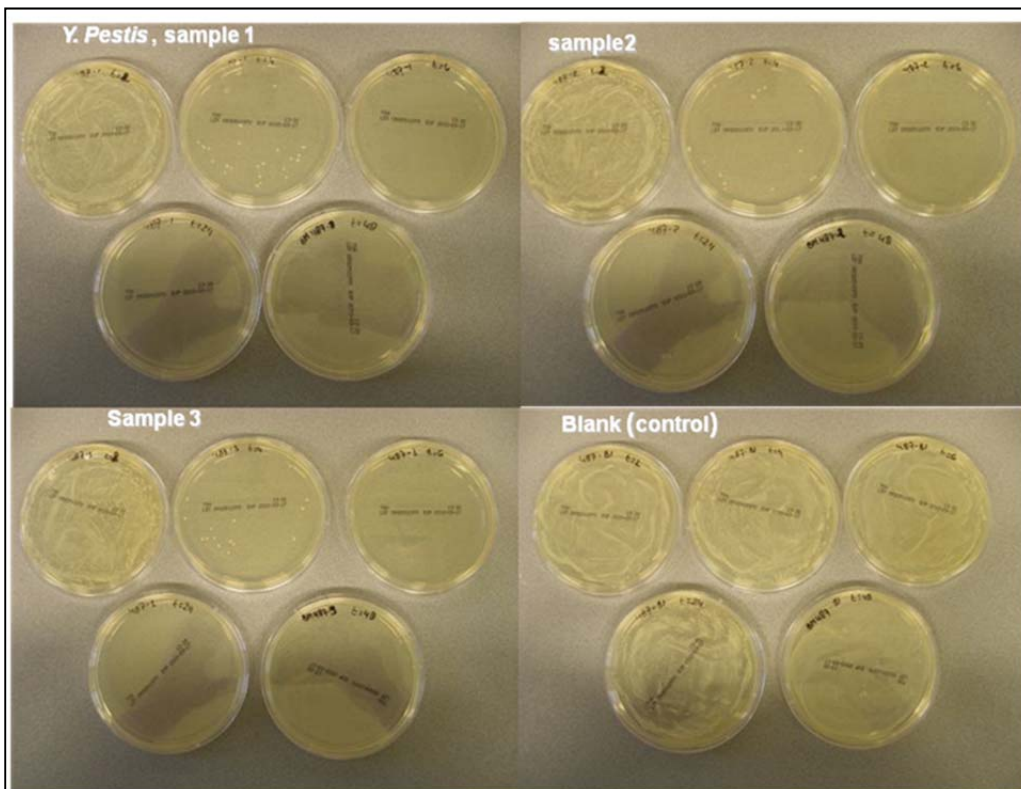


Figure 5.13: Incubated plates of the triplicates treated with *Y. pestis* from time 2h-48 hr

5.4 Evaluation using fluorescent microscopy

Cell viability assays using fluorescent microscopy has been shown to be an effective and very useful tool for toxicity and antimicrobial assays.²¹⁻²³ The key here is using specific fluorescent dyes that can stain certain cell constituents such as DNA, RNA and nucleic acids. Some of these dyes are known commercially as "LIVE/DEAD" BacLight Bacterial Viability kits, these have the capability of monitoring the viability of the bacteria as a function of the cell's membrane integrity.^{24,25} The lysis process in a cell can be monitored with these stains by counting the number of intact and permeable cells at different time points.²⁴

In this work, Fluorescence microscopy was utilized in part to investigate the mode of action of the fibers towards the bacteria cells. For this experiment, two different fluorochromes were used to stain nucleic acids of the bacteria cell for cell viability. Propidium iodide (PI) emits light in the range of the red spectrum. The second fluorochrome a derivative of bis-benzimidazoles (usually referred to by the original manufacturer as Hoechst). The Hoechst fluorochrome (emits blue light when excited), freely diffuses through the membrane, intercalating with the DNA, and therefore indicates viable and non-viable bacteria. In contrast, PI is a DNA intercalater and used as a viability dye to discriminate between viable and non viable cells as it penetrates only bacteria with damaged membranes.²⁶

Experimentally, this was performed by placing a small piece of fiber in the stained diluted bacteria solution (diluted *S. aureus* cells in saline solution 0.85% NaCl) and incubated for at room temperature for 1 hour.

Hoechst (Hoechst 33342, Sigma) and PI (Sigma, P4170), in a 1:200 dilution in silane, were directly added onto diluted *S. aureus* culture, using a final concentration of 50 µg/mL and 1 µg/mL respectively. Incubation took 10 min and images were acquired immediately thereafter.

Samples were observed on an Olympus Cell^{^R} system attached to an IX-81 inverted fluorescence microscope equipped with a F-view-II cooled CCD camera (Soft Imaging Systems). Using a Xenon-Arc burner (Olympus Biosystems GMBH) as light source, images were excited with the 360 nm, 472 nm or 572 nm excitation filter. Emission was collected using a UBG triple- bandpass emission filter cube. For the z-stack image frame acquisition, an

Chapter 5: Antimicrobial evaluation

Olympus Plan Apo N 60x/1.4 Oil objective and the Cell[^]R imaging software have been used. Images were processed and background-subtracted using the Cell[^]R software.

During incubation for 60 min, fluorescent images were taken to monitor changes and the results were compared to a control sample containing no fiber.

Fluorescence-based assays showed that cells incubated with bactericidal fibers for 60 min exhibited a substantial loss in viability (Figure 5.14), indicated by an increased PI signal.

After 60 minutes, the imaging results showed significant reduction of living cells. In fact, the effect was rapid, as the uptake of PI fluorescent cells increased with time. In comparison, bacteria without the fiber treatment (control) showed the Hoechst signal only, with hardly any PI signal. The appearance of red fluorescent cells is explained by PI uptake because all damaged cell membranes become permeable to PI which is thus an indication of cell death. The same response was observed for all active potent fibers. The death of the bacteria cells is most likely as a result of disruptive interaction on the cell wall at the lipid interface damaging the membrane followed by cell lysis.

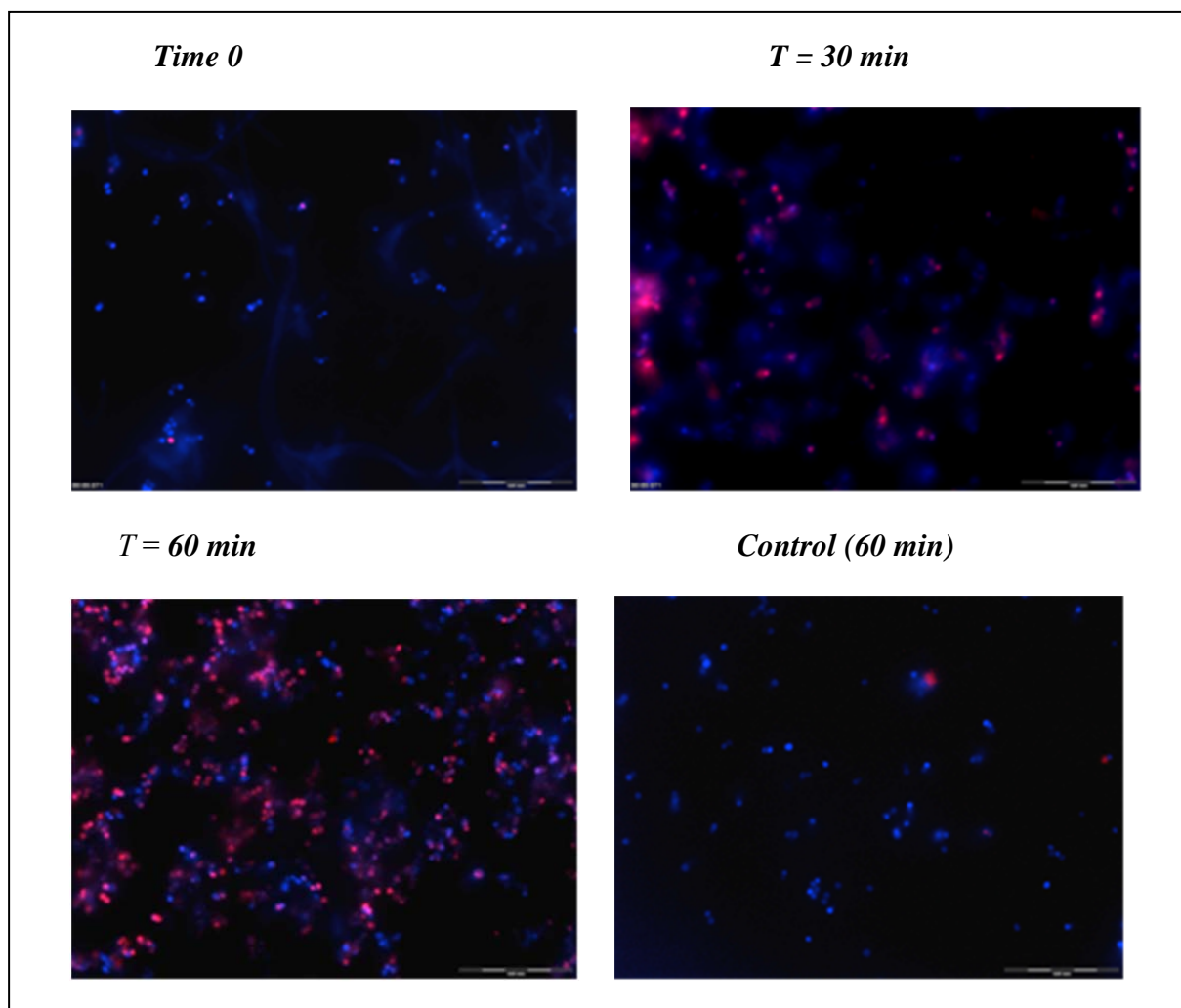


Figure 5.14: Fluorescent microscope images of incubated fibers (SMI-Pq12) with *S. aureus* in saline solution

5.5 Cytotoxicity assay

Biocompatibility of synthetic quaternized polymers besides its antimicrobial activity has attracted considerable attention in recent years.

It is well accepted that most antimicrobial polymers such as quaternary ammonium/phosphonium polymers act by a disruptive interaction on the cell wall at the lipid interface.²⁷ However, the most interesting feature of some antimicrobial polymers is their ability to exhibit higher activity towards bacterial cells than towards mammalian cells.¹⁹ As an indication of the toxicity of the fibers, toxic potency of selective fibers (SMI-Pq1, SMI-Pq4, SMI-Pq8, SMI-Pq12, SMI-P, and SMI-AP) was tested against rat cardiac H9c-2 cells as a mammalian cell culture model.^{28,29}

Chapter 5: Antimicrobial evaluation

H9c-2 Cells were seeded at a density of 10^5 /mL into petri dishes, and grown to a confluency of 70-80 %. Propidium iodide (PI) is a membrane-impermeable dye which intercalates with the DNA. Its uptake is therefore an indication for the loss of membrane integrity, a hallmark of necrotic cell death. In contrast, nuclear condensation (pyknosis) is characterized by condensed chromatin and cell shrinkage, a hall mark of apoptosis.³⁰ The formation of apoptotic bodies can therefore be assessed by the use of the Hoechst fluorochrome. Both, apoptotic and necrotic cell death provide therefore detailed information regarding cell viability and potential cytotoxic effects.

In this assay (Hoechst-33342) and PI (Sigma, P4170), in a 1:200 dilution in PBS, were directly added onto the cells, using a final concentration of 50 μ g/mL and 1 μ g/mL respectively. A consistent small piece of each fiber type in triplicate was incubated with the cells for up to four hours. Fluorescence microscopy was then used to observe the samples during incubation time. Fluorescence was monitored and images were acquired at 1, 2 and after 4 hours incubation time and compared to a control of cells without any fiber. The percentage PI was calculated by counting the red fluorescent cells as a ratio to the total cells in each sample image. The mean average value of each sample was then used for the cell viability assay.

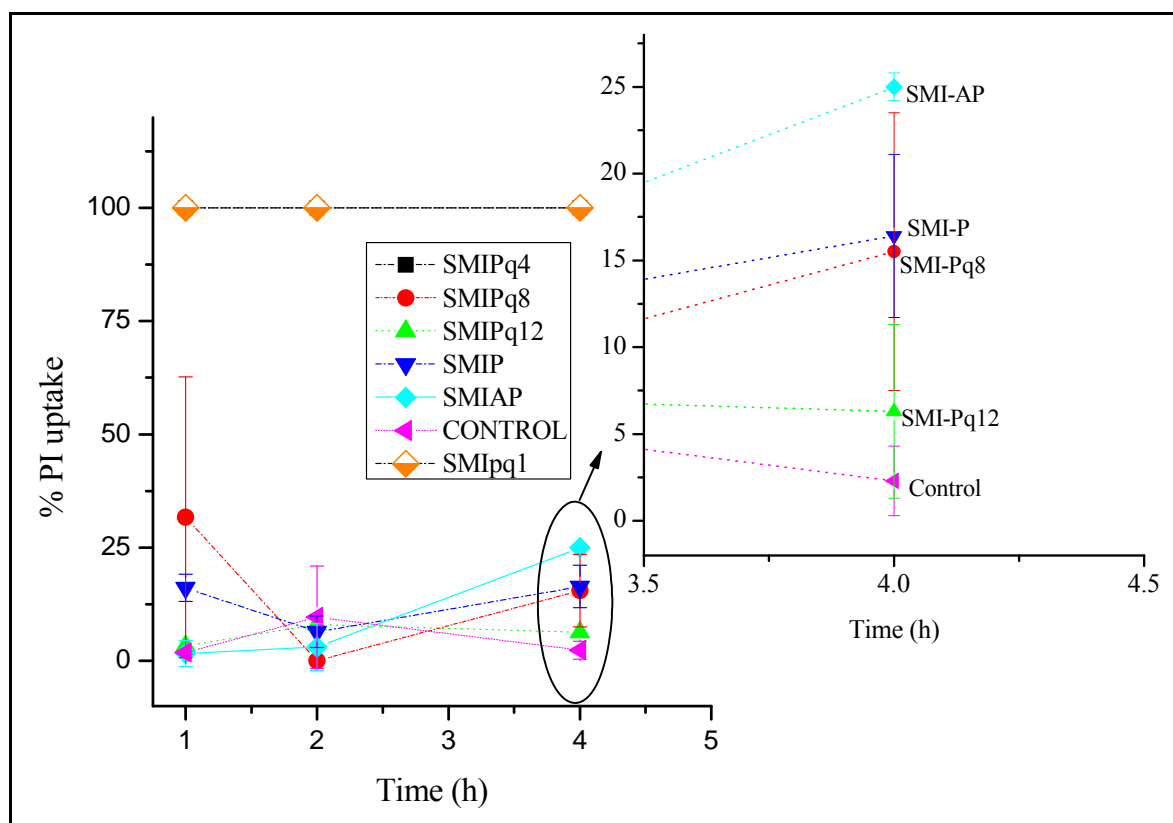


Figure 5.15: (PI) uptake of H9c-2 Cells treated with various antimicrobial fibers. The H9c-2 Cells were incubated with the fibers at room temperature for up to 4 hours. Assays were calculated from fluorescence results acquired after 1, 2 and 4 hours incubation.

Figure 5.15 illustrates the percentage of PI uptake with time for all the tested fibers. It can be seen from the figure that the quaternary ammonium SMI-Pq4 and SMI-Pq1 fibers were extremely toxic as observed by the high (100 %) PI uptake within one hour incubation and zero viable (blue) cells. This was a clear indication of rapid cytotoxicity of both fibers towards H9c-2 cells by compromising the cell membranes, as evident by the PI signal and thus cell death. Thus, the bioactivity of both SMI-Pq1 and SMI-Pq4 fibers indicates that they are nonselectively active, meaning it disrupts both mammalian and bacterial cell membranes.

However, cell viability in contact with the other fibers was much better. Fibers containing tertiary amino groups SMI-P and phenol groups SMI-AP showed a decline in viable cells as the PI uptake was noticed to increase with time. In the case of SMI-AP no significant PI uptake of the cells was observed, in contrast, the viability decreased by around 25% after 4

Chapter 5: Antimicrobial evaluation

hours incubation. On the other hand SMI-P was a little less harmful as 73.6% \pm 4.7 viable cells were observed as judged from the PI signal.

The monitored fluorescence of SMI-Pq12 samples revealed little change in cell viability compared to the control. For example after one hour incubation viable cells calculated 96.5% \pm 1.5 (viability control after 1 h 98.2% \pm 0.3). The PI uptake hardly increased after 4 hour incubation at 93% \pm 5.0 viable cells compared to the control 97.5% \pm 2.0 viable cells.

In a similar study by Milovic *et al.*³¹ it was shown (using Live/Dead fluorescence assay) that polycationic bactericidal *N*-hexyl,methyl- poly(ethylenimine) surface coating, although highly lethal to bacteria, has no harmful effect on mammalian (monkey kidney) cells.

In Summary, this work shows the toxicity of the fibers on H9c-2 cells decreases in the order of SMI-Pq1, SMI-Pq4 > SMI-AP > SMI-P > SMI-Pq8 > SMI-Pq12. Figure 5.16 displays a representation of the results from fluorescence images acquired in the assay, whereby one image per fiber is shown as an example and compared to a control image.

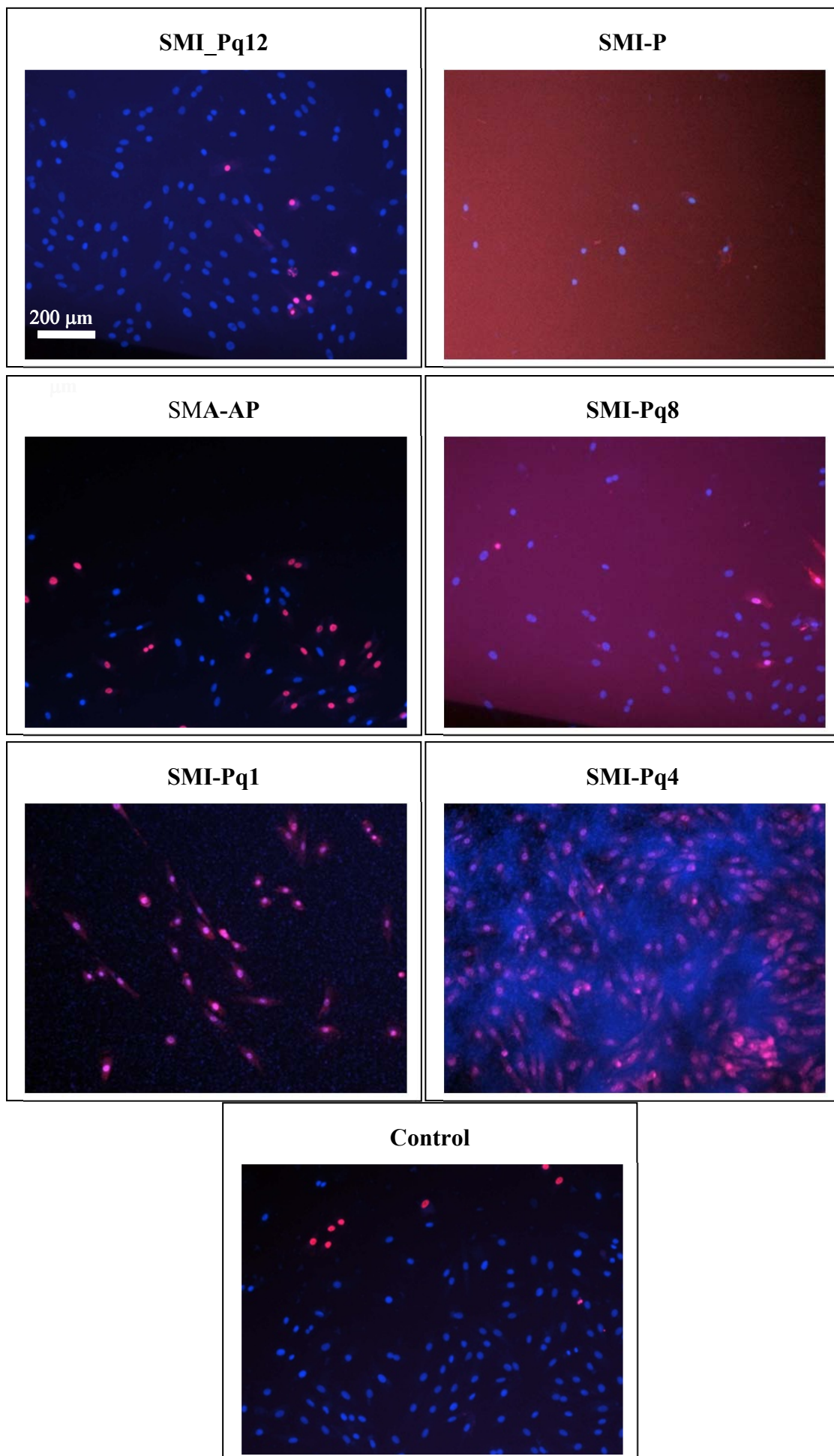


Figure 5.16: Fluorescence microscopy images of H9c-2 cells after incubation for 4 hours with various fibers as indicated in the figure.

5.6. Conclusion:

From the results, it is clear that the polymer fibers of the quaternized SMI-P type derivatives are the most potent for both Gram-negative and Gram-positive bacteria. The quaternized derivatives of the commercially available precursor SMI-C was about 50% less active than those prepared from the alternating precursor SMI-P.

The concentration of the fiber used in the antimicrobial evaluation is reasonably low (126-130 $\mu\text{g/mL}$). Interesting and positive results were obtained for most of the fibers. Functionalized fibers of maleimide-styrene copolymer derivatives such as SMI-AE did not show any significant antimicrobial activity against the tested strains. SMI-NB fibers were slightly active against *E. coli*. SMI-P fibers showed good activity against *S. aureus* and moderate activity against *E. coli*. No significant bactericidal activity was detected for all unquaternized fibers against *P. aeruginosa* except for SMI-AP.

The use of the fluorescence microscopy technique has allowed to monitor bacteria viability based on membrane damage, because PI fluorochrome only penetrates into the bacteria with a damaged membrane. A significant reduction of the viable cells (blue fluorescence) was demonstrated by fluorescent microscopy, suggesting that the bacteria treated by the electrospun fibers had compromised membranes. Membrane damage is therefore one of the most likely causes for the death of the bacteria. Also, using the same set of fluorochromes, an indication of cytotoxicity towards mammalian (cardiac rat) cells was carried out by monitoring fluorescence with time. The quaternized polymer with the longest alkyl chain SMI-Pq12 showed the least toxic effect on the cells. Contrarily, fibers quaternized by short C1 and C4 alkyl chains had very toxic activity against the cells.

5.7 References:

1. Doyle, T. C.; Burns, S. M.; Contag, C. H. *Cellular Microbiology* 2004, 6, (4), 303-317.
2. Sadikot, R. T.; Blackwell, T. S. *The Proceedings of the American Thoracic Society* 2005, 2, (6), 537-540.
3. De Almeida, P. E.; Van Rappard, J. R. M.; Wu, J. C. *American Journal of Physiology - Heart and Circulatory Physiology* 301, (3), H663-H671.
4. Andreu, N.; Zelmer, A.; Wiles, S. *FEMS Microbiology Reviews* 2011, 35, (2), 360-394.
5. Shah, K.; Weissleder, R. *Neurotherapeutics* 2005, 2, (2), 215-225.

Chapter 5: Antimicrobial evaluation

6. Rice, B. W.; Cable, M. D.; Nelson, M. B. *Journal of Biomedical Optics* 2001, 6, (4), 432-440.
7. Marques, C. u. N. H.; Salisbury, V. C.; Greenman, J.; Bowker, K. E.; Nelson, S. M. *Journal of Antimicrobial Chemotherapy* 2005, 56, (4), 665-671.
8. Jeong, J.-H.; Byoun, Y.-S.; Lee, Y.-S. *Reactive and Functional Polymers* 2002, 50, (3), 257-263.
9. Nonaka, T.; Uemura, Y.; Ohse, K.; Jyono, K.; Kurihara, S. *Journal of Applied Polymer Science* 1997, 66, (8), 1621-1630.
10. Kenawy, E.-R.; Abdel-Fattah, Y. R. *Macromolecular Bioscience* 2002, 2, (6), 261-266.
11. McDonnell, G.; Russell, A. D. *Clinical Microbiology Reviews* 1999, 12, (1), 147-179.
12. Lambert, P. A.; Hammond, S. M. *Biochemical and Biophysical Research Communications* 1973, 54, (2), 796-799.
13. Endo, Y.; Tani, T.; Kodama, M. *Applied and Environmental Microbiology* 1987, 53, (9), 2050-2055.
14. Gelman, M. A.; Weisblum, B.; Lynn, D. M.; Gellman, S. H. *Organic Letters* 2004, 6, (4), 557-560.
15. Murata, H.; Koepsel, R. R.; Matyjaszewski, K.; Russell, A. J. *Biomaterials* 2007, 28, (32), 4870-4879.
16. Ikeda, T.; Tazuke, S.; Suzuki, Y. *Die Makromolekulare Chemie* 1984, 185, (5), 869-876.
17. Roy, D.; Knapp, J. S.; Guthrie, J. T.; Perrier, S. b. *Biomacromolecules* 2007, 9, (1), 91-99.
18. Tashiro, T. *Macromolecular Materials and Engineering* 2001, 286, (2), 63-87.
19. Gabriel, G. J.; Som, A.; Madkour, A. E.; Eren, T.; Tew, G. N. *Materials Science and Engineering: R: Reports* 2007, 57, (1-6), 28-64.
20. Ignatova, M.; Voccia, S.; Gilbert, B.; Markova, N.; Mercuri, P. S.; Galleni, M.; Sciannamea, V. r.; Lenoir, S.; Cossement, D.; Gouttebaron, R.; JÃ©rÃ©me, R.; JÃ©rÃ©me, C. *Langmuir* 2004, 20, (24), 10718-10726.
21. Kang, S.; Pinault, M.; Pfefferle, L. D.; Elimelech, M. *Langmuir* 2007, 23, (17), 8670-8673.
22. Schiffman, J. D.; Elimelech, M. *ACS Applied Materials & Interfaces* 2011, 3, (2), 462-468.
23. Grapski, J. A.; Cooper, S. L. *Biomaterials* 2001, 22, (16), 2239-2246.
24. Bunthof, C. J.; van Schalkwijk, S.; Meijer, W.; Abee, T.; Hugenholtz, J. *Applied and Environmental Microbiology* 2001, 67, (9), 4264-4271.
25. Laflamme, C.; Lavigne, S.; Ho, J.; Duchaine, C. *Journal of Applied Microbiology* 2004, 96, (4), 684-692.

Chapter 5: Antimicrobial evaluation

26. Brana, C.; Benham, C.; Sundstrom, L. *Brain Research Protocols* 2002, 10, (2), 109-114.
27. Timofeeva, L.; Kleshcheva, N. *Applied Microbiology and Biotechnology* 2010, 89, 1-18.
28. Hescheler, J.; Meyer, R.; Plant, S.; Krautwurst, D.; Rosenthal, W.; Schultz, G. *Circulation Research* 1991, 69, (6), 1476-1486.
29. Zordoky, B. N. M.; El-Kadi, A. O. S. *Journal of Pharmacological and Toxicological Methods* 2007, 56, (3), 317-322.
30. Loos, B.; Engelbrecht, A.-M. *Autophagy* 2009, 5, (5), 590-603.
31. Milović, N. M.; Wang, J.; Lewis, K.; Klibanov, A. M. *Biotechnology and Bioengineering* 2005, 90, (6), 715-722.

Chapter 6

Chapter 6: Conclusions and Recommendations

The synthesis and characterization of antimicrobial polymer derivatives obtained from styrene-maleic anhydride copolymers was presented in this thesis. All the polymers synthesized in this study were electrospun into nanofibers and evaluated for antimicrobial activity. The main findings and recommendations are discussed in this chapter.

6.1 Conclusions

Modification of Poly(styrene-co-maleic anhydride) (SMA) copolymers

In this study two SMA copolymer grades were chosen. An alternating SMA-P (prepared in this study) and a random SMA-C (obtained commercially) were chemically modified to maleimide derivatives. Conventional free radical polymerization was performed to obtain the alternating SMA-P copolymer with a dispersity of 2.7 and a weight average molecular weight (M_w) 128 000 g mol⁻¹. The imidization of the SMA copolymer was successfully performed using three aliphatic primary amino reagents including *n*-aminobutane, 2-aminoethanol and 3-dimethylaminopropylamine (DMAPA). The resulting imidized polymer products were poly(styrene-co-*n*-butylmaleimide) (SMI-NB), poly(styrene-co-*N*-(2-hydroxyethyl)maleimide) (SMI-AE) and poly(styrene-co-*N*-(3-*N,N*-dimethylaminopropyl)maleimide) (SMI-P).

A fourth amino compound (4-aminophenol) was used to synthesize *N*-(*p*-hydroxyphenyl)maleimide (HPM). Free radical copolymerization of HPM with styrene was performed and poly(styrene-co-*N*-(hydroxyphenyl)maleimide) (SMI-AP) was obtained with M_w 31 000 g mol⁻¹, and dispersity ($D = 2.0$).

The most important maleimide copolymer derivatives among those synthesized were the styrene-co-*N*-(3-*N,N*-dimethylaminopropyl)maleimide copolymers SMI-P and SMI-C. These copolymers were used as essential precursors for the preparation of quaternary ammonium derivatives using alkyl halides with various aliphatic chain lengths, including methyl iodide (C₁), 1-bromobutane (C₄), 1-bromooctane (C₈), and 1-dodecylbromide (C₁₂). All modified styrene-maleimide (SMI) copolymer derivatives were successfully characterized by ATR-FTIR, ¹³C-NMR and ¹H-NMR spectroscopy.

Electrospinning of styrene-maleimide copolymer derivatives

The prepared styrene-maleimide copolymer derivatives were successfully electrospun into nanofiber mats with average fiber diameters below 1000 nm. The thermal properties of the fiber mats was investigated, according to the TGA results, the copolymer derivatives show an increase in thermal stability after imidization of the SMA-P precursor. The quaternized derivatives of SMI-P had lower thermal stability as indicated by the lower decomposition temperatures compared to the tertiary amine-functional precursors SMI-P and SMI-C.

Thermal treatment was a successful method to crosslink the water-soluble quaternized fiber mats. The treatment at 130 °C resulted in crosslinked fibers that are insoluble in either water or other polar solvents such as DMF.

Antimicrobial evaluation

The electrospun nanofiber mats were all subjected to antimicrobial evaluation against different bacterial strains including Gram-positive bacteria *Staphylococcus aureus* Xen 36 and Gram-negative bacteria *Escherichia coli* (Xen 14) and *Pseudomonas aeruginosa* (Xen 5).

Bioluminescence assay

It was shown that the bioluminescence technique can be used as a qualitative method for antimicrobial activity screening of nanofibers. This was achieved by utilizing bacterial strains that contains the *Photobacterium luminescens luxABCDE* operon (*lux* gene) to provide bioluminescence.

Viable cell count assay

The shake flask method was applied for the antimicrobial activity assay of the fibers against Gram-positive strain *S. aureus* Xen 36 and Gram-negative strains *E. coli* Xen 14 and *P. aeruginosa* Xen 5.

With regards to the unquaternized SMI fiber derivatives, the fibers of SMI-AP were the most potent against all bacterial strains. Whereby it killed *S. aureus* populations (6 log) and reduced the populations of *E. coli* Xen 14 and *P. aeruginosa* Xen 5 by 5 log and 3 logs respectively in 24 hours.

Chapter 6: Conclusions and Recommendations

No significant activity was detected against *P. aeruginosa* Xen 5 for SMI-P, SMI-NB and SMI-AE. However, SMI-P fibers were able to reduce the populations of *S. aureus* Xen 36 and *E. coli* Xen 14 by up to 5 logs and 3 logs respectively.

SMI-AE and SMI-NB fibers did not show any significant antimicrobial properties against any of the bacterial strains *S. aureus* Xen 36 and *P. aeruginosa* Xen 5. However, the SMI-NB fibers were able to reduce the population of *E. coli* Xen 14 by 2 logs in 24 hours.

With regards to the antimicrobial activity of the quaternized SMI fibers, all fibers containing quaternary ammonium groups have shown good antimicrobial properties as expected. It was shown that the quaternized polymer fibers based on the prepared SMI-P precursor exhibited the strongest antimicrobial activity against all the tested bacteria. As they were able to completely kill *S. aureus* populations in 24 hours. However, only the quaternized SMI-Pq4 and SMI-Pq12 fibers were able to completely kill *E. coli* Xen 14 populations in 24 hours.

The antimicrobial activity of the quaternized SMI-Pq8 fibers were the most potent against *P. aeruginosa* Xen 5 as it killed all bacterial cells after 24 hours contact. The other quaternized derivatives had moderate activity against *P. aeruginosa* Xen 5, whereby the populations were reduced by 3 logs when treated with SMI-Pq12 fibers and by 2 logs with SMI-Pq4 fibers.

External antimicrobial tests at TNO

Due to technical circumstances only one type of fibers SMI-P was tested against so called “super bugs” or warfare microbes. The SMI-P fibers were tested against *Bacillus anthracis*, methicillin resistant *S. aureus* (MRSA), *Yersinia pestis* and *Vibrio cholerae* at the Netherlands Organization for Applied Scientific Research (TNO). The results indicated that the fibers were able to inhibit the growth of all the strains except the *Bacillus anthracis* spores. The fibers showed excellent activity against *Y. pestis* as it completely killed all the cells after 6 hours of contact.

Mode of action and cytotoxicity

The use of the fluorescence microscopy technique has allowed monitoring bacteria viability based on membrane damage, because PI fluorochrome only penetrates into the bacteria with a damaged membrane. A significant reduction of the viable cells (blue fluorescence) was

Chapter 6: Conclusions and Recommendations

demonstrated by fluorescent microscopy, suggesting that the bacteria treated by the electrospun fibers had compromised membranes. Membrane damage is therefore one of the most likely causes for the death of the bacteria.

Using the same set of fluorochromes, an indication of cytotoxicity towards H9c-2 mammalian (cardiac rat) cells was carried out by monitoring fluorescence with time. The quaternized polymer with the longest alkyl chain SMI-Pq12 showed the least toxic affect on the cells. After 4 hour incubation of the cells with the fibers, calculated to be 93% \pm 5.0 viable cells compared to the control 97.5% \pm 2.0 viable cells. Contrarily, fibers quaternized by short C1 and C4 alkyl chains had very toxic activity against the cells as they completely killed all H9c-2 cells in 1 hour. These findings suggest that the derivatives with the longer hydrophobic chains such as C12 that low cytotoxicity towards mammalian cells could have a degree of selectivity towards pathogens. This interesting property could open doors to extend the applications of the polymer fibers in various biomedical fields.

6.2 Recommendations:

The favorable antimicrobial properties of the materials synthesized in this work, open various pathways for further investigations with regards to the design and the usage of the materials and fibers in general.

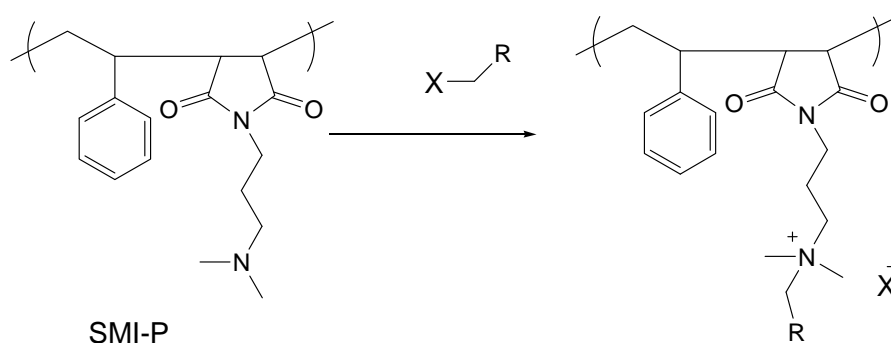
First of all, an increased understanding of the nature of the crosslinking process of SMI-P and its quaternized derivatives will help to design and target selective reactive groups in the polymer chain.

There are a number of interesting points that can be given attention to study or to extend this work. These can be summarized as follows:

- It is worth investigating the quaternized water-soluble polymers in polymer latexes. They could play a dual role as surfactant and as antimicrobial agent. This means that the polymer will stabilize the latex against coagulation and will protect the latex as well as the eventual coating against microbial attack.
- The ability of the quaternized SMI-P fiber derivatives to crosslink via heat treatment makes them excellent candidates for electrospinning. No toxic solvent is required, and obviously water is a greener alternative to prepare the antimicrobial nanofibers.

Chapter 6: Conclusions and Recommendations

- In this work aliphatic halides were used for the quaternization reaction. It is recommended to investigate the quaternization using dihalides as a post-electrospinning step. It would be interesting to study the effect of this reaction on the physical and chemical properties of the functionalized fiber mat and on the antimicrobial properties. Also to investigate the ability for the quaternization reaction to crosslink the fiber mat.
- The styrene-maleimide copolymer derivative SMI-P is a very good precursor for a library of quaternary ammonium compounds. The selection of the halide-containing compound can be used to specifically target certain microorganisms, or for immobilization of specific functionality. See Scheme below.



X= e.g. Cl, Br, I

R= aliphatic, aromatic, heterocyclic ..etc

- There is a continuous need for new classes of antifungal agents. For example pyrimidine derivatives are known as effective fungicides. It is recommended to utilize this technology to quaternize the SMI-P with various known fungicides that contain a halide to form the quaternary ammonium moieties. an activated halide.
- Mixtures of different antimicrobial quaternized derivatives are also an interesting area of research whereby the antimicrobial efficacy and observation of any synergistic effect can be investigated.
- There was a good indication of low cytotoxicity of some of the fiber mats, such as SMI-P and SMI-Pq12. This makes them possible candidates for wound dressings or protective bandages. However, it is recommended to apply Methylthiazol Tetrazolium (MTT) assays to determine the cytotoxicity_of the fibers for biomedical applications.